DEEP LEVEL IMPURITIES IN SEMICONDUCTORS

FOR NUCLEAR RADIATION DETECTION

by

Stephen John
S. J. PEARTON, B.Sc.(Hons)

Submitted in fulfilment of the requirements for the degree of
Doctor of Philosophy

UNIVERSITY OF TASMANIA
HOBART

August 1981

This thesis contains no material which has been accepted for the award of any other degree or diploma in any university and, to the best of my knowledge and belief, contains no copy or paraphrase of material previously published or written by another person, except where due reference is made in the text.

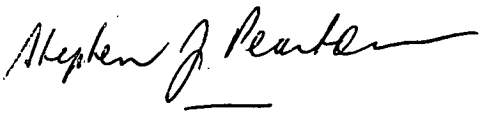

ADDENDA BASED ON EXAMINER'S COMMENTS

1. page vi, "deep level" is a term which must be referenced to the band gap. It physically denotes a localized state. For example, > 0.1 eV from the band edge is "deep" for germanium and silicon, but hydrogenic for gallium phosphide.

2. In Figure 2, the diode is upside-down relative to the W(t) graph.

3. Page 16. Note that the Fermi level position at 25 ^{o}C is well above the defect level, which is therefore always ionised and thus may be susceptible to charge-state effects. No Poole-Frenkel emission was observed for this defect state.

4. Page 17. An exponential dependence of σ vs. I/T has also been characterized as "multiphonon emission". Here, the energy is a configuration excitation required to promote capture.

CONTENTS

CONTENTS (cont'd)

SUMMARY

This thesis describes experiments on the behaviour of deep level defects in the semiconductors Ge, Si and GaAs. High-purity samples of these materials are often used for the fabrication of solid state nuclear radiation detectors; it is within this context that the work has been performed.

Deep level impurities may have considerable effect on the performance of solid state devices. By trapping signal carriers (electrons and holes) they may change the effective lifetimes of these entities, and so affect parameters such as switching times in photoconductors, the efficiency of solid state lasers and light-emitting diodes, and the energy resolution of semiconductor radiation detectors. Positive uses of their effects include the increased switching times of certain Si diodes, higher quantum gain in some photoconductors and the production of high resistance compound semiconductor wafers. The deep level defects may be caused by contamination of the material with other elements, by lattice line and point defects, or associations of these imperfections and impurities. They may be present in the as-grown semiconductor crystal, introduced during processing of the material, or during the operation of the final device (e.g. radiation damage).

No general formalism exists to explain or predict the properties of these deep level impurities, particularly because of their non-hydrogenic nature. A greater understanding of solid state physics than currently exists will need to be achieved to produce a theoretical treatment of their behaviour. The study of their properties is therefore desirable from both a device and a fundamental point of view.

Chapter 1 describes experiments on radiation damage centres in Ge. The γ-irradiation of p-type Ge crystals grown from silica crucibles

under an H_2 atmosphere always produces two deep acceptor levels. We detail evidence showing these are most likely due to oxygen-vacancy complexes. Heat treating samples before irradiation appears to reduce the amount of oxygen available for production of the deep levels, and so these samples are hardened to γ-radiation damage. Similarly, Li ions drifted through the crystal cause radiation hardening of this material, possibly by binding oxygen into stable Li-O pairs, and also by direct passivation of the γ-induced defect centres. The thermal and electrical stability of these centres is also discussed. Proton and neutron irradiation of Ge produced acceptor levels only, whereas γ-damage produced both donor and acceptor levels.

Chapter 2 deals with deep level defects found in single crystal and polycrystalline GaAs. Many different defect species are present - even the high purity epitaxial wafers used to fabricate radiation detectors showed high trap densities. The Poole-Frenkel effect (field enhanced emission) and a magnetic field sensitivity were observed in one of the deep donor levels (E_c - 0.62 eV).

Chapter 3 deals with the fabrication of thin, highly doped contacts to semiconductors by pulsed laser melting of an evaporated dopant layer. The use of Li to produce n^+ layers has met with the most success, and good quality Si and Ge radiation detectors were fabricated in this fashion. The advantage and problems of the technique are discussed.

Chapter 4 deals with the measurement of the energy levels and capture cross sections of defects related to over 25 different elemental impurities deliberately introduced into Ge. There appears to be a band of energies at approximately one-third the band gap of the material (E_g = 0.66 eV) into which many deep metal-related states (particularly donors) fall. The capture cross sections of these

states for majority carriers are generally 10^{-16} to 10^{-18} cm^2. These facts may be related to the notion that many of the energy levels measured for metal-related centres in Ge may be due to defects of complicated nature, rather than simple subsitutional or interstitial defects.

Chapter 5 discusses experiments in which point defects in Ge and GaAs are neutralised by the incorporation of atomic hydrogen. Data on the depth and efficiency of the passivation as a function of hydrogen plasma exposure duration and temperature are presented. Significantly in Ge, copper-related defects may be neutralised to a depth of $\sim$100 μm for a 3 hour plasma exposure at $300^{o}C$.

Miscellaneous experiments on the behaviour of deep level defects are described in Chapter 6. They fall into an 'interest only' category and no detailed data is presented or conclusions drawn.

ACKNOWLEDGEMENTS

The work reported in this thesis was performed and written entirely at the Australian Atomic Energy Commission Research Establishment, and many people contributed or assisted in various ways.

I would like firstly to acknowledge my debt to Dr A.J. Tavendale, Leader of the Semiconductor Radiation Group, who was my supervisor at Lucas Heights. His suggestions and encouragement during the practical work, and his critical reading of the various publications, were of great assistance. He also supplied samples which proved crucial to some experiments.

Mr A.A. Williams and Mr D. Alexiev gave much advice and skilful practical assistance during the course of the project on material preparation, instrumentation, furnaces and vacuum systems. Their help is sincerely appreciated.

Mr G.C. Wall provided most of the Ge used in the project, which was not an insignificant amount. The doped and ultra-pure Ge was grown in the laboratories of Applied Physics Division, AAEC. Also, Dr E.M. Lawson arranged many laser irradiations and provided Rutherford backscattering and optical and scanning electron microscope data on the samples used.

Mr P.J. Lee and Mr A.McG. Beech gave practical assistance in many areas of diode fabrication, while the ^{60}Co γ-irradiations were performed by Mr R.R. Glover, Mr G. Burrell and Mr H.J. Gray (Isotopes Division). The Q-switched ruby laser was operated by Mr A. Rose and Rutherford backscattering measurements were performed by Mr M.D. Scott. Mr L.S. Dale (Chemical Technology Division) provided the SSMS measurements. Proton irradiations were carried out on the 3 MeV Van de Graaff accelerator by Mr D.D. Cohen (Australian Institute of Nuclear Science

and Engineering - AINSE) with assistance from Mr J.P. Fallon and Mr L.H. Russell; electron irradiations were performed by Mr S.G. Kanard (AINSE). SEM samples were measured by Mr K.G. Watson (Materials Division) and Mr C.P. Bock (AINSE) was most helpful in arranging LHe supplies. Mr J. Mellor (Materials Division) provided optical microscope photographs of several samples.

Mr J.E. Eberhardt deserves special mention for his patient refeering of many publications.

Mr G. Watt and Mr W.O. Hill (Instrument Development Group) lent several items of instrumentation for use during the course of the project.

The assistance of the various workshops, maintenance, the Editorial group, the library and the secretarial staff is also acknowledged.

I wish to express in particular, my appreciation to Ms L. Woodland, who did a marvellous job in typing this thesis.

The work was performed with the assistance of a postgraduate studentship from The Australian Institute of Nuclear Science and Engineering. The Institute's interest and encouragement, particularly that of Mr E.A. Palmer (Executive Officer) is appreciated. I wish to thank AINSE and the AAEC for providing me with an opportunity not normally afforded postgraduate students.

At the University of Tasmania I would like to thank Dr K.B. Fenton for his interest and support during the project, and Mr R. Lincolne, who performed a fast neutron irradiation of some Ge samples.

INTRODUCTION

The measurement of deep defect levels in semiconductors by various methods has been fully described in several review articles [Blood and Orton 1978; Sah et al. 1970; Kimerling 1978]. In this thesis, the major technique used has been deep level transient spectroscopy (DLTS) [Lang 1974; Miller et al. 1977], and a brief introduction to the technique is included here for completeness.

BASIS OF THE DLTS TECHNIQUE

The principle of the technique depends on two phenomena. Firstly, the variation of the test p-n junction capacitance with the applied reverse bias (Figure 1) and, secondly, the capture and emission of free charge carriers by defect centres within the diode depletion region. A localised defect level (termed 'deep' if it is greater than ~0.1 eV from the allowed band edge) can alter the space charge density by this carrier trapping, causing a change in depletion depth and thus capacitance. In the DLTS measurement, the applied reverse bias is periodically reduced, filling the localised defect levels. As the trapped carriers are thermally re-emitted, the time dependence of the capacitance is measured by a high sensitivity, fast transient response bridge (Figure 2). The DLTS technique uses the fact that each defect state possesses a unique energy level and capture cross section, which enables a spectroscopic display of the defects present in the depletion region.

The transient capacitance signal is processed so that a selected decay rate produces a maximum output. As the temperature of the test sample is scanned, changing the emission rate of the defect level, a spectrum peak in the signal output versus temperature data occurs when the capacitance decay rate passes through a preset rate window. The rate window may be achieved by various means using a box-car integration [Lang 1974], lock-in amplifier [Kimerling 1976] or, in our case,

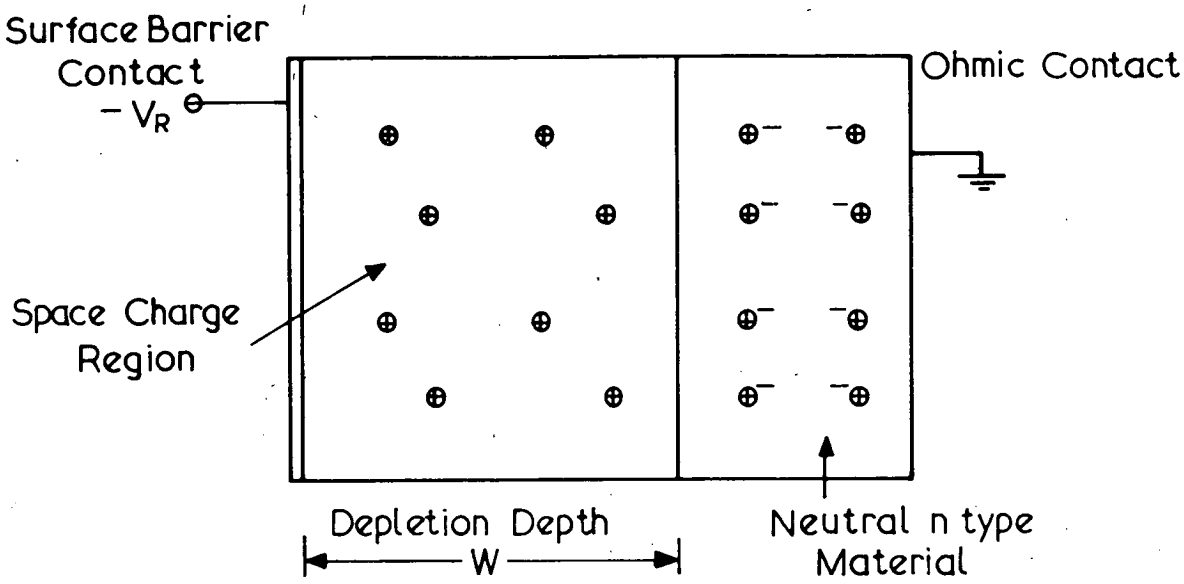

$$\text{Capacitance} \quad C = \frac{\varepsilon A}{W}$$

$$\text{Depletion Depth} \quad W = \left(\frac{2\varepsilon (V_{bi} + V_R)}{qN} \right)^{1/2}$$

FIG. 1 REVERSE BIASED DIODE - AREA A cm^2, FREE CARRIER DENSITY N cm^{-3}, BUILT-IN BIAS V_{bi}

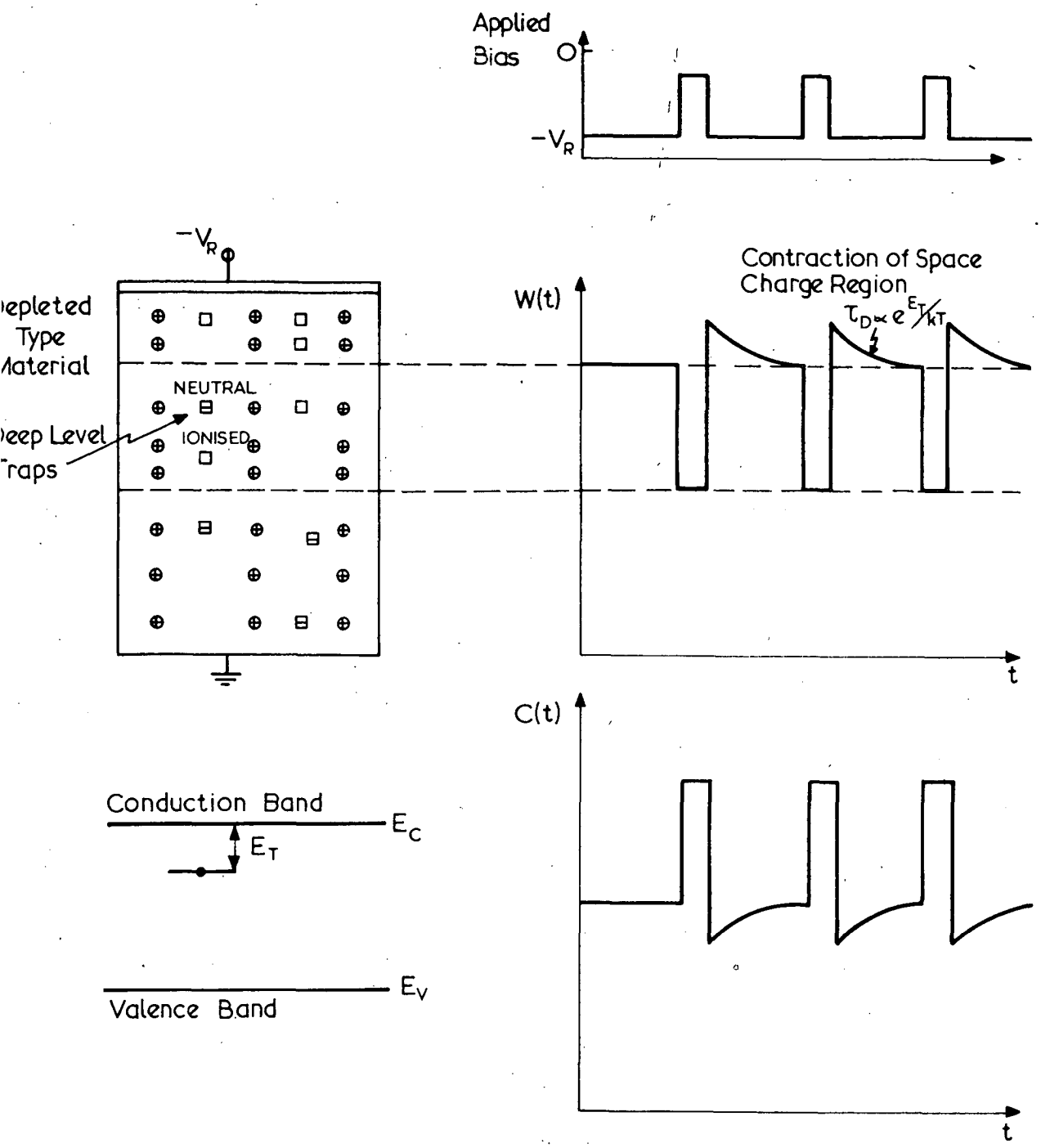

FIG. 2 PULSING WAVEFORMS FOR OBSERVATION OF CAPACITANCE TRANSIENTS

an electronic correlator [Miller et al. 1975]. This instrument generates an exponential waveform whose decay rate may be externally selected. This exponential waveform, and the exponential capacitance decay waveform due to discharging of defects in the test sample, are multiplied together and the resulting signal integrated to give a d.c. output. A maximum output is achieved when the two decay rates are equal. Changing the pre-selected decay rate means the temperature at which the two rates are coincident also changes, and this temperature dependence gives the activation energy for carrier emission from the particular defect level to the appropriate band (Figure 3).

MEASUREMENT OF DEFECT PARAMETERS

The thermal emission rate e has the following temperature dependence:

$$e = \frac{\sigma \langle v \rangle N}{g} \exp\left(-\frac{\Delta E}{kT}\right) \qquad (1)$$

$$\therefore \quad \Delta E = -kT \ln \frac{e}{CT^2} \quad , \quad C = \text{constant}$$

where σ = capture cross section of level,

$\langle v \rangle$ = average thermal velocity of carrier at absolute temperature T,

N = density of states in appropriate band,

g = degeneracy of level,

ΔE = activation energy of level, and

k = Boltzmann's constant.

Thus ΔE may be obtained from the slope of a $\ln e$ versus $\frac{1}{T}$ plot, and σ derived from the intercept of the same plot. To account for the T^2 dependence of the exponential prefactor in equation (1), a correction must be applied to the calculated value of ΔE. The simplest method is to subtract 2kT where T is the average temperature of the data collection [Miller et al. 1977].

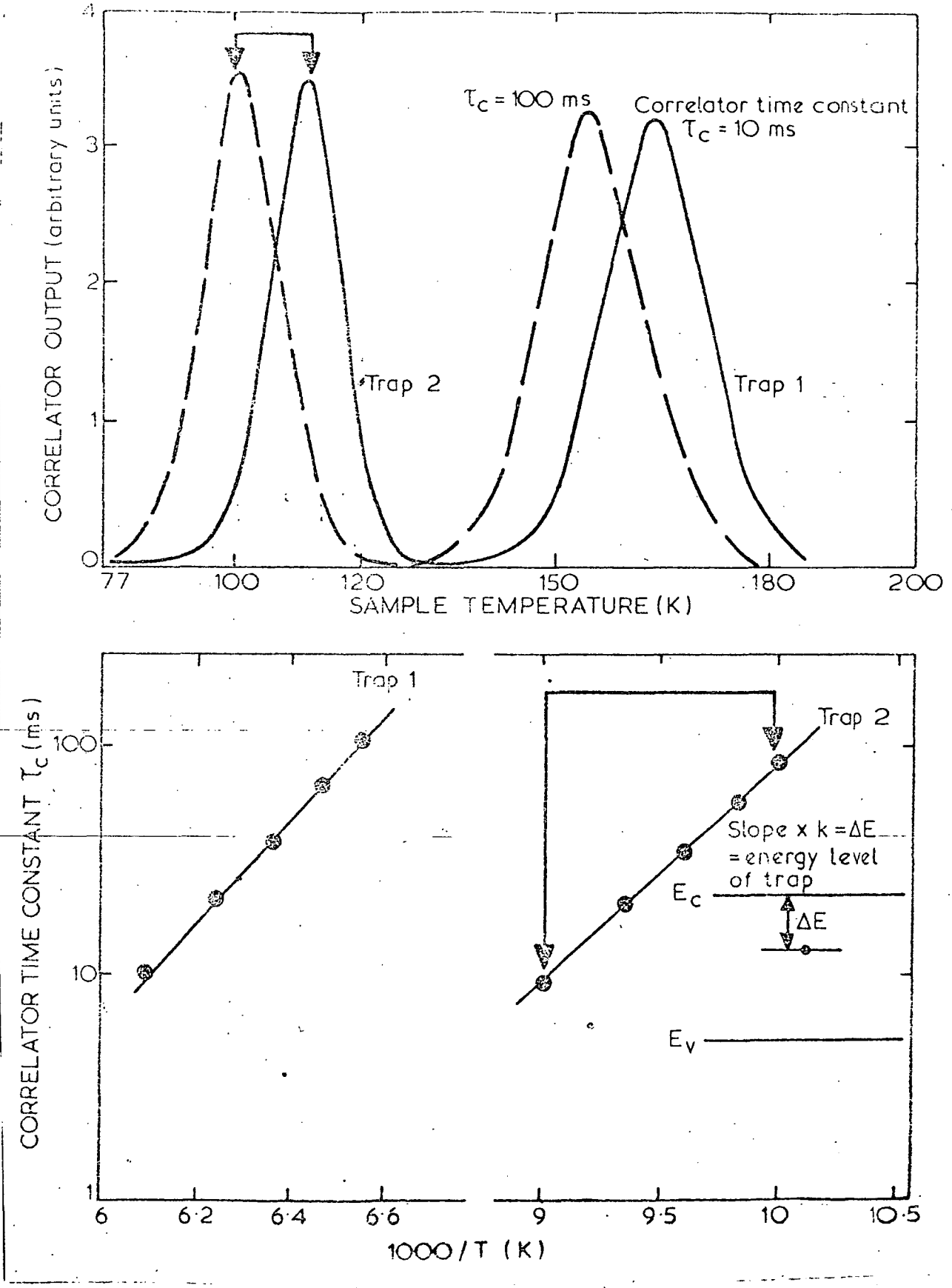
CORRELATOR OUTPUT (arbitrary units)
0
1
2
3
4
77
100
120
150
180
200
SAMPLE TEMPERATURE (K)
τ_c = 100 ms
Correlator time constant
τ_c = 10 ms
Trap 2
Trap 1
CORRELATOR TIME CONSTANT τ_c (ms)
1
10
100
6
6·2
6·4
6·6
9
9·5
10
10·5
1000/T (K)
Trap 1
Trap 2
Slope x k = ΔE
= energy level
of trap
E_c
ΔE
E_v

FIGURE 3.

Capture cross sections may be directly measured by following the capacitance signal output after the pulse as a function of the pulse duration. The capture of the free carriers occurs in the neutral material because of the decrease in space-charge (depletion) width during the bias pulse. The peak height of the DLTS signal is related to the pulse width t by

$$n(t) = N_T \left(1-\exp(-t/\tau)\right) \tag{2}$$

where τ^{-1} = rate of carrier capture by trap, and N_T = trap concentration. The cross section is obtained from the expression

$$\tau^{-1} = \langle v \rangle n\sigma \tag{3}$$

where n = net background doping density. The method is straightforward for majority carrier traps, but poses problems for minority carriers because the injection efficiency of a forward biasing (or LED) pulse is generally unknown, hence the injected carrier density is subject to large calculational errors. In the present case, minority carrier cross sections have been derived from the exponential prefactor of the thermal emission rate. This method is subject to large uncertainties in isolated cases because the factors involved may include field and temperature dependences. A discrepancy usually noted between directly measured and derived cross section is not yet understood, but it may be related to the fact that pulsed bias methods measure cross sections for neutral material, whereas derived values are obtained from thermal emission rates measured in the space-charge region.

Trap concentrations are obtained by measuring the relative change in capacitance signal produced by a small change in the pulse amplitude, V. The defect concentration, N_T, may be profiled using [Lang 1974a,b]:

$$\delta\left(\frac{\Delta c}{c}\right) = \left(\frac{\varepsilon}{qw^2 n}\right)\frac{N_T(x)}{n(x)}\,\delta V \tag{4}$$

where q = electronic charge,

w = depletion layer width,

ε = dielectric constant,

$n(x)$ = free carrier density at depth x, and

n = free carrier density at edge of depletion region.

If a plot of Δc against pulse amplitude is linear, the trap concentration profile is the same as that of the free carrier density profile. An approximation, valid for $\Delta c/c \ll 1$ and the one-sided abrupt junction assumption, is

$$N_T \approx 2n \frac{\Delta c}{c} \qquad (5)$$

where c = capacitance of the device at the quiescent reverse bias, and

Δc = change in capacitance produced by pulsing to zero bias.

Example data for various levels in Ge are shown in Figures 4(a), (b) and (c).

The DLTS technique is now standard for deep level defect measurement in semiconductors because of its unique combination of advantages over other methods (see Table 1). It has been used throughout this thesis in relation to radiation damage, grown-in defects, laser doping damage and metal-related centres.

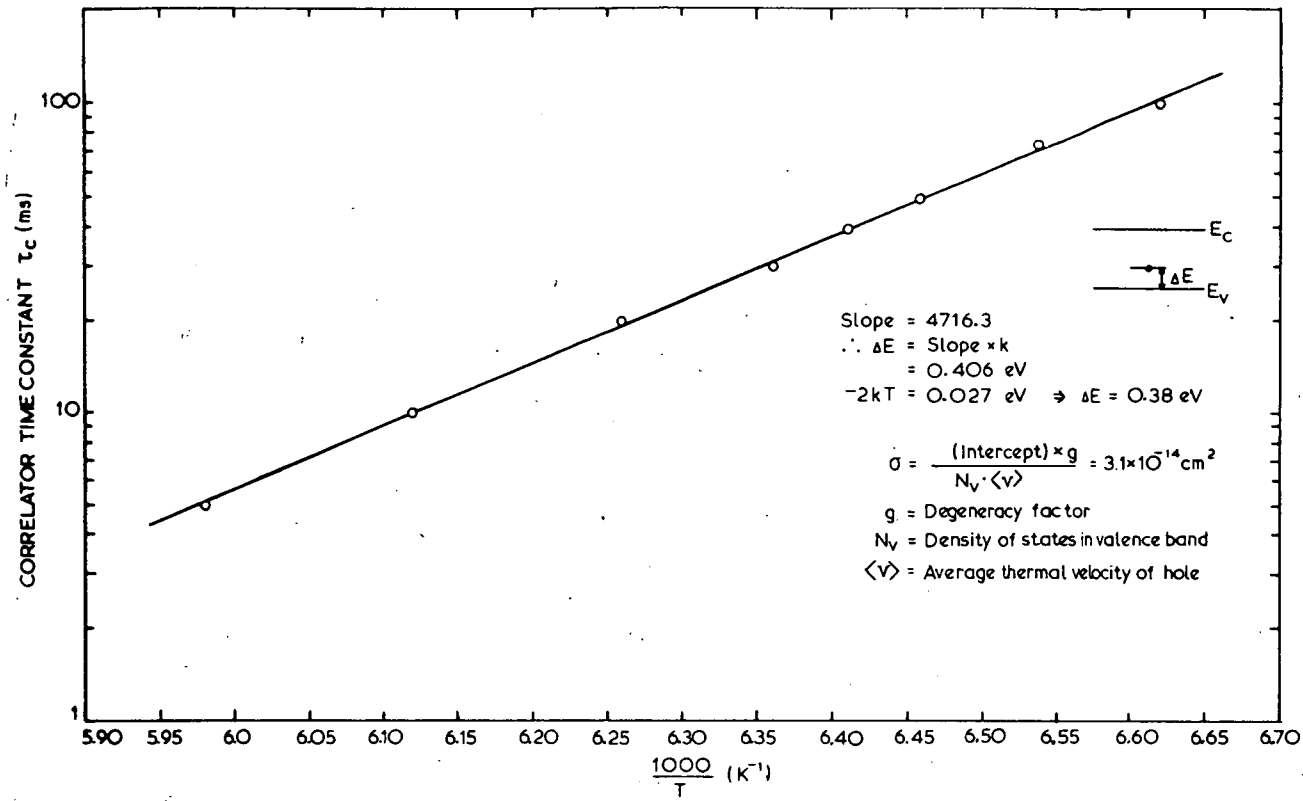

FIG. 4 (a) ARRHENIUS PLOT P-TYPE GERMANIUM ACCEPTOR LEVEL

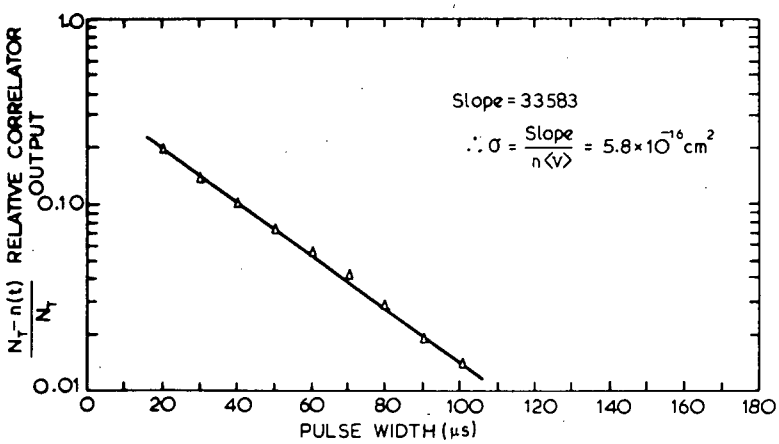

FIG. 4 (b) N-TYPE GERMANIUM DONOR LEVEL

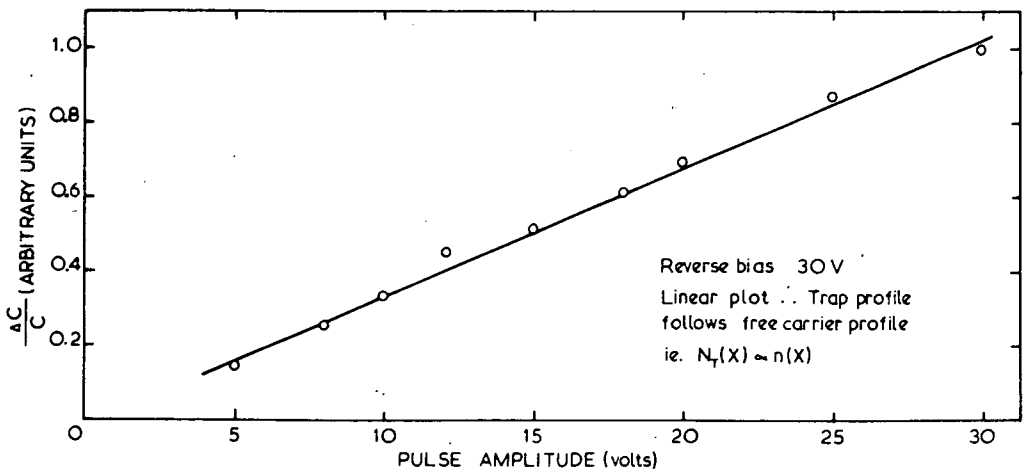

FIG. 4 (c) P-TYPE GERMANIUM ACCEPTOR LEVEL

REFERENCES

Blood, P. and Orton, J. W. [1978] - Reports on Progress in Physics 41(2)157.

Kimerling, L. C. [1976] - IEEE Trans. Nucl. Sci. 23(6)1497.

Kimerling, L. C. [1978] - Int. Conf. Physics of Semiconductors 1978, Edinburgh, Inst. Phys. Conf. Series No. 13.

Lang, D. V. [1974] - J. Appl. Phys. 45:3023.

Miller, G. L., Ramirez, J. V. and Robinson, D. A. H. [1975] - J. Appl. Phys. 46:2638.

Miller, G. L., Lang, D. V. and Kimerling, L. C. [1977] - Ann. Rev. Mater. Sci. 7:377.

Sah, C. T., Forbes, L., Rosier, L. L. and Tasch, A. F. [1970] - Solid-State Electronics 13:759.

TABLE 1

ADVANTAGES OF DLTS AS COMPARED TO OTHER TECHNIQUES

(Hall measurements, infrared absorption, photoluminescence, etc.)

1. Works best for deep (E_T >100 meV) levels, decreasing sensitivity for shallow levels (opposite to other techniques).
2. High sensitivity (typically 10^{-4} of background doping density), greater range of observable trap depths.
3. Observes majority and minority traps.
4. Speed of device characterisation, easy to interpret.
5. Concentration profiling (absolute values of trap density).
6. Direct measure of capture cross sections.
7. Sample in form of actual device (e.g. radiation detector).

DISADVANTAGES

1. Specialised instrumentation.
2. Some states unobservable ('unsaturable' traps).
3. Electrically active states only observed.
4. Some devices give problems (RC time constant of substrate or undepleted material). C must change with reverse bias in general.

CHAPTER 1

RADIATION DAMAGE IN Ge

1.1 γ-INDUCED CENTRES IN Ge

1.1.1 SINGLE CRYSTAL Ge

INTRODUCTION

The electrical (and optical) properties of single crystal semiconductors are extremely sensitive to the production of the relatively stable lattice imperfections caused by γ-irradiation. The effects of irradiation are crucial in many device performance-related areas, particularly in an environment where heavy photon fluxes are prevalent. The ultra-pure (net impurity densities $<4 \times 10^{10}$ cm^{-3}) and single crystal Ge for nuclear radiation detectors, as well as intentionally doped material, provides an excellent environment for the observation of basic γ-radiation damage processes.

Confusion exists as to the exact nature of the resulting defect complexes formed by the γ-irradiation of Ge. In the past 15 years, much work has been performed using a variety of techniques (e.g. Mashovets [1977]), but because of the sensitivity of the radiation damage centres to the experimental conditions during the irradiation and to the type and density of background impurity levels, firm conclusions were often hindered. Measurement is required of the exact levels formed, the effect of the crystal growth conditions and the degree of thermal annealing required for removal of the damage centres. The relatively well-characterised nature and strict crystal growth control of the Ge used for nuclear radiation detectors might allow a better understanding of defect production processes in particular, and deep level impurity states in general.

The deep level transient spectroscopy (DLTS) technique [Lang 1974] provides a spectroscopic display of the deep lying energy states ionizing as the sample temperature is raised, allowing the observation of individual defect levels as a function of radiation dose or annealing

time. In an attempt to clarify the type, density and trapping cross sections of induced defects we have used DLTS to examine devices produced 10 years ago, and doped and high purity material newly irradiated.

EXPERIMENTAL

1. Sample Preparation and Irradiation

The material used was of two classes. The first was γ-compensated n-type nuclear radiation detectors fabricated ten years ago [Lawson 1969] in which compensation of the shallow donor population was achieved by the deliberate introduction of deep level acceptor centres by γ-irradiation [Ryvkin et al. 1965; Lawson 1971]. These Ge(γ) detectors were compared with recently irradiated samples from the same crystals, the only difference being that the original samples had undergone long-term annealing at room temperature. The second class of material consisted of Ge crystals, n- and p-type, with varying growth conditions. The aim was to observe in this second class of samples any differences in the defect energy levels or densities produced by variations in the selected dopants or growth conditions. Table 1 lists the growth conditions.

After being lapped onto discs or cubes (area $\sim$0.6 cm^2, thickness $\sim$0.4 cm) the samples were polished with a slurry of 600 grade SiC grit on pile cloth and etched to a specular finish in a 4:1 mixture of HNO_3 (70 wt %) and HF (40 wt %). An n^+ contact was formed by evaporating Li to one face and diffusing for ten minutes at 325^{0}C; Pd was evaporated onto the opposite face. On p-type samples, this procedure formed a p-n^+ junctions, while Schottky barriers were produced from n-type material. Surface-related DLTS peaks could be identified by examining washed and re-etched samples. Sample purities were determined by 1 MHz C-V measurements performed at 77 K.

All samples with the exception of the previously irradiated Ge(γ) detectors were given a uniform γ-dose of 150 Mrad, performed at ambient temperature (~25°C) in a 2.1 Mrad h^{-1} ^{60}Co facility. Dependent on the initial net electrically active impurity density, this enabled observation of the induced defect behaviour in both lightly and heavily irradiated material. The major levels tabulated were observed usually in three different samples of widely varying purity.

2. DLTS Measurements

Samples were installed in a continuous flow cryostat operating over the temperature range 6 to 180 K, measured using a gold (0.03 at wt % iron)/chromel thermocouple imbedded in a sapphire disc on which the sample was mounted. The DLTS system used a fast capacitance bridge operating at 1 MHz (Boonton model 71A) and an electronic correlator [Miller et al 1975] which used an exponential weighting function for measurement of the transient diode capacitance changes.

An infrared emitting diode was used to inject minority carriers into the n-type Schottky barrier samples although, in most cases, the barriers were leaky enough to permit hole injection by pulsed forward biasing. This injection enabled a qualitative check of acceptor level creation by γ-rays in the n-type samples.

Reverse bias voltages were typically 30 V with leakage currents less than 50 μA for all samples below 180 K. The product of the capacitance of the depletion region and the resistance of the un-depleted material was less than 0.2 μs for every sample; this is small compared to the inverse of the bridge measurement frequency (1 μs).

A trap spectrum was obtained by scanning the temperature of the sample diode [Mashovets 1977]. The energy separation of the defect

from the appropriate band edge was obtained by measuring the thermal emission rate as a function of temperature. Cross sections for carrier capture were obtained by measuring the correlation signal output as a function of bias pulse width. Majority defect concentration profiles were obtained by measuring the change in correlator output for changes in bias pulse amplitude [Lang 1974].

All annealing experiments were performed in an atmosphere of H_2, with the samples mounted on a graphite block. A complete coating of the samples with GaIn alloy provided effective gettering for rapidly diffusing contaminants, most notably Cu.

EXPERIMENTAL RESULTS

Table 1 lists the defect parameters measured for the most common levels observed and the growth conditions for the material used. Defects are labelled by the temperature at which they appear for a correlator time constant of 10 ms. Energy levels have been corrected for the temperature dependence of the exponential prefactor by subtracting 2 kT from the raw energy obtained, where T is the average temperature of the peak position over the set of time constants used [Miller et al. 1977]. Most probable errors for the energies were typically ±7%. Typical errors for the cross sections were ±30%, and for the concentrations ±25%. Results were checked at several diode bias voltages and revealed no field dependence within the stated errors. The free carrier densities used to determine defect concentrations were obtained by C-V measurements (f = 1 MHz) at the peak temperatures.

1. Ge(γ) Detectors

All three of the Ge(γ) detectors (γ-irradiated in 1969, stored at 25°C in air) showed a donor level at E_c - 0.36 eV, with a donor level at E_c - 0.20 eV evident in two of them (Figure 1). One of

TABLE I MEASURED TRAP PARAMETERS

DEFECT	LEVEL (eV)	σ (cm^2)	N_T (cm^{-3})	GROWTH CONDITIONS OF PARENT CRYSTAL
31	E_c - 64 meV	2.4×10^{-14}	2.1×10^{9}	a(i) (iii),c
31	E_v + 35 meV	1.9×10^{-16}	$1.8\text{-}7.2\times10^{11}$	f(i), g(i)
45	E_v + 68 meV	-	$3.2\text{-}8.4\times10^{10}$	f(ii), g(i)
46	E_c - 75 meV	1.4×10^{-14}	3.6×10^{11}	a(iii)
58	E_c - 0.10	2.3×10^{-14}	2.2×10^{9}	a(i) (iii), c
88	E_c - 0.18	2.5×10^{-15}	1.4×10^{11}	e
93(surface)	E_c - 0.18	7.7×10^{-15}	5.1×10^{9}	a(i) (iii), c
103	E_c - 0.19	4.9×10^{-16}	1.6×10^{11}	e
105	E_v + 0.23	7.5×10^{-15}	1.7×10^{10} - 2.9×10^{12}	f(i), g(i)(ii), h(ii)
110	E_c - 0.20	2.9×10^{-14}	9.2×10^{9} - 1.4×10^{12}	a(i) (iii), b, c,
148	E_c - 0.36	1.8×10^{-14}	1.4×10^{10} - 2.2×10^{12}	a(i) (ii) (iii), b, c
152	E_c - 0.27	5.8×10^{-16}	2.3×10^{12}	h(i)
163	E_v + 0.38	4.2×10^{-14}	1.6×10^{11} - 1.3×10^{12}	f(i), g(i) (ii)
165	E_c - 0.42	3.7×10^{-14}	1.6×10^{11} - 2.1×10^{12}	d,e, h(i) (ii)
174 (surface)	E_c - 0.37	7.4×10^{-16}	9.4×10^{11}	c

Growth conditions and treatment of parent crystal

(a) Hoboken (1968), n-type (zone levelled, Czochralski) 3 crystals
- (i) Dose 410 Mrd T = 80°C (1969) ($n = 5\times10^{10}$ cm^{-3})
- (ii) Dose 284 Mrd T = 25°C (1969) ($n = 2.4\times10^{10}$ cm^{-3})
- (iii) Dose 410 Mrd T = 80°C (1969) ($n = 9.9\times10^{12}$ cm^{-3})

(b) As for a(i); annealed~900°C for 3 hours $n = 7.2\times10^{12}$ cm^{-3}

(c) As for (b) Dose 150 Mrd T = 25°C (1979) $n = 3.4\times10^{12}$ cm^{-3}

(d) Phosphorus doped ("Spectrosil" silica crucible, H_2 atmosphere) $n = 8\times10^{13}$ cm^{-3} (2.4×10^{10} cm^{-3})

(e) Arsenic doped ('Spectrosil" silica crucible, H_2 atmosphere) $n = 2.2\times10^{14}$ cm^{-3} (5.9×10^{12} cm^{-3})

(f) As grown ("Spectrosil" silica crucible, H_2 atmosphere)
- (i) p-type $p = 4.3\times10^{10}$ cm^{-3} (4×10^{12} cm^{-3})
- (ii) n-type $n = 3.3\times10^{12}$ cm^{-3} (1.7×10^{11} cm^{-3})

(g) As grown (graphite crucible H_2 atmosphere)p-type (heated 74 hrs at 650°C under N_2 to make H_2 deficient).
- (i) H_2 rich $p = 2.7\times10^{12}$ cm^{-3} (2.4×10^{13} cm^{-3})
- (ii) H_2 poor $p = 9.6\times10^{12}$ cm^{-3} (3.7×10^{13} cm^{-3})

(h) As grown ("Spectrosil" crucible) n-type
- (i) Wet N_2 $n = 3.2\times10^{13}$ cm^{-3} (4.4×10^{12} cm^{-3})
- (ii) Dry N_2 $n = 1.1\times10^{11}$ cm^{-3} (2.6×10^{10} cm^{-3})

NB Net impurity density measured at 77K, (C-V data at 1 MHz) value in brackets is that after irradiation (150MRad).

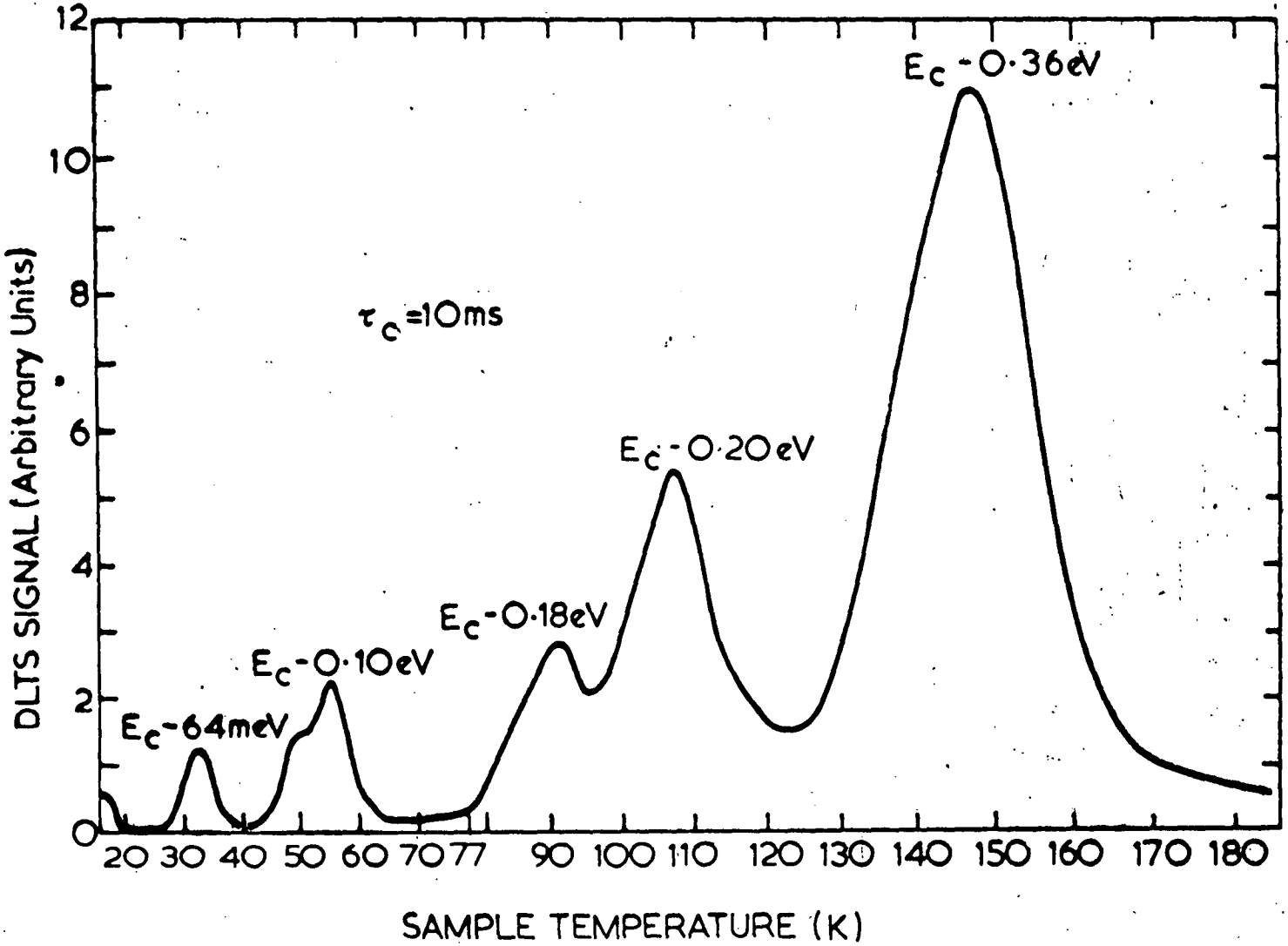

Figure 1 Majority carrier DLTS spectrum for sample subjected to long term room temperature annealing (growth condition 1a(i)) correlator time constant 10 ms. Reverse bias V_R = 25V, capacitance C = 11.9 pF(77K), 24 pF(148K), Area A = 0.8 cm^2.

the diodes (4D2) was annealed for 3 hours at ~900°C to check the stability of the defects, and retested after replacing the contacts. Both of the deep donors were still present, their concentrations having increased in ratio with the free carrier density (two orders of magnitude). No new levels were produced by the annealing. Previously unirradiated samples from the same crystals did not show the donor levels on irradiation, simply a spectrum composed of deep acceptor defects. One of the new samples was annealed for 3 hours at 675°C in an attempt to produce the E_c - 0.36 eV level; the net result was to return the sample to its pre-irradiated state. All these samples remained n-type after irradiation.

2. High Purity and Doped Material

Germanium samples from the second group were also irradiated (150 Mrad) after testing on the DLTS system. The three p-type crystals displayed similar defect spectra: the dominant levels were deep acceptors at E_v + 0.23 eV and E_v + 0.38 eV, whose concentrations were within a factor of three of each other in each of the crystals. Both levels were reduced in concentration in samples taken from the crystal previously heated under N_2 for 74 hours at 675°C to reduce its H_2 content, compared to unannealed companion sections. After irradiation, samples containing these levels could be returned to their original state by annealing at 675°C for 3 hours. Figure 2(a) shows the post-irradiation DLTS spectrum of an originally high purity Ge detector ($N_a-N_d = 4.3 \times 10^{10}$ cm^{-3}), whereas Figure 2(b) shows the post-irradiation spectrum of a section of n-type material (original $N_d-N_a = 3.3 \times 10^{12}$ cm^{-3}) taken from the same crystal. There are no common levels, even though all the defects are acceptors.

A deep donor level (E_c - 0.42 eV) was observed in four of the five n-type samples; it was not created in the crystal with the

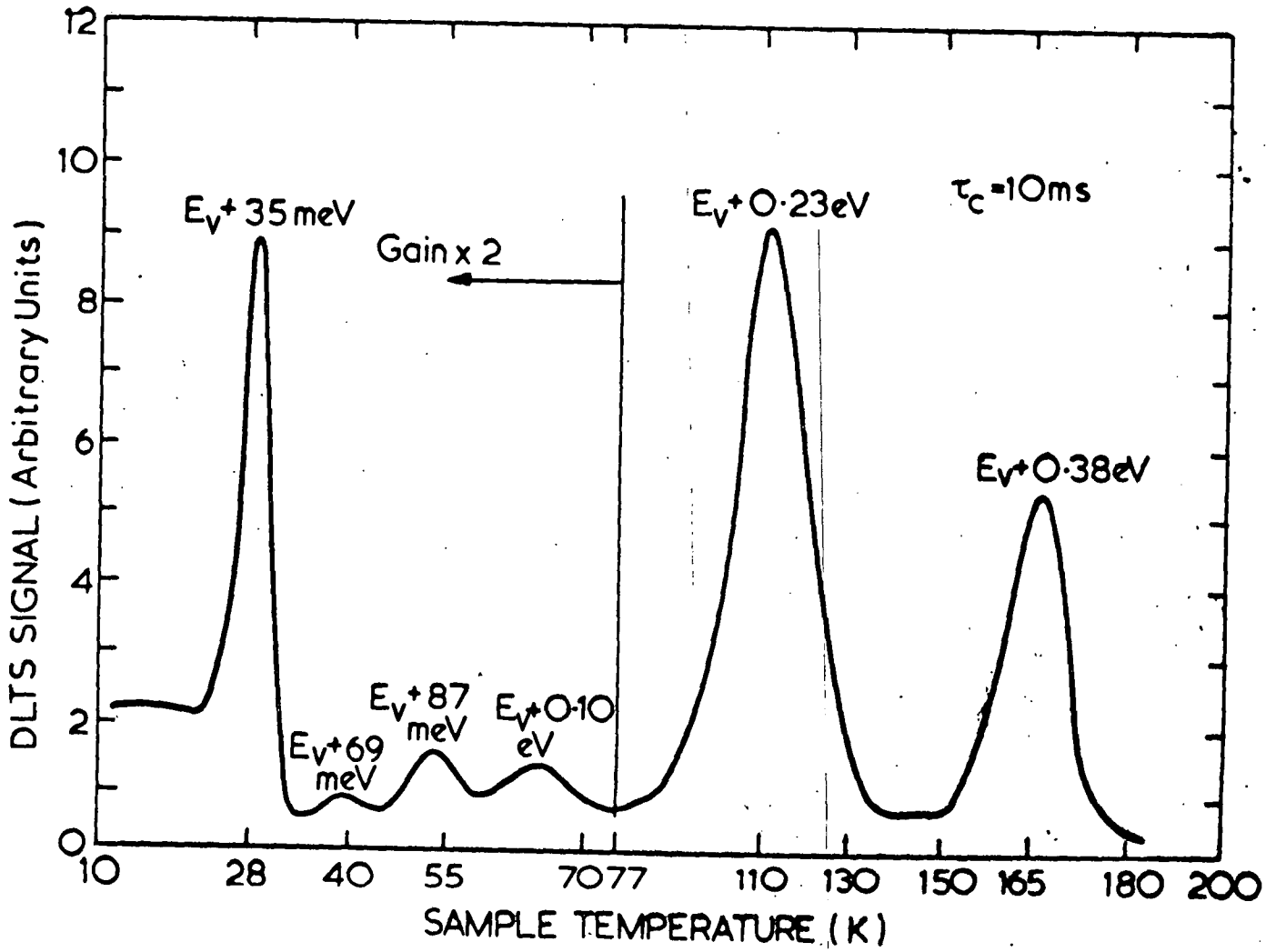

Figure 2a DLTS spectrum of γ-irradiated high purity p-type Ge detector (growth condition 5a). γ-dose = 150 Mrad, correlator time constant 10 ms. V_R = 16V, C = pF,(31K), 80pF(163K), A = 0.4 cm^2.

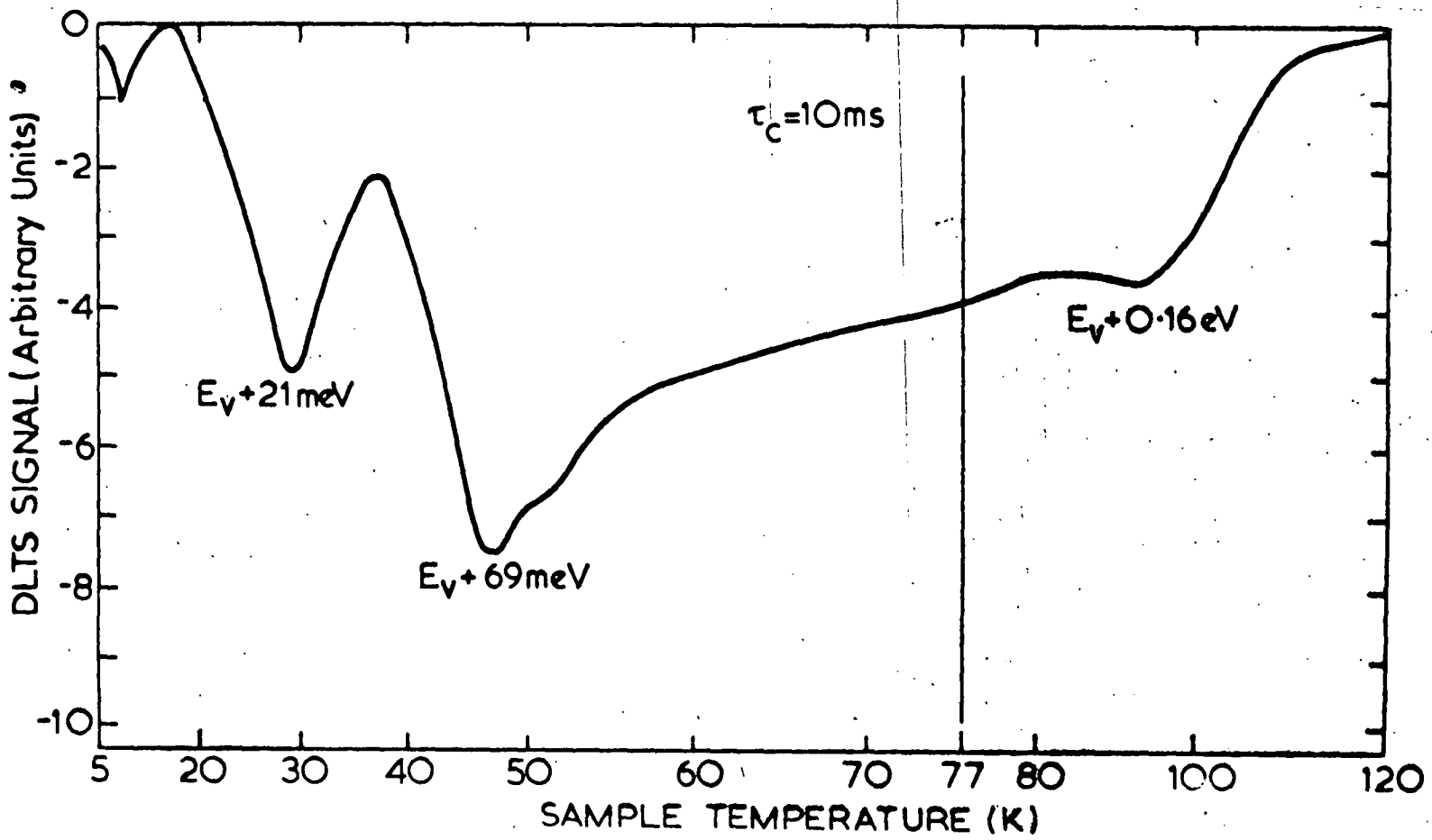

Figure 2b DLTS spectrum of γ-irradiated n-type Ge sample from same crystal as fig. 2a (growth condition 5b). Correlator time constant 10 ms. VR = 20V, C = 5.7 pF(20K), 10 pF(77K), A = 0.14 cm^2.

lowest net impurity density ($\sim 10^{11}$ cm^{-3}). A typical defect spectrum for an irradiated n-type sample is shown in Figure 3; this sample is compensated as shown by the large increase in capacitance on heating. Figure 4 shows the Arrhenius plots of inverse trap emission rate versus inverse temperature for some of the defect levels observed. These plots may be regarded as the signature of the particular trapping centre. Figure 5 shows the data used to measure directly the trapping capture cross sections. That the defect centres were uniformly introduced throughout the diodes is evident from the linearity of the plots produced with the pulse profiling technique (Figure 6).

DISCUSSION

1. Ge(γ) Detectors

The E_c - 0.36 eV level appeared in all of the samples which had undergone long-term annealing at room temperature. It did not appear in the unirradiated original material, nor in the base material subsequently irradiated. It could not be removed by annealing at 900°C for 3 hours. It appears that the level can only be introduced into irradiated material which had undergone considerable annealing at room temperature, and that this process leads to the formation of extremely stable impurity-defect complexes. Later experiments indicate that creation of the donor levels is possible after irradiation by extended thermal annealing at elevated temperatures (section 1.1.3). The Li contacts on the ten year old Ge(γ) detectors were still stable, indicating the complexing of Li into stable Li-O pairs. The presence of oxygen in these crystals leads to the possibility of the formation of stable oxides producing these donor levels. An attempt to promote vacancy motion (and production) by a short, high temperature anneal (3 hours at 675°C) did not produce either of the donor levels in the

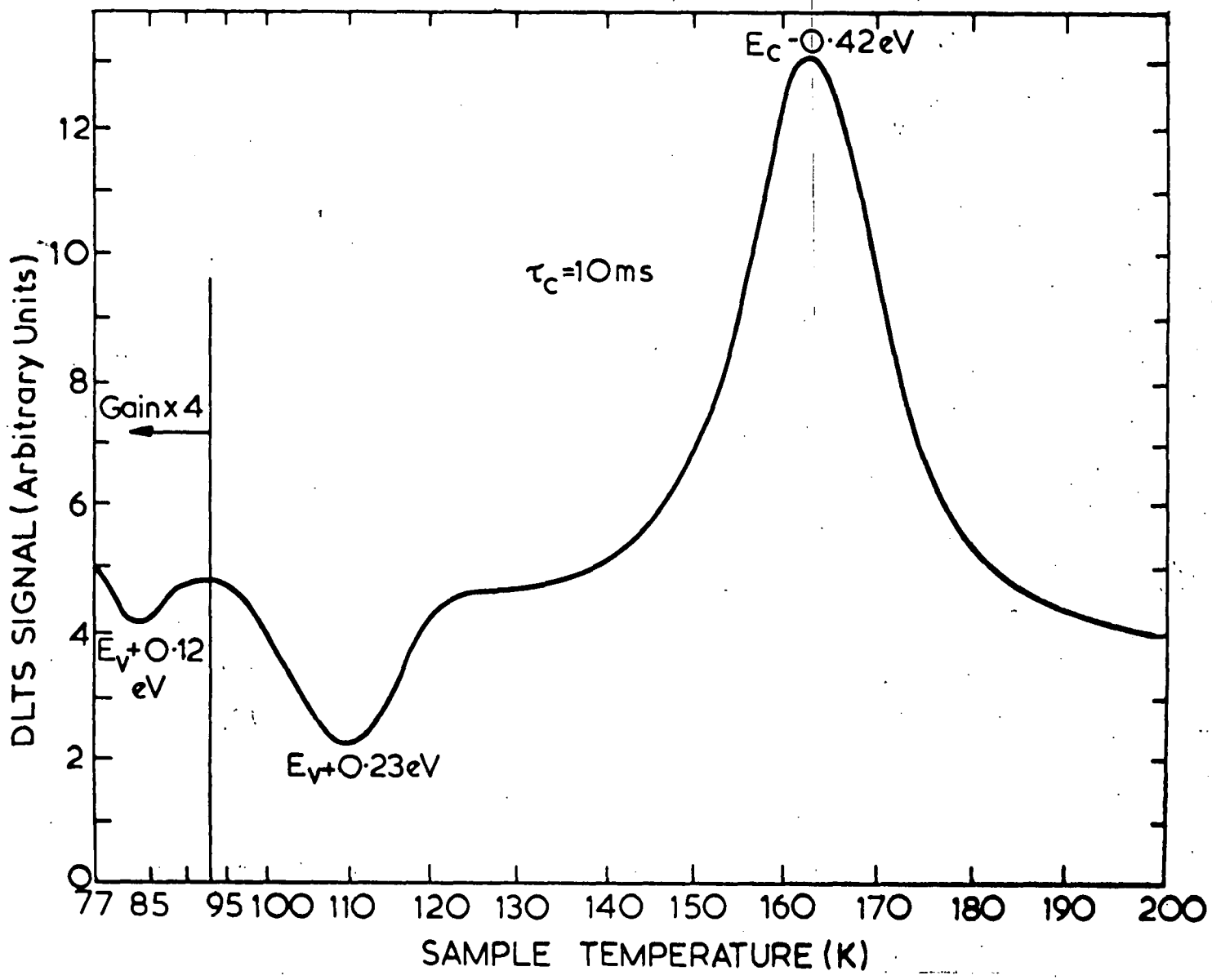

Figure 3 DLTS spectrum of γ-irradiated n-type Ge (growth condition 7b) showing the E_C - 0.42 eV donor level. Correlator time constant 10 ms. V_R = 15V, C = 6.9 pF(77K), 155 pF(165K), A = 0.8 cm^2.

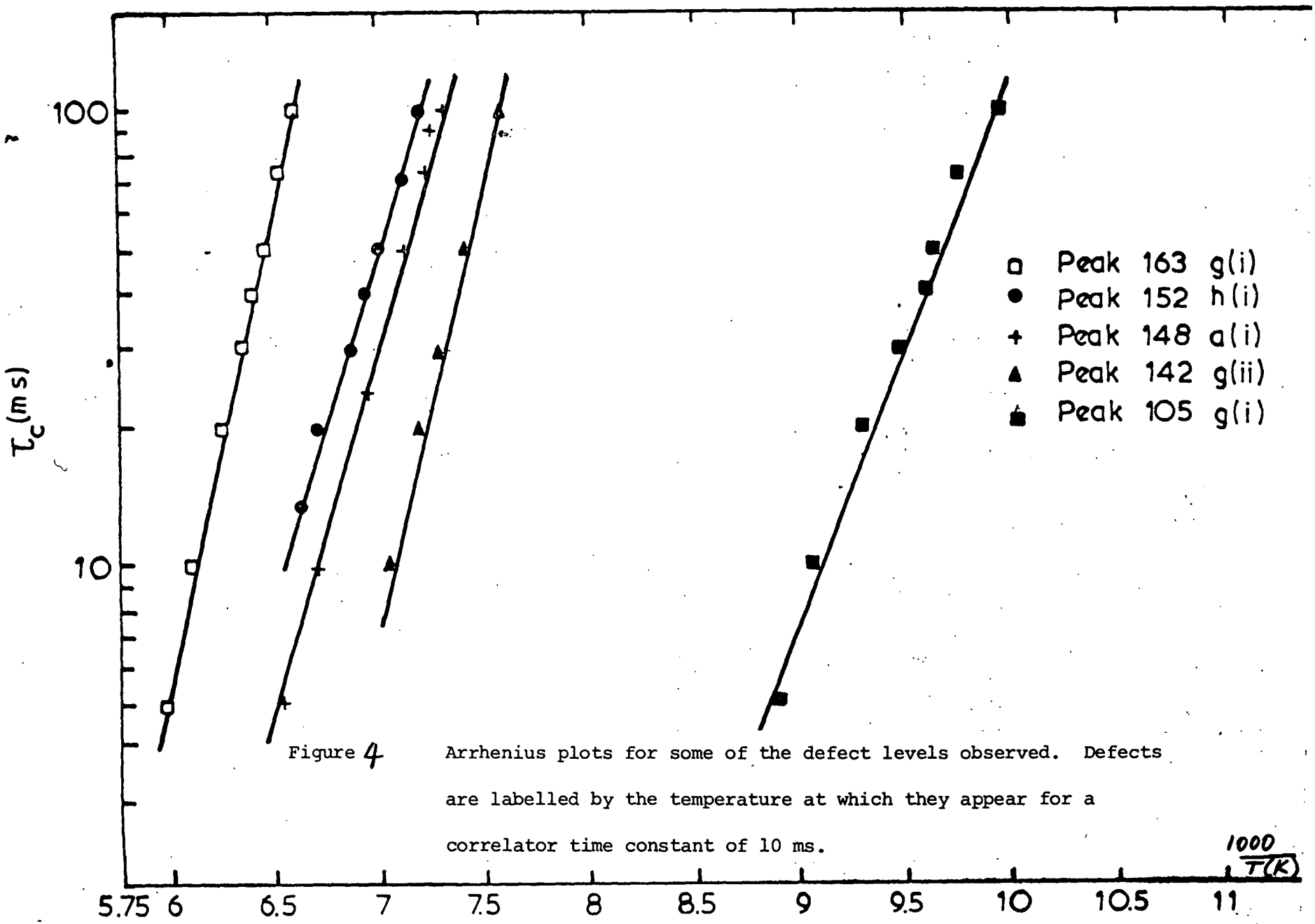

Figure 4 Arrhenius plots for some of the defect levels observed. Defects are labelled by the temperature at which they appear for a correlator time constant of 10 ms.

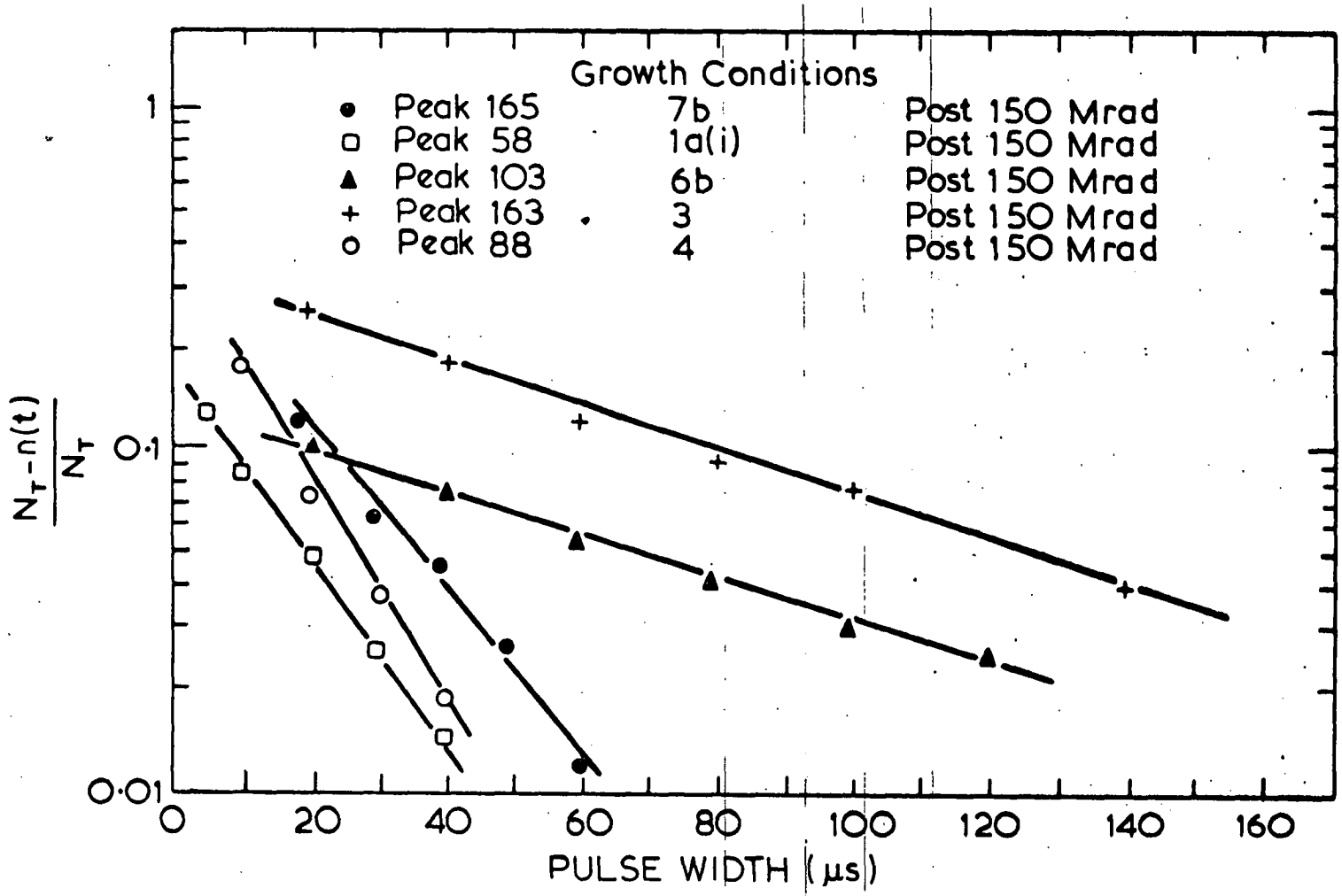

Figure 5. Relative correlator signal output versus pulse width for some of the defect levels observed (growth conditions in Table 1). Bias pulse amplitude equals reverse bias in all cases.

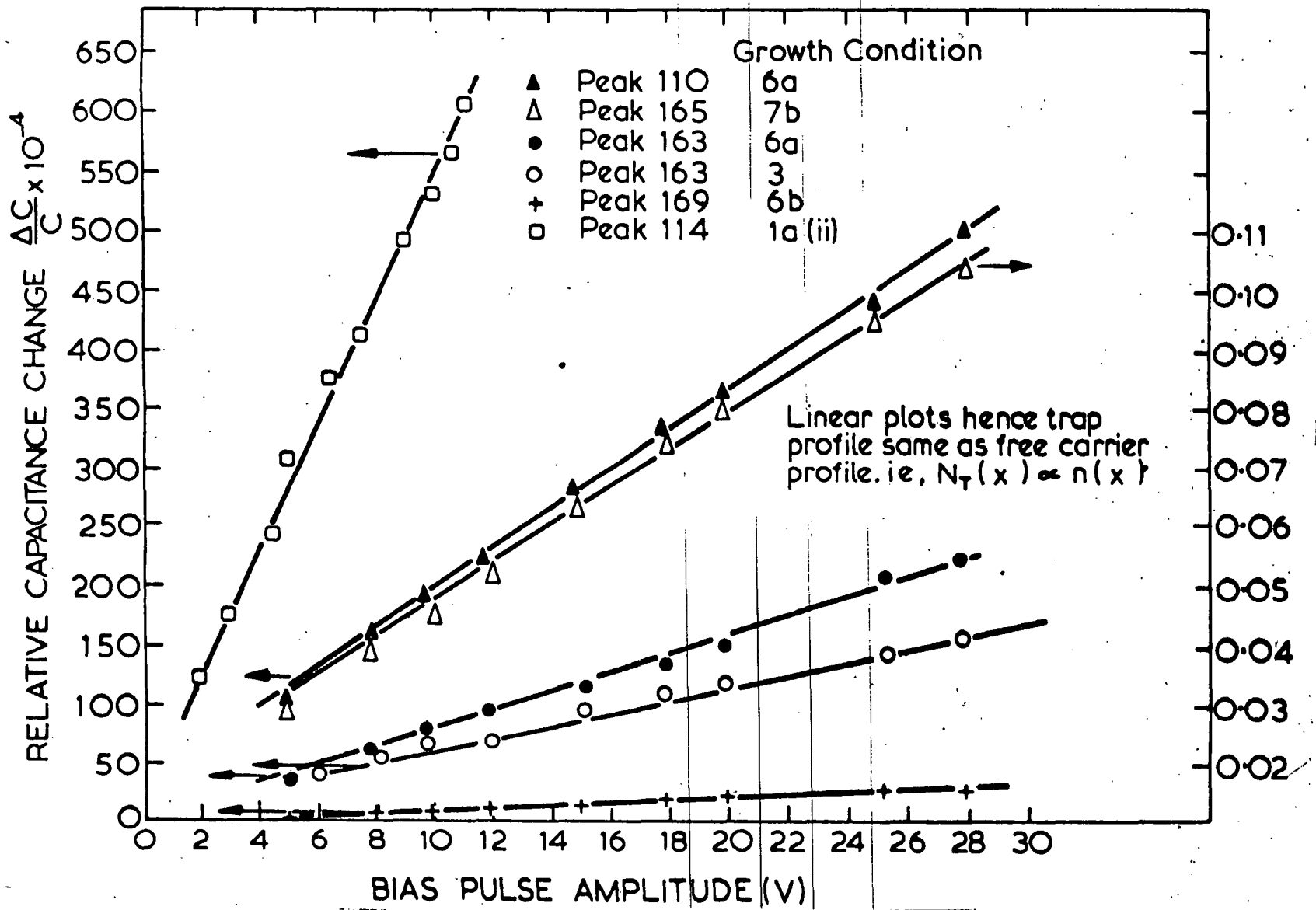

Figure 6 Relative capacitance change versus pulse amplitude for some of the defect levels observed (growth conditions in Table 1).

V_R = 30V for all cases.

newly irradiated material.

2. High-Purity and Doped Material

It is likely that the E_v + 0.38 eV, E_v + 0.23 eV and E_c - 0.42 eV levels are also defect - impurity complexes rather than simple radiation defects. The clearest evidence comes from the high purity crystal in which a junction existed, samples from either side of which were irradiated. No common levels were observed, indicating that segregation of impurities during the crystal growth plays a dominant role in determining the type of complexes formed with radiation defects along the length of a crystal. Overall, the n- or p-type material grown in these laboratories tended to have common defects produced by the irradiation, even though the growth conditions varied, and similarly with the commercially obtained material; however, the two classes of material had few levels in common after irradiation.

3. General

Previous work on γ-irradiation damage in Ge has generally been performed on material with net impurity densities $\gtrsim 10^{13}$ cm^{-3}. It has been commonly accepted that defect impurity interactions play a major role in determining the electrical characteristics of radiation effects and their subsequent annealing behaviour. Clearly this is evident here, even in the more pure material, with a large number of defect levels observed in Ge grown under similar conditions. The effect of O and Si content on the trapping of vacancies produced by the irradiation is likely to be vital and will affect both the formation of the various defect-impurity complexes and their annealing rates.

A comparison of the net free-carrier densities for n-type samples before and after irradiation, taken at 180 K where all defect levels observed were ionized, showed that the formation of electrically inactive donor-acceptor complexes [Mashovets 1977; Emtzev et al. 1972]

was a major component of the compensation process. In most cases, the difference in doping density was approximately an order of magnitude and never less than a factor of two. Crystals intentionally doped with P and As showed no significant differences from nominally undoped crystals.

SUMMARY OF INITIAL EXPERIMENT

New deep donor levels in γ-irradiated n-type Ge and deep acceptors in irradiated p-type Ge, were observed using deep level transient spectroscopy. Room temperature annealing has introduced a donor at E_c - 0.36 eV over the long-term in all 10 year old Ge(γ) detectors and at E_c - 0.20 eV in some samples. These were not observed in recently irradiated material from the same crystals. Annealing at ∿900°C for 3 hours did not remove these levels. Acceptors at E_v + 0.38 eV and E_v + 0.23 eV were introduced in p-type material grown at the AAEC Research Establishment, and a deep donor at E_c - 0.42 eV in n-type material. The acceptors were removed after annealing at 675°C, but the donor remained after this treatment. The levels were observed in both undoped and doped crystals, grown under various conditions. There were total trap densities usually an order of magnitude lower than the original doping density of the n-type material, which supports the hypothesis that compensation is due to electrically inactive vacancy-donor complexing. The deepest levels will not have as large an effect on the energy resolution of a γ-damaged radiation detector as the moderately deep levels, due to their low emission rate at 77 K, the operating temperature of the detector.

REFERENCES

Emtzev, V. V., Mashovets, T. V. and Ryvkin, S. M. [1972] - Radiation Damage and Defects in Semiconductors (Institute of Physics Conf. Series No. 16) p. 17.

Lang, D. V. [1974] J. Appl. Phys. 45:3023.

Lawson, E.M. [1969] - AAEC/TM527.

Lawson, E. M. [1971] - Nucl. Instr. and Meth. 95:131.

Mashovets, T. V. [1977] - Radiation Effects in Semiconductors (Institute of Physics Conf. Series No. 31) p. 30.

Miller, G. L., Lang, D. V. and Kimerling, L. C. [1977] - Ann. Rev. Mater. Sci. pp 377-448.

Miller, G. L., Ramirez, J. V. and Robinson, D. A. H. [1975] - J. Appl. Phys. 46:2638.

Ryvkin, S. M., Matveev, O. A., Stokan, N. B. and Khusainov, A. Kh. [1965] - Z. Tech. Fitz. 34(8) 1535. Trans. Sov. Phys-Tech. Phys. 9(8) 1190 [1965].

1.1.2 ELECTRICAL PROPERTIES OF γ-IRRADIATED POLYCRYSTALLINE Ge

It is also of interest to examine the electrical properties of γ-irradiated polycrystalline Ge to see, for example, whether vacancy complexes produced by the irradiation associate with grain boundaries to produce energy states in the forbidden band gap. The starting material was characterised by I-V, C-V, TSCAP and DLTS measurements prior to irradiation, and is described fully in Chapter 6. The material was HP p-type Ge taken from bars zone refined in silica boats under an H_2 atmosphere. Contacts were formed in the usual fashion by Li diffusion and evaporation of Pd. The samples were irradiated in a 1.8 Mrad h^{-1} ^{60}Co γ-irradiation facility to a dose of 150 Mrad.

RESULTS AND DISCUSSION

Figure 1 shows a typical electrically active defect spectrum from a γ-irradiated polycrystalline p-Ge diode accompanied by the TSCAP spectrum. The two acceptor states E_v + 0.23 eV and E_v + 0.38 eV are seen in single crystal AAEC-grown p-type Ge and are unidentified impurity-defect complexes. Eight polycrystalline diodes were investigated, with all displaying these levels. In several (Figure 2), the E_v + 0.23 eV level signal was inverted (and occasionally the E_v + 0.38 eV level signal also) due either to the extra junction explanation (proposed and discussed in sections 6.3 and 2.2) and occasionally to a signal from the heavily doped side of the junction (Li contact side); the C-V characteristic of Figure 3 shows the diodes to be linearly graded rather than abrupt junctions. The more graded the junction, the worse the leakage current of the diode; a typical 'poor' diode I-V characteristic is shown in Figure 4.

The E_v + 0.23 eV and E_v + 0.38 eV acceptor states induced by γ-radiation in Ge are clearly important to an understanding of defect mechanisms in Ge. They are present in all p-type material grown in our laboratories after irradiation.

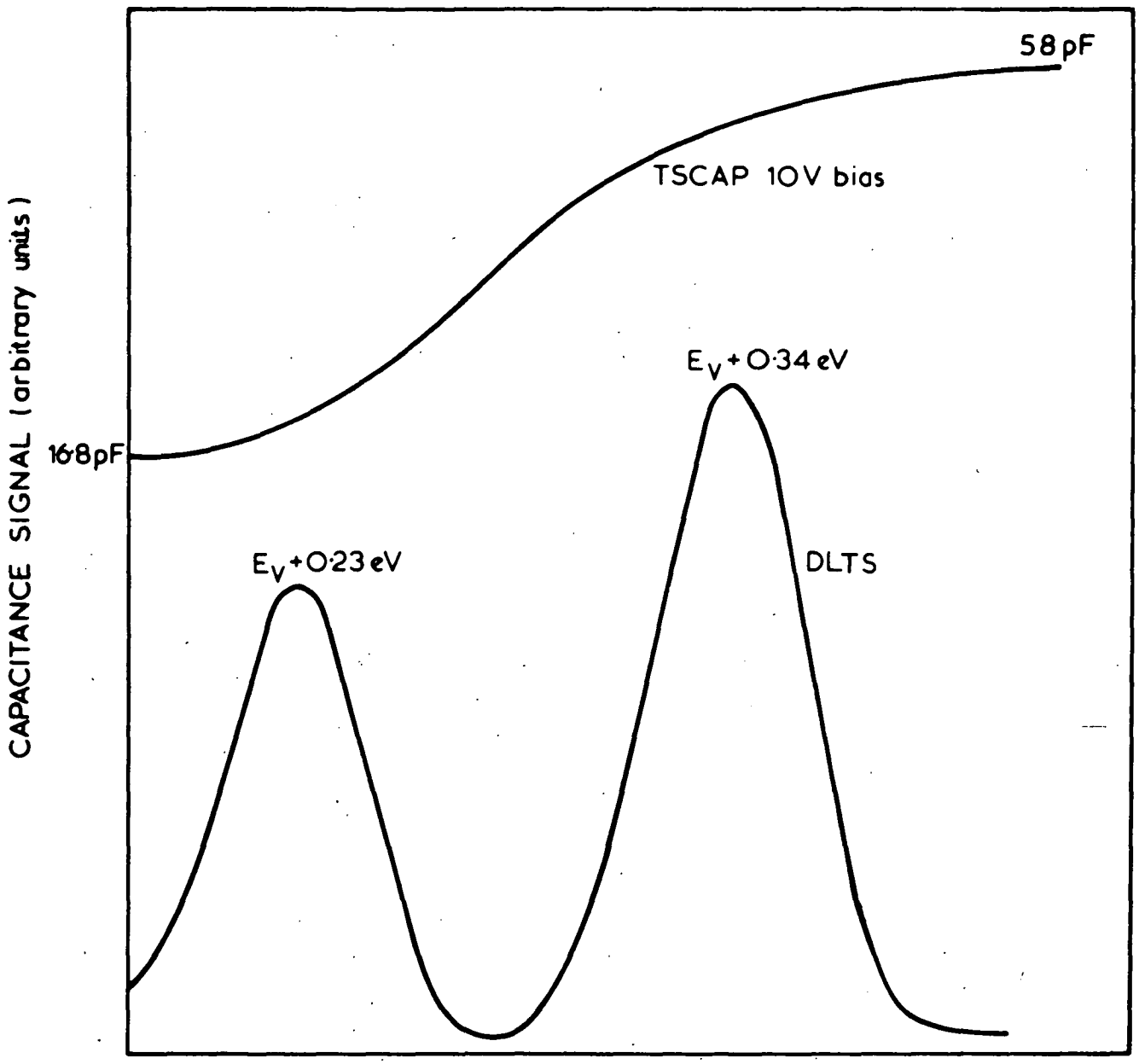

Figure 1. POLYCRYSTALLINE γ-IRRADIATED HIGH PURITY p-TYPE Ge

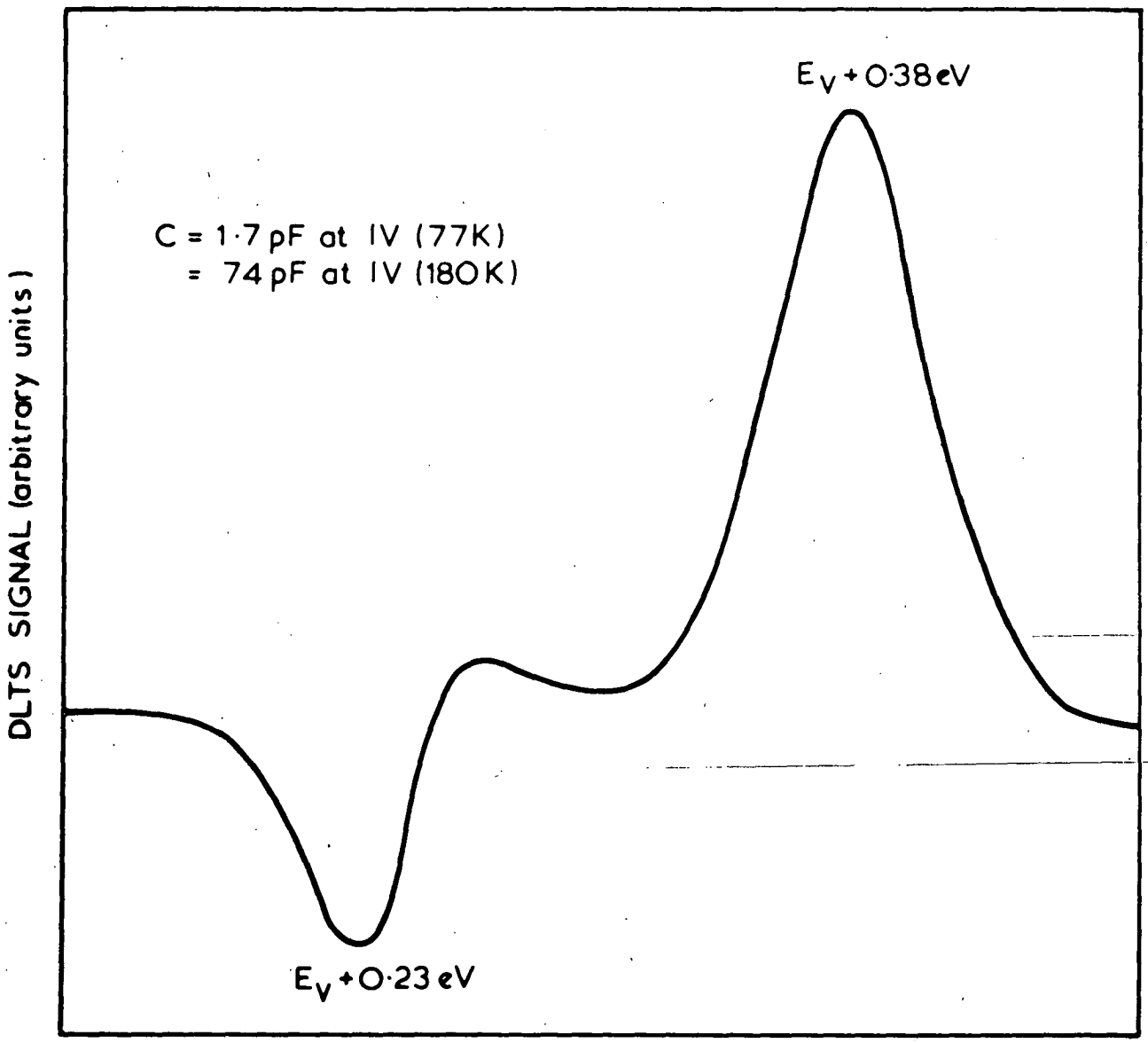

Figure 2. γ-IRRADIATED HIGH PURITY POLYCRYSTALLINE p-TYPE Ge

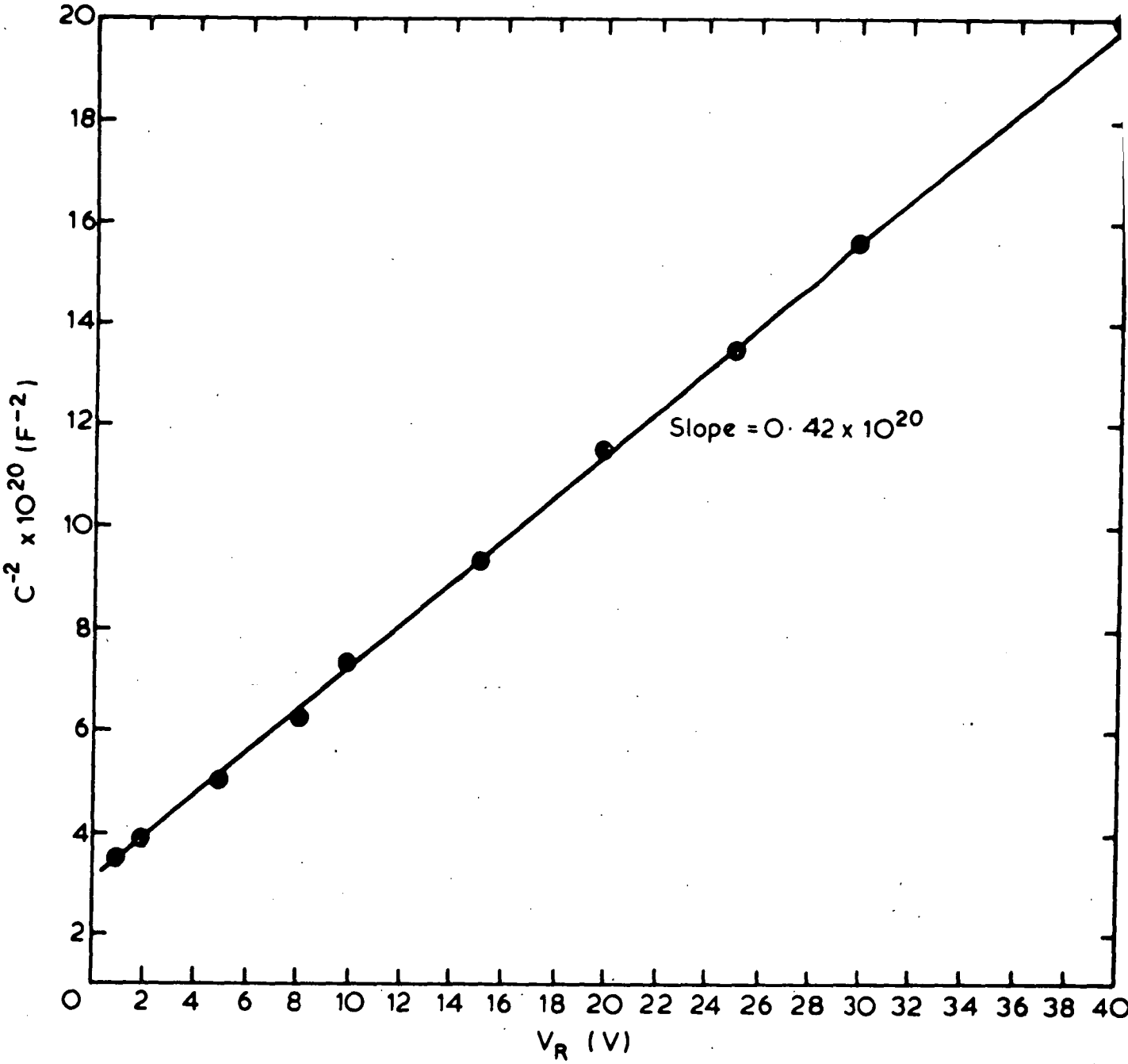

Figure 3. γ-IRRADIATED HIGH-PURITY POLYCRYSTALLINE p-TYPE Ge

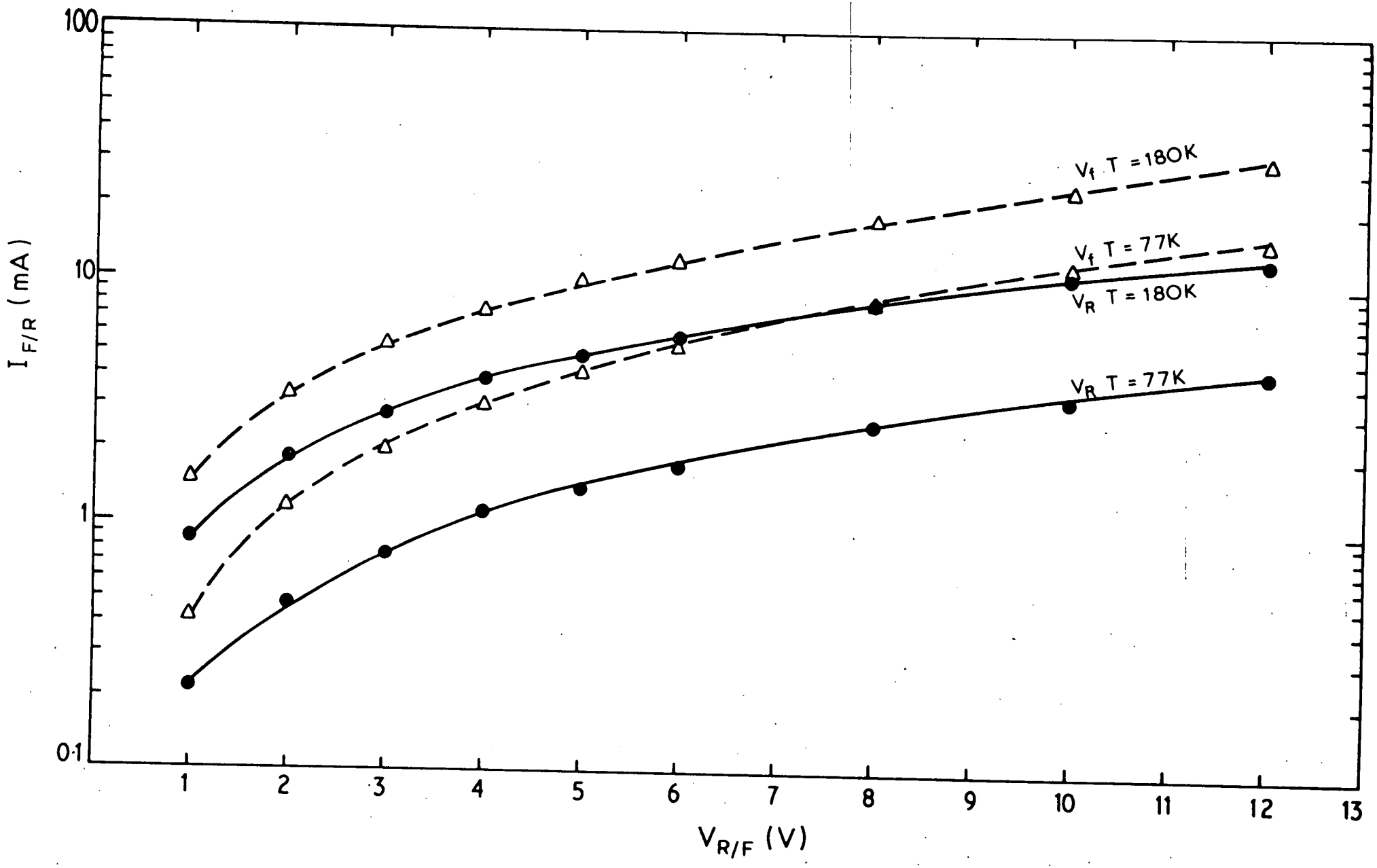

Figure 4. POLYCRYSTALLINE Ge-γ IRRADIATED

1.1.3 THERMAL AND ELECTRICAL STABILITY OF γ-INDUCED CENTRES

INTRODUCTION

Section 1.1.1 investigated the type and density of deep levels produced in ^{60}Co γ-irradiated Ge grown under varying conditions (dopant, gas atmosphere, crucible material). To summarise these earlier results, deep acceptor levels at E_v + 0.23 eV and E_v + 0.38 eV, present in similar concentrations, were observed in all p-type material ($p = 4 \times 10^{10}$ to 4×10^{13} cm^{-3}) grown in the AAEC laboratory, regardless of the crystal growth conditions. In all but the highest purity n-type Ge ($n < 10^{11}$ cm^{-3}) a donor at E_c - 0.42 eV was measured, which proved stable against annealing for 3 hours at 650°C. In commercially obtained n-type material, which had been fabricated into γ-compensated radiation detectors ten years previously, deep donor levels were observed which were stable against annealing for 3 hours at ∿900°C. These centres (E_c - 0.36 eV, E_c - 0.20 eV) were not seen in samples of the same material which were irradiated just prior to measurement. The main conclusion of the earlier work was that even in the highest purity Ge, the γ-ray induced centres were due to γ-defect-impurity complexes. In the present work, we have made further measurements along these lines, observing the stability of ^{60}Co γ-ray induced defects to thermal annealing, electric and magnetic fields and stress effects, as well as monitoring differences in defect centre behaviour in different types of material. The main measuring technique used has again been DLTS [Lang 1974].

RESULTS

(a) Long-Term Room Temperature Annealing

(i) AAEC material

The E_v + 0.23 eV and E_v + 0.38 eV levels appeared in all p-type crystals grown from silica crucibles under H_2 atmospheres, including

material from the AAEC, General Electric (USA) and Lawrence Berkeley Laboratory (USA). The long-term stability of the E_v + 0.23 eV and E_v + 0.38 eV centres in various types of p-Ge may provide some clues to their identity. Figure 1(a) shows the DLTS spectra over 15 months for a γ-irradiated p-type sample grown in an H_2 atmosphere from a graphite crucible. The concentrations of the two levels showed a steady decline over the long term at room temperature and were essentially below the sensitivity of the DLTS technique after about 14 months. The DLTS spectra over 15 months of a p-type sample grown under similar conditions, but in a silica crucible, are shown in Figure 1(b). The stability of these centres in this class of material is greater than that in the graphite grown material. The major difference between the two samples is in the higher oxygen content of the silica grown material. Cleland [1972] has also observed stabilising of γ-induced defects in material of high O content.

It should be noted that a sample from the graphite grown material was post-growth annealed for 75 hours at 675°C under an N_2 atmosphere before irradiation to reduce its H_2 content; it showed similar stability of the acceptor levels at room temperature to its unannealed companion. Thus H_2 content appears to have no significant effect on the defect stability at room temperature. One other difference between the samples in Figures 1(a) and 1(b) of course is the higher carbon content of the graphite grown material.

Other experiments have provided considerable evidence that silicon content has no effect on the introduction of the E_v + 0.23 eV and E_v + 0.38 eV acceptor levels, but that oxygen itself is almost certainly a component of these centres. Also, it has been found that annealing the material prior to irradiation has considerable influence on the concentrations of the two acceptors produced by the γ-rays (sections 1.4 and 1.5).

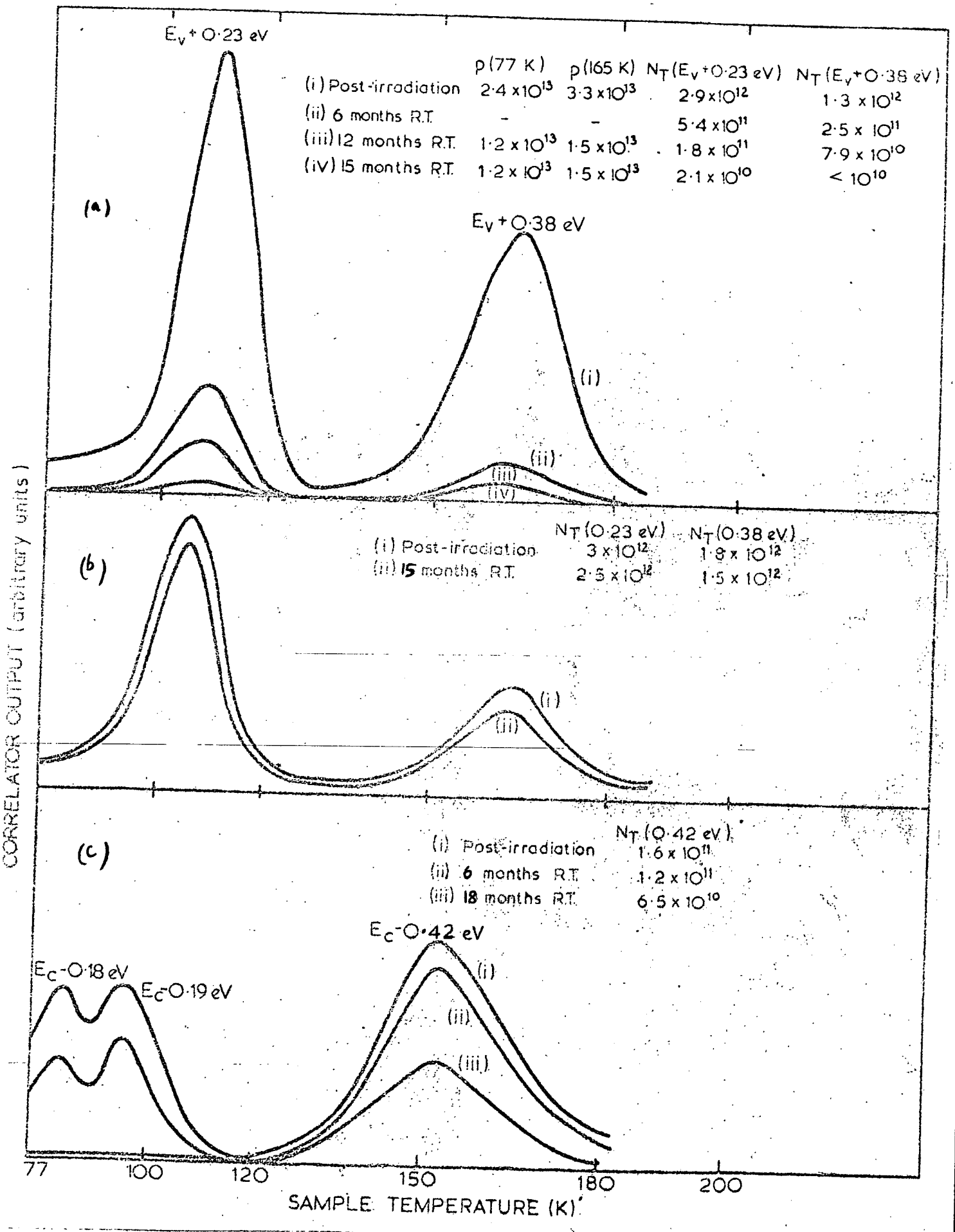
(a)
$E_V + 0{\cdot}23$ eV
$E_V + 0{\cdot}38$ eV
(i) Post-irradiation
(ii) 6 months R.T.
(iii) 12 months R.T.
(iv) 15 months R.T.
p(77 K)
p(165 K)
$N_T(E_V + 0{\cdot}23$ eV)
$N_T(E_V + 0{\cdot}38$ eV)
$2{\cdot}4 \times 10^{13}$
$3{\cdot}3 \times 10^{13}$
$2{\cdot}9 \times 10^{12}$
$1{\cdot}3 \times 10^{12}$
$5{\cdot}4 \times 10^{11}$
$2{\cdot}5 \times 10^{11}$
$1{\cdot}2 \times 10^{13}$
$1{\cdot}5 \times 10^{13}$
$1{\cdot}8 \times 10^{11}$
$7{\cdot}9 \times 10^{10}$
$1{\cdot}2 \times 10^{13}$
$1{\cdot}5 \times 10^{13}$
$2{\cdot}1 \times 10^{10}$
$< 10^{10}$
(b)
(i) Post-irradiation
(ii) 15 months R.T.
$N_T(0{\cdot}23$ eV)
$N_T(0{\cdot}38$ eV)
3×10^{12}
$1{\cdot}8 \times 10^{12}$
$2{\cdot}5 \times 10^{12}$
$1{\cdot}5 \times 10^{12}$
(c)
(i) Post-irradiation
(ii) 6 months R.T.
(iii) 18 months R.T.
$N_T(0{\cdot}42$ eV)
$1{\cdot}6 \times 10^{11}$
$1{\cdot}2 \times 10^{11}$
$6{\cdot}5 \times 10^{10}$
$E_C - 0{\cdot}42$ eV
$E_C - 0{\cdot}18$ eV
$E_C - 0{\cdot}19$ eV
77
100
120
150
180
200
SAMPLE TEMPERATURE (K)
CORRELATOR OUTPUT (arbitrary units)

FIGURE 1

The deep donor (E_c - 0.42 eV) observed in most n-type material also anneals over the long-term at room temperature. Figure 1(c) shows the DLTS spectra recorded over an 18 month period after irradiation for an As-doped (N_d-N_a = 2 x 10^{14} cm^{-3}) sample. This diode has been taken from a crystal grown in a silica crucible under an H_2 atmosphere.

(ii) Hoboken (Belgium) material

The hypothesis from the earlier work was that extremely stable deep donor levels formed over a considerable time in this Sb-doped n-type Ge (n = 5 x 10^{13} cm^{-3}) sample after irradiation. Figure 2 shows the DLTS spectra recorded over a one year period for an irradiated sample. The acceptor levels present immediately after the irradiation gradually anneal, coinciding with the growth of the stable donor level at E_c - 0.36 eV. There is considerable variance in the time required for the donor to appear. In the zone levelled sample of Figure 2, the donor was evident after six months at room temperature. In Czochralski grown samples of the same class of material, the acceptors were still annealing 18 months after irradiation and no donor was then evident. One can speculate again that the oxygen content of the material plays a major role in the room temperature stability of γ-ray induced defects.

(b) Thermal Annealing

(i) AAEC material

The two dominant acceptor levels in p-type material require $\sim$3 hours at 200°C for 50% removal and $\sim$5 hours at 200°C for complete removal. These results were obtained in a variety of material (N_a-N_d = 4 x 10^{10} to 3 x 10^{13} cm^{-3}), the growth conditions (crucible material, gas atmosphere) appearing to make no significant difference. The E_c - 0.42 eV level in n-type material is stable against annealing

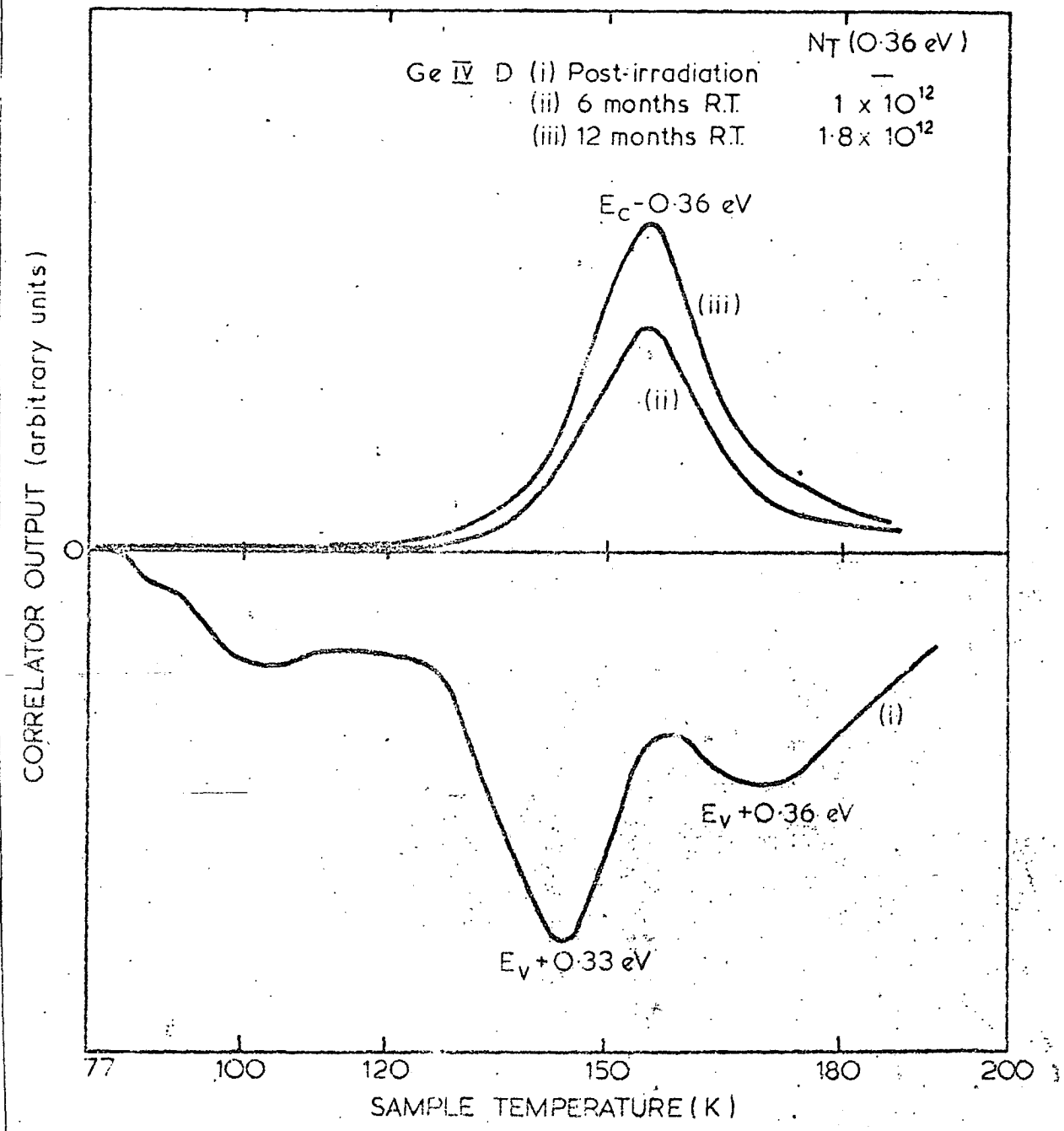
Ge IV D (i) Post-irradiation
(ii) 6 months R.T.
(iii) 12 months R.T.
N_T (0·36 eV)
—
1 x 10^12
1·8 x 10^12
E_c - 0·36 eV
(iii)
(ii)
O
(i)
E_v + 0·36 eV
E_v + 0·33 eV
CORRELATOR OUTPUT (arbitrary units)
77
100
120
150
180
200
SAMPLE TEMPERATURE (K)

FIGURE 2.

for 3 hours at 650°C, 8 hours at 650°C reduces its concentration by ∿60% and 8 hours at 750°C by 95%. The latter data was obtained from P- and As-doped samples ($n = 5 \times 10^{12}$ to 5×10^{14} cm^{-3}) grown from silica crucibles

(ii) Hoboken (Belgium) material

Once formed, the deep donors in this class of material were stable against annealing for 3 hours at 900°C (melting point Ge 936°C). After irradiation, the formation of the centres can be accelerated by extended thermal annealing at elevated temperatures. The donors were produced after irradiation by heating samples to 675°C for periods ranging from 100 to 500 hours; the sample which did not show the donors after 18 months at room temperature required 150 hours at 675°C for their appearance.

(c) Electric and Magnetic Fields and Stress Effects

No electric field dependence of energy level or capture cross section of the γ-induced centres was evident to average fields of 5.2×10^3 V/cm. Similarly, no effect on these parameters was observed with axial magnetic fields up to 2 kG. Representative samples were installed in an apparatus to produce stress within the diodes; no effects were discerned for applied pressures of 8.8×10^6 Pa.

Baruch [1961] was the first to observe the motion of radiation-induced defects in Ge under the influence of the electric field of a reverse-biased p-n junction, using C-V measurements. We have observed the stability of γ-induced defects in electric fields, using both DLTS and C-V measurements.

Samples of the Hoboken material were irradiated with ^{60}Co γ-rays (dose - 150 Mrad) and then annealed for 500 hours at 657°C to produce significant concentrations of the stable deep donors, E_c - 0.20 eV and E_c - 0.36 eV. The material had net doping densities in the range

$n = 4 \times 10^{12}$ to 4×10^{13} cm^{-3} at 77 K and samples were in the form of Schottky diodes (Pd evaporated front contact, Li diffused ohmic back contact). The junctions were reverse-biased to 170 V at 25°C producing average electric fields in the depletion region of $\sim 6 \times 10^3$ V/cm and were regularly checked with the DLTS apparatus during the bias application.

Defect centres were removed during the bias application, as is evident from the data of Figure 3, which shows the variation of device capacitance with junction bias, for several stages during the bias application. However, during the defect removal, the concentration profile of the two donor levels was constant across the depletion region. This cannot be explained by a drift of the defects out of the depletion region under the action of an electric field or local loss of the defect centres by motion to sinking sites. In both cases, one would expect a monotonic variation in the defect concentration across the depletion region, because of the shape of the electric field profile. One possible explanation is that a gradual change of charge state occurs during the electric field application, as the defect centres are isolated in the depletion region. Charge-dependent annealing might then take place, as seen in the P-V centre in Si [Kimerling 1976]. Indeed, this behaviour may be quite common in radiation damage centres and may have application in identifying (and removing) certain damage sites. Field strengths of 3.5×10^3 V/cm (T = 25°C) also caused some removal of the E_c - 0.42 eV donor level in As-doped AAEC material, though at a rate approximately five times less than the rate observed in the Hoboken material.

The motion of the E_v + 0.23 eV and E_v + 0.38 eV defect centres in electric fields could not be determined as these samples were in the form of n^+p junctions, the n^+ contact being Li diffused; the Li

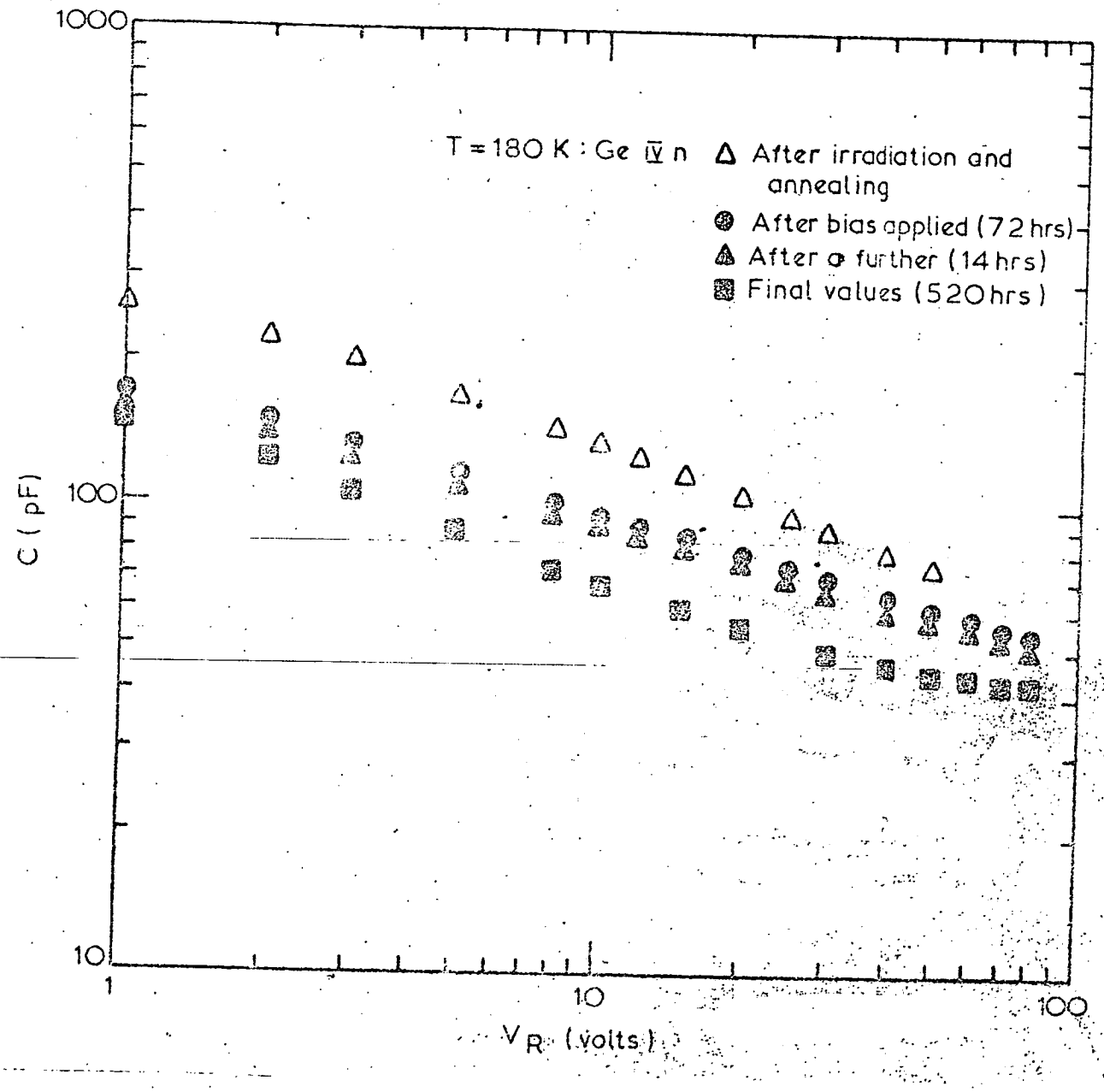
1000
100
10
1
10
100
C (pF)
V_R (volts)
T = 180 K : Ge IV n
After irradiation and annealing
After bias applied (72 hrs)
After a further (14 hrs)
Final values (520 hrs)

FIGURE 3.

ions themselves are highly mobile in electric fields [Pell 1960].

(d) Carrier Capture Models

There are several available mechanisms for free carrier capture by impurity centres, as discussed by Grimmeiss et al. [1980]. By plotting the logarithm of the capture cross section assuming various temperature dependences, one may test the likelihood of the various models. Figure 4 shows the temperature dependence of the electron capture cross section of the E_c - 0.36 eV donor level in Hoboken material. Our data, albeit over a limited temperature range, lie on a straight line of slope -2.6, close to the value of -3.0 used in the cascade model of Abakumov et al. [1978]. This model is based on a cascade capture process involving a series of closely spaced excited states near the conduction band.

If the data is plotted as log (σT^2) vs $\frac{1}{T}$ (Figure 5), an activation energy of 7±3 meV is obtained. This is interpreted in the two-stage capture model of Gibb et al. [1977] to be the energy separation between the lowest excited state of the cascade process and the conduction band. However, as the chemical nature of the defect is unknown, one cannot compare this value with theory. Furthermore, in the two-stage cascade capture model a plot of the logarithm of emission rate or inverse detrapping time constant of a particular trap versus inverse temperature gives an activation energy which corresponds to the energy between the lowest excited state and the ground state, provided this latter transition is not thermally activated. From the data of Figure 6 we obtain a value of E_c - 357±25 meV. Adding 7 meV to this gives 364 meV, in good agreement with the result obtained by taking into account the temperature dependence of the electron capture cross section, i.e. from a plot of $\tau T^{-0.6}$ vs $\frac{1}{T}$, enthalpy ΔH = 365±27 meV (Figure 7). Thus the results support both capture models, as found by

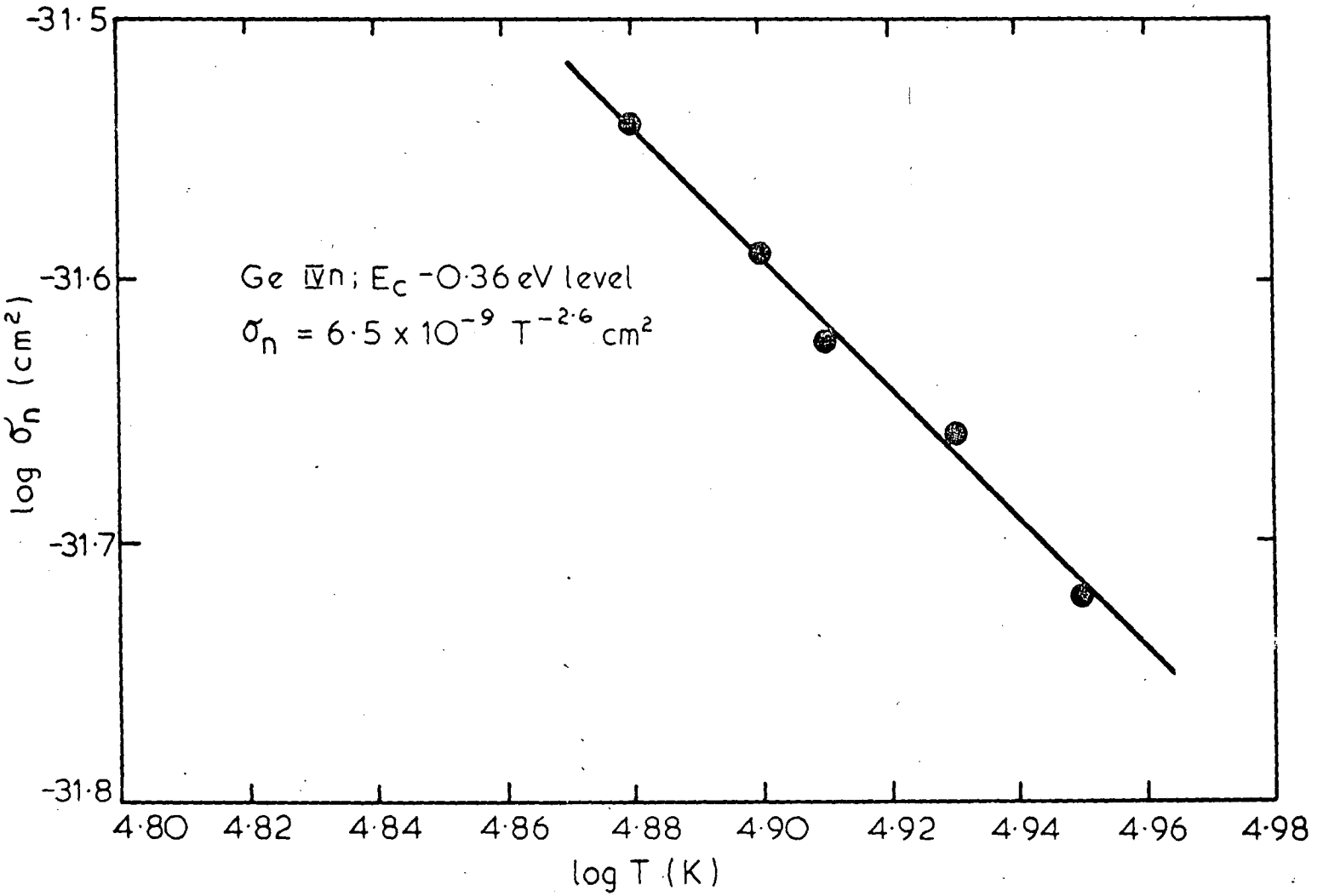

FIGURE 4

Temperature dependence of the electron capture cross-section of the E_c-0.36 eV donor level in γ-irradiated n-type Ge sample, assuming a cascade capture process.

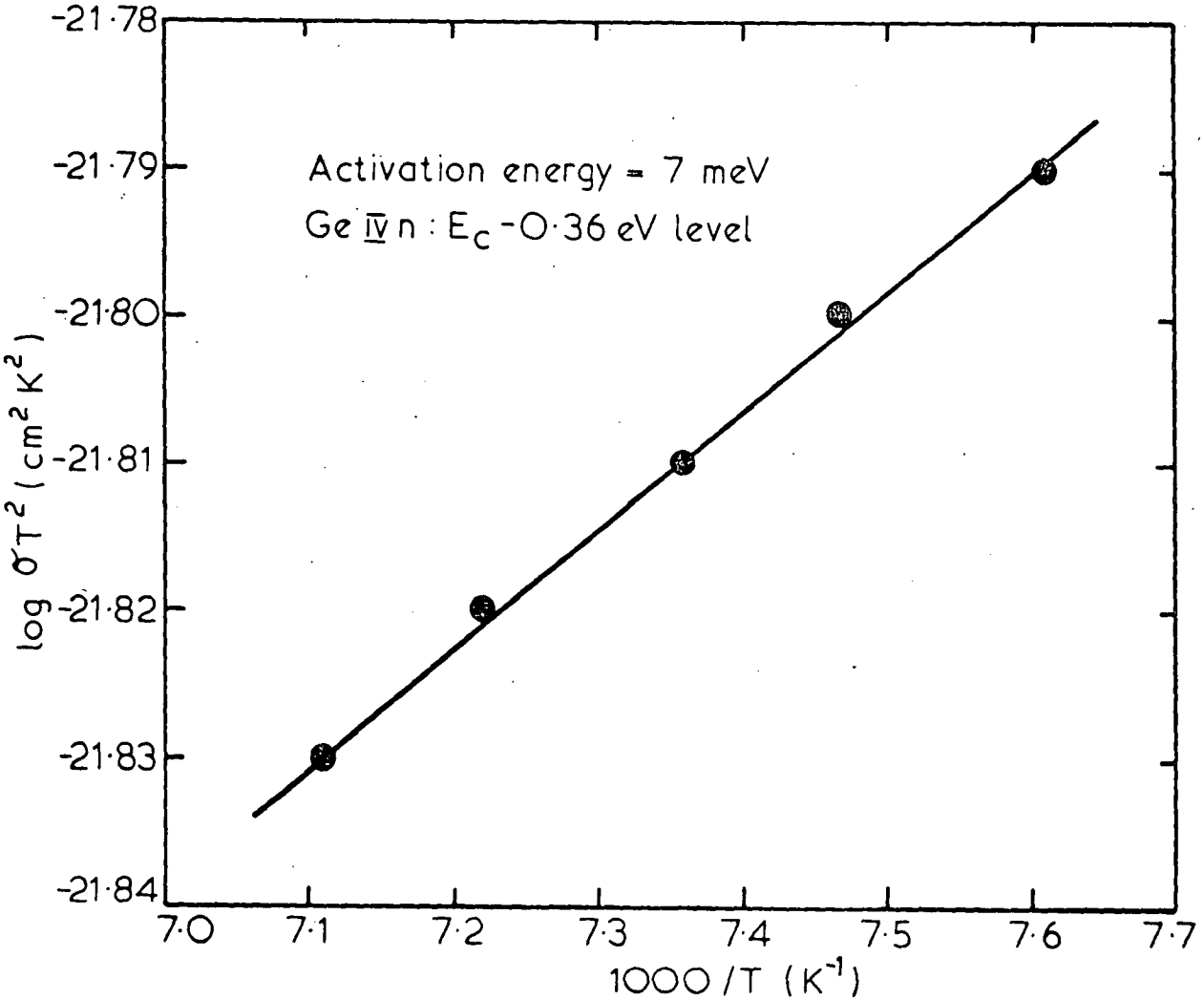

FIGURE 5

Temperature dependence of the electron capture cross-section of the E_c - 0.36 eV donor level assuming a two stage capture model.

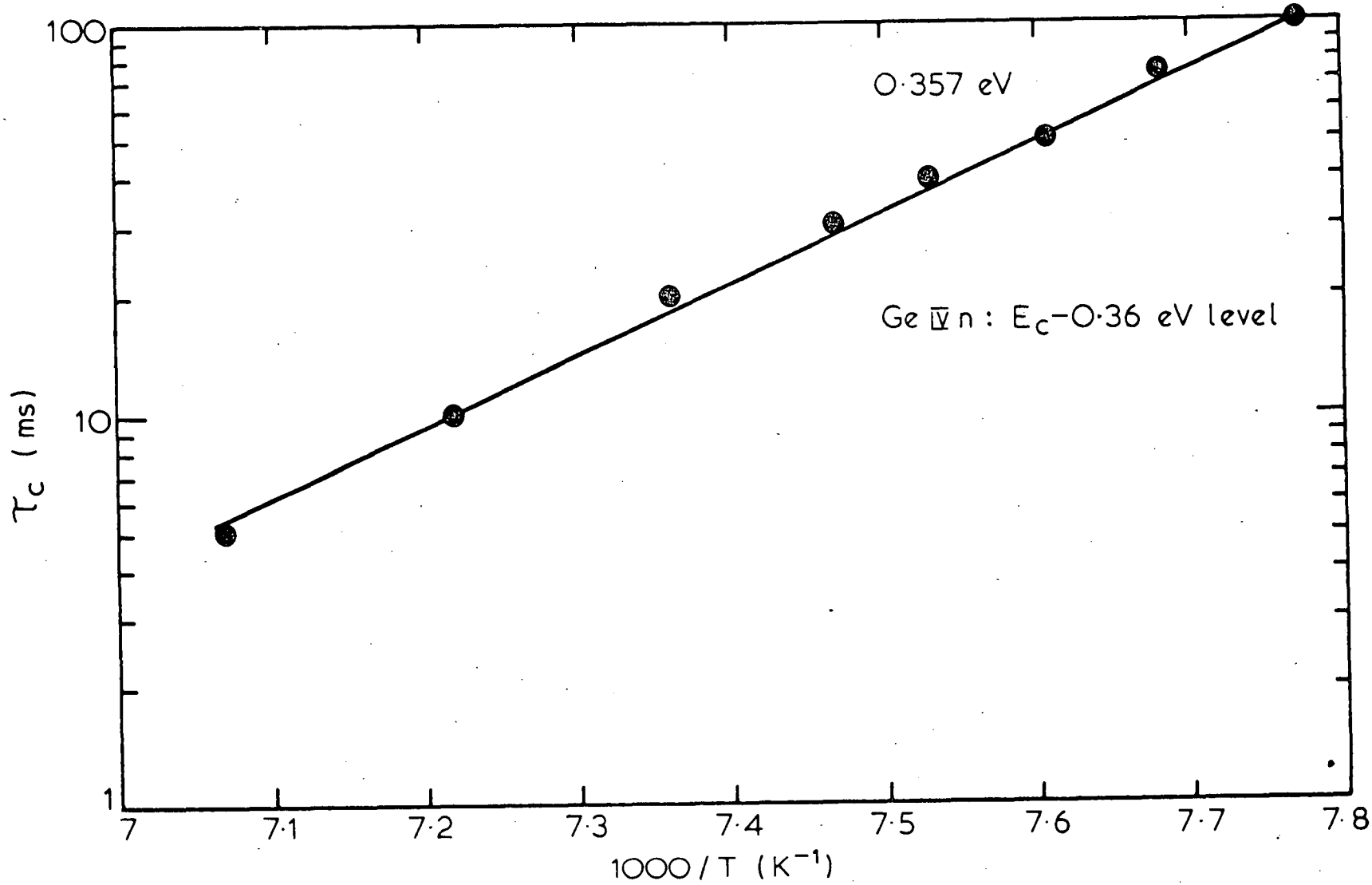

FIGURE 6

Electron detrapping time constant vs inverse temperature at the E_c - 0.36 eV donor level.

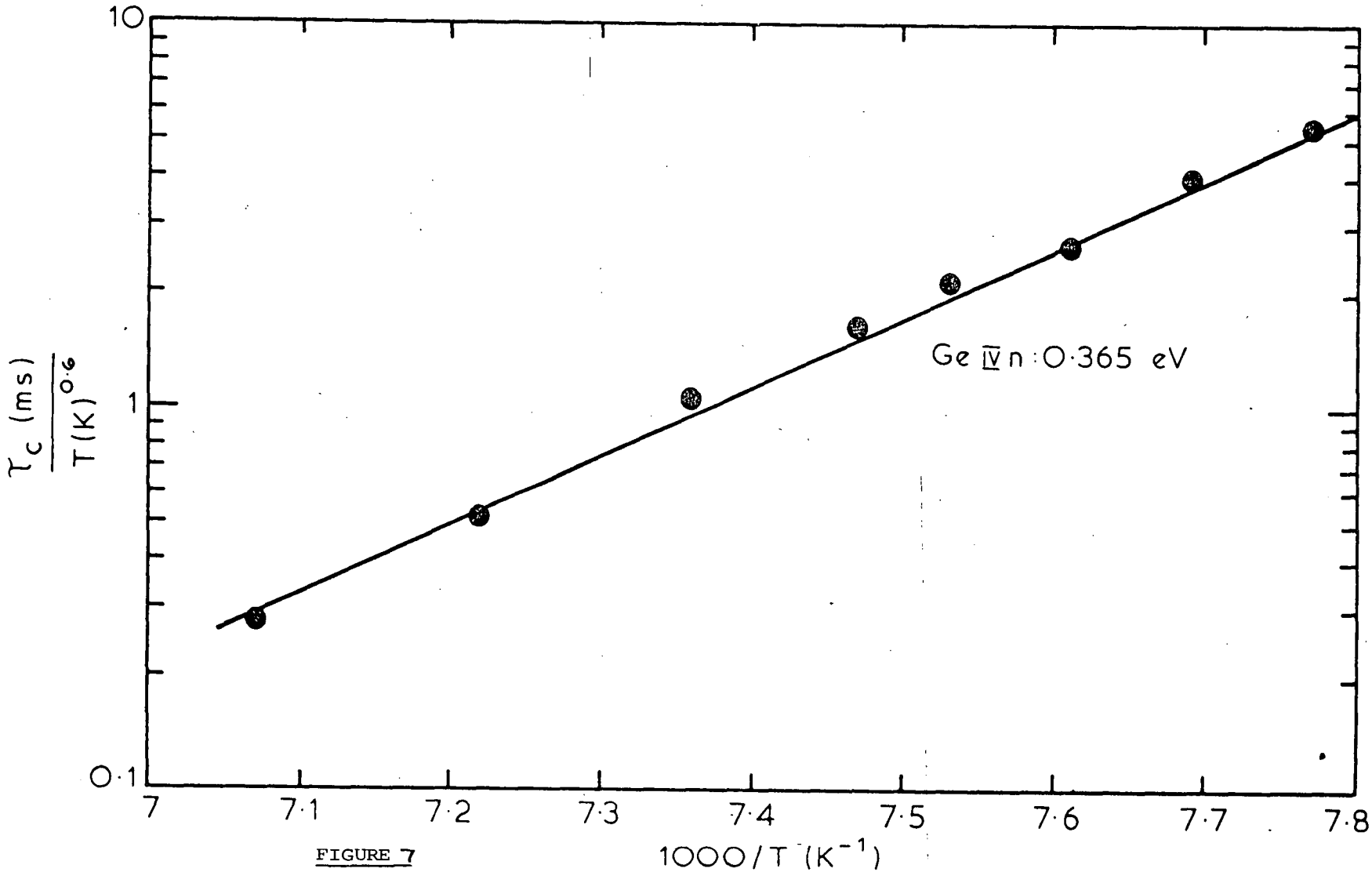

FIGURE 7

Electron detrapping time constant vs inverse temperature at the E_c - 0.36 eV donor level taking into account the temperature dependence of the capture cross section. The slope of the plot gives the enthalpy of the centre.

Grimmeiss et al. [1980]. It may be that the two models are essentially equivalent in measurements such as reported here. The series of closely spaced levels near the conduction band may effectively be the same as one level near the conduction band.

A similar analysis for the two deep acceptors found in irradiated AAEC, silica grown p-type material and the deep (E_c - 0.42 eV) donor in n-type material gives the following temperature dependence:

$$E_v + 0.23 \text{ eV}: \quad \sigma = 5.9 \times 10^{-8} \quad T^{-3.4} \text{ cm}^2$$

$$E_v + 0.38 \text{ eV}: \quad \sigma = 2.4 \times 10^{-8} \quad T^{-2.9} \text{ cm}^2$$

$$E_c - 0.42 \text{ eV}: \quad \sigma = 6 \times 10^{-11} \quad T^{-1.5} \text{ cm}^2$$

Following the same analysis as that used for the E_c - 0.36 level gives a similar good agreement with the cascade capture models for the two acceptor levels, but poor agreement for the deep E_c - 0.42 eV centre.

From these results it is possible to say that the cascade capture process is a likely mechanism for carrier capture by the two acceptors, but not for the deep donor level.

DISCUSSION

The results discussed in this paper have relevance to radiation-damaged Ge devices, as the material investigated was typical of that used for high-purity nuclear radiation detectors (AAEC, General Electric, Lawrence Berkeley crystals) or grown for transistor manufacture (Hoboken crystals used here). While γ- (and electron) radiation damage is seldom as important to device operation as fast neutron or charged particle damage, it enables observation of damaged induced point defects, whose role in device degradation is still not clear [Darken et al. 1980].

The density of background impurities and the thermal history of the crystal have been shown to have considerable effect on its sensitivity to radiation damage. The role of Si and O content of

γ-irradiated crystals is likely to have considerable influence on the resulting defect complexes due to vacancy trapping at the oxygen centres and the interaction of Si and O themselves. The observed stabilising of defects in irradiated material of higher O content, the suspected formation of highly stable oxides as the cause of donor levels in the long-term annealed n-type Hoboken material and the almost certain presence of oxygen in the E_v + 0.23 eV and E_v + 0.38 eV centres in irradiated p-type, silica grown Ge, are examples of this.

SUMMARY

Data is presented on the stability of the most common γ-induced defects in n- and p-type Ge on long-term annealing and in electric and magnetic fields. Evidence from carrier capture data for the possible presence of excited states for both donor and acceptor centres is discussed. The observed response of some γ-induced centres to electronic stimulation such as electric fields, may lead to novel methods of removing radiation damage in Ge devices and, indeed, of identifying their chemical nature.

REFERENCES

Abakumov, V.N., Perel, V.I. and Vasrevich, I.N. [1978] - Sov. Phys. Semicond. 12.

Baruch, P. [1961] - J. Appl. Phys. 32(4)653.

Cleland, J.W. [1972] - IEEE Trans. Nucl. Sci. 19(6)224.

Darken, L.S., Trammell, R.C., Raudorf, T.W., Pehl, R.H. and Elliott, J.H. [1980] - Nucl. Instr. and Meth. 171:49.

Gibb, R.M., Rees, G.J., Thomas, B.W., Wilson, B.L., Hamilton, B., Weight, D.R. and Mott, N.F. [1977] - Philos. Mag. 36:1021.

Grimmeiss, H.G., Janzen, E. and Skarstam, B. [1980] - J. Appl. Phys. 51(7)3740.

Kimerling, L.C. [1976] - IEEE Trans. Nucl. Sci. 23(6)1497.

Lang, D.V. [1974] - J. Appl. Phys.. 45:3023.

Pell, E.M. [1960] - J. Appl. Phys. 31:291.

1.1.4 THE NATURE OF THE E_v + 0.23 eV AND E_v + 0.38 eV CENTRES

INTRODUCTION

During the course of the work on the radiation damage centres in Ge, we have observed that two deep acceptor levels in γ-irradiated p-type Ge are predominant. Using deep level transient spectroscopy, the energy levels are measured as E_v + 0.23 eV and E_v + 0.38 eV. They occur in all typical crystals for nuclear radiation detection (grown from silica crucibles under an H_2 atmosphere), irespective of the supplier of the material (AAEC, General Electric or Lawrence Berkeley Laboratory). Their concentrations are always similar (within a factor of three) and their capture cross sections for holes are also similar: σ_p (E_v + 0.23 eV) = 8 x 10^{-15} cm^2, σ_p (E_v + 0.38 eV) = 3 x 10^{-14} cm^2. Clearly, they are fundamental to an understanding of the defect chemistry of Ge - the components of these defect states must be common to virtually all Ge.

Three elements are common electrically inactive impurities in Ge: oxygen, hydrogen and silicon. Oxygen has long been known to have considerable influence on the defects induced in Ge by γ-radiation [Whan 1965]; the actual defect states involving oxygen, however, have not been identified. The amount of oxygen incorporated in the Ge crystal during its growth depends on both the gas ambient and the crucible material; a typical crystal grown from a silica crucible under an H_2 atmosphere may contain ∿6 x 10^{13} oxygen atoms cm^{-3}. Using a N_2 atmosphere may increase this to ∿10^{14} cm^{-3}, while growth from a graphite crucible under H_2 may reduce the oxygen content to ∿5 x 10^{13} cm^{-3} [Hubbard and Haller 1980]. Apart from oxygen, silicon is the other important electrically inactive impurity found in most Ge; this is more easily controlled and may be detected by spark source mass spectrometry (SSMS). Typical crystals intended for use as high

purity nuclear radiation detectors may contain 10^{14} to 10^{17} silicon atoms cm^{-3} [Hubbard and Haller 1980]. Crystals grown under H_2 atmospheres also typically contain $\sim 10^{13}$ hydrogen molecules cm^{-3} [Hubbard and Haller 1980].

The other impurities always present in p-type Ge are the electrically active shallow level acceptor impurities, generally, B, Al or Ga. These control the electrical purity of the material and crystals with net impurity densities of $<10^{10}$ cm^{-3} are available. Deliberate doping may increase this to $>10^{16}$ cm^{-3}. The problem, therefore, is this: all p-type Ge grown from silica crucibles shows two deep acceptor levels on γ-irradiation, the levels having similar concentrations and hole capture cross sections. One component of the centres is almost certainly a vacancy induced by the γ-irradiation, as the levels are not observed in unirradiated material. All p-type Ge contains electrically active impurities such as B, Al or Ga. All p-type Ge contains at least some electrically inactive oxygen and silicon. All other impurities may be disregarded because, if a wide range of crystals is investigated, results cannot be influenced by stray contaminants. What then are the components of the $E_v + 0.23$ eV and $E_v + 0.38$ eV centres?

EXPERIMENTAL

A large number of crystals from various suppliers were used in this investigation (Table 1). The material was obtained from General Electric Company (USA), Lawrence Berkeley Laboratory (USA), Sylvania Electric Incorporated (USA), Hoboken (Belgium), as well as crystals grown at the AAEC Research Establishment. Samples were prepared in the usual manner, with Li diffused n^+ contacts (10 minutes, 350°C) with evaporated Pd ohmic contacts. Several were also prepared with Sb diffused n^+ contacts. The irradiations were performed in a

1.6 Mrad h^{-1} ^{60}Co γ-irradiation facility.

Defect spectra were measured by the DLTS technique [Lang 1974] in the usual manner. Net doping densities were measured at 77 K and 180 K by C-V measurements (1 MHz).

RESULTS

Table 1(a) shows the crystals which displayed the two deep acceptor centres after γ-irradiation. DLTS spectra from two of the samples which displayed the levels are shown in Figure 1 (General Electric HP p-type Ge) and Figure 2 (Lawrence Berkeley Laboratory HP Ge). In Lawrence Berkeley and General Electric material prepared with Sb diffused contacts, copper contamination was picked up during the heating - the Cu did not appear to interact with the radiation damage centres (Figure 3).

Samples from various of these crystals were annealed for various times (1 to 1000 hours) at either 500°C or 675°C prior to irradiation. These samples were considerably hardened to radiation damage compared to their unannealed companions, even though net doping densities had not significantly changed (see section 1.1.5). Annealing under N_2 or H_2 appeared to make no significant difference, thus hydrogen does not appear to be a component of either of the acceptor centres, as long term annealing under N_2 ambients leads to the outdiffusion of hydrogen [Hall and Soltys 1978].

The presence of Li reduces the density of these levels. Figures 4(a) and 4(b) show the relative damage caused in a Li drifted sample, compared to an undrifted companion. The regions investigated are identical (≈80 μm from the Li diffused contact). This passivation of the defects by Li has been observed many times on the 'tail' of Li diffused contacts on p-type γ-irradiated samples.

Silicon concentrations of General Electric and Lawrence Berkeley

TABLE 1(a): p-TYPE CRYSTALS DISPLAYING TWO ACCEPTOR LEVELS ON IRRADIATION

Supplier	Crystal No.	(N_a-N_d) 77 K	Gas Atmosphere	Crucible Material	Dose (Mrad)	$\frac{N_T\ (0.38\ eV)}{(N_a-N_d)\ 180\ K}$	Comment
AAEC	78-93	4×10^{10}	H_2	silica	100	0.11	
AAEC	80-25	3×10^{11}	H_2	silica	100	0.11	
AAEC	80-23	3×10^{13}	cylinder H_2	Al_2O_3	150	0.09	
AAEC	78-8	3×10^{12}	H_2	graphite	150	0.06	Li contacts stable for >18 months at R.T.
AAEC	78-8	10^{13}	annealed 75 h 675°C, N_2		150	4×10^{-3}	Radiation hardened
AAEC	78-8	7×10^{12}	annealed 75 h 675°C, N_2 then 75 h 675°C, H_2		300	8×10^{-3}	Radiation hardened
AAEC	78-8	10^{13}	annealed 75 h 675°C, H_2		300	1.5×10^{-2}	Radiation hardened
AAEC	80-11	10^{13}	H_2	silica	150	0.17	
AAEC	80-11	10^{13}	annealed 75-1000 h 675°C, N_2		150	0.06	Radiation hardened
AAEC	78-31	1×10^{10}	H_2	silica	100	0.18	
AAEC	78-31	1×10^{10}	annealed 20-200 h 500°C, N_2		100	0.10	Radiation hardened
AAEC	77-71	5×10^{10}	H_2	silica	100	0.16	
AAEC	77-71	5×10^{10}	annealed 20-200 h 500°C, N_2		100	0.05	Radiation hardened
AAEC	78-86	10^{14}	H_2	silica	200	0.02	Ga doped
AAEC	crystallites Z.R. bars	3×10^{9} - 5×10^{11}	H_2	silica	100	~0.10	
GEC	4	3×10^{10}	H_2	silica	50	0.14	[Si] = 0.08 ppm
GEC	6*	1.3×10^{10}	H_2	silica	50	0.12	[Si] = 0.008 ppm
GEC	7	1.4×10^{10}	H_2	silica	50	0.13	
LBL	436-11.7*	1×10^{11}	H_2	pyrocarbon coated silica	50	0.12	[Si] = 3 ppm
LBL	450-11.8	7×10^{11}	H_2	pyrocarbon coated silica	50	0.11	[Si] = 0.008 ppm
LBL	469-1.9	4×10^{11}	H_2	silica	50	0.14	[Si] = 0.008 ppm
LBL	441-2.0*	5×10^{10}	H_2	silica	50	0.14	[Si] = 2.5 ppm
LBL	438-2.3	5×10^{10}	H_2	pyrocarbon coated silica	50	0.17	[Si] = 0.025 ppm

TABLE 1(b): p-TYPE CRYSTALS NOT DISPLAYING TWO ACCEPTOR LEVELS ON IRRADIATION

Supplier	Crystal No.	(N_a-N_d) 77 K	Gas Atmosphere	Crucible Material	Dose (Mrad)	$\frac{N_T\ (0.38\ eV)}{(N_a-N_d)\ 180\ K}$	Comment
AAEC	79-9	9×10^{14}	H_2	graphite	1000	$<10^{-4}$	Al-doped Li contacts precipitated in less than one hour
Sylvania	409H-1	8×10^{15}	zone levelled		700	$<10^{-4}$	Zn-doped
Sylvania	413C-1	1×10^{16}	zone levelled		700	$<10^{-4}$	Zn-doped
Hoboken	R	2×10^{13}	zone levelled		115	$<10^{-4}$	1 of 4 sections showed levels at $\sim 3 \times 10^{-4}$ background doping
Hoboken	B29	2×10^{13}	zone levelled		115	$<10^{-4}$	Normal Li-driftable Ge

NB: AAEC 79-9 had Sb diffused (1 h 500°C) n^+ contact, all others Li diffused n^+ contact (10 min 350°C). Samples of GEC and LBL material shown with an asterisk indicate these were radiation hardened when prepared with Sb, rather than Li contacts.

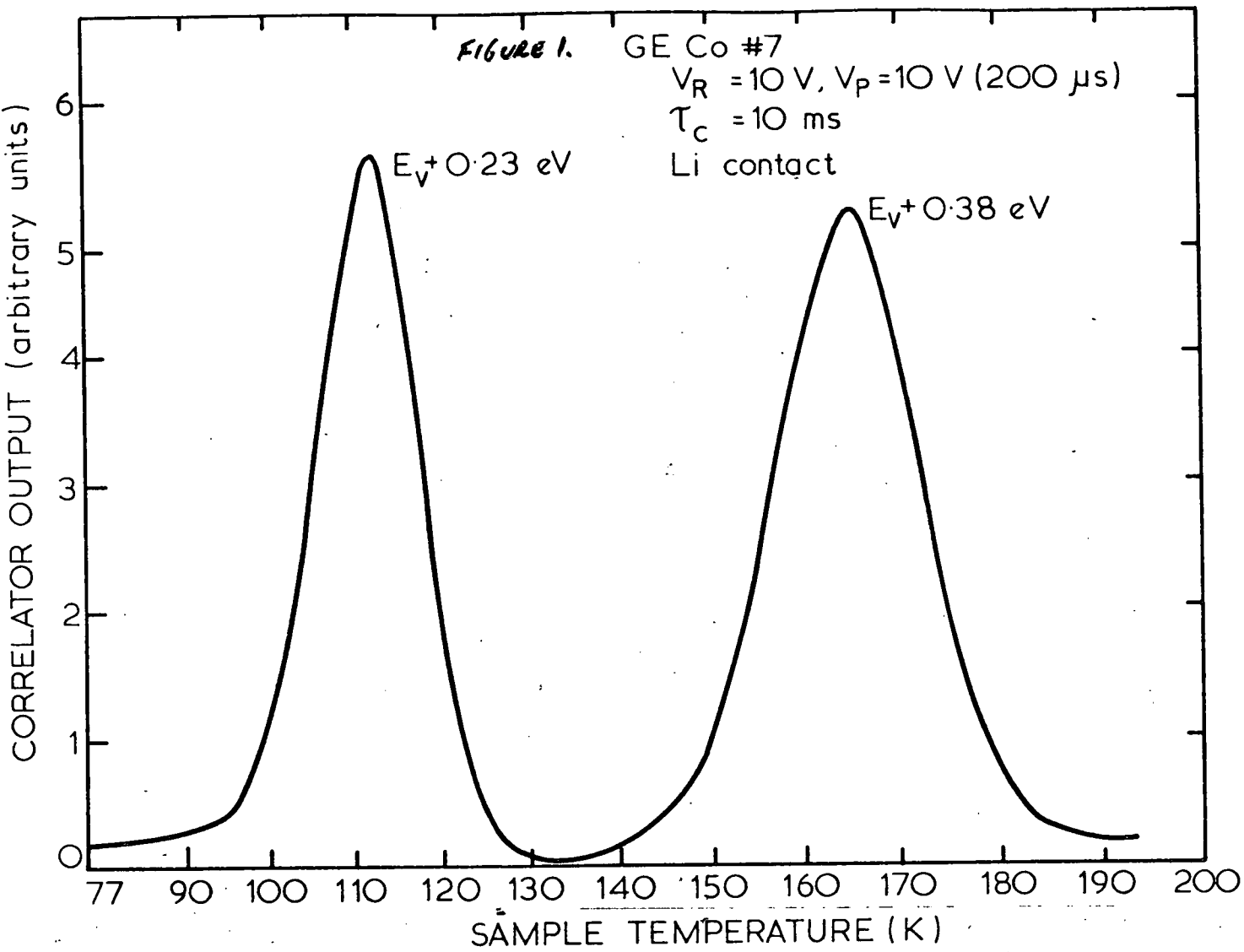
FIGURE 1.
GE Co #7
V_R = 10 V, V_P = 10 V (200 μs)
τ_c = 10 ms
Li contact
E_V+0·23 eV
E_V+0·38 eV
CORRELATOR OUTPUT (arbitrary units)
0
1
2
3
4
5
6
77
90
100
110
120
130
140
150
160
170
180
190
200
SAMPLE TEMPERATURE (K)

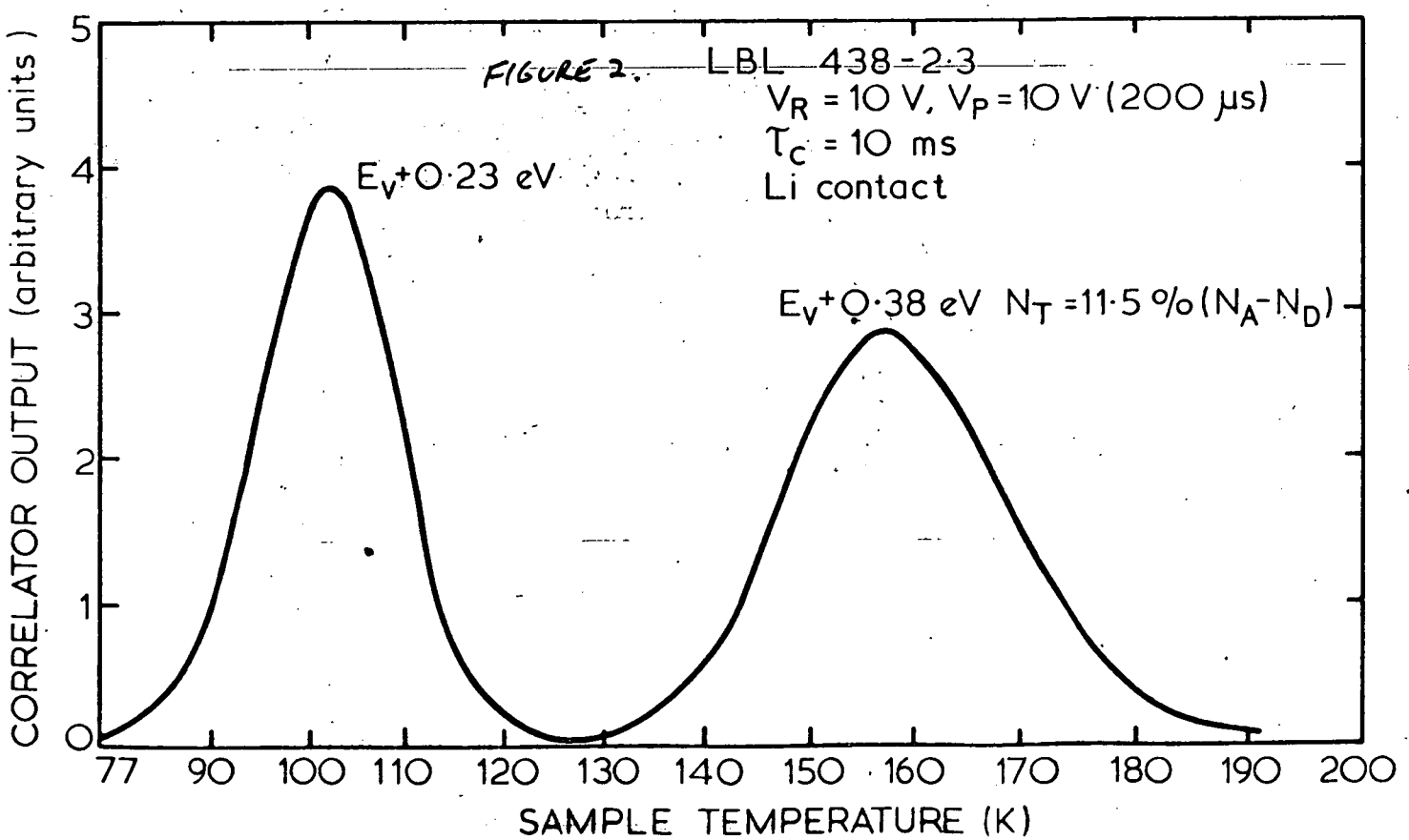
FIGURE 2.
LBL 438-2-3
V_R = 10 V, V_P = 10 V (200 μs)
τ_c = 10 ms
Li contact
E_V+0·23 eV
E_V+0·38 eV N_T = 11·5 % (N_A-N_D)
CORRELATOR OUTPUT (arbitrary units)
0
1
2
3
4
5
77
90
100
110
120
130
140
150
160
170
180
190
200
SAMPLE TEMPERATURE (K)

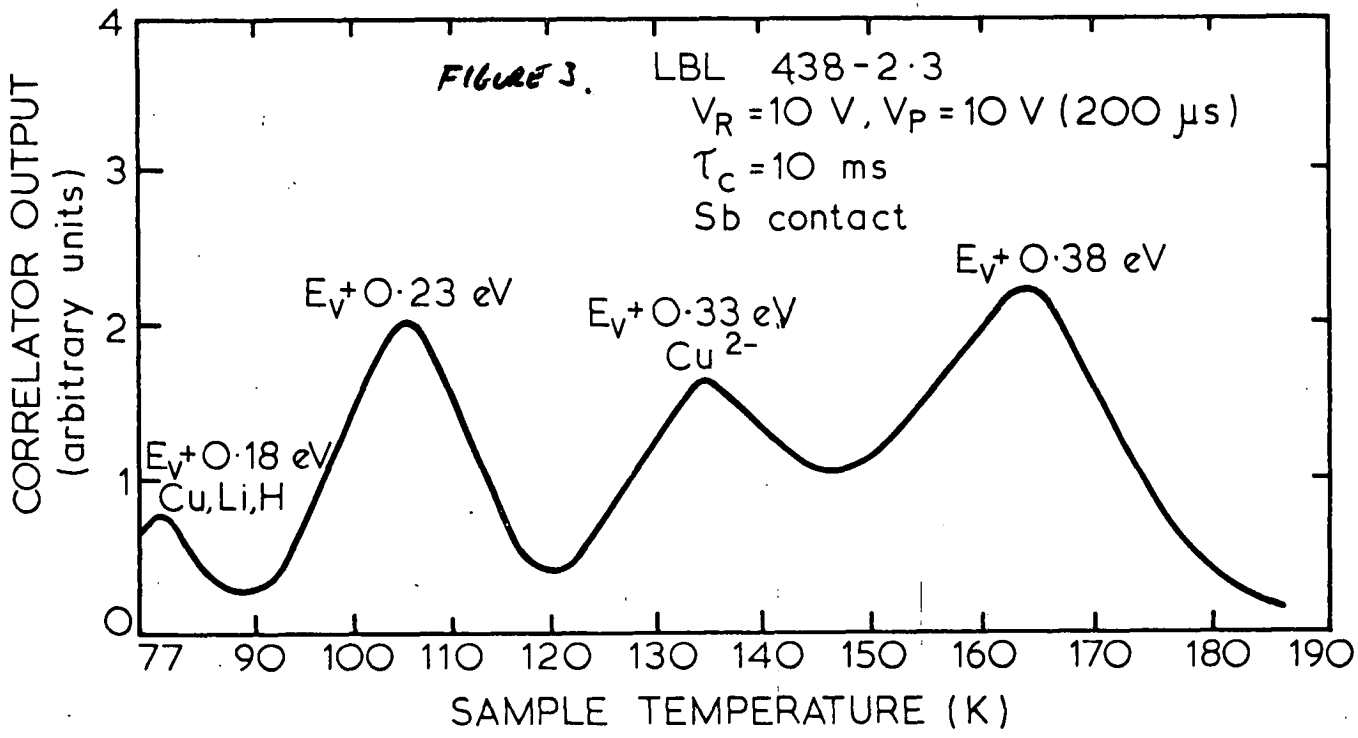
FIGURE 3.
LBL 438-2·3
V_R = 10 V, V_P = 10 V (200 μs)
τ_c = 10 ms
Sb contact
E_V+0·18 eV
Cu, Li, H
E_V+0·23 eV
E_V+0·33 eV
Cu^{2-}
E_V+0·38 eV
CORRELATOR OUTPUT
(arbitrary units)
0
1
2
3
4
77
90
100
110
120
130
140
150
160
170
180
190
SAMPLE TEMPERATURE (K)

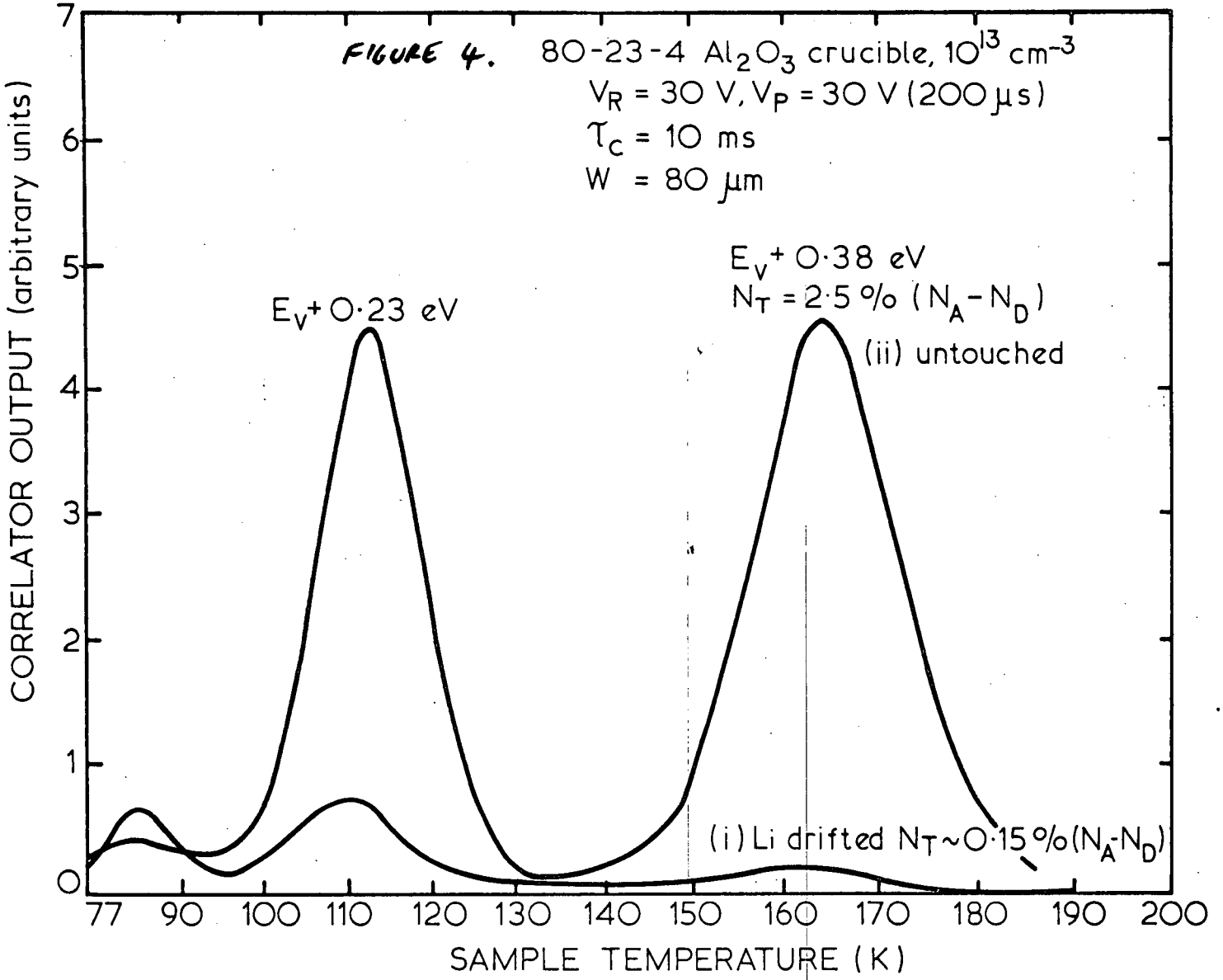
FIGURE 4. 80-23-4 Al_2O_3 crucible, 10^{13} cm^{-3}
V_R = 30 V, V_P = 30 V (200 µs)
τ_c = 10 ms
W = 80 µm
E_V+ 0·38 eV
N_T = 2·5 % (N_A − N_D)
(ii) untouched
E_V+ 0·23 eV
(i) Li drifted N_T ~ 0·15 % (N_A-N_D)
CORRELATOR OUTPUT (arbitrary units)
0
1
2
3
4
5
6
7
77
90
100
110
120
130
140
150
160
170
180
190
200
SAMPLE TEMPERATURE (K)

Laboratory crystals were determined by SSMS to be in the range 0.008 to 3.0 ppm. Crystals with high silicon concentrations were deliberately doped to obtain high levels of this element. The results from these samples show that silicon cannot be a part of the deep acceptor centres. It should be noted at this stage that four different crucible materials had been used for various crystals investigated: the usual silica, graphite and pyrocarbon coated silica and Al_2O_3. Stray contaminants (except oxygen) leached from the crucible during crystal growth can therefore be fairly safely dismissed as possibilities, particularly as the samples came from crystals grown in three different laboratories; no systematic contamination would be expected in all these crucibles.

At this point it was clear that all normal high purity Ge crystals grown for nuclear radiation detection display the two acceptor centres on irradiation. However, samples from three 'special' crystals did not show the levels ((Table 1(b)). A deliberately Al-doped AAEC sample grown from a graphite crucible showed no evidence of the levels after a dose of 1000 Mrad (Figure 5). This sample had an extremely low oxygen content as determined by the rate of Li precipitation; a normal Li diffused contact (10 minutes 350°C) precipitated completely in less than an hour, as determined by a thermal probe used for measuring the conduction type of Ge crystals. Consequently, these samples were prepared for irradiation by diffusing Sb for one hour at 500°C to form an n^+ contact. Even allowing for possible radiation hardening, the centres should be evident at concentrations of ∿1% of the net background doping density, judging from other material; instead there is no evidence for them down to the sensitivity of the DLTS technique, $<10^{-4}$. The ultimate sensitivity of our system is believed to be $\sim 10^{-5}$ of the background doping density.

The second class of material not to show these levels was

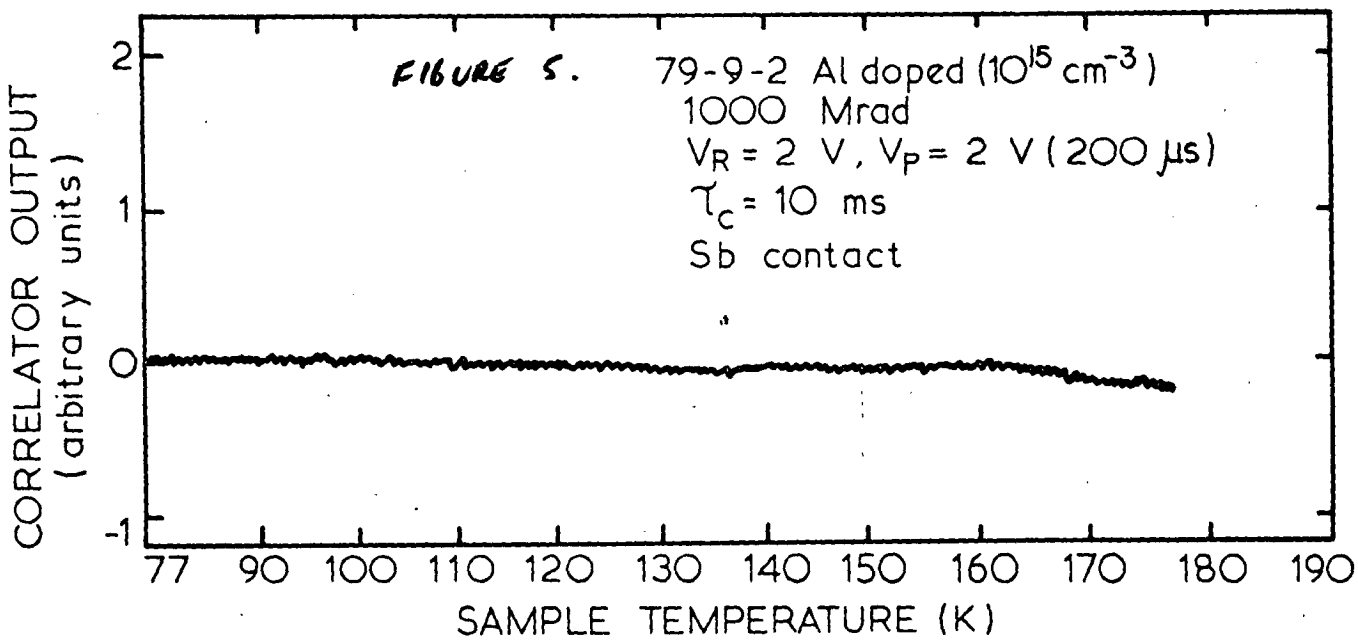
FIGURE 5.
79-9-2 Al doped (10^{15} cm^{-3})
1000 Mrad
V_R = 2 V, V_P = 2 V (200 μs)
τ_c = 10 ms
Sb contact
CORRELATOR OUTPUT
(arbitrary units)
2
1
0
-1
77 90 100 110 120 130 140 150 160 170 180 190
SAMPLE TEMPERATURE (K)

deliberately Zn doped crystals obtained from Sylvania Electric. These crystals were specifically grown for Li drifting, and therefore low oxygen content was aimed for. This was also the aim of the crystal growth of the third class of material not to show the levels, normal grade Li drifting Ge from Hoboken. Sections from one of these crystals, denoted 'R' in Table 1(b), had previously shown normal Li drift rates. One of four sections from this crystal not previously drifted did show a very low concentration of the acceptor defects after irradiation (N_T $\sim 3 \times 10^{-4}$ of the background doping density). Figures 6(a) and 6(b) show DLTS spectra from this and one of its companion sections, which showed no evidence of the levels. For the dose received (115 Mrad) the defects should have been present at concentrations of several per cent of the background doping density. Lithium contacts to these samples proved stable for the three days required for the irradiation.

DISCUSSION

Let us examine the evidence more closely. Firstly, hydrogen and silicon do not appear to be components of either the acceptor centres. High purity (N_a-N_d $\sim 5 \times 10^{10}$ cm^{-3}) samples which were over-irradiated so that the net doping density at 77 K rose by at least orders of magnitude (N_a-N_d $\sim 2 \times 10^{12}$ cm^{-3}) due to the introduction of deep radiation induced acceptors showed high concentrations of the E_v + 0.23 eV and E_v + 0.38 eV centres ($\sim 10^{12}$ cm^{-3}), far in excess of the net impurity concentration at 77 K before irradiation; that is, the shallow level impurities are unlikely to be part of the two acceptor centres, although it must be stressed that the doping densities measured for the samples are net impurity densities (N_a-N_d).

This leaves oxygen as the likely component of the γ-induced centres in a complex with vacancies. The three crystals with known low oxygen content showed either no evidence of the deep acceptor levels,

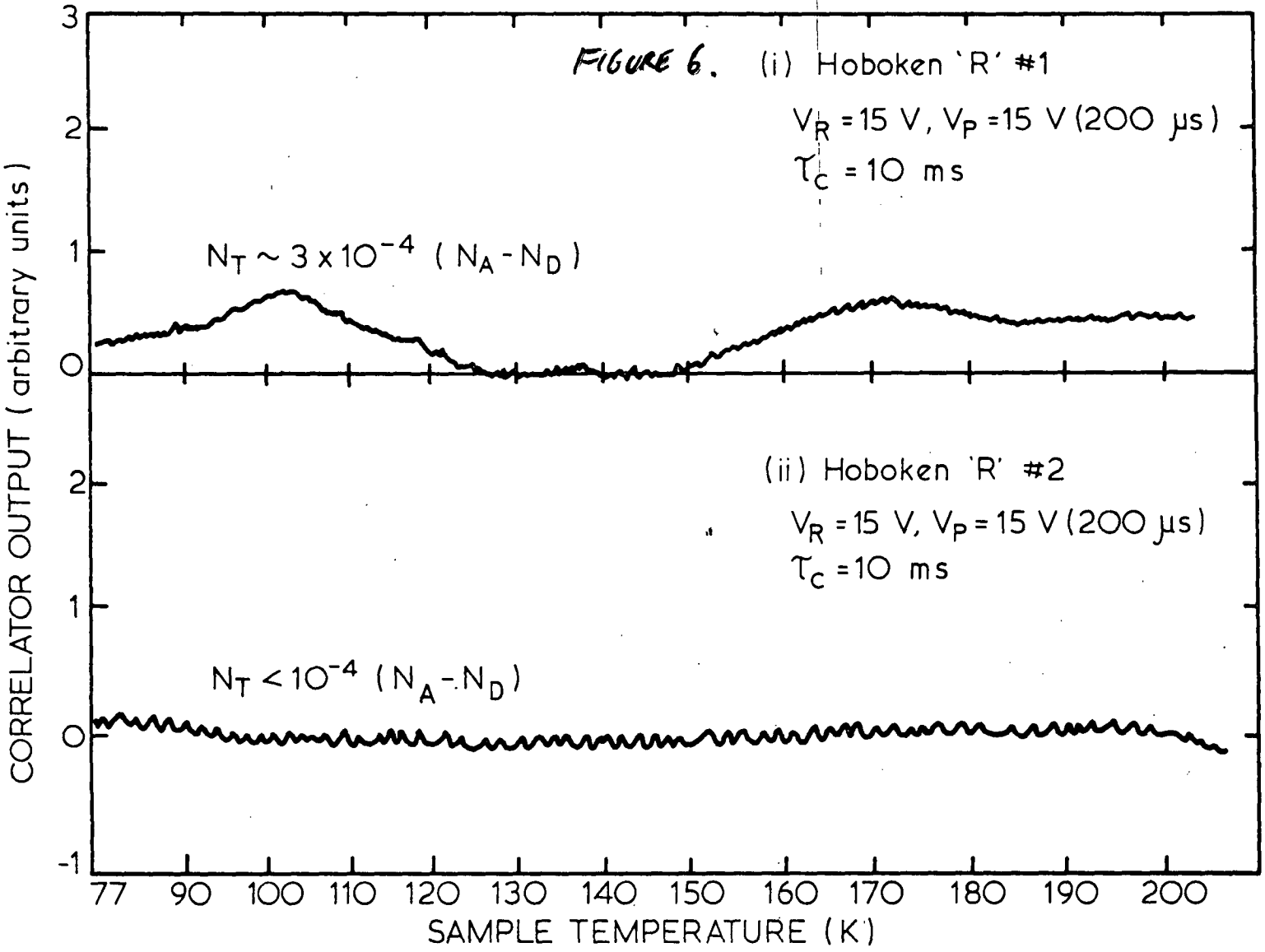
FIGURE 6.
(i) Hoboken 'R' #1
V_R = 15 V, V_P = 15 V (200 μs)
τ_c = 10 ms
$N_T \sim 3 \times 10^{-4}$ ($N_A - N_D$)
(ii) Hoboken 'R' #2
V_R = 15 V, V_P = 15 V (200 μs)
τ_c = 10 ms
$N_T < 10^{-4}$ ($N_A - N_D$)
CORRELATOR OUTPUT (arbitrary units)
3
2
1
0
2
1
0
-1
77 90 100 110 120 130 140 150 160 170 180 190 200
SAMPLE TEMPERATURE (K)

or else an abnormally low concentration of them. All silica-grown crystals will have significant oxygen content, as discussed above. The graphite-grown AAEC crystal (78-8) should have had low O content, but Li contacts on samples from this crystal remained stable for 718 months at room temperature, meaning that this crystal did in fact have quite a high O concentration. The pyrocarbon-coated silica crucibles used for some of the Lawrence Berkeley Laboratory crystals will also enable enough O to be incorporated into the melt during crystal growth, so that significant concentrations of the acceptor centres are produced on irradiation.

Additional evidence comes from the hardening of annealed material to these centres; it is known that the form of oxygen content can change during heating, for example being incorporated into electrically active, shallow donor or acceptor centres [Joos et al. 1980]. Also, The oxygen-vacancy centre at E_c - 0.18 eV is the dominant level introduced in electron- or γ-irradiated Si crystals pulled in similar fashion to the Ge used here [Kimerling 1977].

The E_v + 0.23 eV centre displays sensitivity in some samples to infrared illumination (Figure 7), which may determine how the two acceptor states are populated. The E_v + 0.38 eV level does not show this sensitivity but, in some samples, the concentrations of both levels are a function of the thermal cycling of the sample while being illuminated (Figure 8). Shallow level defects containing oxygen are also sensitive to infrared illumination [Hall 1975].

The reduced concentration of the two acceptors in the presence of Li is most likely due to the capture of oxygen into stable Li-O pairs, as well as a much lesser component due to direct passivation of the induced levels by the Li, as with laser-induced defects (Chapter 3). It is postulated, therefore, that the E_v + 0.23 eV and E_v + 0.38 eV

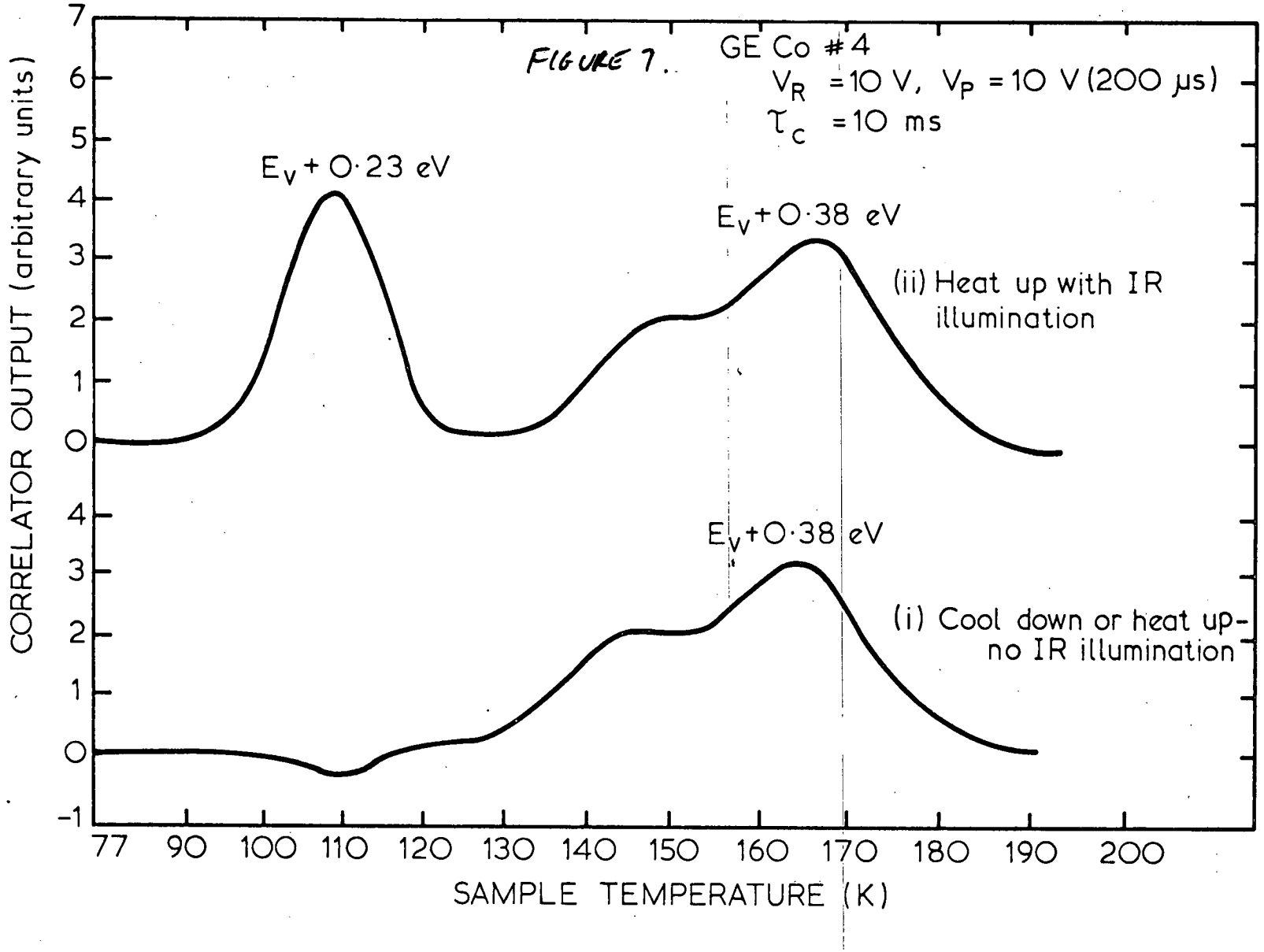
FIGURE 7.
GE Co #4
V_R = 10 V, V_P = 10 V (200 μs)
τ_c = 10 ms
E_V + 0·23 eV
E_V + 0·38 eV
(ii) Heat up with IR illumination
E_V + 0·38 eV
(i) Cool down or heat up- no IR illumination
CORRELATOR OUTPUT (arbitrary units)
7
6
5
4
3
2
1
0
4
3
2
1
0
-1
77
90
100
110
120
130
140
150
160
170
180
190
200
SAMPLE TEMPERATURE (K)

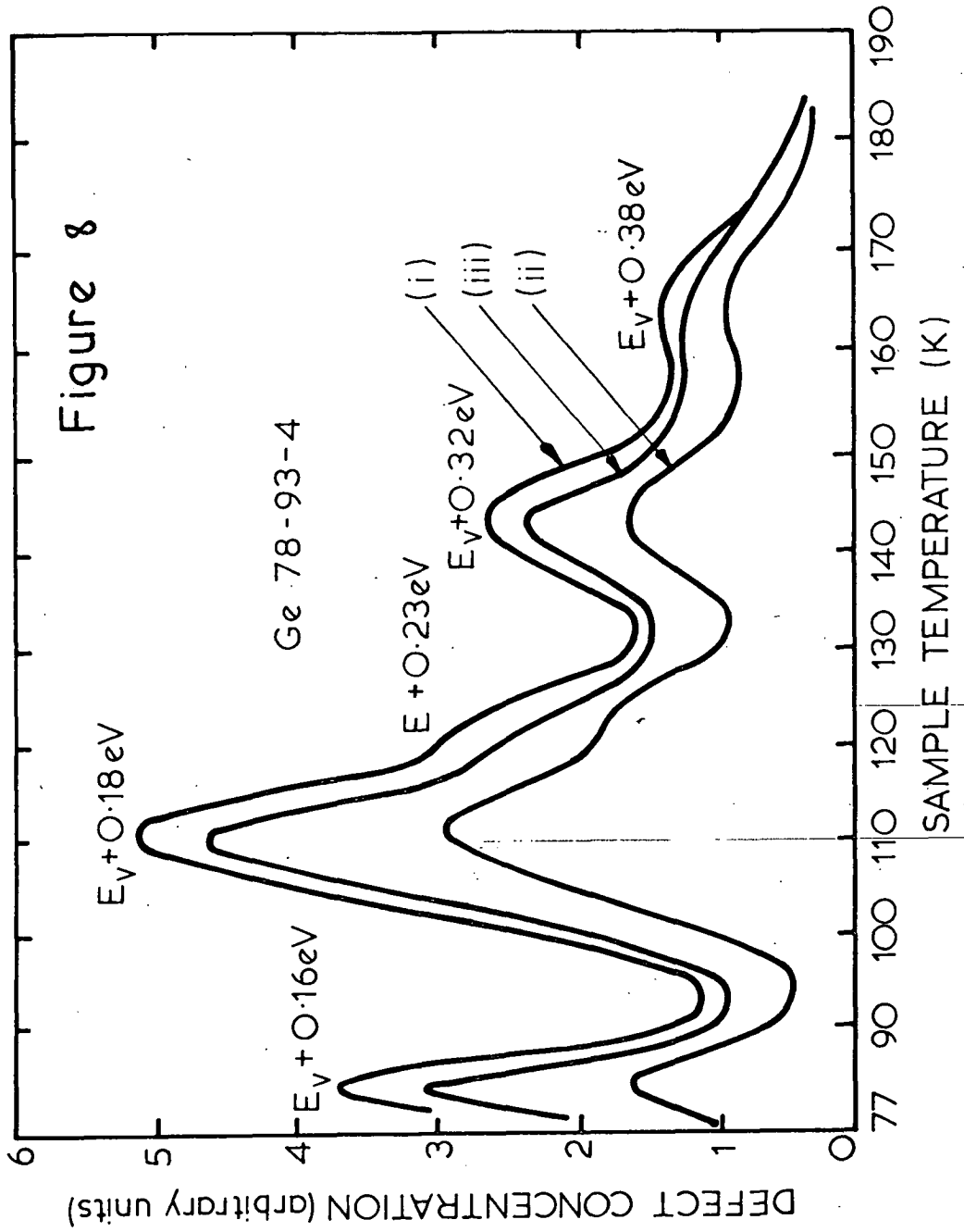

Figure 8 (i) Reverse biased (10V pulsing 10V) spectrum of γ-irradiated HP p-Ge (cool down spectrum)

(ii) Heat up spectrum under conditions in (i) after infra-red illumination

(iii) Cool-down spectrum after heating above the detrapping temperature of the defects

acceptor centres in γ-irradiated Ge are vacancy associations with oxygen. The levels may be caused by two charge states of the same defect; this remains to be proven.

REFERENCES

Hall, R. N. [1975] - Inst. Phys. Conf. Series No. 23, p. 190.

Hall, R. N. and Soltys, T. J. [1978] - IEEE Trans. Nucl. Sci. 25(1)385.

Hubbard, G. A. and Haller, E. E. [1980] - IEEE Trans. Nucl. Sci. 27(1)235.

Joos, B., Haller, E. E. and Falicov, L. M. [1950] - Phys. Rev. B 22(2)832.

Kimerling, L. C. [1977] - Radiation Effects in Semiconductors, Inst. Phys. Conf. Series No. 31, p. 221.

Lang, D. V. [1974] - J. Appl. Phys. 45:3023.

Whan, R. E. [1965] - Phys. Rev. 140(2A)A690.

1.1.5 RADIATION HARDENING BY THERMAL ANNEALING

INTRODUCTION

It is known that heating of crystals containing oxygen can affect the form in which it appears, for example, quenching of high-purity Ge can produce shallow level impurities involving oxygen [see, for example, Joos et al. 1980]. In this experiment we observe the effect of post growth annealing p- and n-type Ge crystals, then irradiating and comparing the radiation damage produced in this material to that produced in its untreated form.

Other authors have previously considered the effect of the extraction of impurities by thermal treatment in γ-damage formation rates [Khansevarov et al. 1967]. Improvements in Ge crystal purity and methods of observing deep level defects such as deep level transient spectroscopy [Lang 1974], should enable further understanding of the defect chemistry of Ge.

EXPERIMENTAL TECHNIQUE

Samples from four AAEC grown crystals were used. Two were high-purity p-type (N_a-N_d = 1-5 x 10^{10} cm^{-3}), one a moderately pure p-type (N_a-N_d = 10^{13} cm^{-3}) crystal and the other an n-type crystal (N_d-N_a = 3 x 10^{13} cm^{-3}). All were grown by the Czochralski process from silica crucibles in an H_2 atmosphere. After annealing, contacts were formed by a Li diffusion (300°C, 10 minutes) on one face, followed by a Pd evaporation to the opposite face. The rectangular prism-shaped samples had areas 0.5 to 1.3 cm^2 and were $\sim$0.4 cm thick.

For comparison, samples from two p-type crystals ($N_a-N_d \simeq 2 \times 10^{10}$ cm^{-3}) obtained from General Electric and five p-type crystals (N_a-N_d = 5 x 10^{10} to 7 x 10^{11} cm^{-3}) obtained from Lawrence Berkeley Laboratory, were prepared. One set was fabricated with Li diffused contacts (5 minutes, 250°C) and a second set with Sb diffused

n^+ contacts (1 hour, 500°C). The relative amounts of E_v + 0.23 eV and E_v + 0.38 eV levels produced by irradiation were compared in these two sets of samples, without additional heating.

The AAEC grown samples were coated in GaIn eutectic alloy to prevent Cu contamination during the heating and annealed under flowing N_2 gas for periods between 20 and 1000 hours at 500° or 675°C in a resistively heated furnace. The samples were allowed to cool slowly to ambient temperature (∿3 hours) and, after contacting, were irradiated in a 1.8 Mrad/h ^{60}Co γ-irradiation facility. The integrated doses of 50 to 150 Mrad were sufficient to create significant radiation damage. Hall effect and C-V measurements at 77 K determined no significant difference between the net impurity densities of heat treated and control samples prior to irradiation (Figure 1).

RESULTS

Figure 2(a) shows DLTS spectra from a high purity AAEC grown sample prior to irradiation and for the irradiated heat treated and control samples. Noting that the sample dimensions are the same, it is seen that the heat treated (20 hours at 500°C) sample has significantly less damage than the irradiated control sample, even though a new defect level (E_v + 0.18 eV) has been introduced. This is emphasised in the thermally stimulated capacitance scans of Figure 2(b); the capacitance of the heat treated sample is less because fewer deep level acceptors have been introduced by the irradiation. The defect concentrations in samples annealed at 500°C for various periods were typically one-third of those in the control samples. In Table 1 we have defined a parameter which allows comparison between samples. This is the sum of the observed trap densities above 77 K, divided by the net impurity concentrations at 77 K. As no significant difference was observed for annealing times between 20 and 1000 hours, the numbers in Table 1 are

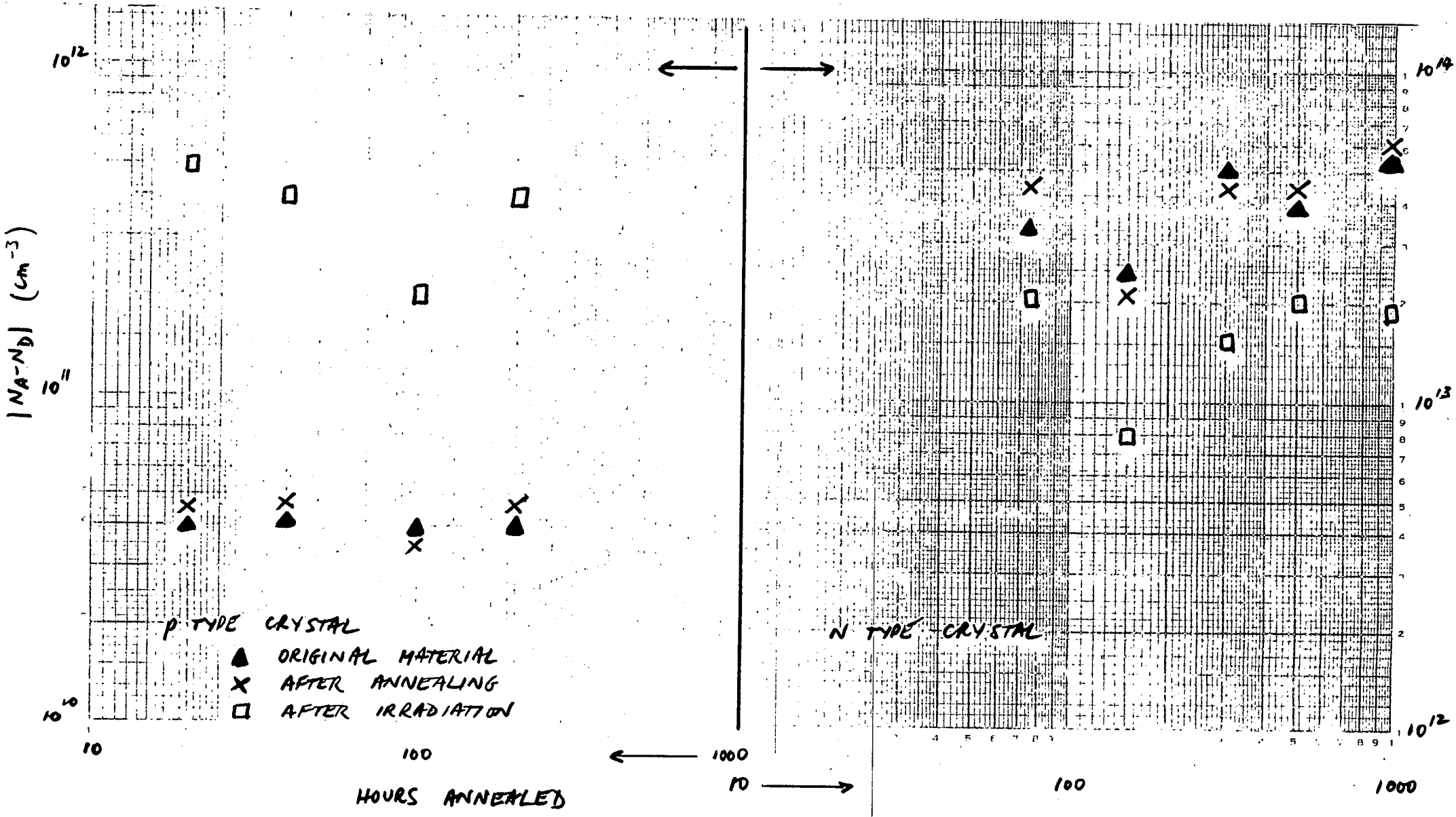

FIGURE 1. HALL EFFECT MEASUREMENTS OF NET CARRIER DENSITY OF CONTROL, HEAT TREATED AND IRRADIATED SAMPLES.

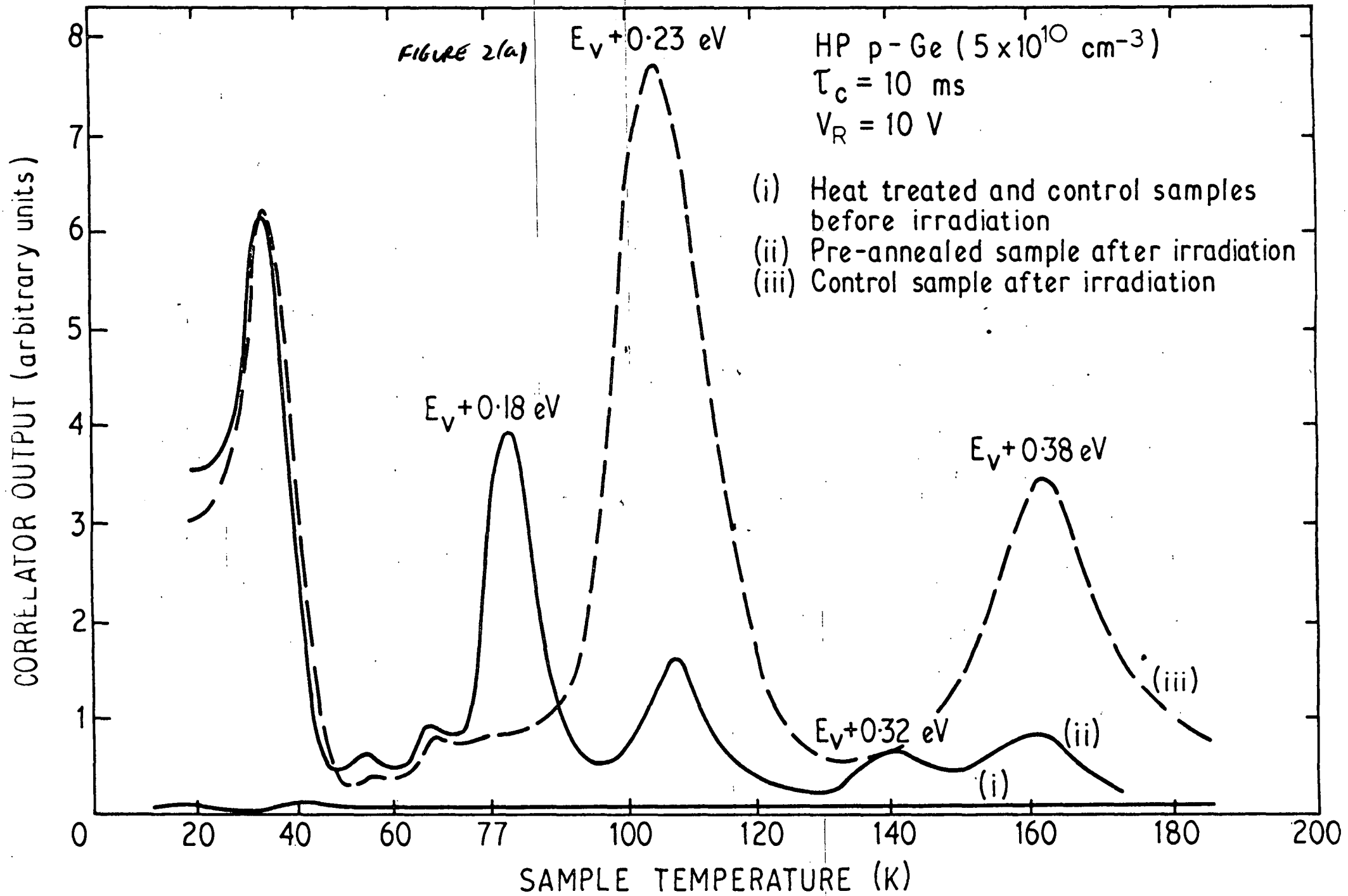
FIGURE 2(a)
E_v+0·23 eV
HP p-Ge (5 x 10^{10} cm^{-3})
τ_c = 10 ms
V_R = 10 V
(i) Heat treated and control samples before irradiation
(ii) Pre-annealed sample after irradiation
(iii) Control sample after irradiation
E_v+0·18 eV
E_v+0·38 eV
E_v+0·32 eV
(i)
(ii)
(iii)
CORRELATOR OUTPUT (arbitrary units)
SAMPLE TEMPERATURE (K)
0
1
2
3
4
5
6
7
8
20
40
60
77
100
120
140
160
180
200

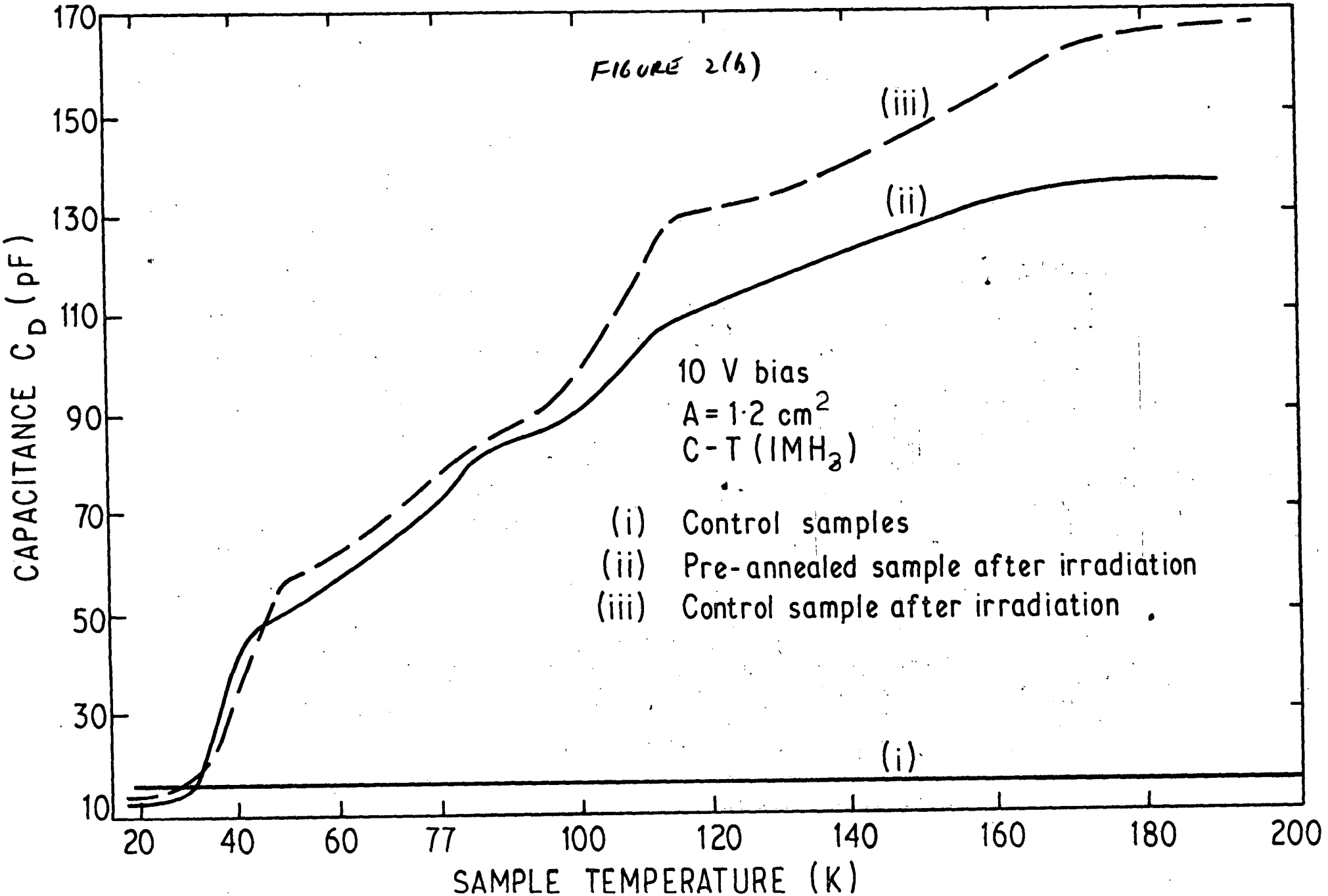
FIGURE 2(b)
170
150
130
110
90
70
50
30
10
CAPACITANCE C_D (pF)
20
40
60
77
100
120
140
160
180
200
SAMPLE TEMPERATURE (K)
(iii)
(ii)
(i)
10 V bias
A = 1·2 cm^2
C-T (IMH$_3$)
(i) Control samples
(ii) Pre-annealed sample after irradiation
(iii) Control sample after irradiation

TABLE 1 The effect of heating times on relative defect concentrations produced in Ge by γ-irradiation

CRYSTAL TYPE	SAMPLES	$\frac{\Sigma N_T}{\text{AV. } N_A-N_D/77K}$ (%)	AV. DEFECT CONCENTRATION RELATIVE TO CONTROL SAMPLE (%)
p-type 5×10^{10} cm^{-3}	Control	32.5	
annealed at 500°C	Heat treated	10.7	33
p-type 1×10^{10} cm	Control	35.5	
annealed at 500°C	Heat treated	20.5	58
p-type $10^{13}cm^{-3}$	Control	36.3	
annealed at 675°C	Heat treated	12.7	35
n-type 3 $\times10^{13}cm^{-3}$	Control	1.7	
annealed at 675°C	Heat treated	0.8	47

the average from the 15 heat treated and 5 control samples used from each crystal.

It is interesting to note that not only does p-type, silica grown Ge of a wide range of purity (10^{10} to 10^{13} cm^{-3}) show the effect, but also n-type Ge, in which the induced acceptor levels (filled by pulsed IR illumination) are not the oxygen-related centres observed in the p-type material. Figure 3 shows the relative amount of damage induced in a heat treated (75 hours at 675°C) n-type sample compared to an untreated sample.

Samples from one of the two General Electric crystals were radiation hardened after heat treatment (1 hour, 500°C), while samples from two of the five Lawrence Berkeley Laboratory crystals showed hardening after a similar treatment. These two crystals had high Si concentrations (2.5 to 3.0 ppm) compared to the other three crystals (0.008 to 0.025 ppm Si) as determined by SSMS.

To be useful as a radiation hardening method, heat treatment must not introduce other defects after irradiation which cannot be thermally removed at temperatures for which restoration of the irradiated control sample is possible. Complete restoration of all the p-type samples was achieved by annealing for ∿5 hours at 200°C, while the n-type material required ∿1 hour at 200°C. Figures 4(a) and 4(b) show DLTS spectra from γ-irradiated heat treated and control samples after post-irradiation annealing for 3 hours at 200°C. Similar degrees of defect removal are seen.

DISCUSSION

There are several possible explanations for the observed radiation hardening of the pre-annealed material:

(a) The formation of electrically inactive complexes during the heat treatment, which occur during the irradiation break up due to photodisintegration or electronic processes.

FIGURE 3.

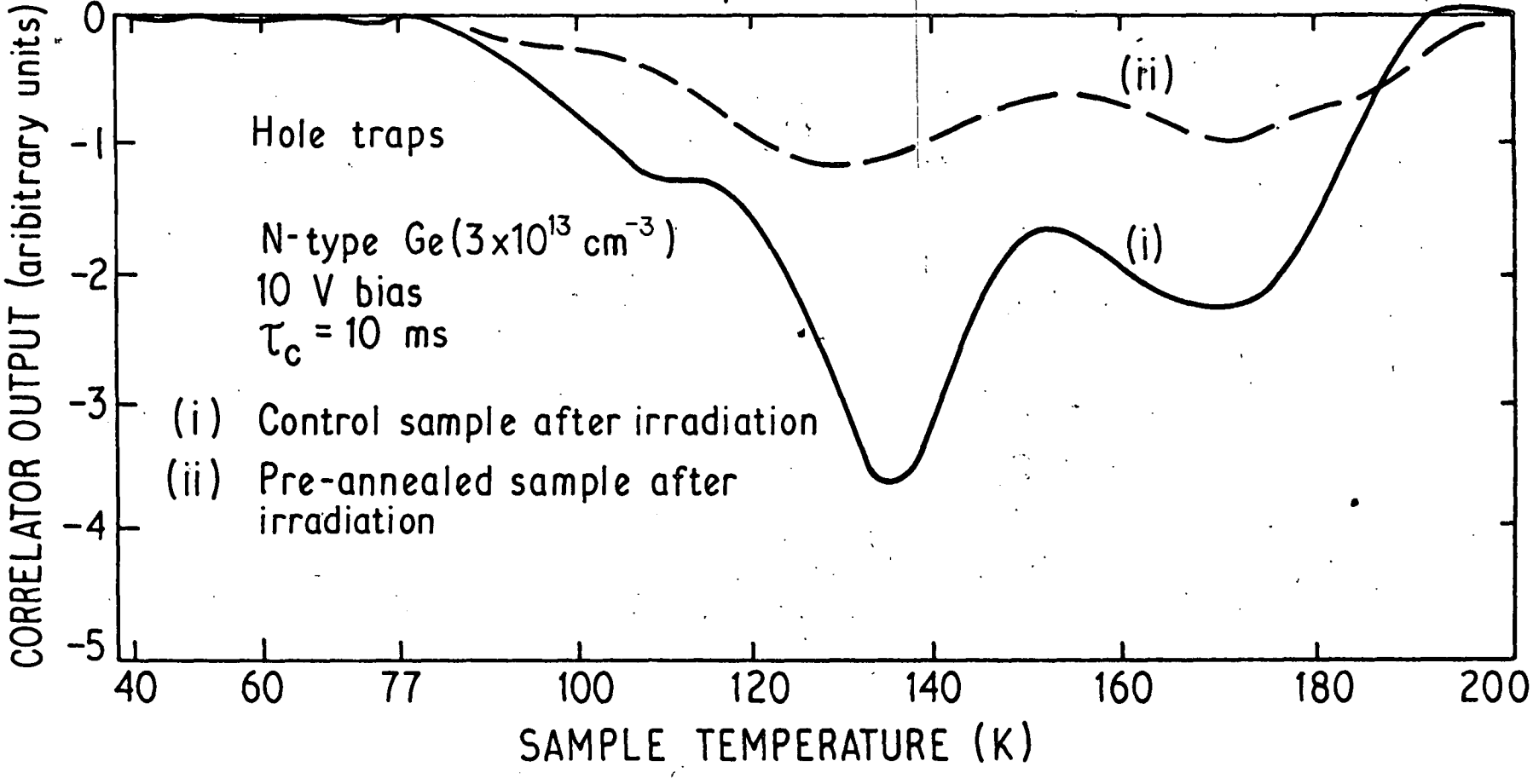
CORRELATOR OUTPUT (aribitrary units)
0
-1
-2
-3
-4
-5
Hole traps
N-type Ge(3x10^13 cm^-3)
10 V bias
τc = 10 ms
(i) Control sample after irradiation
(ii) Pre-annealed sample after irradiation
(ii)
(i)
40
60
77
100
120
140
160
180
200
SAMPLE TEMPERATURE (K)

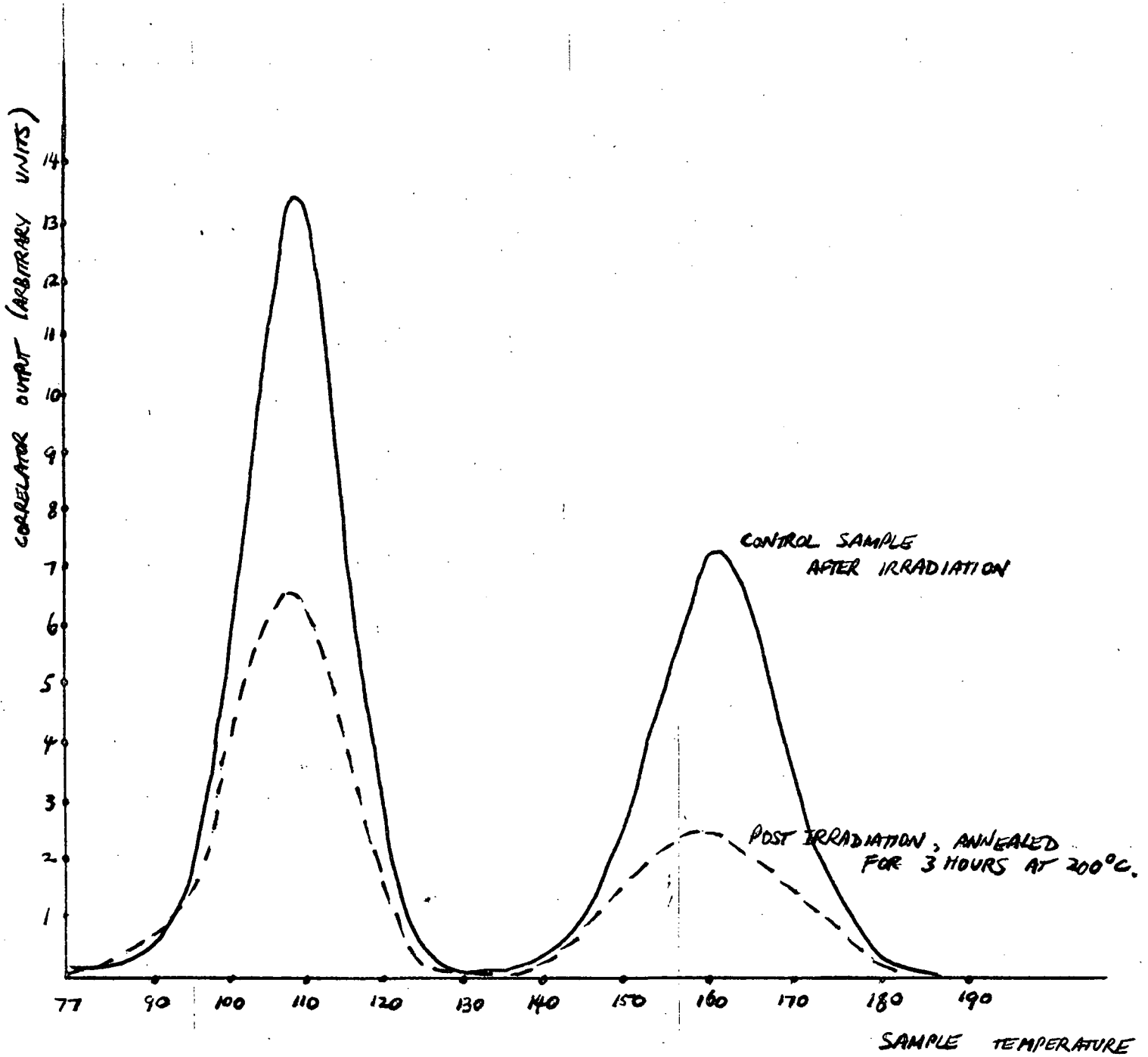

FIGURE 4 (a) REDUCTION IN DEFECT DENSITY WITH POST-IRRADIATION ANNEALING.

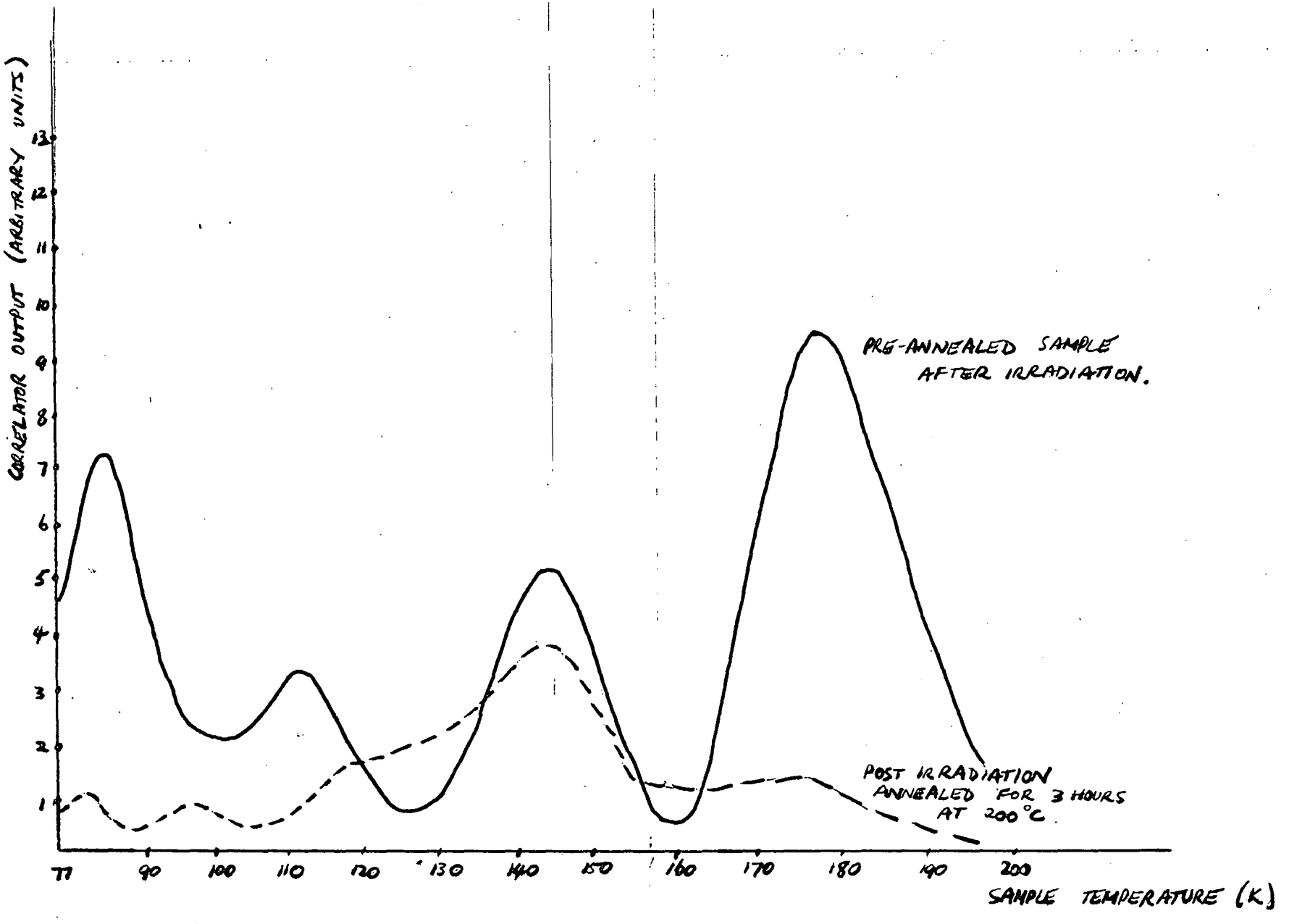

FIGURE 4(b). REDUCTION IN DEFECT DENSITY WITH POST-IRRADIATION ANNEALING.

(b) The aggregation of oxygen during the annealing.

(c) The interaction of Si and O during the annealing.

(d) The loss or re-ordering of hydrogen during the annealing.

(e) Dislocation movement.

Each of the possibilities will be discussed in turn.

(a) A tentative model along these lines could be proposed as follows:

1. Extended low temperature annealing favours the formation of electrically-inactive complexes of two forms. The first will be donor-acceptor pairs

$$D^+ + A^- \underset{k_2}{\overset{k_1}{\rightleftarrows}} (DA)^o \qquad (1)$$

leaving the effective impurity concentration unchanged after annealing. In either conductance type there will be a population of shallow level minority carriers. The rates k_1 and k_2 will be dependent on the concentration of these shallow level minority carriers and hence these reactions will be less important for low residual impurity concentrations. The second form will consist of conglomerate defects involving neutral impurities

$$X^o + Y^o \underset{k_4}{\overset{k_3}{\rightleftarrows}} (XY)^o \qquad (2)$$

In this model $k_3 > k_4$ at the temperature of the anneals used in this experiment. These conglomerates could be in the form of electrically-inactive oxides or possibly silicates.

2. Upon irradiation there will be a dynamic balance between shallow donor D_S-deep acceptor A_D complex formation, leading to compensation of n-type material with reactions of the form

$$D_S^+ + A_D^- \rightleftarrows (D_S A_D)^O \qquad (3)$$

$$D_S^+ + 2A_D^- \rightleftarrows (D_S A_D A_D)^- \qquad (4)$$

(higher vacancy-donor complexes are increasingly less likely)

$$Ge_I + (D_S A_D)^O \rightarrow D_S^+ \qquad (5)$$

the production of vacancy aggregates leading to increasing p-typeness for p-type material

$$Ge + \gamma \rightarrow A_D^- \qquad (6)$$

and reactions of the form

$$(DA)^O + \gamma \rightarrow D_S^+ + A_D^- \qquad (7)$$

$$(XY)^O + \gamma \xrightarrow{k_5} X^O + Y^O \qquad (8)$$

$$\xrightarrow{k_6} (XA_D)^- + (YA_D)^- \qquad (9)$$

The rate of reaction (7) will be low compared to that of reaction (8) because of the small initial formation of $(DA)^O$ compared to $(XY)^O$. Reactions (3) to (7) may be summarised as being of the form

$$V + Ge \underset{k_b}{\overset{k_a}{\rightleftarrows}} (V\text{-}Ge)$$

where V are acceptor-like (vacancy) defects. At the temperature of irradiation (300 K) this model would require $k_5 > k_a, k_6 >> k_b, k_3$. The probability of photodisintegration of a complex impurity is small, thus some form of electronic process such as ionization enhanced annealing would be

h as ionization

required to explain the dominance of reaction (8). Cross sections for displacement of Ge atoms by 1.2 MeV γ-rays are ~0.05 to 0.5 barn/atom respectively for a threshold energy of displacement of E_d = 15 or 30 eV [Vavilov and Ukhin 1977]. The cross sections for interaction with electrically neutral conglomerates are unknown, but are likely to be of the same order.

It is hard to see neutral impurities being the cause of the hardening, because of the very low cross sections for dissociation by γ-rays and also the fact that annealing for 20 or 1000 hours seems to make little difference.

(b) This is the most likely explanation, because oxygen in Ge is known to undergo changes of form upon heating, as mentioned in the introduction. Evidence for the formation of new oxygen complexes on annealing comes from the production of the E_v + 0.18 eV level in the p-type samples studied and, to a lesser extent, the E_v + 0.32 eV level; these are not observed in the irradiated control samples and possibly result from the complexing of a neutral oxygen-related conglomerate with a radiation induced defect. The E_v + 0.18 eV level was detected at lower concentrations in the samples heated at 500°C for 1 hour than those annealed for longer periods.

(c) Two sets of samples from the General Electric and Lawrence Berkeley Laboratory crystals were prepared, one set with Li diffused (5 minutes, 280°C) n^+ contacts, the other with Sb diffused (1 hour, 500°C) n^+ contacts. The silicon concentration of these samples, as determined by SSMS, was in the range 0.008 to 3.0 ppm. In the Li diffused samples, the introduction of the E_v + 0.23 eV and E_v + 0.38 eV levels was unaffected by the Si content of the sample, or the type of crucible from which the parent crystal was grown (silica or pyrocarbon

coated silica). In the Sb diffused samples, which had been heated to 500°C for 1 hour, radiation hardening of these levels was observed in three of the seven samples; two had high Si content (2.5 and 3.0 ppm) and were grown in pyrocarbon coated crucibles, but the other had low Si content (0.008 ppm) and was grown in a silica crucible. It should be noted that a crystal with higher Si content (0.08 ppm) grown from a silica crucible showed no radiation hardening after 1 hour at 500°C.

(d) Annealing under N_2, rather than H_2, appeared to make no significant difference to the properties of the base material even though outdiffusion of hydrogen would be occurring for the longer annealed samples [Chen and McKay 1968; Hall and Soltys 1978]. Similarly, samples annealed for 75 hours under H_2 showed similar degrees of hardening to those annealed for the same period under N_2.

(e) Removal of dislocations to the surface was not an explanation, as the etch pit densities on annealed samples were generally similar and at most 20 to 30% lower than on unannealed control samples (800 cm^{-2}). They consisted of isolated pits (randomly scattered, nearest neighbour distances ~400 μm) and lines of pits. It must not be forgotten, however, that radiation induced vacancies may aid in dislocation climb and movement and may eventually themselves be sunk by the dislocation.

CONCLUSIONS

The method of radiation hardening by thermal annealing has been proven only for γ-ray damage and may be less efficient for more heavily damaging radiation, such as protons or fast neutrons. It is hoped that continuing experiments along these lines will assist in the understanding of radiation damage defect behaviour in semiconductors in general, as the ultra-pure Ge provides the opportunity to study defect processes in a nearly perfect lattice.

REFERENCES

Chen, G. and McKay, J. W. [1968] - Phys. Rev. 167:745.

Hall, R. N. and Soltys, T. J. [1978] - IEEE Trans. Nucl. Sci. 25(1)385.

see, for example, Joos, B., Haller, E. E. and Falicov, L. M. [1980] - Phys. Rev. B 22(2)832.

Khansevarov, R. Yu., Mashovets, T. V. and Vitovskii, N. A. [1967] - Phys. Stat. Solidi 22:K103.

Lang, D. V. [1974] - J. Appl. Phys. 45:3023.

Vavilov, V. S. and Ukhin, N. A. [1977] - Radiation Effects in Semiconductors and Semiconductor Apparatuses, Consultants Bureau, New York.

1.2 FAST NEUTRON AND PROTON DAMAGE IN Ge

From the point of view of semiconductor radiation detector operation, the most important radiation damage is that created by fast neutrons and protons. The strongly disordered regions within the crystal lattice created by these particles trap free charge carriers created by the ionizing radiation of interest. This trapping means the carriers are either lost entirely to the charge collection process, or are collected with reduced efficiency, depending on the time for which they are held at the defect sites. The consequence for the detector user is that spectral peaks broaden on the low energy side with a corresponding degradation in resolution. Many common areas of use for HP or Li drifted Ge detectors involve considerable background fluxes of damaging radiation, such as astronomical applications [Hicks et al. 1974], nuclear reaction studies using accelerators [Kraner 1980], or the use of detectors as charged particle telescopes in high energy accelerator experiments [Pehl et al. 1978].

Considerable information exists regarding threshold fluxes for significant damage by fast neutrons and protons and the annealing conditions required to remove the radiation damage [Kraner 1980]. A model has been proposed to explain the effect of fast neutron damage on HP Ge detectors [Darken et al. 1980], which did not rule out the possibility of point defects also playing a major role in the effects of the damage, as well as the more obvious defect clusters. In this experiment we examine the point defects produced by the fast neutron and proton irradiation of Ge.

EXPERIMENTAL PROCEDURE

Samples were prepared in the standard way with Li diffused n^+ contacts (10 minutes at 325°C) and Pd barrier contacts. Growth conditions of the parent crystals have been reported earlier (Table 1,

section 1.1.1). Both n- and p-type Ge were examined, with net free carrier densities in the range 1 x 10^{11} to 2 x 10^{14} cm^{-3} prior to irradiation. In some cases, contacts and part of the sample were lapped off and the contact remade so that damage deep in the sample could be observed. This helped to differentiate more clearly between proton and neutron damage.

The room temperature irradiations were performed at the University of Tasmania's Central Science Laboratory using a Kaman Sciences Corporation A-711 neutron generator. The unit has a maximum total output of 10^{11} neutrons/s and uses the (D,T) reaction (neutron energy 14.7 MeV). The samples were contained in polyethylene packets which acted as converters to produce knock-on protons. The total integrated dose was 1.5 x 10^{8} neutrons/cm^2 estimated from Cu activated during the same exposure. This translates to 1.4 x 10^{5} protons/cm^2 using the knock-on proton cross section of $\sim$1 barn [Adair 1950]. The samples were, to a certain extent, self-collimating, with area 1 cm^2 and being 30 cm away from the neutron source. They were mounted orthogonal to the source for the irradiation.

RESULTS

The damage produced by the irradiation may be divided into three regions:

1. A region of slight proton damage plus neutron damage.
2. A heavily damaged region caused by protons at the end of their range.
3. Fast neutron damage only.

Table 1 lists the parameters measured for the observed defects. The outstanding difference between proton and neutron damage reported here and the γ-ray damage reported earlier, is that here only acceptor level defects were observed. The defects produced by p- and n-

TABLE 1: OBSERVED DEFECT LEVEL PARAMETERS

a) Neutron Plus Proton Damage Region

Defect	Level	Cross-Section cm^2	Trap Density cm^{-3}	Sample (DOPING DENSITY AFTER IRRADIATION)
32	E_v + 30meV	6.9×10^{-20}	1.4×10^{9}	undoped n = 7×10^{10} cm^{-3} (10K)
38	E_v + 67meV	7.8×10^{-16}	1.5×10^{9}	undoped n = 7×10^{10} cm^{-3} (10K)
51	E_v + 71meV	7×10^{-18}	3.2×10^{10}	undoped (H poor) p = $10^{13} cm^{-3}$ (77K)
96	E_v + 0.11eV	1.6×10^{-19}	3.0×10^{9}	undoped n = 3×10^{10} cm^{-3} (77K)

b) Proton Induced (Nuclear Stopping Damage)

89	E_v + 0.16eV	4.1×10^{-16} (1.4×10^{-16} direct	7.5×10^{10}	undoped (H_2 poor) p = 10^{13} cm^{-3} (77K)
103	E_v + 0.13eV	2×10^{-18}	6×10^{11}	As-doped n = 8×10^{12} cm^{-3} (77K)
145	E_v + 0.29eV	9.4×10^{-16}	6.6×10^{11}	P-doped n = 2×10^{13} cm^{-3} (77K)

c) Neutron Induced

118	E_v + 0.23eV	5.3×10^{-16}	4.8×10^{9}	undoped n = 4×10^{10} cm^{-3} (77K)
146	E_v + 0.36eV	1.5×10^{-14}	3.6×10^{9}	undoped n = 2.5×10^{11} cm^{-3} (77K)
			8.0×10^{10}	undoped (H_2 poor) p = 10^{13} cm^{-3} (77K)

irradiation in general had lower trapping cross sections and many of the peaks were broad, indicating clustered defects or unresolved energy levels.

DLTS spectra from an undoped silica grown n-type sample and an undoped silica grown p-type sample are shown in Figures 1 and 2(a). The thermally stimulated capacitance scan of the latter is shown in Figure 2(b). The minority carrier injection in the n-type sample was obtained by infrared illumination. Arrhenius plots for some of the levels are shown in Figure 3.

Annealing *in vacuo* at 130^{o}C for 2 hours removed the proton damage completely in a n-type sample grown under a wet N_2 atmosphere ($n = 4 \times 10^{13}$ cm^{-3}) and reduced by ∿30% the trap density in a companion sample from the same crystal, but grown under an atmosphere of dry N_2. It has been reported that *in situ* annealing of neutron and proton damaged detectors can be achieved at temperatures of 150^{o}C for extended periods (>5 hours) [Pehl 1978] and this would tend to be confirmed by the results here.

DISCUSSION

The P-doped sample displayed a proton induced level at E_v + 0.29 eV on the first occasion it was tested (about one week after irradiation). This defect was tracked into the sample and was definitely not a surface level. On a subsequent test, this level had disappeared and the bulk capacitance of the device had increased, due to an increase in the net free carrier density from 2.1×10^{13} cm^{-3} to 5.3×10^{13} cm^{-3}. This is still below the pre-irradiation value of 8×10^{13} cm^{-3}. Similar behaviour was displayed by the level E_v + 0.13 eV in the As-doped sample, in which n had reduced from 2×10^{14} cm^{-3} to 8.2×10^{12} cm^{-3} after irradiation, and on a second insertion into the DLTS system had returned to 2.1×10^{13} cm^{-3} (the diode was stored in a freezer between

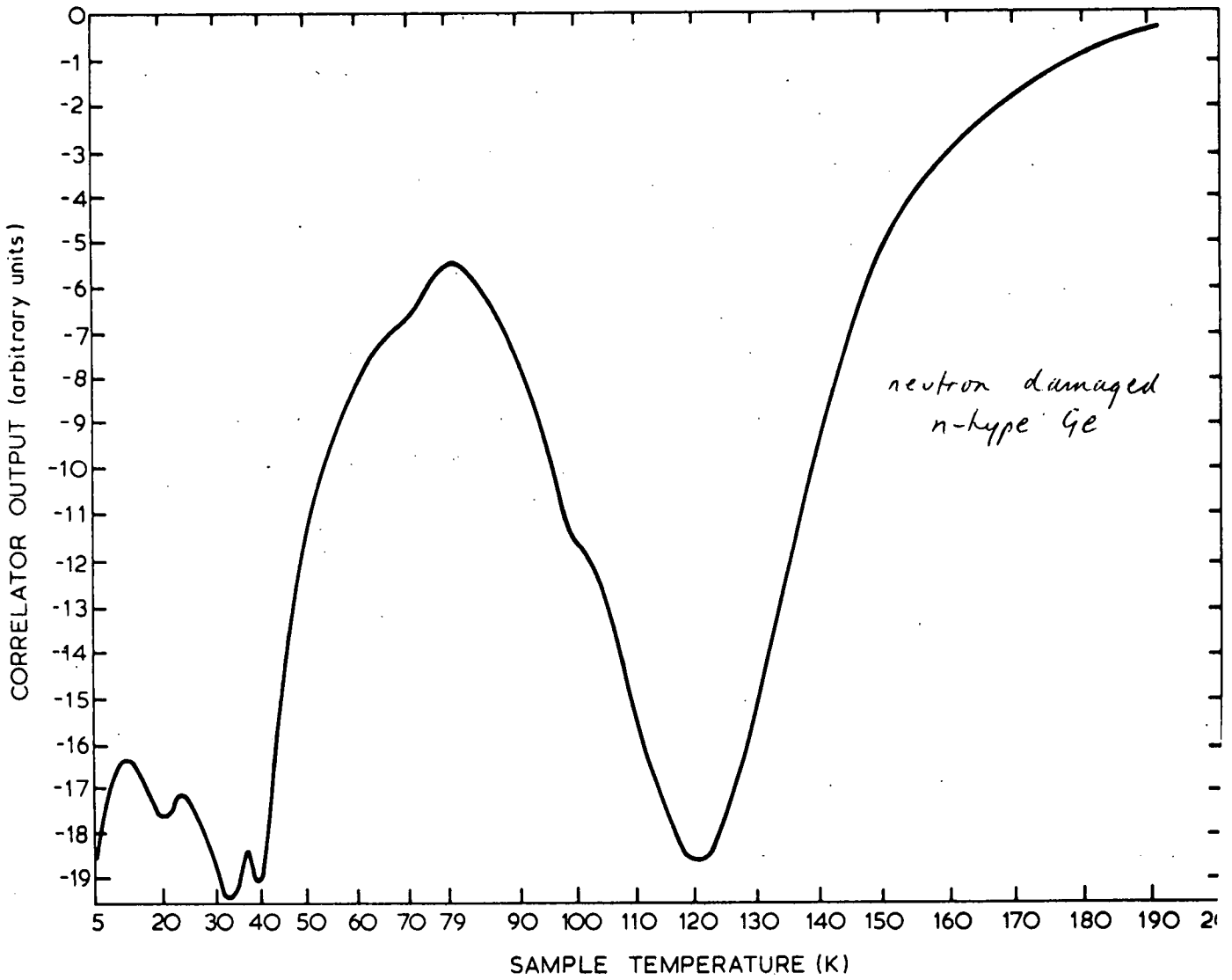
CORRELATOR OUTPUT (arbitrary units)
0
-1
-2
-3
-4
-5
-6
-7
-8
-9
-10
-11
-12
-13
-14
-15
-16
-17
-18
-19
5
20
30
40
50
60
70
79
90
100
110
120
130
140
150
160
170
180
190
SAMPLE TEMPERATURE (K)
neutron damaged
n-type Ge

Figure 1

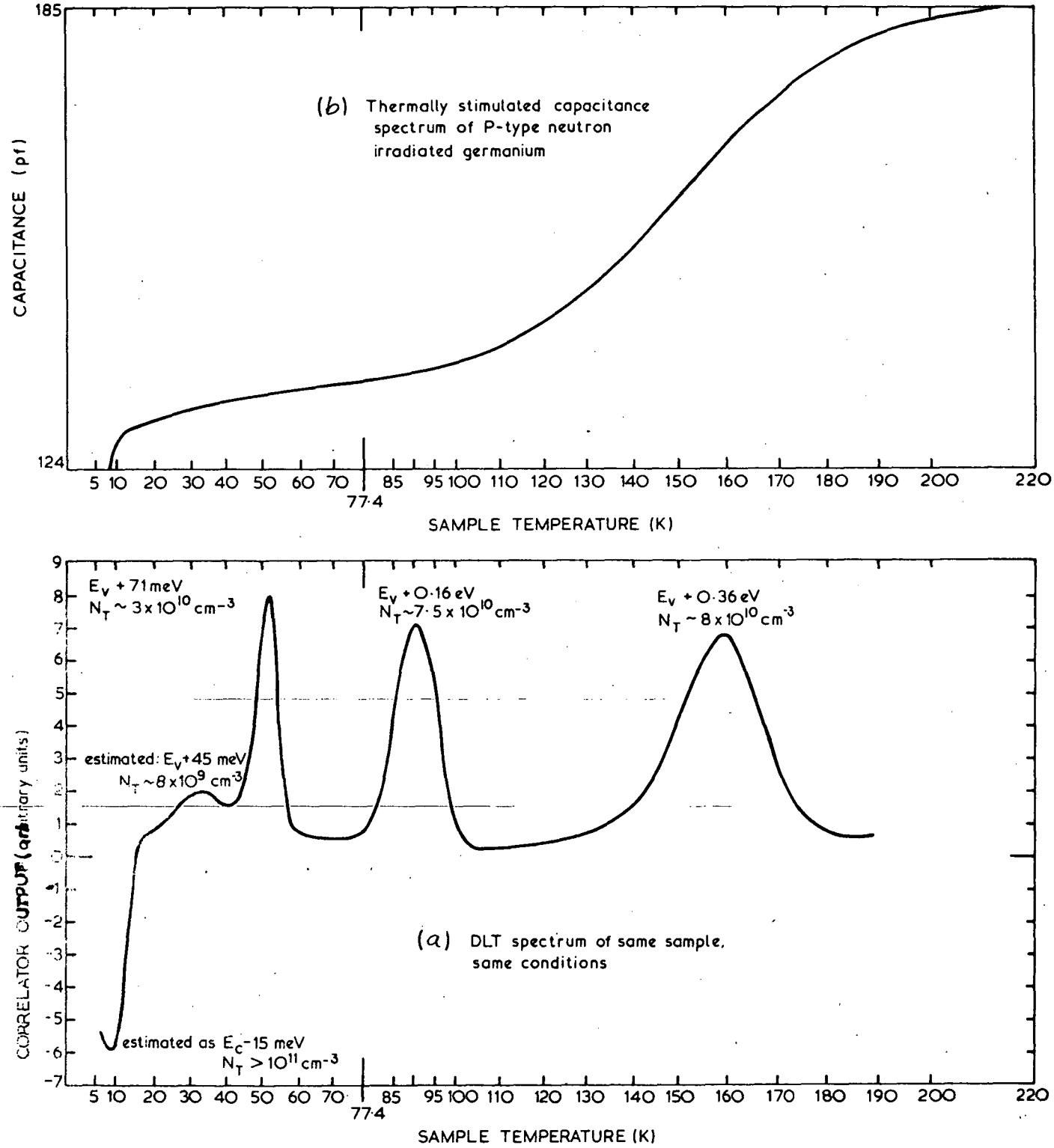
185
124
CAPACITANCE (pf)
(b) Thermally stimulated capacitance spectrum of P-type neutron irradiated germanium
5 10 20 30 40 50 60 70 85 95 100 110 120 130 140 150 160 170 180 190 200 220
77·4
SAMPLE TEMPERATURE (K)
E_V + 71 meV
$N_T \sim 3 \times 10^{10}$ cm^{-3}
E_V + 0·16 eV
$N_T \sim 7{\cdot}5 \times 10^{10}$ cm^{-3}
E_V + 0·36 eV
$N_T \sim 8 \times 10^{10}$ cm^{-3}
estimated: E_V + 45 meV
$N_T \sim 8 \times 10^{9}$ cm^{-3}
CORRELATOR OUTPUT (arbitrary units)
(a) DLT spectrum of same sample, same conditions
estimated as E_C − 15 meV
$N_T > 10^{11}$ cm^{-3}
9 8 7 6 5 4 3 2 1 0 -1 -2 -3 -4 -5 -6 -7
5 10 20 30 40 50 60 70 85 95 100 110 120 130 140 150 160 170 180 190 200 220
77·4
SAMPLE TEMPERATURE (K)

Figure 2.

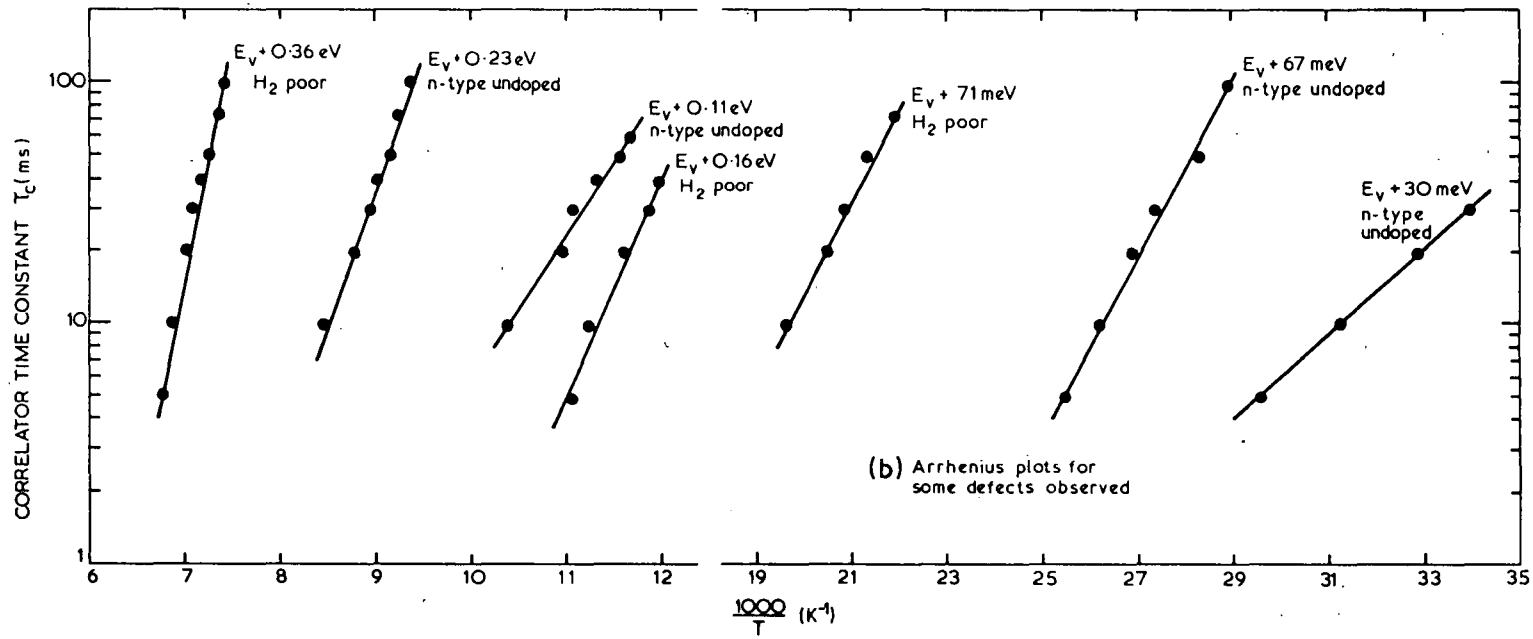
CORRELATOR TIME CONSTANT τ_c (ms)
100
10
1
E_v + 0·36 eV
H_2 poor
E_v + 0·23 eV
n-type undoped
E_v + 0·11 eV
n-type undoped
E_v + 0·16 eV
H_2 poor
E_v + 71 meV
H_2 poor
E_v + 67 meV
n-type undoped
E_v + 30 meV
n-type
undoped
(b) Arrhenius plots for
some defects observed
6
7
8
9
10
11
12
19
21
23
25
27
29
31
33
35
$\frac{1000}{T}$ (K^{-1})

Figure 3

DLTS scans). It has been suggested previously that the charge of a radiation induced defect can affect its annealing behaviour [Baruch 1961]. Thus one possible explanation is that on the first DLTS scans the diodes were taken below the freeze-out temperature of the defects involved and, being in the neutral state, they proceeded to anneal. This could be useful in the repair of particle-damaged detectors: to leave them for a period of hours with a slight forward bias to inject minority carriers in n-type material and, in the case of HPGe detectors, to cycle them in temperature. It may be necessary for the application of bias (changing the Fermi level) before the traps are formed, and on going below freeze-out that they convert to an electrically inactive complex, in which state they remain.

No levels were observed in the p-type sample grown under an atmosphere of H_2, while its companion from the same crystal which was heated under N_2 to remove H_2, showed three levels (E_v + 71 MeV, E_v + 0.16 eV, E_v + 0.36 eV). The effect of hydrogen 'tying-up' dangling bonds produced by the radiation damage may be an explanation for this result, but one cannot speculate further on the basis of two samples.

Another feature of the experiment was the observation in two samples of the inversion of the transient capacitance signal from the Boonton 71A bridge. One explanation could be that p-type regions are present in the bulk n-type material. These could have been formed by radiation induced decompensation of originally slightly p-type regions, or the conversion of originally slightly n-type regions. The effect has been observed previously in neutron irradiated Ge [Evseev et al. 1977].

The charge carrier trapping centres formed cannot completely account for the observed free carrier compensation, indicating that

neutral complexes were formed, as with γ-compensated Ge. In all cases, the density of neutral complexes is of the same order of magnitude as the electrically active defect population.

DLTS measurements therefore reveal significant numbers of point defects produced by fast neutron and proton irradiation of Ge. Point defect densities of 10^9 to 10^{11} cm^{-3} for a neutron flux of $\sim 10^8$ neutrons/cm^2 were observed. It is possible these could have an important effect in the resolution transients observed in Ge radiation detectors [Darken et al. 1980].

REFERENCES

Adair, R. K. [1950] - Rev. Mod. Phys. 22:249.

Baruch, P. [1961] - J. Appl. Phys. 32:653.

Darken, L. S., Trammell, R. C., Raudorf, T. W., Pehl, R. H. and Elliott, J. H. [1980] - Nucl. Instr. and Meth. 171:49.

Evseev, V. G., Konopleva, R. F. and Yuferev, A. A. [1977] - Radiation Effects in Semiconductors 1976, IOP Conf. Series 31, pp. 319-325.

Hicks, D. B. and Jacobsen, A. S. [1974] - IEEE Trans. Nucl. Sci. 21(1)169.

Ishino, S. and Matsutani, Y. [1977] - Inst. of Phys. Conf. Series 31, 292.

Kraner, H. W. [1980] - IEEE Trans. Nucl. Sci. 27(1)218 and references contained therein.

Kraner, H. W., Chasman, C. and Jones, K. W. [1967] - Semiconductor Nuclear Particle Detectors and Circuits, eds. W. L. Brown et al. (National Academy of Science, Washington) pp. 339-361.

Kraner, H. W., Chasman, C. and Jones, K. W. [1968] - Nucl. Instr. and Meth. 62:173.

Lang, D. V. [1974] - J. Appl. Phys. 45:3023.

Pehl, R. H., Varnell, L. S. and Metzyer, A. E. [1978] - IEEE Trans. Nucl. Sci. 25:409.

CONCLUSIONS

This chapter makes no claim to being a complete work on radiation damage centres in Ge, only to being a start towards some clear knowledge of what the common levels in radiation damaged HP Ge are. The basic technique used has been DLTS, but obviously Hall effect results over a wide temperature range, careful isochronal and isothermal annealing experiments on the various damage levels, and infrared spectroscopy measurements, are also needed. Unnecessary speculation has been kept to a minimum, as radiation damage is complex and confusing enough without adding to it. The well-known sensitivity of the damage centres to background impurities and experimental conditions adds to this complexity. We have performed the work from the context of Ge for nuclear irradiation detectors, and confusing comparisons with lower resistivity material have been avoided.

The one clear-cut result has been in γ-irradiated p-type Ge grown by the Czochralski technique from silica crucibles, under an H_2 atmosphere. Two levels are observed, due to oxygen-vacancy complexes. Studies on these levels could augment knowledge about the corresponding case in Si, and lead to a more general understanding of the interaction of defects and impurities in the elemental semiconductors.

CHAPTER 2

DEEP LEVEL DEFECTS IN GaAs

INTRODUCTION

Unambiguous identification of impurity levels in compound semiconductors is difficult because of stoichiometric problems, high concentrations of intrinsic lattice defects and impurity-defect interactions. As part of a program to fabricate solid state radiation detectors we had on hand small quantities of a wide range of n-type GaAs. However, with no active crystal growth program it was unrealistic to attempt to identify defects by controlled doping. Therefore in this Chapter, we investigate material of a wide range of purities, some of which was used to construct nuclear radiation detectors. The work is reported from that point of view, to give some feel for the effect of impurities on actual GaAs devices.

2.1 GaAs for Nuclear Radiation Detection

SUMMARY

Deep level transient spectroscopy (DLTS) has been applied for the first time to the study of deep level defects in n-GaAs nuclear radiation detectors. Devices made from commercial bulk and epitaxial material with net donor impurity densities in the range 5×10^{13} to 3×10^{16} cm^{-3} have been studied and several common levels observed. The Poole-Frenkel effect has been identified in three levels (E_v + 0.19 eV, E_c - 0.62 eV, E_c - 0.73 eV) in the epitaxial GaAs. A value for the Poole-Frenkel constant of $\beta = 4.7 \pm 1.4 \times 10^{-4}$ eV $V^{-\frac{1}{2}}$ $cm^{\frac{1}{2}}$ was obtained, compared to the theoretical value for GaAs of 2.3×10^{-4} eV $V^{-\frac{1}{2}}$ $cm^{\frac{1}{2}}$.

INTRODUCTION

The need for cooling of silicon and germanium nuclear gamma-radiation detectors, and their relatively low efficiency, are well-known. In an effort to overcome these disadvantages, attention has been focused on the production of detector grade crystals from the compound semiconductors GaAs, CdTe and HgI_2. Gallium arsenide detectors made from thin, high purity epitaxial layers (thickness ≈100 μm) were first demonstrated at the AAEC Research Establishment, Lucas Heights [Eberhardt et al. 1971]. High resolution operation was obtained up to approximately 100 keV γ-ray energy, but efficiencies were small because of the small active volumes (approximately 0.2 mm^3). The prospects for advancement of such detectors rely on the production of larger active volumes without a corresponding degradation in charge collection efficiency due to charge carrier trapping.

In this work, the technique of deep level transient spectroscopy (DLTS) [Lang 1974] has been used to study, for the first time, trapping levels in bulk, liquid phase epitaxial (LPE) and vapour phase epitaxial (VPE) n-GaAs for nuclear radiation detectors. The low net impurity density (approximately 5×10^{13} cm^{-3}) of some of the diodes, combined with the sensitivity of the technique (defect concentrations $<10^{-4}$ of the net background doping density) has allowed the observation of low level defect concentrations (down to 6×10^{9} cm^{-3} or 1 part in 10^{13} atomic concentration).

EXPERIMENTAL PROCEDURE

1. Material Preparation

Detector fabrication closely followed that of Eberhardt et al. [1971]. Some of the diodes used here had been used in the former work. Briefly, ohmic contacts were produced by alloying GaIn eutectic over the full wafer area (n^+ substrate for epitaxial samples) and rectifying

contacts formed by evaporating gold surface barriers of 2 mm diameter on the front face, after carefully polishing and etching with $3HNO_3:2H_2O:1HF$ at room temperature for ten seconds. Materials used in this study were grown by LPE at the Research Establishment and the Standard Telecommunications Laboratory (UK) and VPE at the Massachusetts Institute of Technology, USA; commercially produced bulk synthesis material was acquired from MCP Electronics Pty Ltd (UK). Twenty-five diodes were examined, with net impurity densities in the range 5×10^{13} to 3×10^{16} cm^{-3}.

2. Measurements

The experimental arrangement has been described elsewhere [Pearton et al. 1980]. Briefly, a fast capacitance bridge (Boonton model 71A) measures the exponential capacitance transients caused by pulsed reduction of the reverse bias on the sample diode. An electronic correlator [Miller et al. 1975] matches the decay of these transients with its own internally generated exponential waveform, producing a maximum output when this weighting function coincides with the decay of a particular trap. A trap spectrum is obtained by scanning the sample diode temperature. The emission rate e_n for an electron is given by

$$e_n = \frac{\sigma_n \langle v_n \rangle N_c}{g} \exp\left(-\frac{\Delta E}{kT}\right) \qquad (1)$$

where σ_n = capture cross section of trap, $\langle v_n \rangle$ = average thermal velocity of carrier, N_c = density of states in the conduction band, g = degeneracy of level (assumed = 2), ΔE = energy separation of defect from conduction band edge, k = Boltzmann's constant, and T = absolute temperature.

An appropriate correction [Miller et al. 1977] to the slope obtained from an Arrhenius plot gives the activation energy of the

level; the capture cross section may be derived from the intercept of such a graph. Cross sections may be measured directly by observing the change in correlator output for changes in bias pulse width, and defect concentrations can be profiled by measuring the change in correlator output for changes in bias pulse amplitude [Lang 1974]. A light-emitting diode (LED) is used to introduce minority carriers into the Schottky barrier structure.

DISCUSSION

1. General

Table 1 lists the measured trap parameters and possible identifications and comparisons. Defects are labelled by their peak temperatures for a correlator time constant of 10 ms. Estimated levels have been obtained assuming an exponential prefactor of 10^{12} in equation (1) [Lang et al. 1976]. The data have been corrected for the temperature dependence of the product $\langle v_n \rangle N_c$ but no correction has been made for the possible temperature dependence of the cross section, although in isolated levels this may be significant [Lang and Logan 1975]. Typically, the most probable errors (obtained from least squares fitting) for the activation energies of the traps are ±7 per cent, ±30 per cent for the cross sections, and ±25 per cent for the concentrations. For the estimated activation energies, the most probable errors are ±10 per cent.

To give some feel for the purity of the material, spark source mass spectrometry (SSMS) results of three low resistivity samples (MCP bulk material and two sealed tube vapour transport grown crystals) are shown in Tables 2- 4. For this low resistivity material Al, Mg, Ca, Si, K and P are common contaminants.

The common impurities iron, copper and chromium, are evident, as well as the unidentified levels A and B [Lang and Logan 1976]. The

TABLE 1

MEASURED TRAP PARAMETERS

(a) LPE Material

Defect	Level (eV)	σ (cm^2) Direct Measure	σ (cm^2) From Intercept	Trap Density N_T(cm^{-3})	Net Doping Density n(cm^{-3}) of Particular Sample	Observations and Comparisons
28	E_c - 59 meV	-	-	2×10^{10}/6.2×10^{9}	5.5×10^{13} (77 K)/	
77	E_c - 0.13	1.2×10^{-17}	2.5×10^{-16}	4.5×10^{11}/2.1×10^{11}	1.03×10^{14} (295 K)	
194	E_v + 0.42	-	2.9×10^{-15}	2.5×10^{12}	1.8×10^{14} (295 K)	(a) Level A
168	E_c - 0.36	-	3.2×10^{-14}	1.7×10^{11}		
208	E_c - 0.38	1.2×10^{-17}	1.3×10^{-16}	7.5×10^{11}	$5.1\text{-}6.0 \times 10^{13}$ (77 K)	
254	E_c - 0.59	2.3×10^{-15}	1.4×10^{-13}	9.9×10^{11}	$5.8\text{-}7.2 \times 10^{13}$ (295 K)	
310	E_c - (0.73-0.78)	6.1×10^{-15}	3.8×10^{-14}	1.5×10^{12}		(b) Cr
278 (est.)	E_v + 0.55	-	-	1.9×10^{12}	5.3×10^{13} (77 K)	(c) Fe
275 (100 ms)	E_v + 0.60	-	-	2.4×10^{12}	6.1×10^{13} (295 K)	
196	E_v + 0.45	-	3.8×10^{-14}	4.8×10^{12}	5.2×10^{13} (77 K)	(a) Cu
310 (est.)	E_v + 0.70	-	-	3.2×10^{12}	7.9×10^{13} (295 K)	(b) Level B
98	E_v + 0.27	-	$\sim 5 \times 10^{-18}$	8.4×10^{10}	7.4×10^{13} (77 K)	
149	E_v + 0.35	-	6.7×10^{-17}	3.0×10^{11}	8.7×10^{13} (295 K)	
189	E_c - 0.51	-	5.4×10^{-12}	5.1×10^{12}		
280	E_v + 0.59	3.1×10^{-18}	2.0×10^{-18}	4.1×10^{12}		
239	E_v + 0.19	2.9×10^{-19}	7.2×10^{-22}	1.3×10^{13}	3.4×10^{14} (77 K)	
91 (est.)	E_c - 0.21	-	-	4.5×10^{13}		
126	E_c - 72 meV	4.9×10^{-19}	2.7×10^{-22}	6.8×10^{13}	3×10^{15} (77 K)	
192	E_c - 0.46	$\sim 5 \times 10^{-13}$	1.7×10^{-13}	3.9×10^{13}	4.4×10^{15} (300 K)	

Material grown at : AAEC Research Establishment

Standard Telecommunications Laboratory (UK)

TABLE 1 (Continued)

(b) Bulk Material

Defect	Level (ev)	Direct Measure (cm^2)	From Intercept (cm^2)	Trap Density $N_T(cm^{-3})$	Net Doping Density $n(cm^{-3})$ of Particular Sample	Observations and Comparisons
42 (est.)	E_c - 83 meV	-	-	1.3×10^{13}	1.2×10^{16} (77 K)	
173	E_c - 0.37	5.2×10^{-15}	1.5×10^{-14}	2.8×10^{15}	1.2×10^{16} (77 K)	Seen in LPE
267	E_c - 0.70	1.3×10^{-14}	1.3×10^{-13}	2.1×10^{14}	2.2×10^{16} (297 K)	Cr, seen in LPE
75 (est.)	E_v + 0.14	-	-	6.1×10^{12}		
114 (est.)	E_v + 0.22	-	-	5.1×10^{12}	7.9×10^{14} (77 K)	
155 (est.)	E_v + 0.30	-	-	2.5×10^{13}	1.9×10^{15} (300 K)	
216	E_v + 0.20	-	8×10^{-21}	1.7×10^{14}		
186	E_v + 0.40	-	4.1×10^{-14}	3.0×10^{14}	2.5×10^{14} (77 K)	Level A
198	E_v + 0.44	-	1.1×10^{-15}	2.4×10^{14}	4.3×10^{14} (300 K)	Cu, seen in LPE
223	E_v + 0.57	-	6.8×10^{-15}	4.2×10^{12}	6.5×10^{13} (77 K)	Fe, seen in LPE
302	E_c - 0.73	-	6.4×10^{-14}	2.8×10^{12}	8.2×10^{13} (300 K)	Cr, seen in LPE
	Material grown at : MCP Electronics Pty Ltd (UK), AAEC-RE					

(c) VPE Material

Defect	Level (ev)	Capture Cross Section (cm^2) Direct Measure	Capture Cross Section (cm^2) From Intercept	Trap Density $N_T(cm^{-3})$	Net Doping Density $n(cm^{-3})$ Particular Sample	Observations and Comparisons
100	E_v + 0.18	-	8.4×10^{-17}	4.3×10^{11}		
165	E_c - 0.36	-	2.7×10^{-15}	1.6×10^{11}		Seen in LPE, Bulk
204	E_c - 0.40	1.4×10^{-17}	9.4×10^{-16}	5.4×10^{11}		Seen in LPE
306	E_c - 0.62	3.0×10^{-17}	1.1×10^{-16}	3.2×10^{12}	$1.03\text{-}2.50 \times 10^{14}$ (77 K)	
290 (100 ms)	E_c - 0.73	-	-	2.1×10^{12}		Cr, seen in LPE, Bulk
28	E_c - 59 meV	-	-	6.2×10^{9}		Seen in LPE
77	E_c - 0.13	1.2×10^{-17}	2.5×10^{-16}	2.1×10^{11}		Seen in LPE
	Material grown at : Massachusetts Institute of Technology					

(a) Lang et al. [1976]

(b) Lang and Logan [1976]

(c) Lang [1974]

TABLE 2.

SPARK SOURCE MASS SPECTROMETRY

REPORT SHEET

REPORT NO: 249 SAMPLE GaAs (VAPOUR PHASE - AAEC)

PLATE NO: 570

SAMPLE NO: 78/3125 (GaAs - VP - 78 - 40)

Element	ppm wt	Element	ppm wt
Lithium	< 0.002	Silver	< 0.06
Beryllium	< 0.002	Cadmium	< 0.1
Boron	< 0.004	Indium	< 0.03
Fluorine	—	Tin	< 0.1
Sodium	Interference	Antimony	< 0.06
Magnesium	< 0.008	Iodine	< 0.03
Aluminium	0.007	Tellurium	< 0.1
Silicon	0.03	Cesium	< 0.04
Phosphorus	< 0.008	Barium	< 0.05
Sulphur	—	Lanthanum	< 0.04
Chlorine	—	Cerium	< 0.04
Potassium	0.1	Praseodymium	< 0.04
Calcium	0.01	Neodymium	< 0.1
Scandium	< 0.01	Samarium	< 0.2
Titanium	< 0.02	Europium	< 0.08
Vanadium	< 0.01	Gadolinium	< 0.2
Chromium	< 0.02	Terbium	< 0.04
Manganese	< 0.01	Dysprosium	< 0.2
Iron	< 0.02	Holmium	< 0.04
Nickel	< 0.06	Erbium	< 0.1
Cobalt	< 0.02	Thulium	< 0.04
Copper	< 0.02	Ytterbium	< 0.1
Zinc	< 0.04	Lutecium	< 0.05
Gallium	MATRIX	Hafnium	< 0.1
Germanium	Contamination	Tantalum	Contamination
Arsenic	MATRIX	Tungsten	< 0.2
Bromine	< 0.04	Rhenium	< 0.08
Selenium	< 0.04	Osmium	< 0.2
Rubidium	< 0.03	Iridium	< 0.08
Strontium	< 0.09	Platinum	< 0.2
Yttrium	< 0.2	Gold	< 0.5
Zirconium	< 0.1	Mercury	< 0.2
Niobium	< 0.02	Thallium	< 0.08
Molybdenum	< 0.1	Lead	< 0.1
Ruthenium	< 0.08	Bismuth	< 0.05
Rhodium	< 0.03	Thorium	< 0.06
Palladium	< 0.1	Uranium	< 0.06

ANALYST: AR

CHECKED: [signature]

COMMENTS: .....

.....

TABLE 3. REPORT SHEET

REPORT NO: 217 SAMPLE Ga As (VAPOUR PHASE, AAEC)

PLATE NO: 496

SAMPLE NO: 77-1002

Element	ppm wt	Element	ppm wt
Lithium	<0.0007	Silver	<0.02
Beryllium	<0.0008	Cadmium	CONTAMINATION *
Boron	<0.005	Indium	<0.01
Fluorine	-	Tin	<0.04
Sodium	*	Antimony	<0.02
Magnesium	0.008	Iodine	<0.01
Aluminium	0.002	Tellurium	CONTAMINATION *
Silicon	0.003	Cesium	<0.01
Phosphorus	0.08	Barium	<0.02
Sulphur	0.09	Lanthanum	<0.01
Chlorine	-	Cerium	*
Potassium	0.04	Praseodymium	<0.01
Calcium	0.004	Neodymium	<0.05
Scandium	<0.004	Samarium	<0.05
Titanium	<0.006	Europium	<0.03
Vanadium	<0.004	Gadolinium	<0.06
Chromium	<0.005	Terbium	<0.01
Manganese	*	Dysprosium	<0.05
Iron	0.2	Holmium	<0.01
Nickel	*	Erbium	<0.04
Cobalt	0.005	Thulium	<0.02
Copper	0.08	Ytterbium	<0.05
Zinc	0.1	Lutecium	<0.02
Gallium	MATRIX	Hafnium	<0.04
Germanium	<0.02	Tantalum	CONTAMINATION
Arsenic	MATRIX	Tungsten	<0.05
Bromine	-	Rhenium	<0.03
Selenium	<0.01	Osmium	<0.06
Rubidium	<0.01	Iridium	<0.03
Strontium	<0.009	Platinum	<0.05
Yttrium	<0.008	Gold	0.02
Zirconium	<0.02	Mercury	<0.06
Niobium	<0.008	Thallium	<0.03
Molybdenum	<0.04	Lead	<0.03
Ruthenium	<0.03	Bismuth	<0.02
Rhodium	<0.009	Thorium	<0.02
Palladium	<0.03	Uranium	<0.02

ANALYST: JR

CHECKED: JR

COMMENTS: * Interference

* Contamination from previous CdTe samples

TABLE 4. SPARK SOURCE MASS SPECTROMETRY

REPORT SHEET

REPORT NO: 230 SAMPLE GaAs (COMMERCIAL MCP MATERIAL)

PLATE NO: 518

SAMPLE NO: 78-741

Element	ppm wt	Element	ppm wt
Lithium	< 0.0007	Silver	< 0.02
Beryllium	< 0.0008	Cadmium	< 0.03
Boron	< 0.001	Indium	< 0.01
Fluorine	–	Tin	< 0.04
Sodium	*	Antimony	< 0.02
Magnesium	0.003	Iodine	< 0.01
Aluminium	0.007	Tellurium	< 0.03
Silicon	0.03	Cesium	< 0.01
Phosphorus	0.003	Barium	< 0.02
Sulphur	0.009	Lanthanum	< 0.01
Chlorine	0.04	Cerium	< 0.01
Potassium	0.1	Praseodymium	< 0.01
Calcium	0.01	Neodymium	< 0.05
Scandium	< 0.004	Samarium	< 0.05
Titanium	< 0.006	Europium	< 0.03
Vanadium	< 0.004	Gadolinium	< 0.06
Chromium	0.005	Terbium	< 0.01
Manganese	< 0.005	Dysprosium	< 0.05
Iron	0.005	Holmium	< 0.01
Nickel	< 0.007	Erbium	< 0.04
Cobalt	< 0.005	Thulium	< 0.02
Copper	< 0.008	Ytterbium	< 0.05
Zinc	0.01	Lutecium	< 0.02
Gallium	MATRIX	Hafnium	< 0.04
Germanium	CONTAMINATION	Tantalum	CONTAMINATION
Arsenic	MATRIX	Tungsten	< 0.05
Bromine	< 0.01	Rhenium	< 0.03
Selenium	< 0.01	Osmium	< 0.06
Rubidium	< 0.01	Iridium	< 0.03
Strontium	*	Platinum	< 0.05
Yttrium	*	Gold	0.02
Zirconium	< 0.05	Mercury	< 0.06
Niobium	< 0.008	Thallium	< 0.03
Molybdenum	< 0.04	Lead	< 0.03
Ruthenium	< 0.03	Bismuth	< 0.02
Rhodium	< 0.009	Thorium	< 0.02
Palladium	< 0.03	Uranium	< 0.02

ANALYST: R

CHECKED:

COMMENTS: * INTERFERENCE

Zn result is near detection limit

latter levels did not appear together in all LPE samples and were completely absent from several diodes. Defect 28 (E_c - 59 meV), seen in both LPE and VPE materials, has been observed at a level of 6×10^{-5} of the background doping density. The level at E_c - (0.75-0.83) eV, commonly assigned in the past to oxygen, was not observed as it typically occurs at approximately 350 K under the conditions used here and levels were recorded only in the range 5-320 K. Useful tabulations of data on hole and electron traps in bulk and epitaxial GaAs crystals have been published by Martin et al. [1977], and Mitonneau et al. [1977].

Figures 1 to 4 show typical DLT spectra obtained from the bulk and epitaxial GaAs crystals. Figure 2 shows an LPE sample with trap levels at 77 K and room temperature which would most likely degrade its spectral response. In germanium, trapping and retention of 10^{-4} of the charge released by ionising radiation leads to tailing on energy spectrum peaks [Haller et al. 1979]. Here, the ratio of trap density to net doping density is approximately 10^{-2} and, even allowing for differences in carrier mobilities, the effect of charge trapping would most likely be evident at peak trap temperatures. The detector gave its best energy resolution when operated at 122 K (see Figure 7 of Eberhardt et al. [1971])- 1.1 per cent FWHM and worsened to 4.2 per cent FWHM at 300 K. The similarity between the defect spectra of VPE (Figure 4) and LPE (Figure 2) samples is quite striking, arguing for common contaminants such as those seen in the SSMS results, or intrinsic defects being responsible.

Figure 5 displays the Arrhenius plots for some of the more common defect levels measured. The activation energy of the trap is obtained from the slope of these graphs. Figure 6 shows the data used to measure the capture cross section of the defect centres. From Figure 7 Figure 7

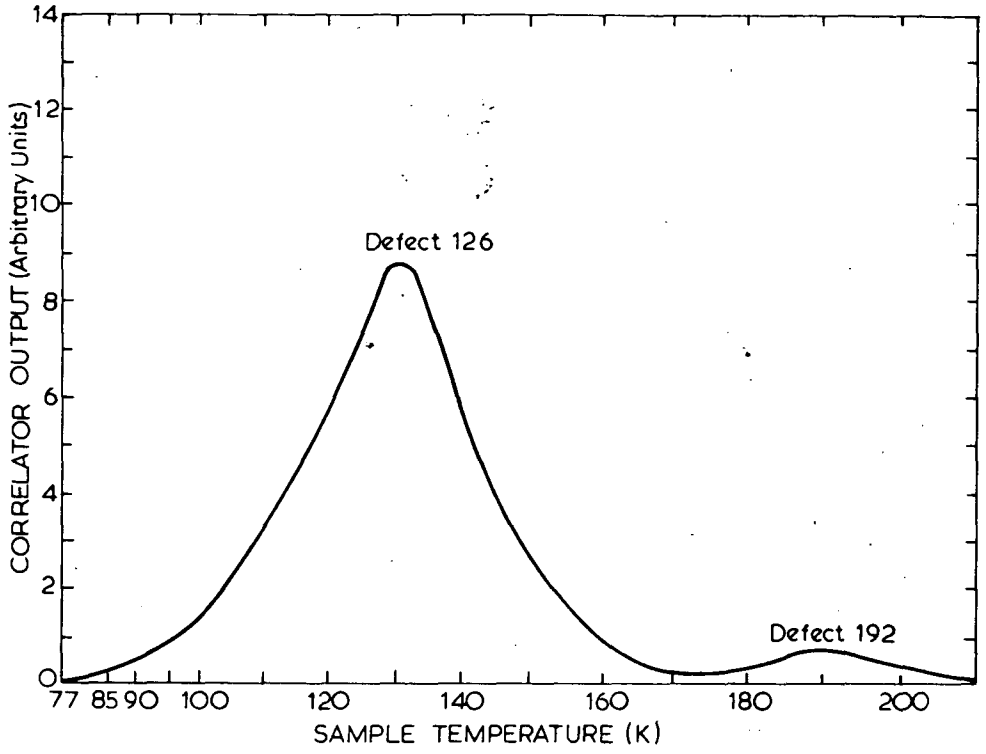

FIGURE 1. A TYPICAL DLT SPECTRUM OF AAECRE LPE n-GaAs (73-10) FOR A CORRELATOR TIME CONSTANT OF τ_c = 5 ms AND REVERSE BIAS OF 15 V

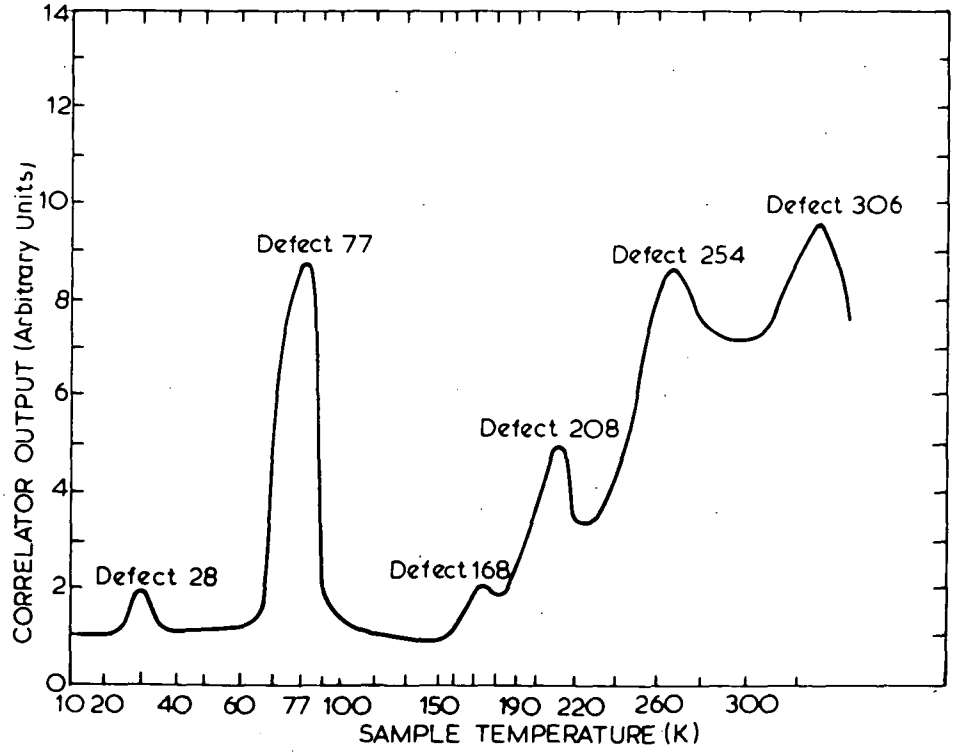

FIGURE 2. A TYPICAL DLT SPECTRUM OF SIL LPE n-GaAs (No. 5) FOR A CORRELATOR TIME CONSTANT OF τ_c = 5 ms AND REVERSE BIAS OF 30 V

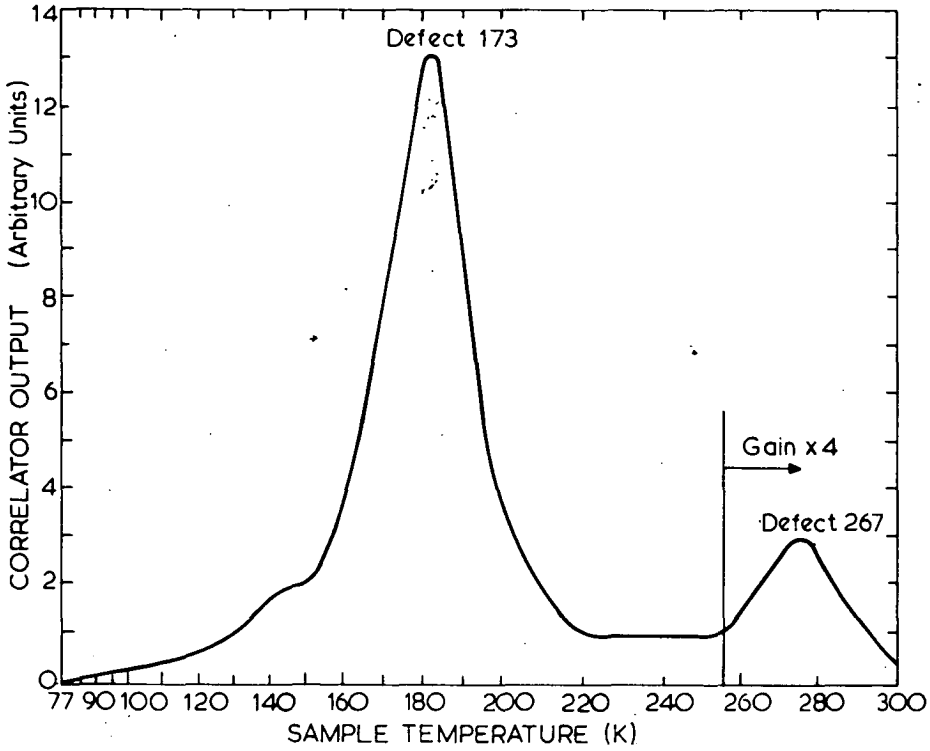

FIGURE 3. DLT SPECTRUM OF BULK n-GaAs FOR A CORRELATOR TIME CONSTANT OF τ_c = 5 ms AND REVERSE BIAS OF 10 V

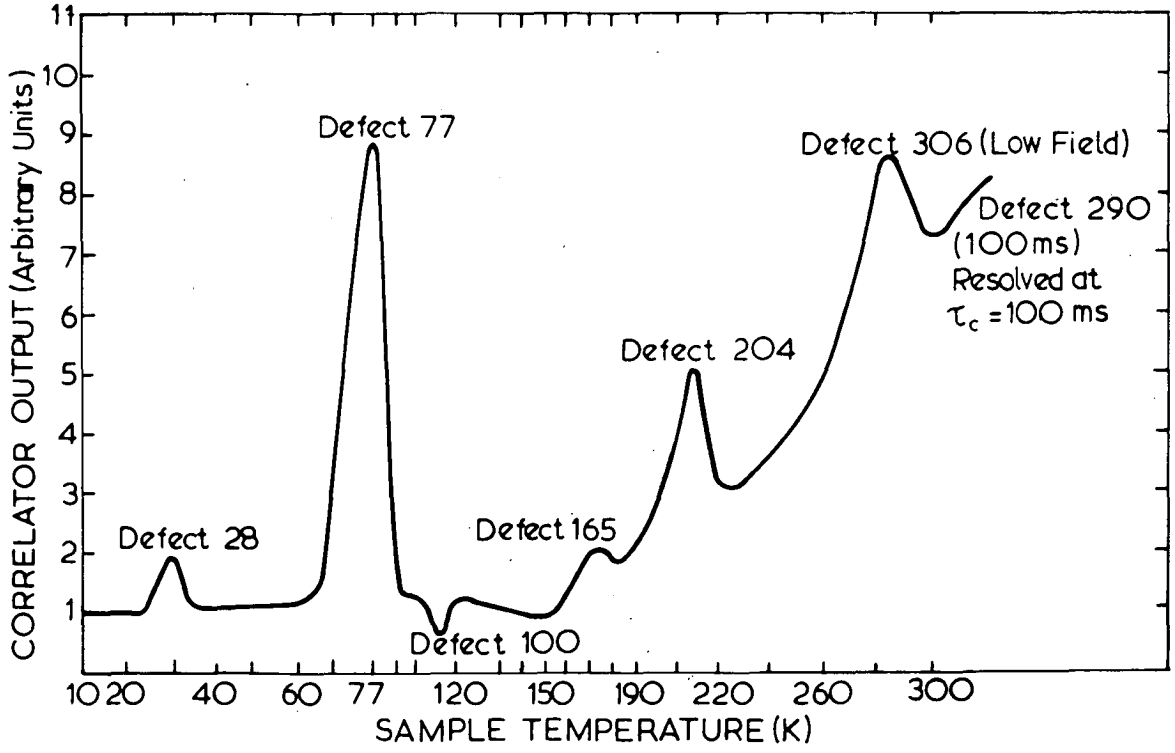

FIGURE 4. DLT SPECTRUM OF MIT VPE n-GaAs (No. 15) FOR A CORRELATOR TIME CONSTANT OF τ_c = 10 ms AND REVERSE BIAS OF 30 V

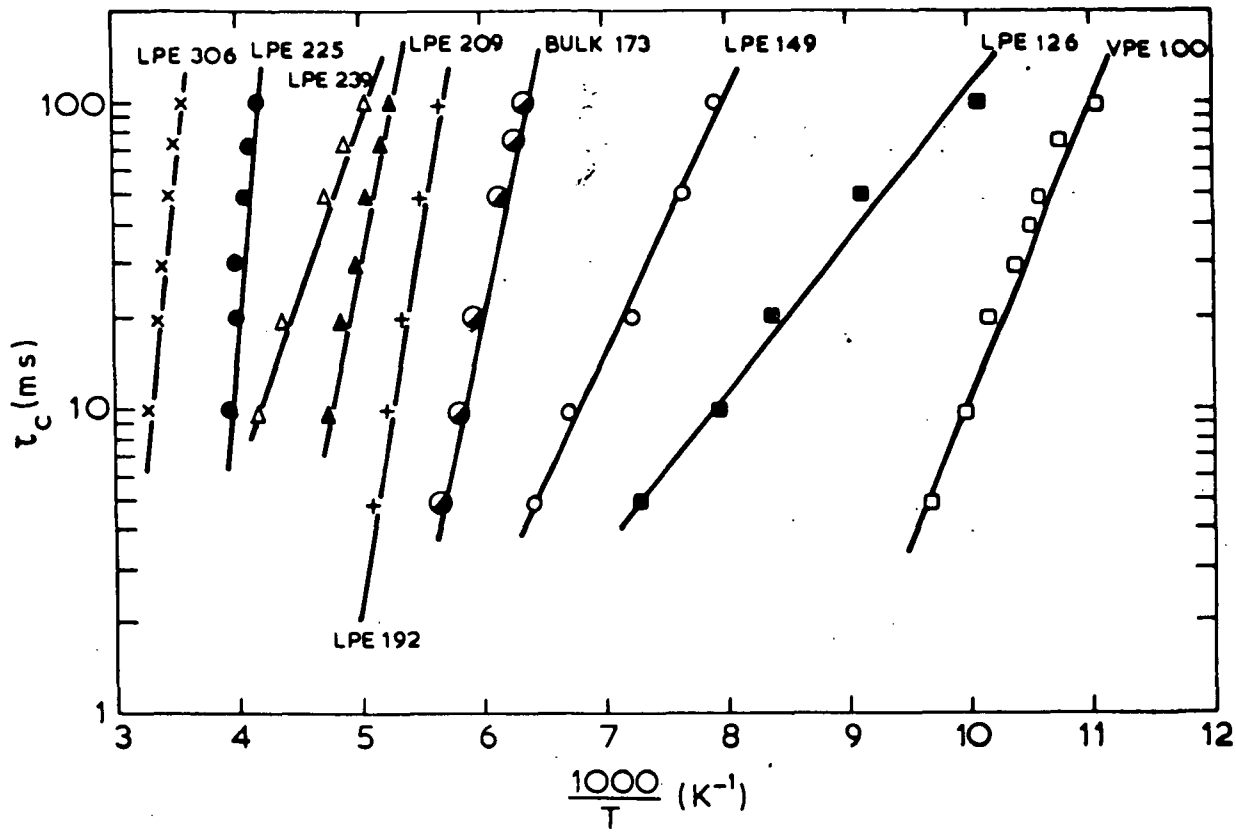

FIGURE 5. ARRHENIUS PLOTS FOR SOME OF THE DEFECT LEVELS OBSERVED IN n-GaAs

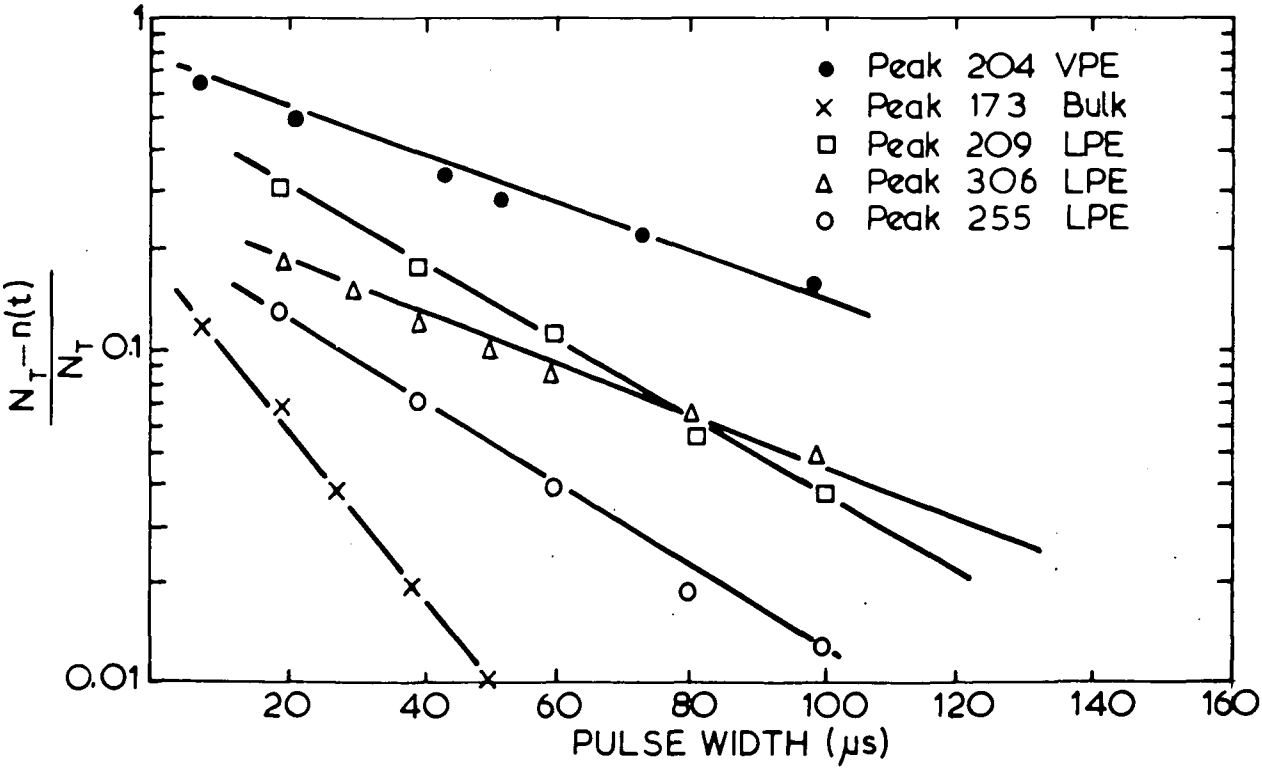

FIGURE 6. RELATIVE SIGNAL OUTPUT v. PULSE WIDTH FOR SOME DEFECT LEVELS

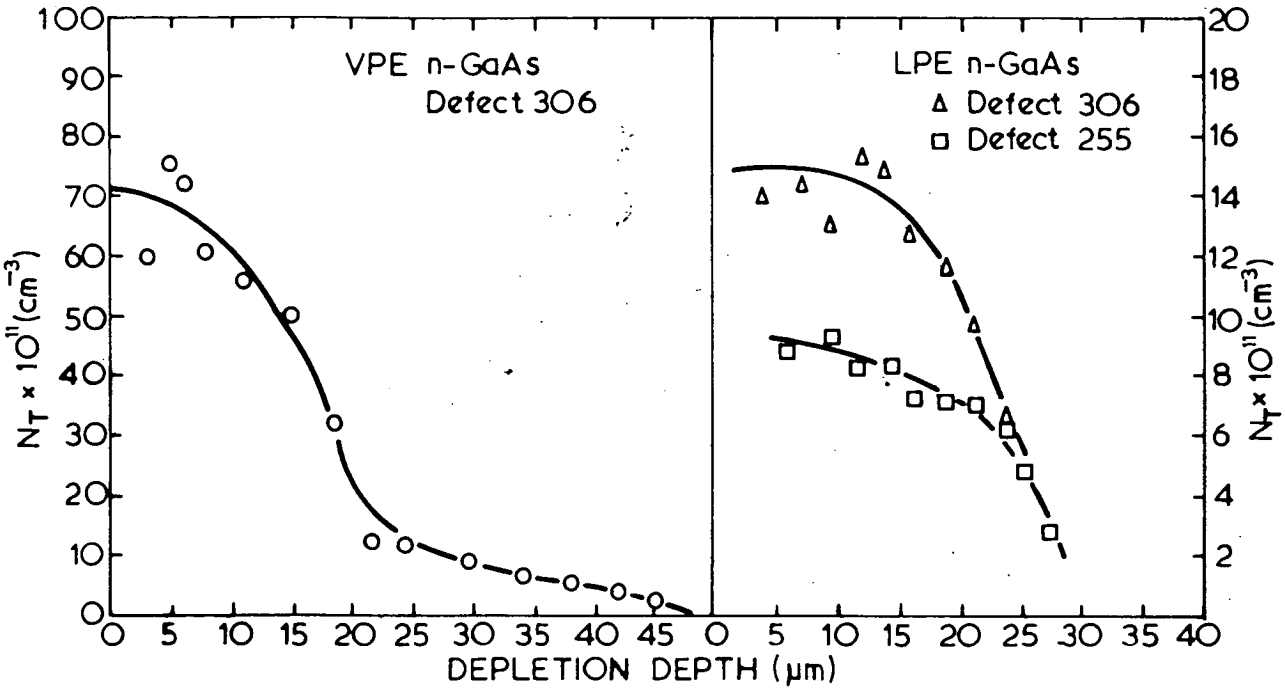

FIGURE 7. CONCENTRATION PROFILES OF SOME DEFECTS

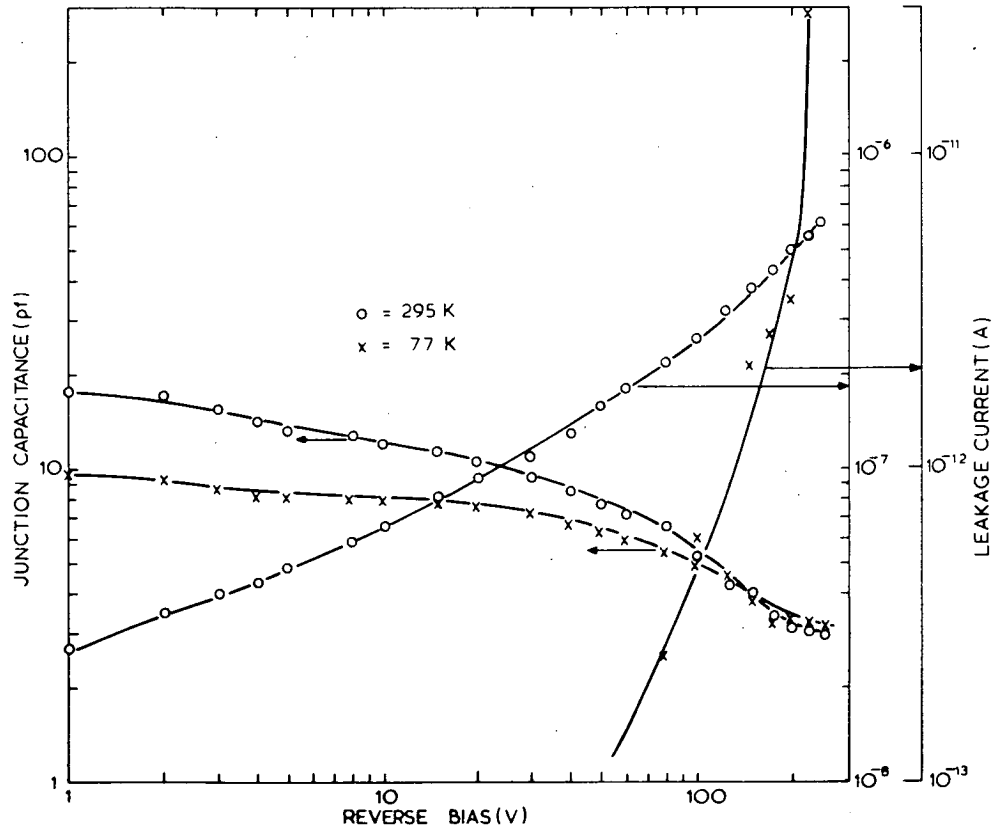

FIGURE 8. LEAKAGE CURRENT AND JUNCTION CAPACITANCE vs. REVERSE BIAS FOR STL LPE n-GaAs (No. 13)

it is seen that surface contamination during processing, or possibly the in-diffusion of chemical impurities during the crystal growth, caused some of the deep levels, resulting in a trap concentration profile that decreases away from the surface. Concentration profiles are more accurately measured using double correlation DLTS (DDLTS) in the constant capacitance mode, which does not suffer from the effect of the depletion width changing significantly as the traps unload [Johnson et al. 1979]. However, the defect concentrations here are so low that this effect has no bearing on the resulting profiles. Figure 8 shows leakage current and junction capacitance versus reverse bias for a typical GaAs detector. The values are comparable to those obtained when this particular detector was constructed in 1971.

On depleting to the anomalous interface region between epitaxial layer and substrate on some LPE samples [Eberhardt et al. 1971], a large number of closely spaced and mostly unresolved peaks were obtained. Copper was definitely identified as one of the impurities [Lang and Logan 1975]. Interface states have been studied by conventional DLTS [Lang and Logan 1977].

2. Field-enhanced Emission

Figures 9 and 10 show the effect of increasing the electric field on the emission rate from defect 306 (E_c - 0.62 eV). The variation in slopes of the various Arrhenius plots is not understood. At least two mechanisms may be involved in field-assisted detrapping:

(i) The Poole-Frenkel effect - lowering the Coulomb potential well by a sufficiently high electric field [Frenkel 1938; Hartke 1968].

(ii) The tunnel effect, leading to a temperature-independent detrapping time.

The Poole-Frenkel effect leads to the relation

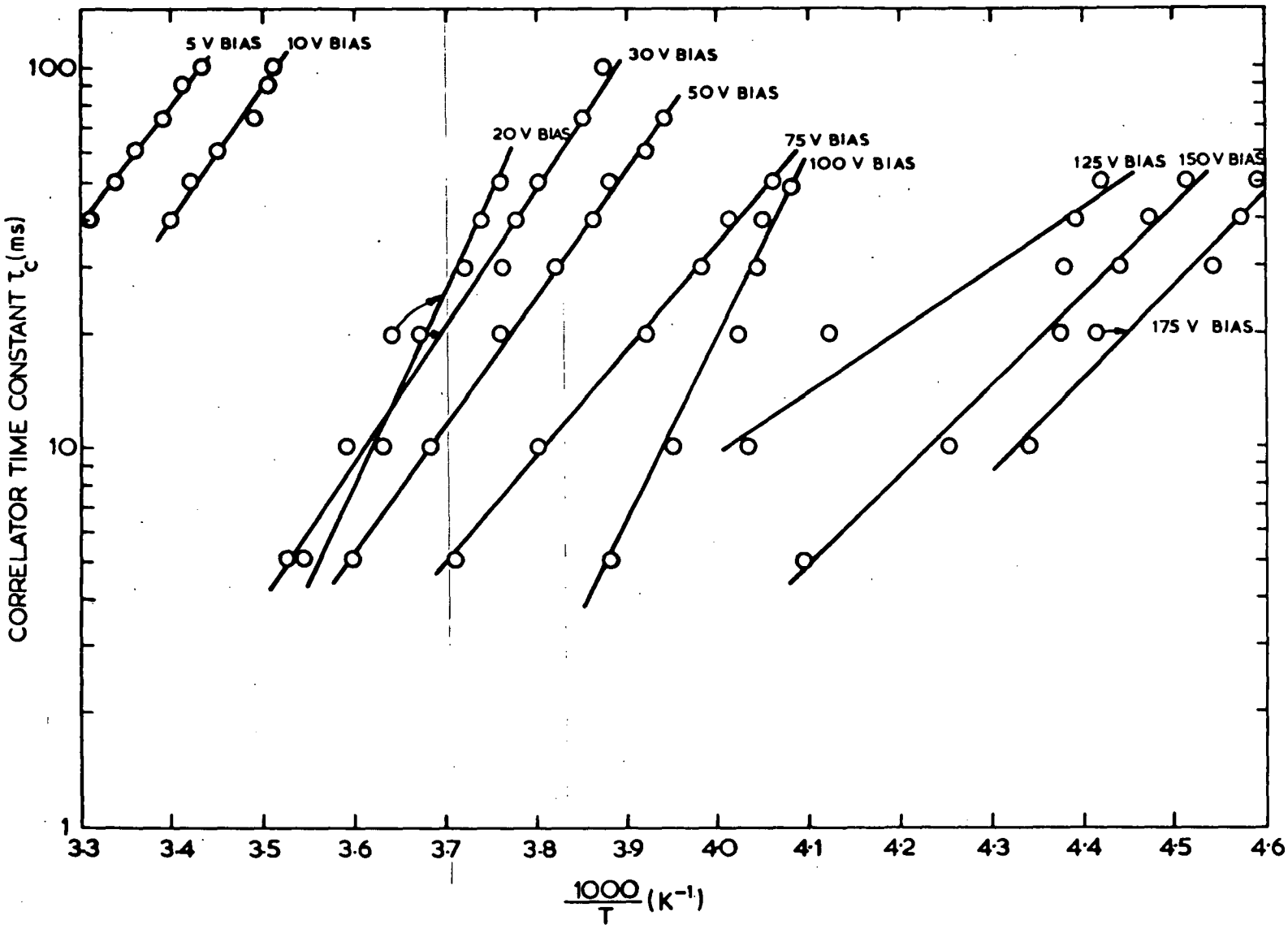

FIGURE 9. BIAS DEPENDENCE OF ARRHENIUS PLOTS FOR DEFECT 306 IN VPE n-GaAs

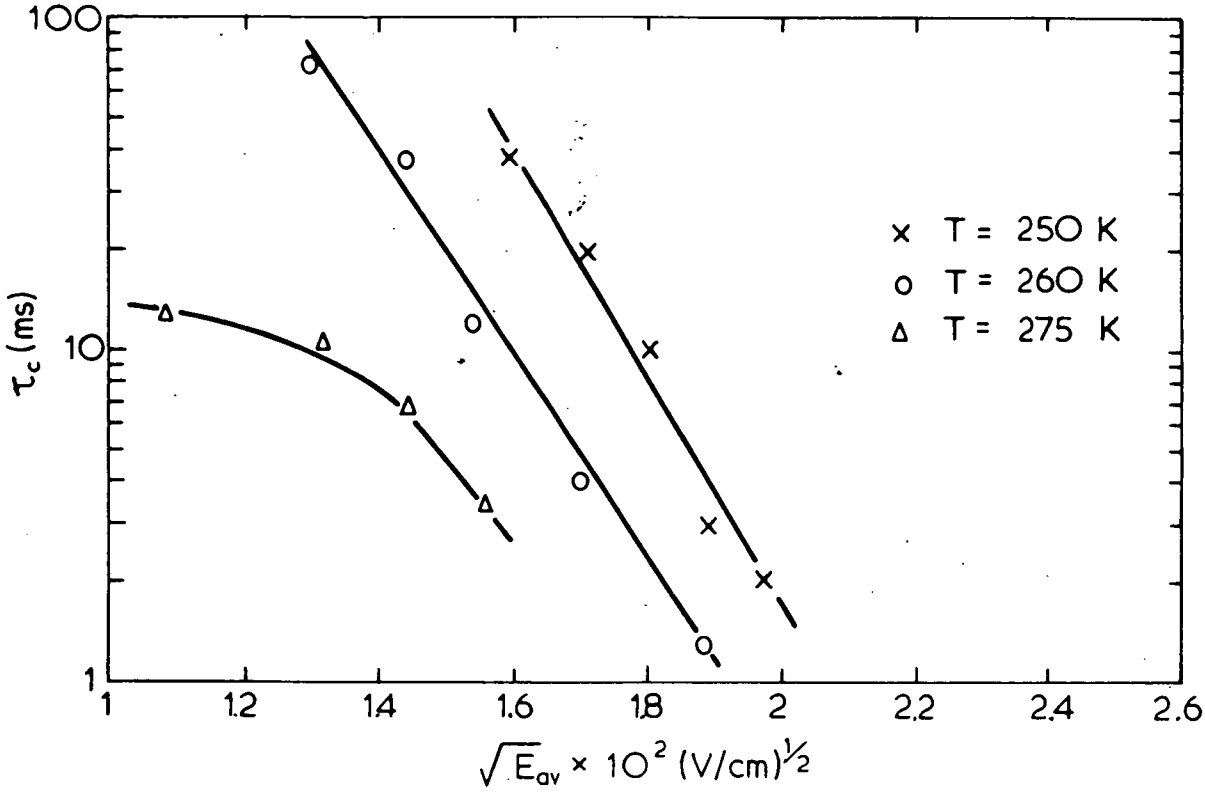

FIGURE 10. BIAS DEPENDENCE OF EMISSION RATE FOR DEFECT 306 IN VPE n-GaAs

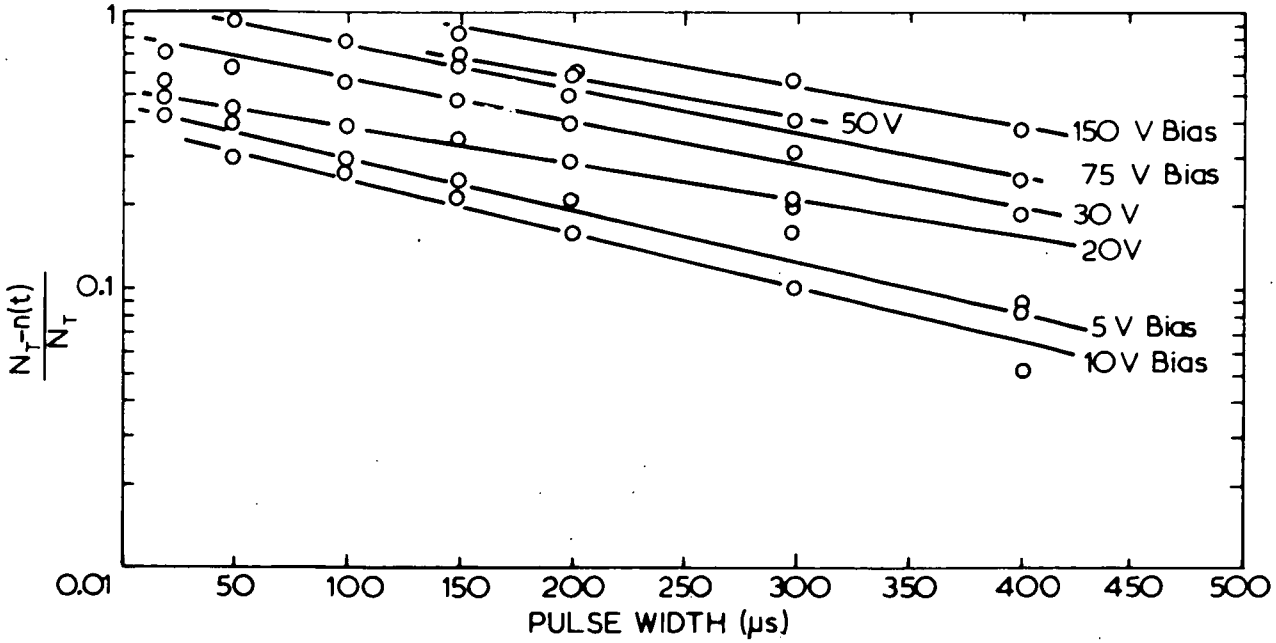

FIGURE 11. BIAS DEPENDENCE OF RELATIVE SIGNAL OUTPUT v. PULSE WIDTH FOR DEFECT 306 IN VPE n-GaAs

$$e_n \propto \exp\left(\frac{\beta\sqrt{E}}{kT}\right) \qquad (2)$$

where $\beta = \left(\frac{q^3}{\pi\varepsilon\varepsilon_o}\right)^{\frac{1}{2}}$

= Poole-Frenkel constant,

= 2.3×10^{-4} eV $V^{-\frac{1}{2}}$ $cm^{\frac{1}{2}}$ for GaAs,

E = average electric field strength,

q = electronic charge,

ε = relative dielectric constant of material, and

ε_o = permittivity of free space.

From the linear portions of Figure 10, a least squares fit to the data yielded a value of $\beta = 4.7 \pm 1.4 \times 10^{-4}$ eV $V^{-\frac{1}{2}}$ $cm^{\frac{1}{2}}$. Data at the highest temperature (275 K) and the lowest fields were used to minimise the contribution from tunnelling effects. However, the discrepancy between theoretical and experimentally determined values may still be due to the presence of tunnelling effects also. The assumption of a doubly-charged trapping centre in both the Frenkel and Hartke theories leads to an increase in the value of β by a factor of 2, i.e. $\beta = 3.25 \times 10^{-4}$ eV $V^{-\frac{1}{2}}$ $cm^{\frac{1}{2}}$, which could explain the discrepancy. Hole emission from the electron trap may also be present, though this was not observed. The field-enhanced emission from the deep trap should lead to a cross section varying as $E^{-\frac{3}{2}}$ [Dussel and Bube 1966]. Figure 11 shows the effect of the electric field on the data used to obtain the capture cross section, and Figure 12 shows a plot of σ_n versus $E^{-\frac{3}{2}}$. A least squares fit yielded a slope of 3.31×10^{-13} $cm^{\frac{1}{2}}$ $V^{-\frac{3}{2}}$ for the latter. This level is also affected by external magnetic fields (Chapter 6). The behaviour in an electric field could not be explained by the recent Pons and Makram-Ebeid [1979] model. Field-enhanced emission was also observed in defect 239 (E_v + 0.19 eV) in

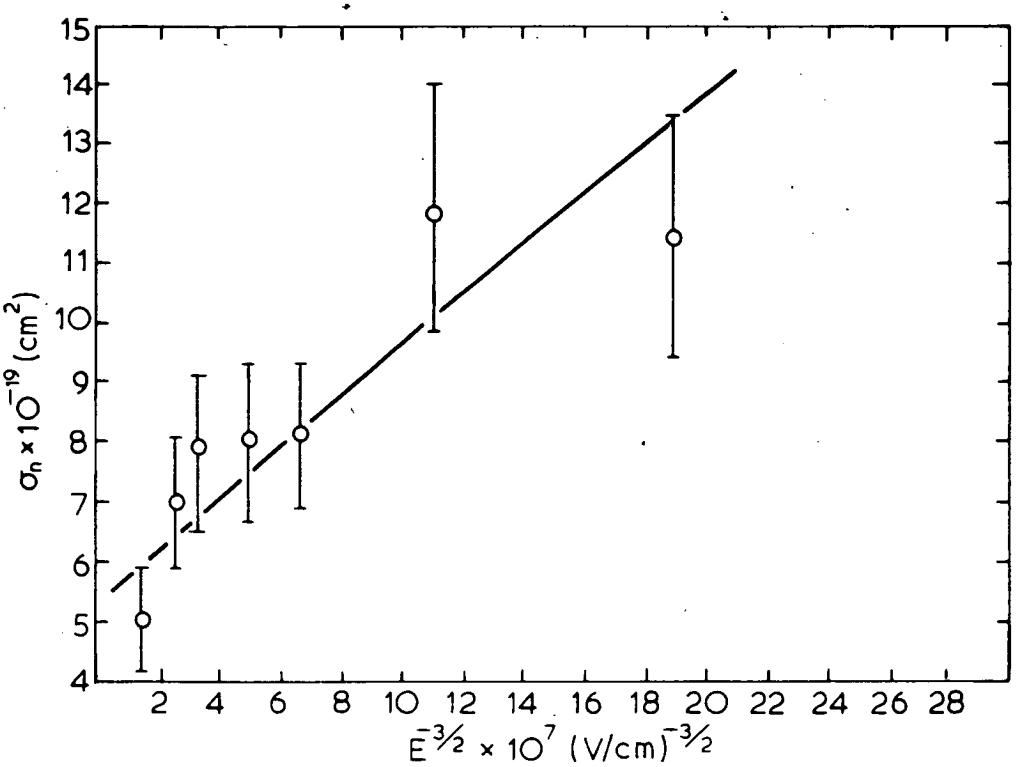

FIGURE 12. BIAS DEPENDENCE OF CROSS SECTION FOR DEFECT 306 IN VPE n-GaAs

LPE material and defect 290 (100 ms) (E_c - 0.73 eV) in VPE material. For the latter, a value of $\beta = 6.2 \pm 1.6 \times 10^{-4}$ eV $V^{-\frac{1}{2}}$ $cm^{\frac{1}{2}}$ was obtained from limited data. It is not known whether effects such as internal stress on the diode could affect the result.

CONCLUSIONS

It is commonly accepted that, in principle, epitaxial layers of up to approximately 1000 μm thickness could be grown. A corresponding decrease in net donor impurities to approximately 10^{11} cm^{-3} would be required for depletion at moderate bias voltage and, from the work reported here, a similar decrease (greater than two orders of magnitude) would be required in the deep level trap densities. Clearly, the spectral response of the epitaxial layers investigated earlier gave superior performance because their small volumes minimised the trapping effects which would be evident in thicker wafers. A simple calculation, using the best value for γ-ray energy resolution at 300 K gives the mean free path λ of a free carrier as ≈1200 μm, i.e. $\lambda \simeq 12\ W_d$, where W_d is the depletion layer thickness. For W_d ≈1000 μm then $\lambda \simeq W_d$ and severe degradation in the spectral response would be evident. Note that the Poole-Frenkel effect at the operating voltages helps reduce the energy resolution degradation by trapping at room temperature by removing the effects of some of the trapping centres to lower temperatures. The requirement remains to produce thicker layers and reduce the net impurity densities while simultaneously reducing the deep trapping centre densities.

REFERENCES

Dussell, G.A. and Bube, R.H. [1966] - J. Appl. Phys. 37:2797.

Eberhardt, J.E., Ryan, R.D., Tavendale, A.J. [1971] - Nucl. Instr. and Meth. 94:463.

Frenkel, J. [1938] - Tech. Phys. - USSR 5:685; Phys. Rev. 54:647.

Hartke, J.L. [1968] - J. Appl. Phys. 39:4871.

Haller, E.E., Li, P.P., Hubbard, G.S. and Hansen, W.L. [1979] - IEEE Trans. Nucl. Sci. 26(1)265.

Huber, A.M., Link, N.T., Valladon, M., Debuen, J.L., Martin, G.M., Mitonneau, A. and Mircea, A. [1979] - J. Appl. Phys. 50(6)4022.

Johnson, N.M., Bartelink, D.J., Gola, R.B. and Gibbons, J.F. [1979] - J. Appl. Phys. 50(7)4828.

Lang, D.V. [1974] - J. Appl. Phys. 45:3023.

Lang, D.V. and Logan, R.A. [1975] - J. Electron. Mater. 4:1053.

Lang, D.V. and Logan, R.A. [1976] - J. Appl. Phys. 47(4)1533.

Lang, D.V. and Logan, R.A. [1977] - Appl. Phys. Lett. 31(10)683.

Lang, D.V., Cho, A.G., Gossard, A.C., Illegems, M. and Weiginan, W. [1976] - J. Appl. Phys. 47(6)2558.

Martin, G.M., Mitonneau, A. and Mircea, A. [1977] - Electron. Lett. 13(7)191.

Miller, G.L., Ramirez, J.V. and Robertson, D.A.H. [1975] - J. Appl. Phys. 46(6)2638.

Miller, G.L., Lang, D.V. and Kimerling, L.C. [1977] - Ann. Rev. Mater. Sci., pp. 377-448.

Mitoneau, A., Martin, G.M. and Mircea, A. [1977] - Electron. Lett. 13(22)667.

Pearton, S.J., Williams, A.A., Tavendale, A.J. and Lawson, E. M. [1980] - AAEC/E501.

Pons, D. and Makram-Ebeid, S. [1979] - J. de Phys. 40:1161.

Schulz, M. and Johnson, M.M. [1977] - Appl. Phys. Lett. 31(9)622.

Wang, K.L. [1979] - IEEE Trans. Electron. Devices, ED-26(5)819.

2.2 Electrical Properties of Polycrystalline GaAs

INTRODUCTION

Gallium arsenide is among the most efficient converters of solar radiation to electrical energy [Sze 1969]. High densities of line or point defects in the crystals cause marked reduction in solar cell power output and thus their observation is of practical interest. Simple I-V and C-V measurements on diode structures provide useful information, while direct observation of the defects by the powerful capacitance spectroscopy (DLTS) [Lang 1974] and thermally stimulated capacitance (TSC) techniques allow measurement of emission rate, concentration and capture cross section of point defects. In this work we have applied these techniques to discrete defects in polycrystalline GaAs, following previous work on single crystal GaAs [Pearton et al. 1980].

EXPERIMENTAL TECHNIQUE

Polycrystalline samples were cut from AAEC vapour phase grown crystals, lapped to obtain two plane parallel faces and polished on a slurry of #600 grade grit on glass. After etching for three minutes in a mixture of $3HNO_3:2H_2O:1HF$, ohmic contacts to the n-type material were formed by alloying (in air) GaIn onto one face. Gold surface barrier contacts (2 mm diameter) were evaporated onto the other face to provide a rectifying contact.

All measurements were performed in vacuo (3×10^{-6} torr) at room temperature and 77 K in the DLTS cryostat described previously [Williams et al. 1980]. A Boonton 71A capacitance bridge (operating at 1 MHz) was used for the DLTS and TSC scans and the C-V results, while I-V characteristics were recorded with a Lambda power supply (LP-415A-FM-VI) and Avo-meter. Diode behaviour was checked by resistance and I-V measurement at room temperature.

RESULTS AND DISCUSSION

Figure 1 shows a typical electrically active defect spectrum for a polycrystalline n-GaAs diode, accompanied by the diode capacitance as a function of temperature. The latter displays a large increase between 77 and 300 K, indicative of many deep lying energy states ionizing. The transient capacitance spectrum is more illuminating; it shows four separate donor levels ionizing over this temperature range. Energy level parameters are recorded in Table 1; virtually all the measured levels are common in single crystal GaAs and thus result from native defects or impurities introduced during the synthesis or growth of the material. Note should be taken of the concentrations measured for these levels: in semiconductor terms they are very high and are undoubtedly affecting free charge carrier transport. The net ionized shallow level density at 77 K was obtained by C-V measurements over a limited range. Generally the slopes of the characteristics indicated graded rather than abrupt junction structures. It should be stressed that samples from five different crystals displayed roughly similar C-T plots, an increase from ∿200 to 300 pF 77 K to 2000 to 3000 pF at 300 K. Arrhenius plots for the energy levels of the various donor defects are shown in Figure 2.

Figure 3 shows the current-voltage characteristic of a typical polycrystalline GaAs diode. For low forward bias voltages the characteristics can be expressed by the equation:

$$J_F = A \exp\left(- \frac{qV}{nkT} \right) \quad ,$$

where A and n are constants. Typical values of the ideality factor n were 3 to 5, consistent with a generation-recombination mechanism caused by large densities of deep defect states; the I-V characteristics also show that there is no saturation of the reverse current at any temperature and that the rectification ratios are poor - the

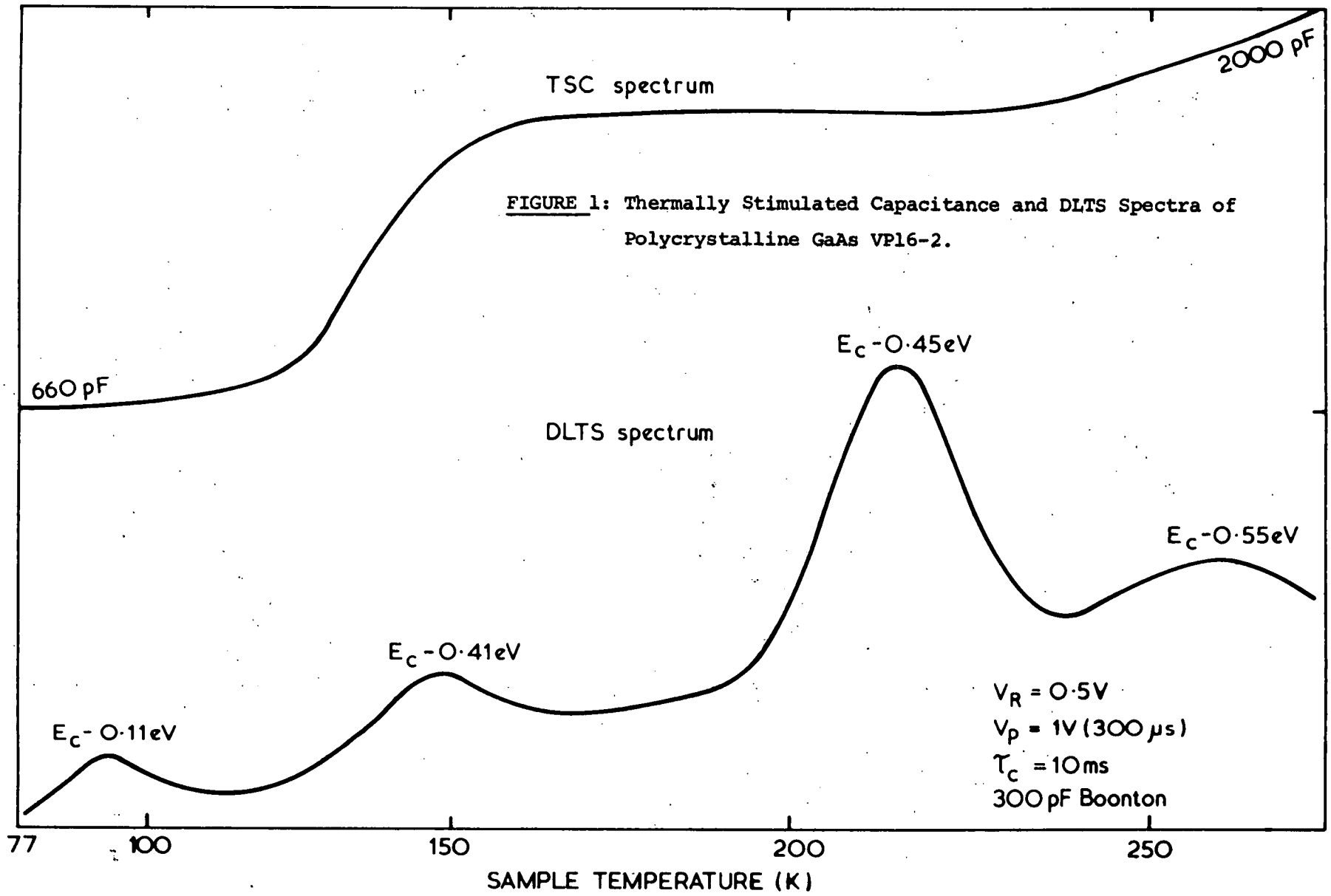

FIGURE 1: Thermally Stimulated Capacitance and DLTS Spectra of Polycrystalline GaAs VP16-2.

Figure 1

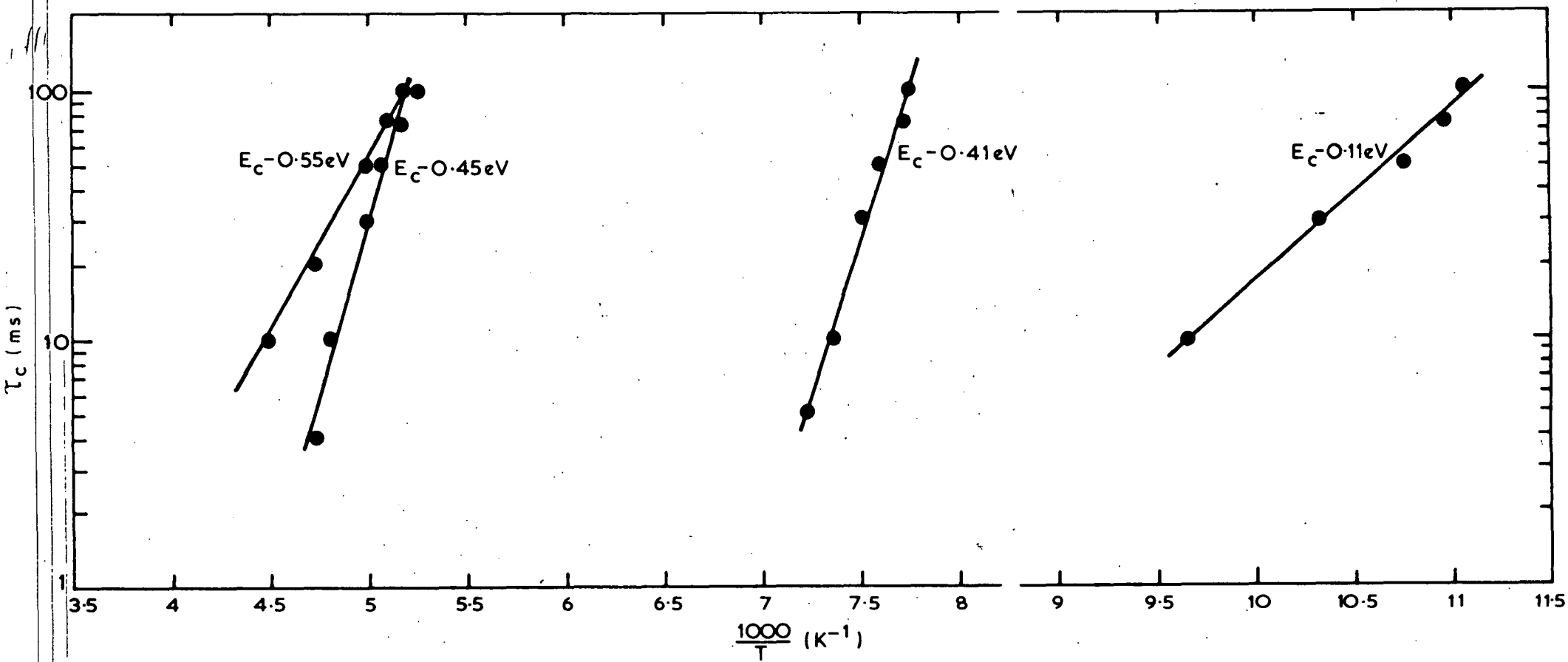

Figure 2 Arrhenius Plots of Donor Levels Detected in Polycrystalline n-GaAs Diodes.

TABLE 1: Discrete Donor Levels in Polycrystalline GaAs

Sample	Levels (eV)	σ (cm^2)	N_T (cm^{-3})	n (cm^{-3})	Comment
VP 16-2,-6,-8	E_c - 0.41	3×10^{-12}	1.5×10^{14}	$2\text{-}10 \times 10^{16}$ (77K)	both common in VPE material
	E_c - 0.45	10^{-17}	5×10^{15}		
VP 7,18,16	E_c - 0.11	1×10^{-18}	1.5×10^{13}	3×10^{15} - 1×10^{17} (77K)	-
	E_c - 0.55	1×10^{-12}	3.6×10^{14}		seen in VPE material

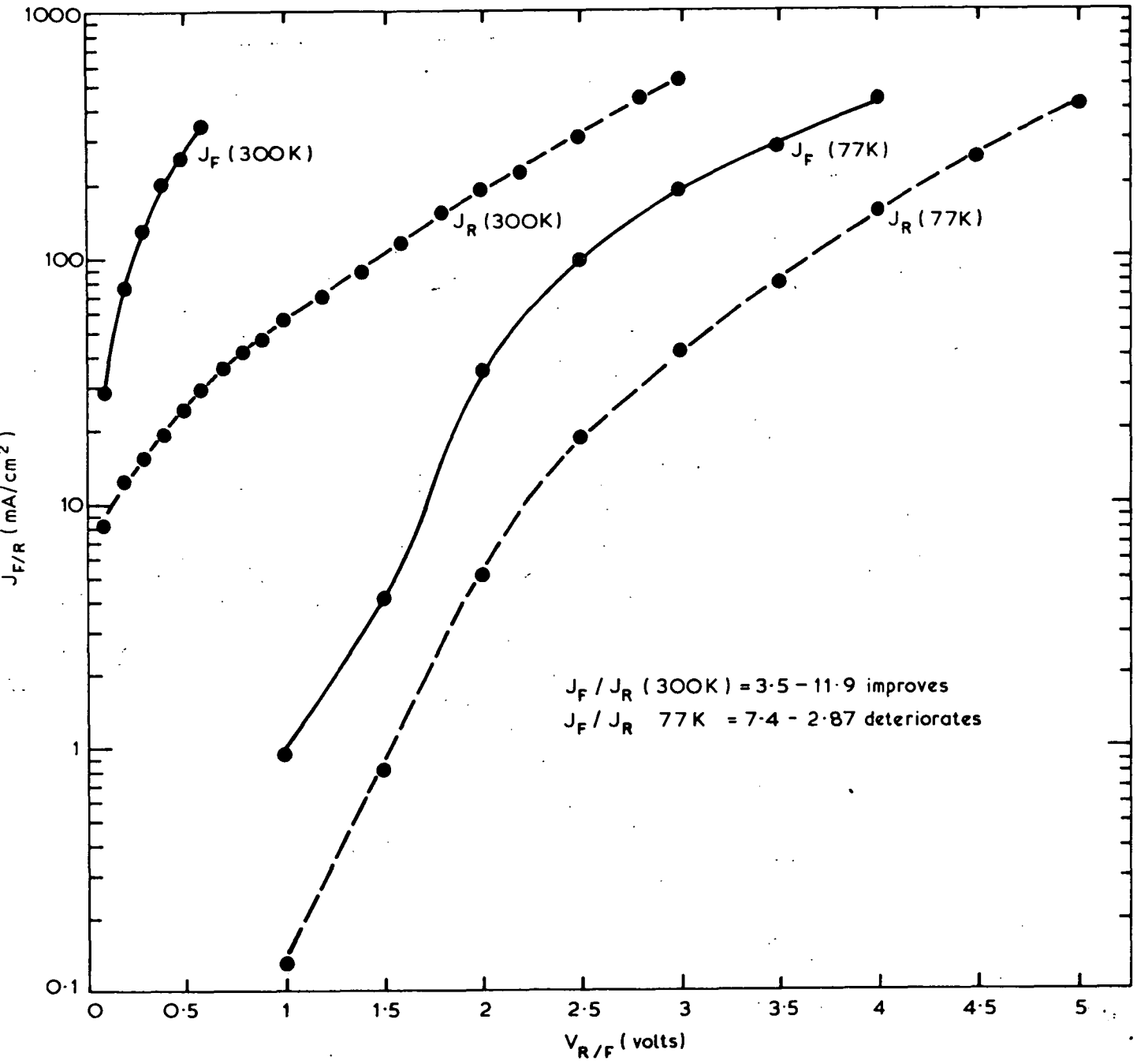

Figure 3 Current Density vs. Voltage for VP16-2.

best measured ratio was 15 (measured at room temperature). When the forward current is dominated by the generation-recombination component, a plot of $J_F \simeq Jgen$ against $(V_{bi}+V)^{\frac{1}{3}}$ and $(V_{bi}+V)^{\frac{1}{2}}$ can determine whether the diode is an abrupt junction or is linearly graded. For the three samples checked in this way, a graded junction was indicated.

Clearly the electrical properties of the material are dominated by deep level defect states, rendering it useless for most applications. Possibly internal junctions between various grain boundaries are injecting whichever polarity bias is applied or, more simply, the gold barrier is not purely rectifying but partially resistive as well. Evidence for the former comes from the observation of an inverted transient capacitance signal during many DLTS scans. The appearance of the inverted ΔC was always noted as the diode temperature was reduced and hence deep donors were freezing out and the depletion depth increasing, possibly reaching an extra junction which is forward biased. The singular lack of improvement of leakage current with temperature on most of the diodes also points to forward biased junctions and/or resistive components. A qualitative check of the response of a single crystal n-GaAs diode to white light (essentially trap-free material) compared to a polycrystalline GaAs diode showed a far reduced relative response for the latter.

SUMMARY

The electrical characteristics of polycrystalline GaAs were investigated by I-V, C-V, thermally stimulated capacitance and deep level transient spectroscopy measurements. Diode structures had poor rectification ratios (<15 for T = 77 to 300 K) and high reverse leakage currents (50 mA/cm^2 for 1 V at 300 K) dominated by generation-recombination centres. High densities $\left(\frac{N_T}{n} > 5\% \right)$ of discrete deep level donors were detected, though none could be correlated with grain boundaries.

REFERENCES

Lang, D. V. [1974] - J. Appl. Phys. 45:3014.

Pearton, S.J., Alexiev, D., Tavendale, A.J. and Williams, A.A. [1980] - AAEC/E503.

Sze, S.M. [1969] - Physics of Semiconductor Devices (Wiley).

Williams, A.A., Pearton, S.J. and Alexiev, D. [1980] - AAEC/TN147.

2.3 Electrical Properties of γ-irradiated Polycrystalline GaAs

INTRODUCTION

The previous section in this chapter dealing with polycrystalline material concluded that native and impurity defect centres dominated and that no centres associated with grain boundaries were detected. A logical extension of this work is the study of γ-ray induced centres in polycrystalline GaAs to determine whether vacancy complexes associate with grain boundaries to produce energy states in the forbidden band gap. Standard characterisation techniques (I-V, C-V, TSCAP, DLTS) were used to examine the n-type GaAs from the previous section which had subsequently been irradiated.

EXPERIMENTAL TECHNIQUE

The samples were irradiated in a 1.8 Mrad h^{-1} ^{60}Co γ-irradiation facility. The samples received an integrated dose of 550 Mrad. After etching and the evaporation of new Pd or Au contacts, the diodes were installed in the DLTS cryostat.

RESULTS AND DISCUSSION

Before irradiation, the n-GaAs surface barrier diodes had typical capacitances of 200 to 300 pF at 77 K, increasing to ∿2000 to 3000 pF at 300 K. Their DLTS spectra displayed four common levels and rectification ratios were typically <15 for T = 77 to 300 K, with high reverse leakage currents (50 mA/cm^2 for 1 V at 300 K). After irradiation the samples were compensated at 77 K and displayed resistive I-V characteristics (Figure 5). The DLTS spectra were essentially unchanged from the pre-irradiation state, though the TSCAP scans reveal the extent of the capacitance change (Figure 6). A C-V characteristic from the only sample (out of five) which did display a change in capacitance with reverse bias at 77 K indicated a net ionized donor concentration of $N_d - N_a = 3.5 \times 10^{11}$ cm^{-3}

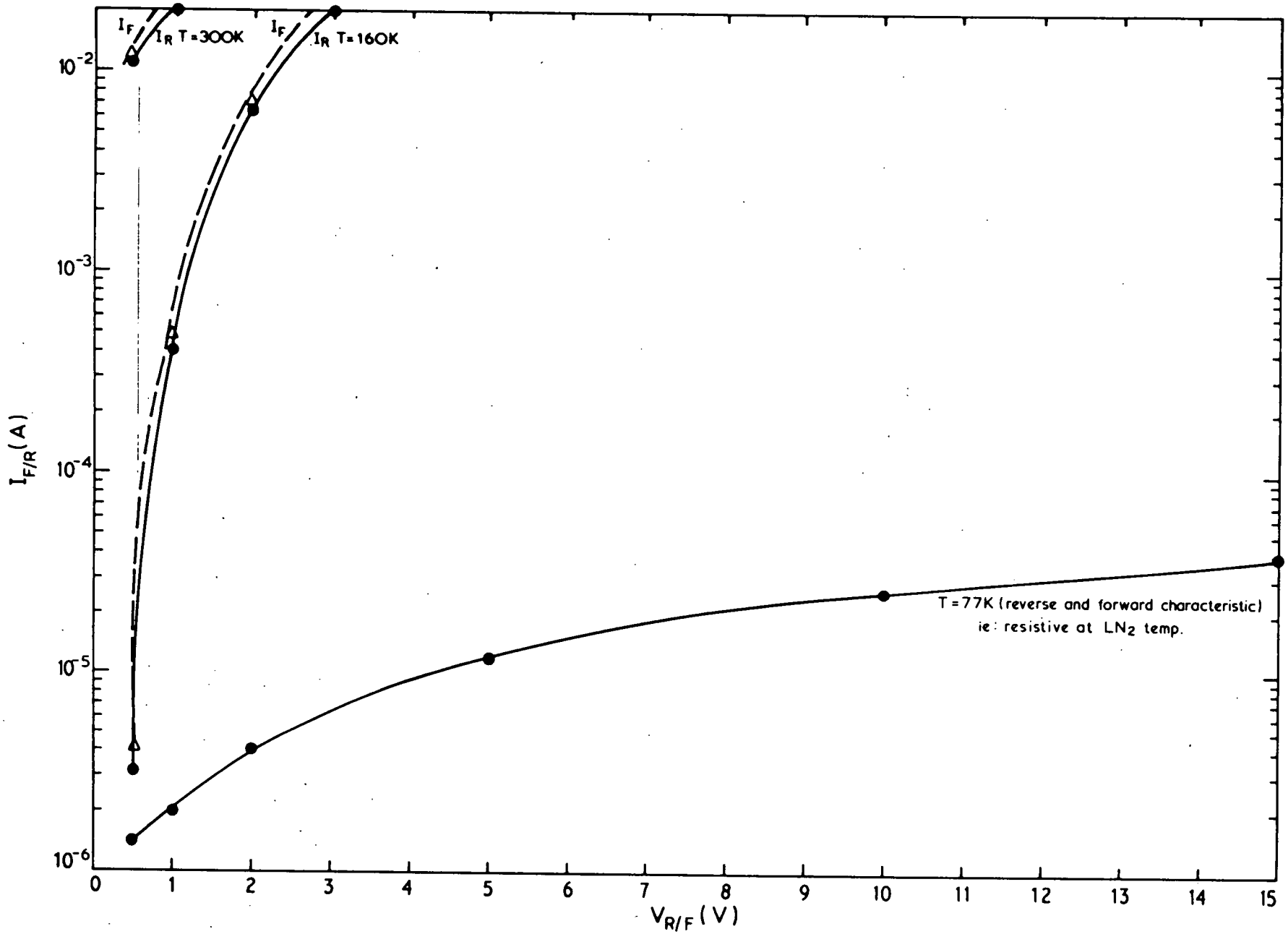

Figure 5. GaAs VP 18 POLYCRYSTALLINE GaAs γ-IRRADIATED 550 MRd

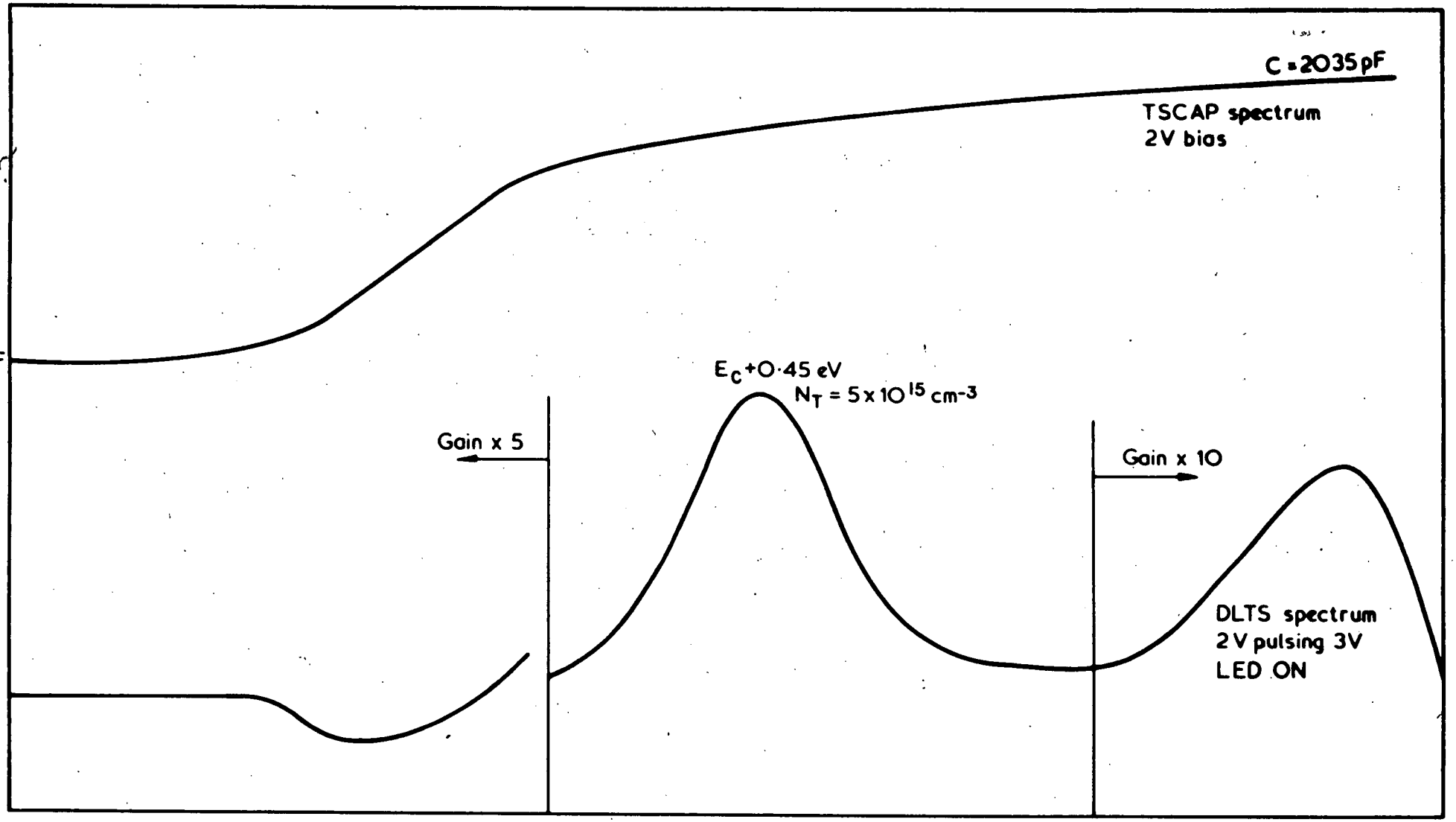

Figure 6 γ-IRRADIATED POLYCRYSTALLINE GaAs

(Figure 7); the doping density at 300 K was similarly measured as $N_d - N_a = 6.6 \times 10^{16}$ cm^{-3}. The samples were poor diodes at 300 K (rectification ratios generally 2 to 5, $I_L \gtrsim 70$ mA/cm^2 for 1 V).

The γ-irradiation must have produced large concentrations of deep level acceptor centres which compensate the shallow donor population at 77 K. These are unobservable by DLTS because the samples are no longer diodes at 77 K; also the acceptors may have extremely large (or small) capture cross sections which render them invisible to the pulsed refilling method.

It is to be noted that no extra DLTS peaks were observed from the pre-irradiation state.

CONCLUSIONS

Nothing unexpected was observed in the γ-irradiation polycrystalline GaAs. No extra defect states were observed showing that vacancy association with grain boundaries is a small effect compared to impurity-defect complexing. The n-type GaAs showed a marked decrease in $N_d - N_a$, as expected. The irradiation of p-GaAs, possibly using lasered Sn as the rectifying contact, and Au as the ohmic contact, may be of interest in order to check the similarities, if any, with the compensation process in the n-type material. Hydrogenation of the defects in these diodes, in the presence of the grain boundaries, could also be interesting.

SUMMARY

The electrical characteristics of γ-irradiated polycrystalline low resistivity n-type GaAs were investigated by I-V, C-V, TSCAP and DLTS measurements. No extra defect peaks, other than those expected, were observed, indicating that vacancy-grain boundary association effects are small compared to the usual impurity-defect complexing. The GaAs is compensated at 77 K; TSCAP scans reveal a five magnitude increase in net ionized impurity concentrations from 77 to 300 K.

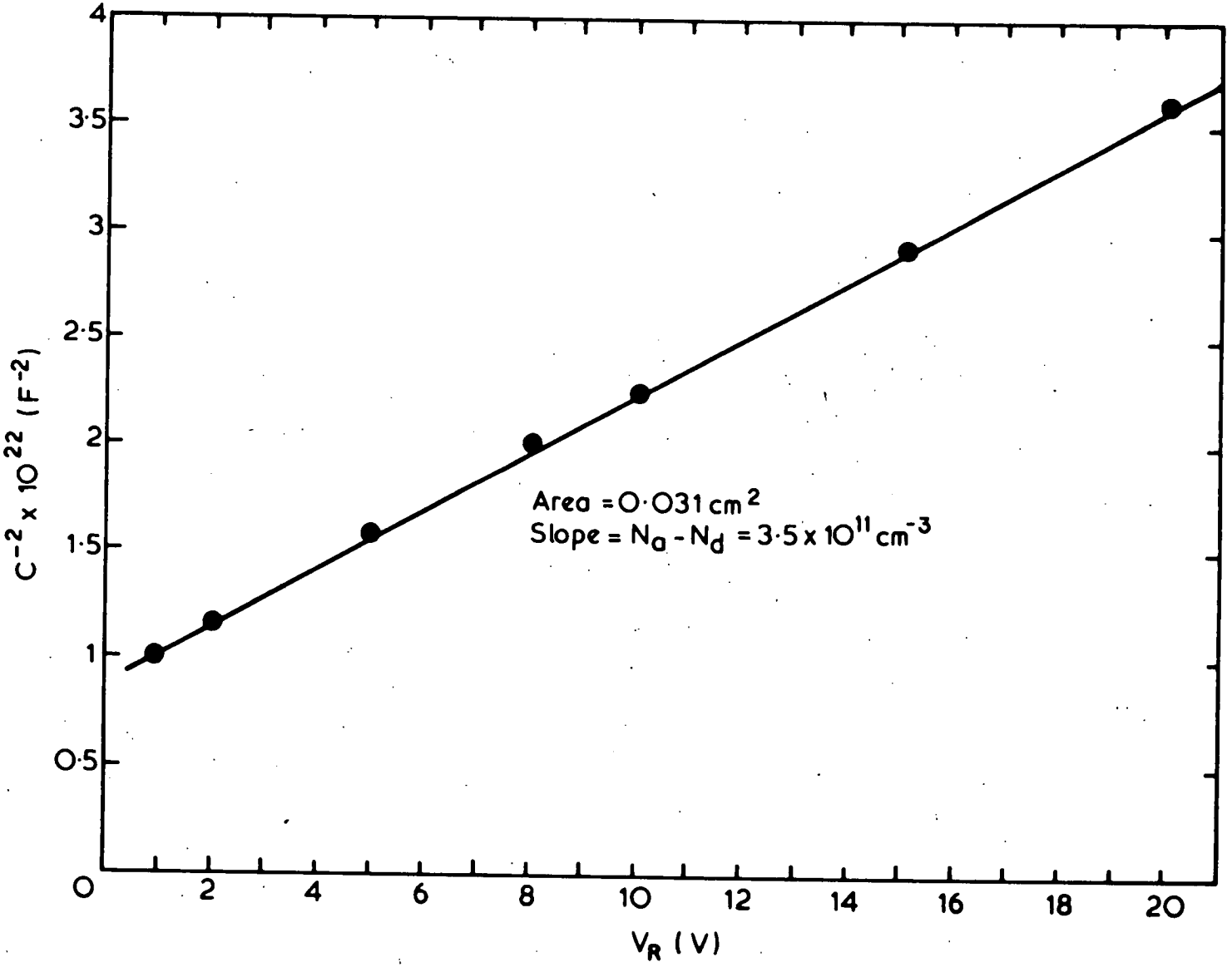

Figure 7. γ-IRRADIATED GaAs AT 77K

CHAPTER 3

LASER AIDED DOPED CONTACTS TO SEMICONDUCTORS

INTRODUCTION

Laser aided doping is a method which uses a pulse of energy from a laser to melt and mix the top surface region of a semiconductor and an evaporated dopant layer. The result can be an extremely thin, robust, highly doped contact to the semiconductor material.

High powered pulsed (Q-switched) or continuous wave (CW) lasers are currently used in many laboratories [see, for example, Laser and Electron Beam Processing of Materials, eds. C.W. White and P.S. Peercy] to anneal ion implantation damage, producing highly doped regions free of extended crystallographic defects. The mechanisms of damage removal are generally thought to be different for the two types of laser irradiation. Continuous wave laser annealing [Gat et al. 1978] is thought to produce solid phase regrowth of ion-implanted layers, while pulsed laser irradiation [White et al. 1979] is thought to produce epitaxial regrowth of a region actually melted during the laser pulse. We have used the latter mode to produce contacts to Si and Ge nuclear radiation detectors and low resistivity GaAs slices.

3.1 Elemental Semiconductors Si and Ge

SUMMARY

Ultra-thin (<0.1 μm), highly doped Li contacts have been fabricated on n- and p-type Ge and Si nuclear radiation detectors by the Q-switched ruby laser melting technique. Full width half maximum resolutions for 5.48 MeV α-particles of 17.4 keV on 2 kΩ cm p-type Si, 21.7 keV on 300 Ω cm p-type Si and 15.3 keV on p-type Ge ($N_a - N_d$ = 1.7 x 10^{10} cm^{-3}) were obtained. Best resolutions for 662 keV ^{137}Cs γ-rays were 2.3 keV for n-type Ge ($N_d - N_a$ = 1 x 10^{10} cm^{-3}) and 4.6 keV (pulser resolution 3.4 keV) for p-type Ge ($N_a - N_d$ = 6 x 10^{10} cm^{-3}). Used as an ohmic contact on a 90 kΩ cm, n-type Si X-ray detector at 80 K, the contact allows operation at 1300 V (depletion at 235 V). Crystal heating data and deep level transient spectroscopy results show significant laser damage in the contacts fabricated on Ge, but far less damage on Si. Owing to the narrow fluence range, careful control of the homogenised laser output energy is necessary for good fabrication yields.

INTRODUCTION

The simplest and most common blocking contact used with high-purity p-type Ge for nuclear radiation detectors is fabricated by Li diffusion from a vacuum-evaporated source. Typically, the diffusion step is performed at ∿300°C for 5 to 10 minutes, yielding a contact thickness of ∿300 μm. Reducing the diffusion temperature to ∿180°C may produce heavily doped layers in the range 10 to 50 μm [Amann et al. 1975]. However, for many applications, most importantly the stacked detectors used in charged-particle counter telescopes, these contacts are less than optimum. Ion-implanted phosphorus contacts are thin (<0.2 μm) [Protić and Riepe 1977], but require annealing at temperatures ∿400°C, which may introduce rapidly diffusing deep level impurities (e.g. copper), thus degrading the detector resolution. In this section we describe the simple fabrication of thin, stable Li contacts by melting an evaporated surface layer by laser, a technique not requiring the bulk crystal to be processed at high temperature.

EXPERIMENTAL PROCEDURE

1. Sample Preparation

Seven detectors were fabricated from high purity p-type Ge grown at the AAEC Research Establishment, and five detectors were fabricated from General Electric (USA) and AAEC high purity (HP) n-type Ge. After cutting and lapping to remove mechanical damage, the material was etched for six minutes in a mixture of hot $4HNO_3$:1HF to achieve a specular surface finish, and Li evaporated onto one face. The thickness of the evaporated layer was not monitored and was not critical to the final performance of the detectors. The completed detectors were typically 4 mm thick with 50 mm^2 areas.

For Si detector fabrication a similar procedure was followed,

although slices were etched initially for 15 minutes in a mixture $8HNO_3$:1HF:1CH_3COOH (at room temperature). Materials used were 90 kΩ cm n-type (Wacker-Chemie), 2 kΩ cm p-type (Wacker-Chemie) and 300 Ω cm p-type (Materials Research Corporation) Si.

Detectors were stored for up to 10 days in air or N_2 before being irradiated by the laser pulse. However, a contact with a more uniform appearance was produced by laser melting within a day of the Li evaporation; this was probably due to the less complete oxidation of the Li layer.

2. Laser Melting and Initial Testing

The samples were irradiated by a homogenised 25 ns FWHM pulse from a Q-switched ruby laser (Figure 1). It was found that the quality of the homogeniser, a tapered Perspex or silica lightguide [Cullis et al. 1979] was critical. Typically a Perspex homogeniser may last 10 to 15 shots before developing large flaws, generally at the 90^{o} bend. These produce structural damage, clearly visible to the naked eye, in the laser-aided doped (LAD) contact, particularly on Ge. In general, this indicated dead layers or, alternatively, p-regions produced by heavy laser damage within the doped n^{+} contact. As well, the output face of the homogeniser is polished on cloth after lapping on #600 paper, which normally leaves a bowed rather than an optically flat surface. This also produced unwanted focusing effects, normally leaving a halo of p-type damage, or less heavily doped n-type regions, around the LAD (Li) contact.

The output power density of the laser was in the range 80 to 240 MW cm^{-2} before passing through the homogeniser, which has an output face of 8 to 10 mm diameter for Perspex and 16 mm for silica. To avoid divergence of the beam out of the lightguide, the gap between sample and output face was kept at less than 1 mm. The two

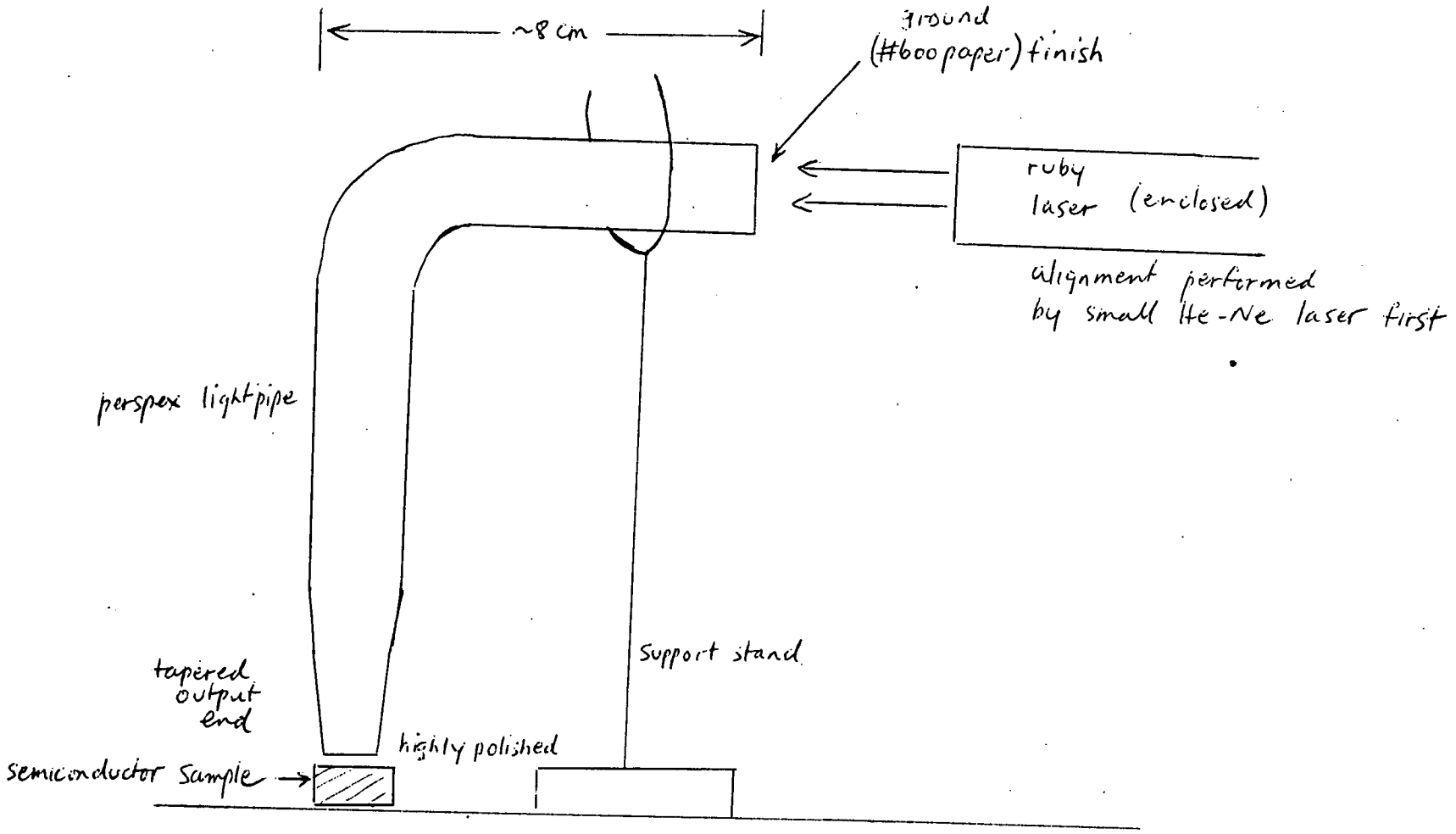

FIGURE 1 EXPERIMENTAL SET-UP FOR LASER DOPING

surfaces were aligned coplanar (by eye) to ensure constant power density across the beam diameter.

The typical melt pattern of transient surface melting - an irregularly rippled 'orange peel' finish - was identified by optical microscopy. More simply, a metallic silver appearance indicated a strongly doped n^+ layer. The samples were then either washed thoroughly in distilled water or soaked in HCl to remove excess Li, and a check on the contact was performed using a thermal probe (hot junction at $100^{o}C$, cold at room temperature) based on the Seebeck effect. This indicated that the degree of doping for the LAD Li contacts was comparable to that for a conventional layer. However, use of the thermal probe should be minimised to avoid mechanical damage to the contact.

The contact was then masked using paint-on apiezon wax in xylene, plus masking tape, and then etched for 4 minutes in $4HNO_3$:1HF, quenched in distilled water, washed in methanol and rinsed thoroughly in distilled water before drying with a jet of boil-off N_2. The wax is removed by washing in trichloroethylene, distilled water, methanol and distilled water. The contact is then tape-masked again and the diode etched for 30 seconds in $4HNO_3$:1HF, rinsed three times with distilled water, blown dry and installed in a LN_2 cold trapped diffusion pump evaporator. A 200 Å Pd ohmic contact is evaporated onto the opposite face of the diode at $\leq 10^{-6}$ torr. Both contacts are then tape-masked and the detector given a final one minute etch in $4HNO_3$:1HF before rinsing and drying in the usual way. Alternatively, an oxide finish produced by etching is used: 15 seconds $4HNO_3$:1HF, rinsed H_2O, 40 seconds $1H_2O_2$:1HF, 40 seconds 1HF:$1H_2O$, rinsed H_2O [Beech 1981]. The detector is then mounted in a spring contacted Al can, installed in a vacuum chamber and cooled to $\sim$80 K via a copper cold finger dipped in LN_2.

DETECTOR PERFORMANCE

1. p-type Germanium

One of the most fruitful areas for application of LAD (Li) layers is as rectifying contacts on HP p-type Ge. High energy particle telescopes require thin front and back contacts and generally some combination of implanted B or P ions, low temperature thermal diffusion of Li, or evaporated Pd has been used to provide the ohmic and rectifying contacts.

Figure 2 shows the best ^{241}Am particle spectrum obtained by irradiating the detector through the LAD (Li) contact. The measured total resolution of 15.3 keV shows that the doped layer was extremely thin. The pulser resolution was 4.1 keV at 5.48 MeV. An estimate of the thickness can be made, based on the method described by Protić and Riepe (1977). Using the measured (uncollimated) α-resolution, the contact thickness is ≤100 nm.

An estimate of the contact thickness can also be obtained by irradiating the detector through the LAD (Li) contact with 5.48 MeV ^{241}Am α-particles. Figures 3 shows α-spectra recorded with the source parallel and at 45^{o} to a LAD (Li) contact on a good quality HP p-Ge detector. The peak shift corresponds to 7.4 keV which translates to an approximate thickness of 0.04 μm. It is interesting that the dopant does not appear to be incorporated over the full melt region (typically assumed to be ∿1 μm [White et al. 1979]).

Figure 4 shows the response to 662 keV γ-rays of a typical LAD (Li) detector. A 2N4416 room temperature FET preamplifier was used in conjunction with a Canberra 2010 main shaping amplifier. The detector resolution of 3.1 keV (measured resolution minus electronic contribution) is typical for a LAD (Li) detector. In general, the leakage currents are slightly higher than one would expect from small, high purity

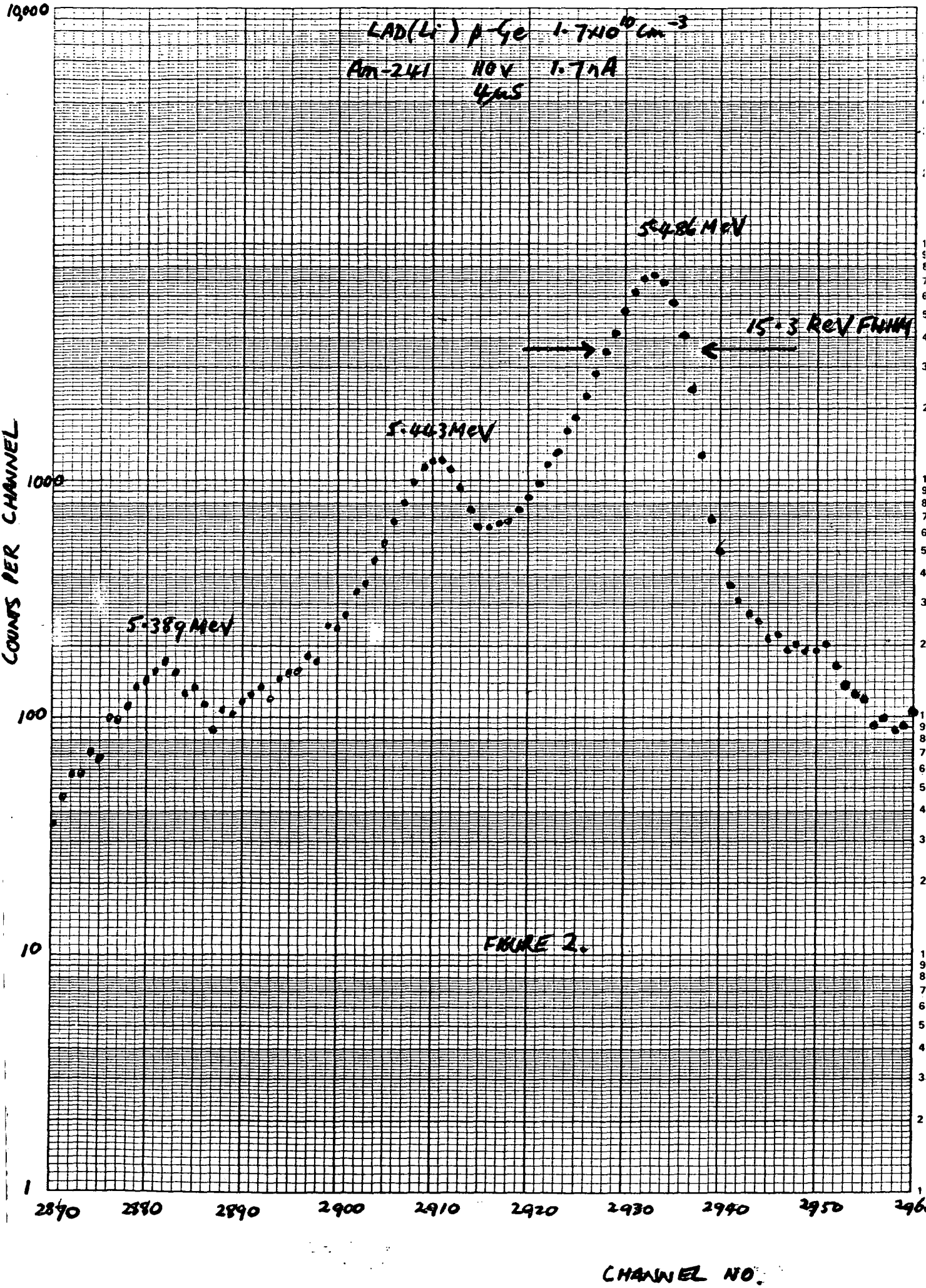
LAD(Li) p-Ge 1·7×10^10 cm^-3
Am-241 HOV 1·7nA
4μs
5·486 MeV
15·3 KeV FWHM
5·443MeV
5·389 MeV
COUNTS PER CHANNEL
CHANNEL NO.
10,000
1000
100
10
1
2870
2880
2890
2900
2910
2920
2930
2940
2950

FIGURE 2.

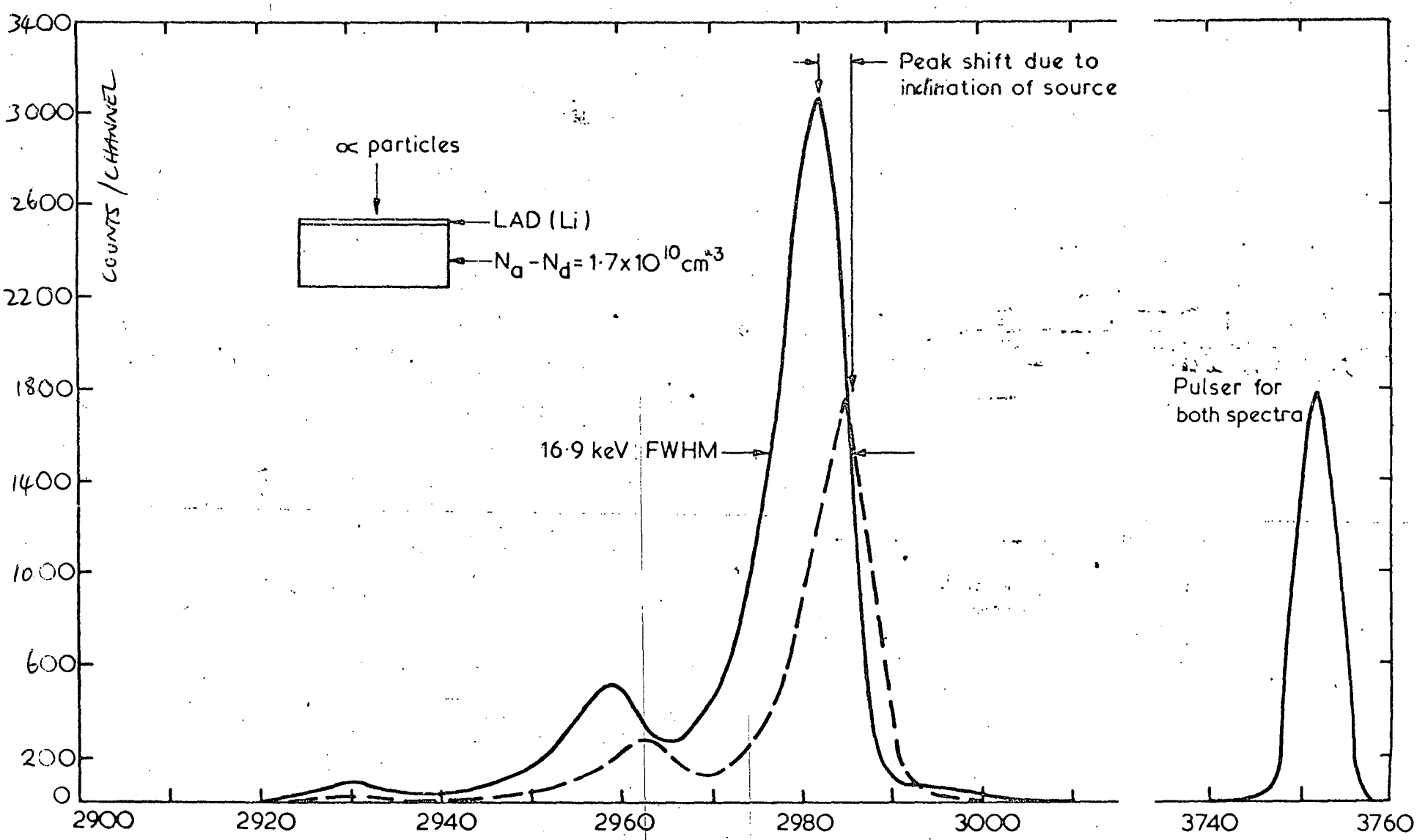

Figure 3 Peak shift of 5.48 MeV α-spectrum recorded through the LAD(Li) contact of a HP p-type Ge ($N_a - N_d = 1.7 \times 10^{10} cm^{-3}$) detector when the α-source is tilted at an angle of 45° to the detector. This measurement gives the contact thickness as ≈0.04 μm.

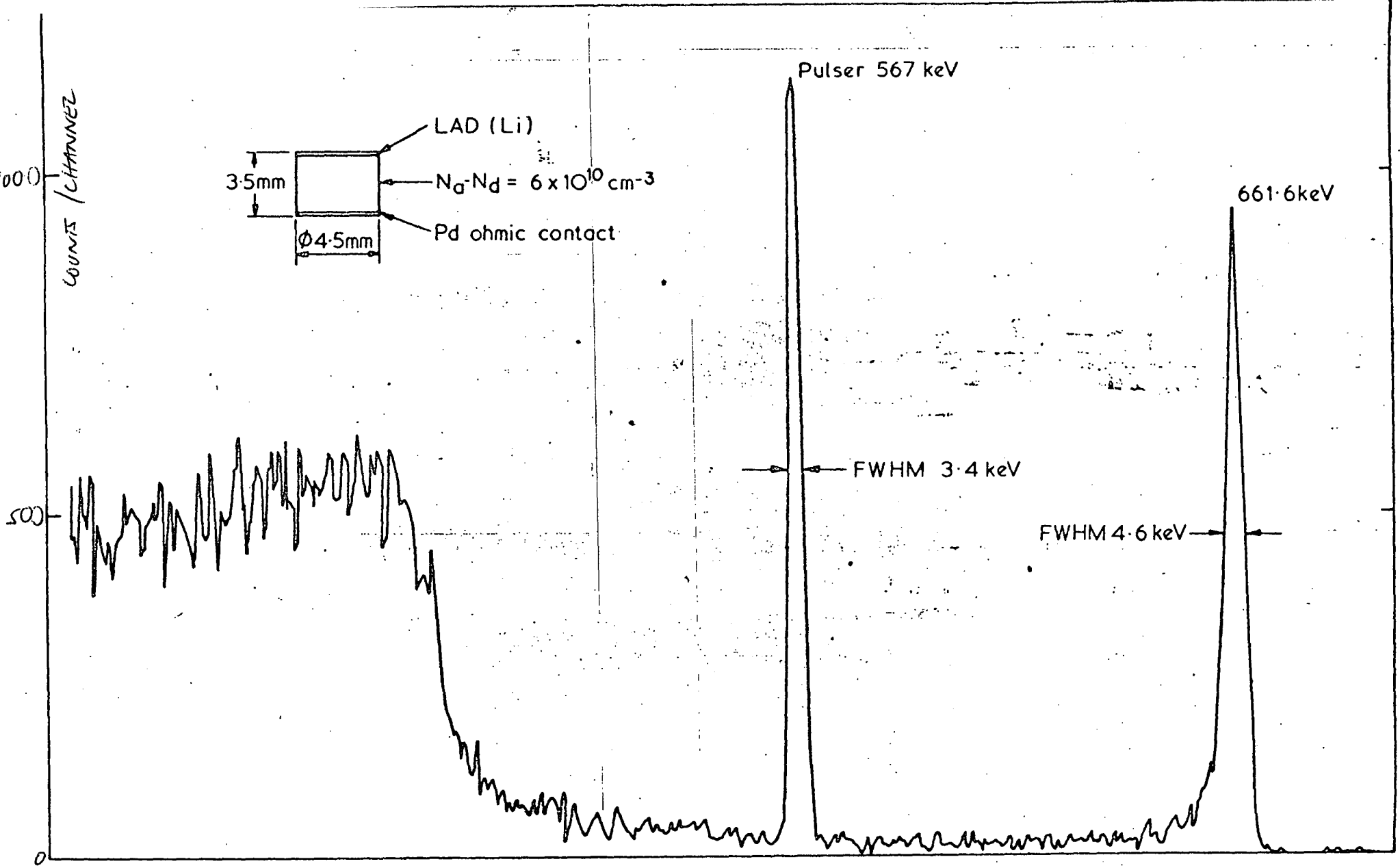

Figure 4. HP p-type Ge LAD(Li) detector response to 662 keV γ-rays fr ^{137}Cs. Effective impurity concentration of material is $6x10^{10}$ cm^{-3}, 36 V bias, $1.8x10^{-9}$ A leakage current, 4 μs time constant on shaping amplifie This resolution is typical for LAD(Li) p-type Ge devices.

detectors. A typical I-V characteristic is shown in Figure 5. The higher leakage currents are most likely due to the laser induced damage centres in the melt region. The damage is probably one of two types: acceptor point defects (see section 4) or poor crystallinity during regrowth of the melt region. Clearly, control of the laser output energy and focusing is of paramount importance in minimising these contributions.

Figure 6 is the forward bias characteristic of a LAD (Li) device. The slope of the initial region of the curve is 127.9 V^{-1} compared to an ideal device slope of 150.6 V^{-1} at 77 K. In general, ideality factors n = 1.2 to 1.6 were found for these detectors.

The contact remained stable during repeated cycling to room temperature; LAD (Li) layers have remained stable at room temperature for periods of several months and none have yet degraded in terms of spectral response or in the indication of the degree of doping. Seven detectors of this type were fabricated on high-purity p-type germanium; all were useful γ-spectrometers and had ^{241}Am α-particle resolutions of $\leq$25 keV.

2. n-type Germanium

One test of the quality of a doped region is to use it as an ohmic contact, applying overvolts if possible.

Figure 7 shows a fully depleted HP n-type detector (5 mm ϕ, 3 mm thick) response to 662 keV ^{137}Cs γ-rays. The applied reverse bias of 42 V corresponds to full depletion according to the C-V characteristic of Figure 8(a). The I-V characteristic of this detector is most revealing. Figure 8(b) shows an immediate increase in leakage current on depleting to the LAD (Li) contact, to the point where the application of an overvoltage of 2 or 3 V would markedly degrade the spectral response. As stated in section 1, it is most likely that poor

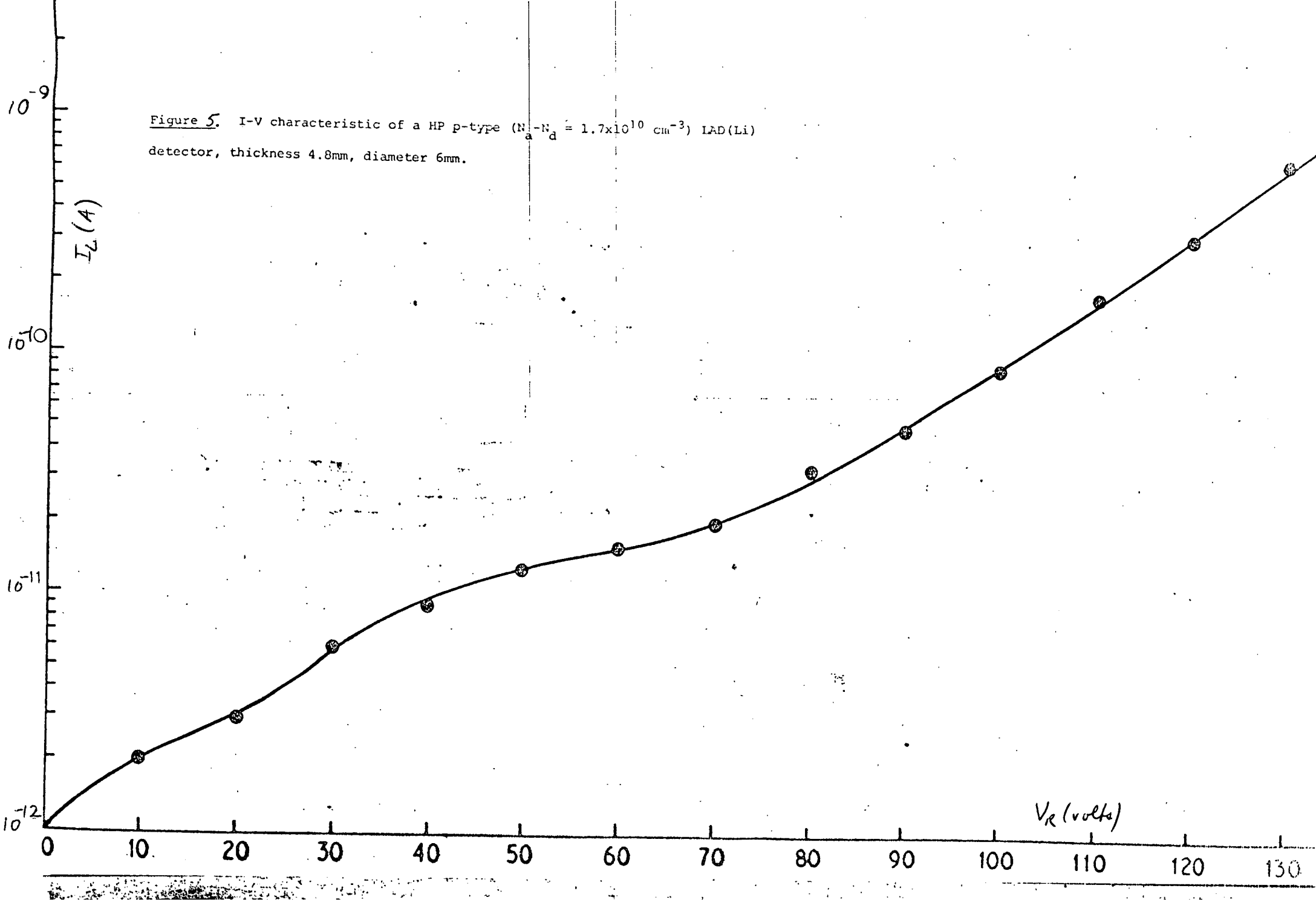

Figure 5. I-V characteristic of a HP p-type ($N_a - N_d = 1.7 \times 10^{10}$ cm^{-3}) LAD(Li) detector, thickness 4.8mm, diameter 6mm.

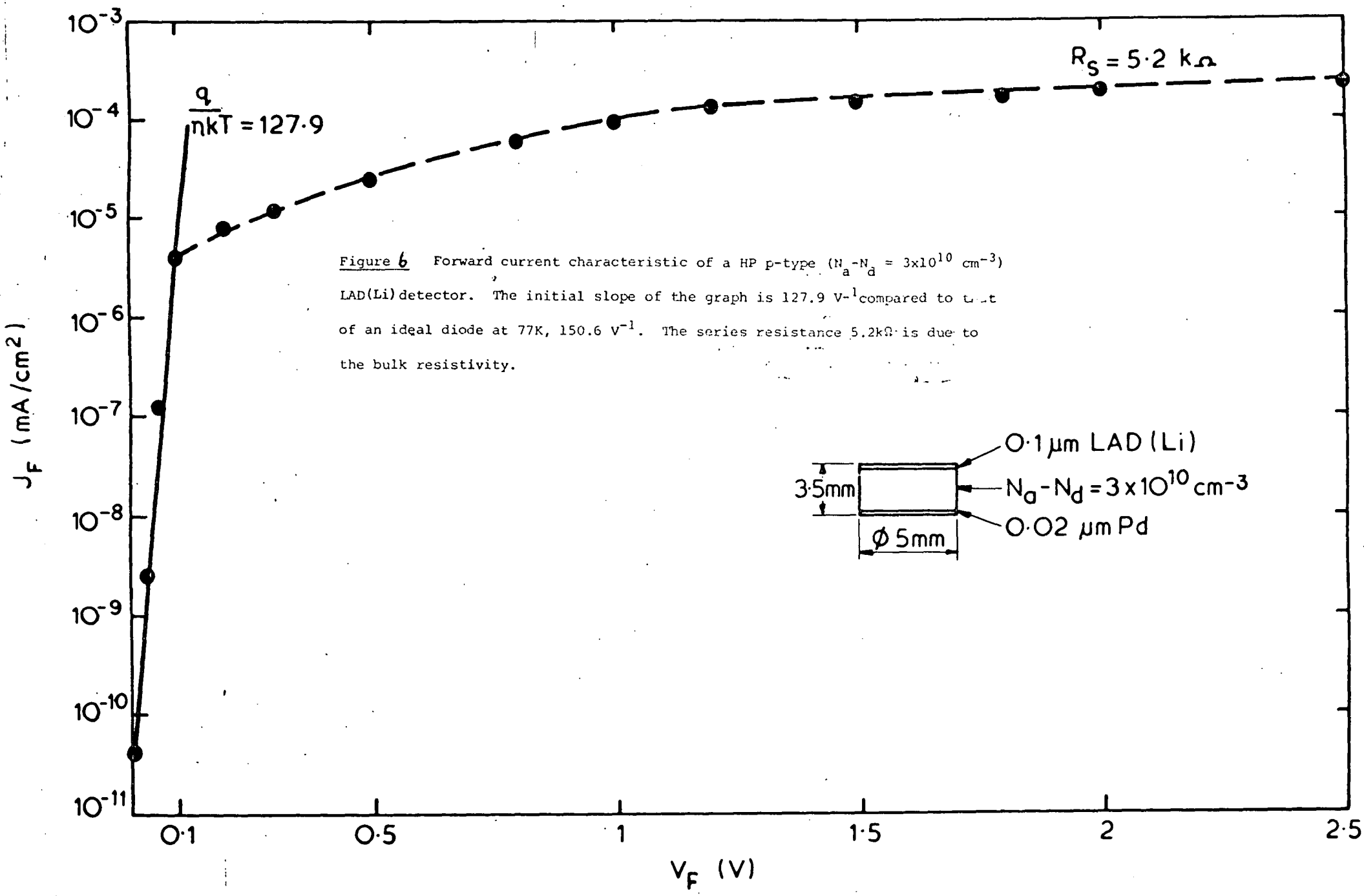

Figure 6 Forward current characteristic of a HP p-type ($N_a - N_d = 3 \times 10^{10}$ cm^{-3}) LAD(Li) detector. The initial slope of the graph is 127.9 V^{-1} compared to that of an ideal diode at 77K, 150.6 V^{-1}. The series resistance 5.2kΩ is due to the bulk resistivity.

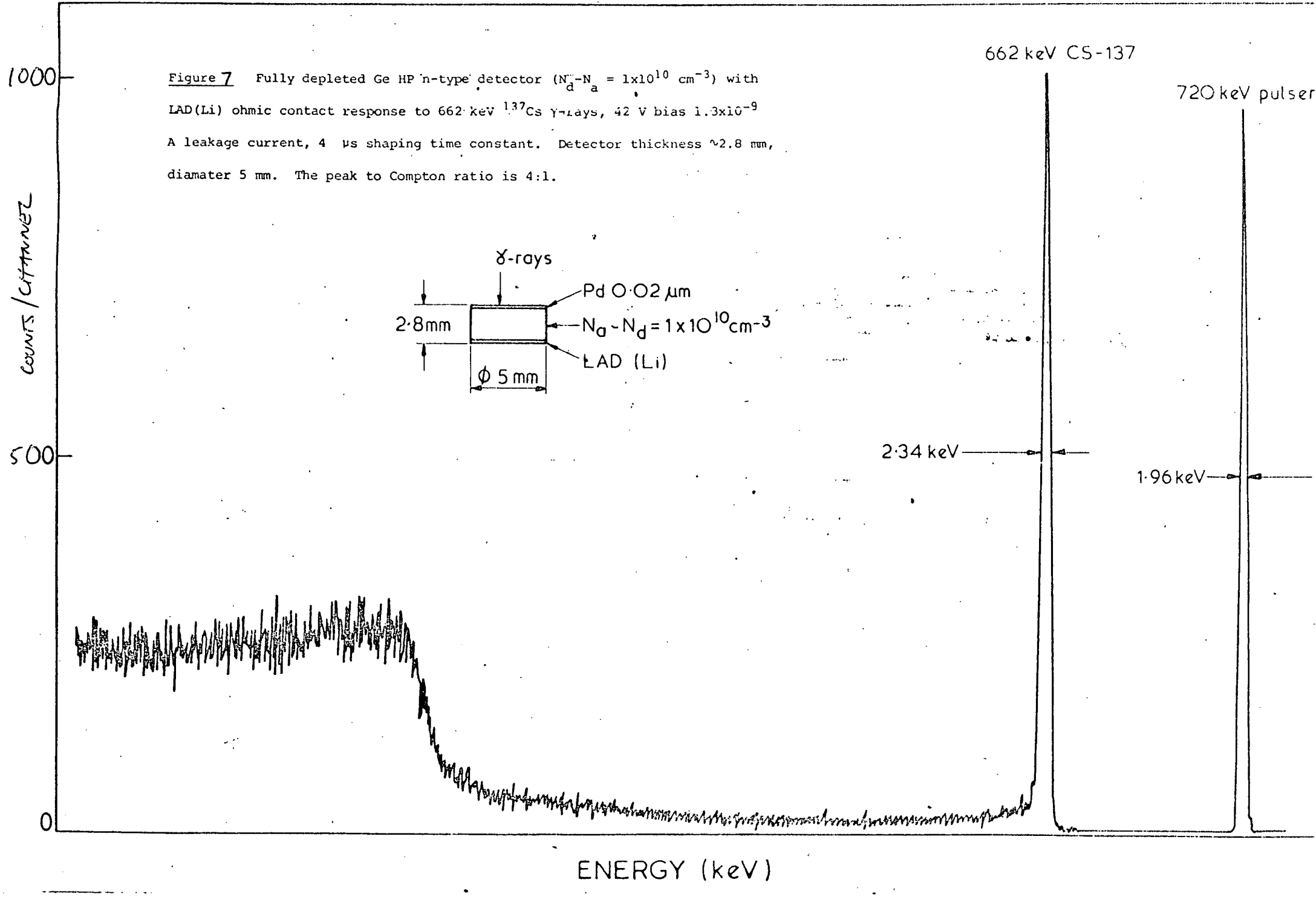

Figure 7 Fully depleted Ge HP n-type detector ($N_d - N_a = 1 \times 10^{10}$ cm^{-3}) with LAD(Li) ohmic contact response to 662 keV ^{137}Cs γ-rays, 42 V bias 1.3×10^{-9} A leakage current, 4 μs shaping time constant. Detector thickness ~2.8 mm, diamater 5 mm. The peak to Compton ratio is 4:1.

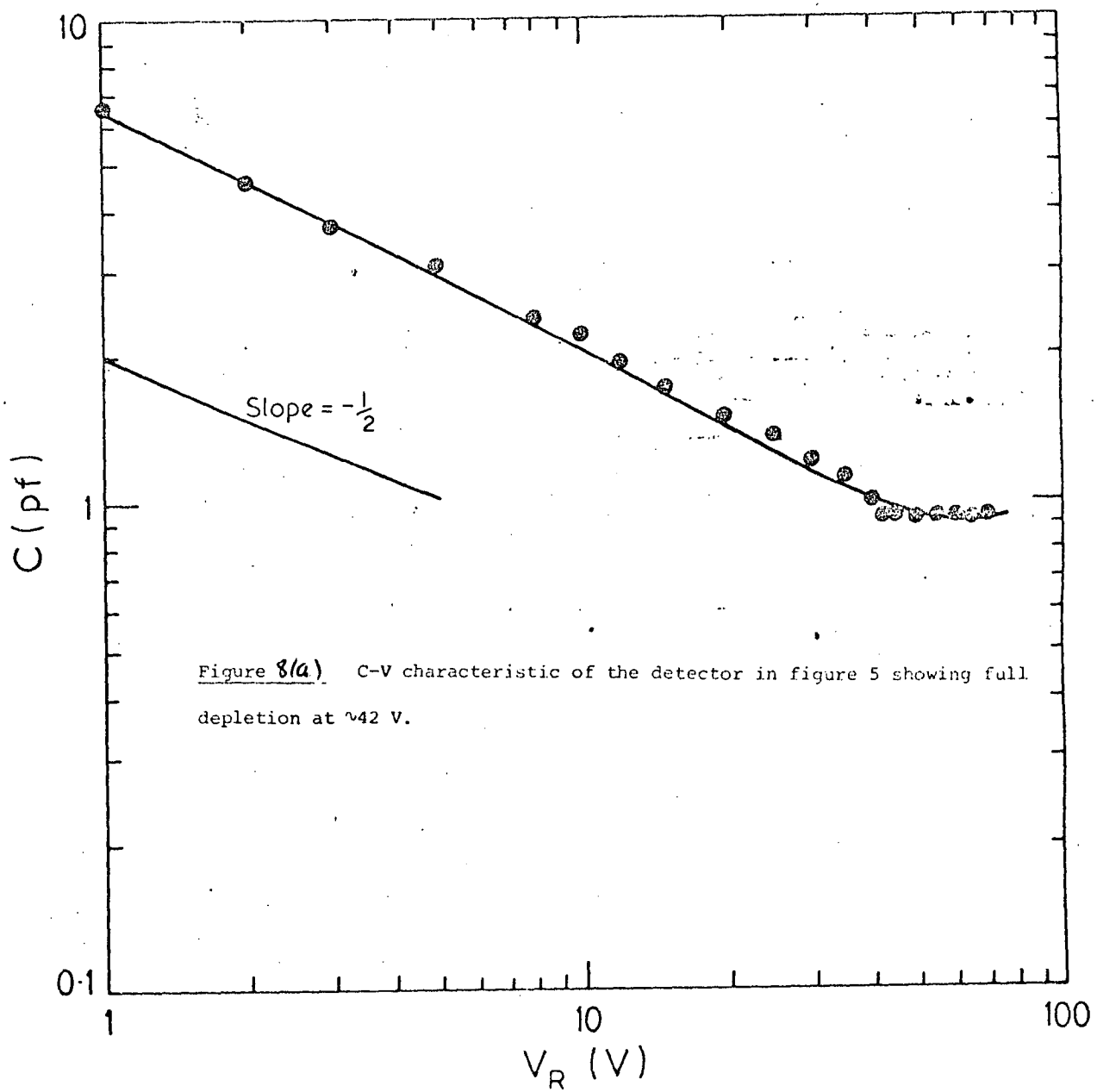

Figure 8(a) C-V characteristic of the detector in figure 5 showing full depletion at ~42 V.

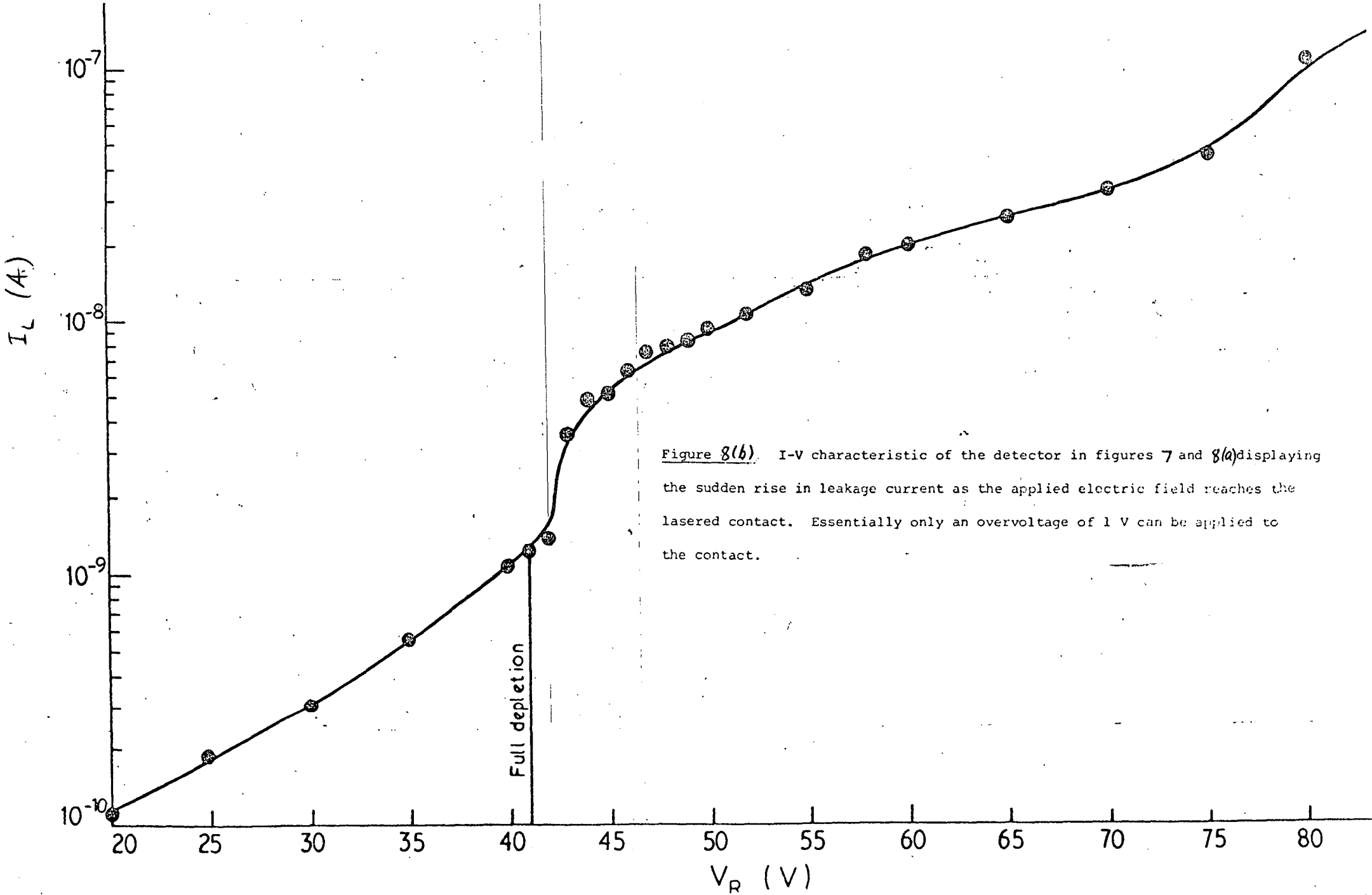

Figure 8(b) I-V characteristic of the detector in figures 7 and 8(a) displaying the sudden rise in leakage current as the applied electric field reaches the lasered contact. Essentially only an overvoltage of 1 V can be applied to the contact.

crystallinity on regrowth of the melt region causes current injection when the applied electric field reaches the LAD (Li) contact. Full depletion was achieved on two of the five n-type detectors fabricated and similar I-V characteristics were recorded for both.

3. p-type Silicon

Silicon α-particle detectors are normally fabricated on n-type material using a Au surface barrier contact, although a special p-type Si/Al contact configuration is available commercially [Ortec Catalogue 1980]. It would be useful to have an alternative and more simple fabrication technique for p-type material to be used as α-particle spectrometers.

A slice of 300 Ω cm p-type Si of area 2.1 cm^2 and thickness 1.5 mm was prepared and irradiated by laser in the normal way. Because of the propensity for Li contacts on Si to oxidise, the centre section of the contact was masked with tape and the perimeter soaked for one minute in a mixture of $1HF:3H_2O$ to remove the oxide. A 400 Å Ni layer was evaporated onto the perimeter to provide contact to the n^+ region. A second evaporation of 200 Å of Pd on the opposite face provided an ohmic contact. An α-resolution of 21.6 keV FWHM at 5.48 MeV was obtained.

A second set of α-particle detectors was fabricated from 2 kΩ cm p-Si. Using the thermal probe, it was noted that good quality LAD (Li) contacts do not appear to oxidise, possibly because, unlike a normal Li-diffused contact, they have a tendency to emulate the behaviour of a Li-Si metal alloy. Because of this, 2 kΩ diodes were fabricated without the evaporated Ni ring. Figure 9 shows the spectral response of a typical detector (at 80 K) having a contact area of 50 mm^2 and an operating bias of 250 V (7 nA leakage current).

One of these detectors was drifted for 200 hours at 550 V (40°C). The Li drifted region was delineated by plating with copper staining

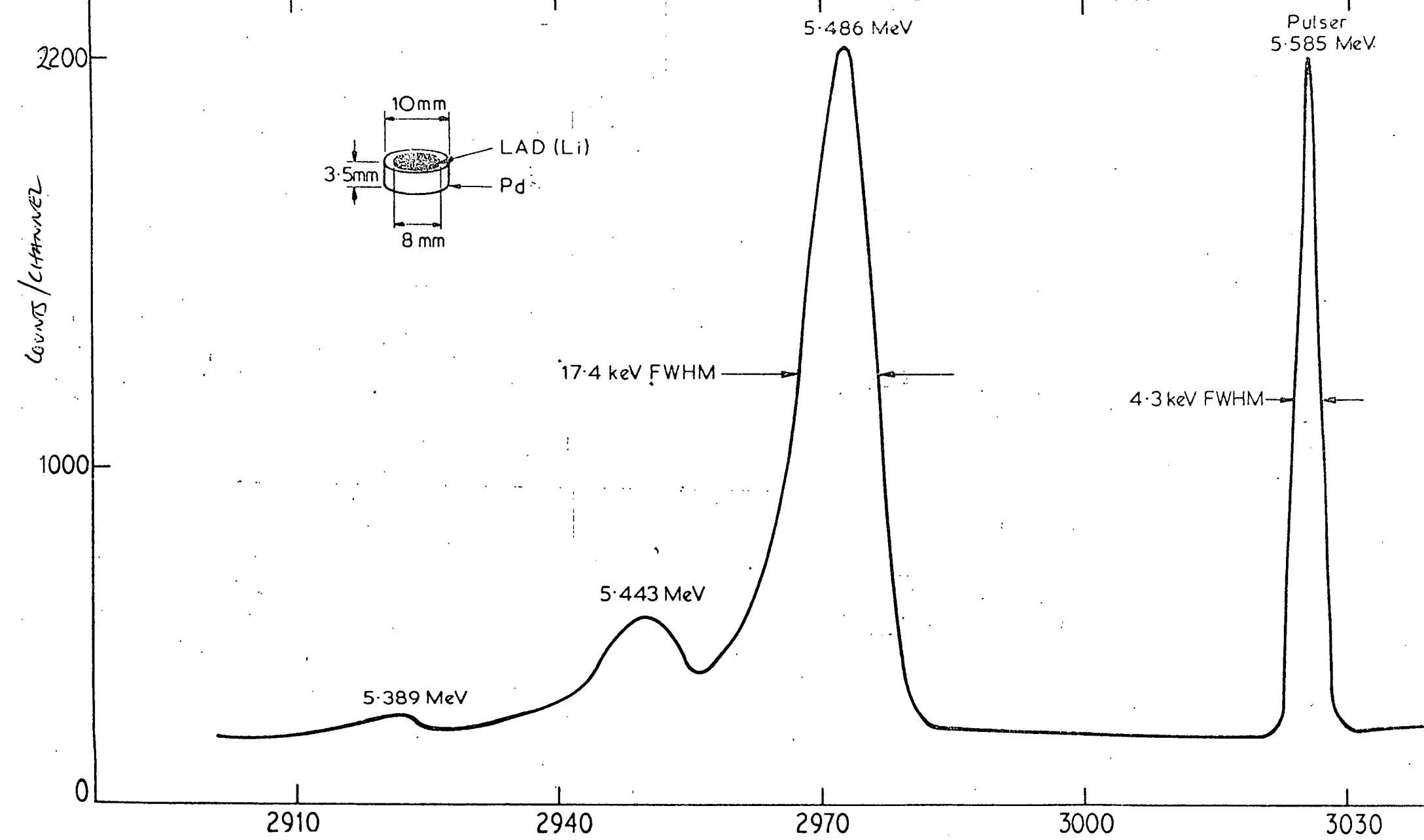

FIG. 9 ^{241}Am α-particle spectrum recorded through the LAD(Li) contact of a 2kΩ cm p-type Si detector. Bias 250 V, leakage current 7×10^{-9} A, 4 μs shaping time constant, detector diameter 8 mm.

solution and was measured at ∿220 μm. This is below the expected drift depth of ∿500 μm, but conventionally drifted samples of this material were also below the expected depth. The significance of this is that because of the low sheet resistivity of the LAD (Li) contact, slices may be Li drifted without Ni-plating the laser irradiated area.

4. n-type Silicon

One of the possible uses for LAD (Li) contacts is in X-ray fluorescence detectors which conventionally use heavy metal contacts; the lower atomic number of Li would reduce extraneous fluorescence peaks. The two types of material used for high-resolution X-ray detection are Si(Li) and HP N-Si. The high purity detectors (60 to 90 kΩ cm) typically have an Au surface barrier contact, with a guarded Li-diffused, ohmic contact which is Ni-plated; X-rays enter the thin Au contact. These detectors normally operate with 10 to 50% overvoltage.

A section of 90 kΩ cm n-type Si was prepared with a LAD (Li) contact, on which a guard ring was cut using a N_2 jet abrasive unit. After masking the collector and guard regions, the diode was etched for a total of 22 minutes in $8HNO_3$:$1HF$:$1CH_3COOH$, and a 200 Å gold surface barrier evaporated onto the opposite face. The spectral response of the diode at 80 K to ^{241}Am X- and γ-rays aimed through the LAD (Li) contact and to ^{57}Co X-rays is shown in Figures 10 and 11 respectively. The operating characteristics of this detector are worth noting: there was no measureable improvement in resolution from 250 to 1300 V operating bias (pinch-off bias = 235 V, total $I_L = 3 \times 10^{-11}$ Å). This result is in contrast to that obtained with overvoltage to an ohmic contact on HP n-Ge. Clearly the laser powers were near optimum to melt Si, whereas they were excessive for the lower melting point Ge, the excess energy leading to lattice damage.

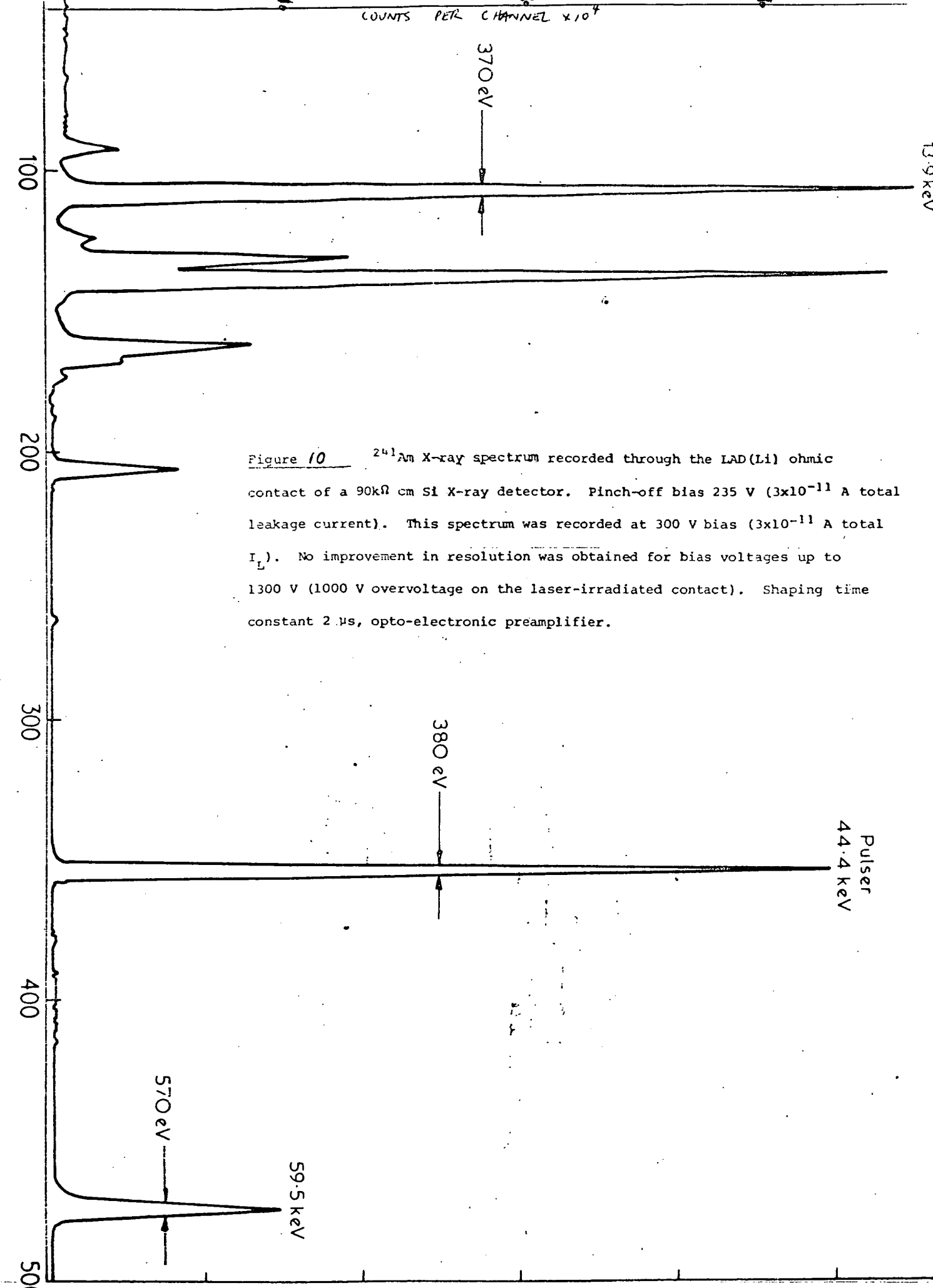

Figure 10 ^{241}Am X-ray spectrum recorded through the LAD(Li) ohmic contact of a 90kΩ cm Si X-ray detector. Pinch-off bias 235 V (3×10^{-11} A total leakage current). This spectrum was recorded at 300 V bias (3×10^{-11} A total I_L). No improvement in resolution was obtained for bias voltages up to 1300 V (1000 V overvoltage on the laser-irradiated contact). Shaping time constant 2 μs, opto-electronic preamplifier.

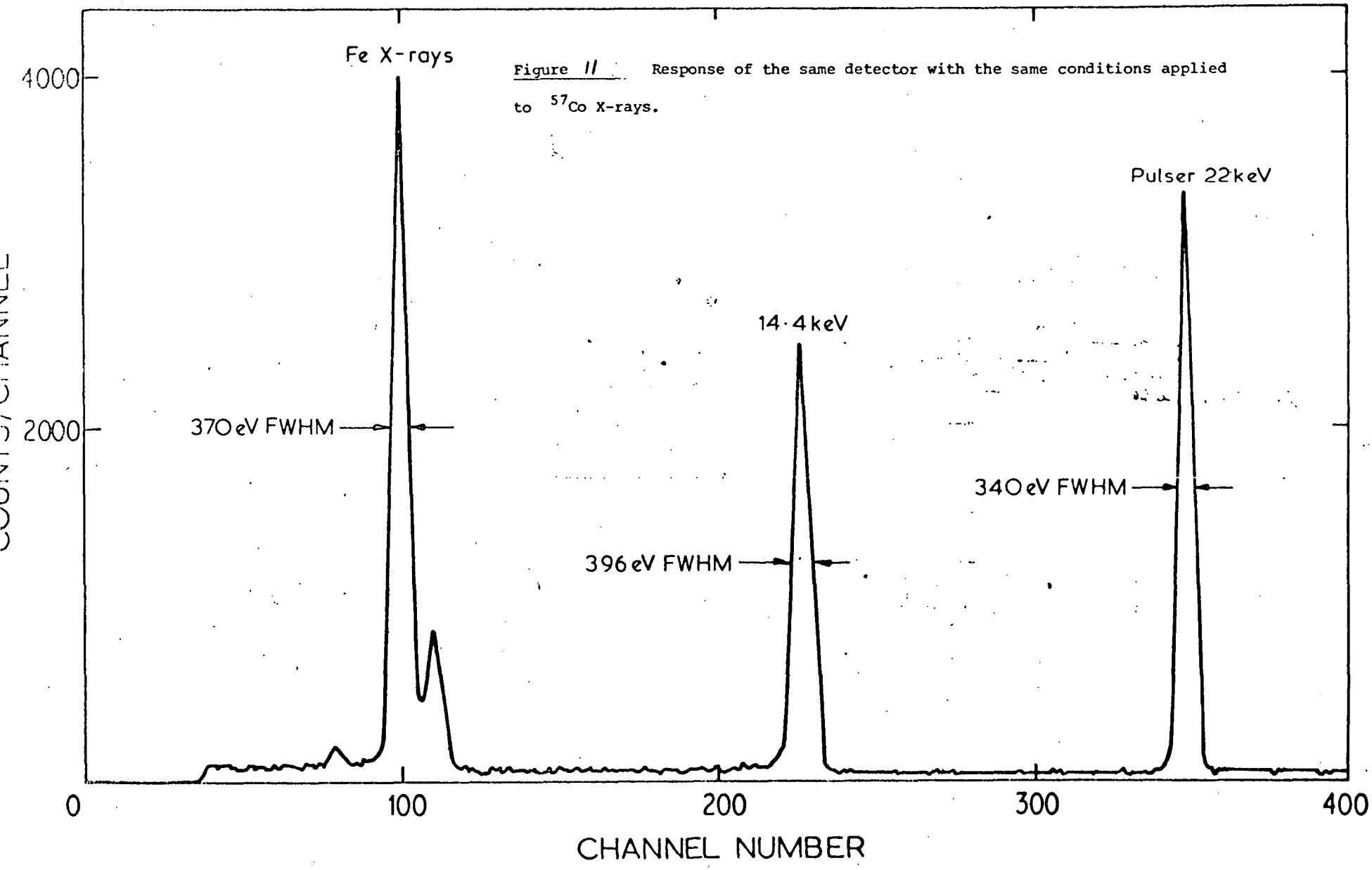

Figure 11 Response of the same detector with the same conditions applied to ^{57}Co X-rays.

Use of a suitable low atomic number p-type dopant (e.g. B) as a laser doped p^+ contact could mean construction of a XRF detector without the easily damaged metal contacts. More simply, Au/LAD (Li) XRF detectors such as described above, could be used with the X-rays beaming through the Li contact, just as was done above. Extraneous fluorescence peaks would not be a problem in this configuration.

CRYSTAL HEATING AND DEEP LEVEL TRANSIENT SPECTROSCOPY

The ultra-thin LAD (Li) contacts have been stable for periods greater than four months at room temperature. However, this is not the case at elevated temperatures. The excess laser energy used on many contacts, particularly on Ge, produces damage centres at which the interstitial Li ions precipitate. Figure 12 shows the times required at various temperatures before the laser-irradiated contact precipitates. These were determined with the thermal probe which displays the heavy laser damage remaining after precipitation as a strong p-type reading. A comparison of the deflection of a precipitated contact with other well-characterised Ge samples showed that the p-skin remaining after Li precipitation had an approximate doping density of $N_a - N_d \approx 5 \times 10^{13}$ cm^{-3}.

The results on Ge are particularly startling; just two minutes at 120°C can turn a formerly highly doped n^+ region into a moderately doped p-region.

The results on Si are less obvious; the points plotted for Si are arbitrarily taken at the stage at which the laser-irradiated contact gives probe readings that are 30% of its original value, i.e. the region is converting from n^+ to n. The Seebeck effect is less obvious in Si than in Ge, and the thermal probe results are less reliable. Clearly, no detector with a LAD (Li) contact can be heated without the danger of precipitating the contact; this is their single

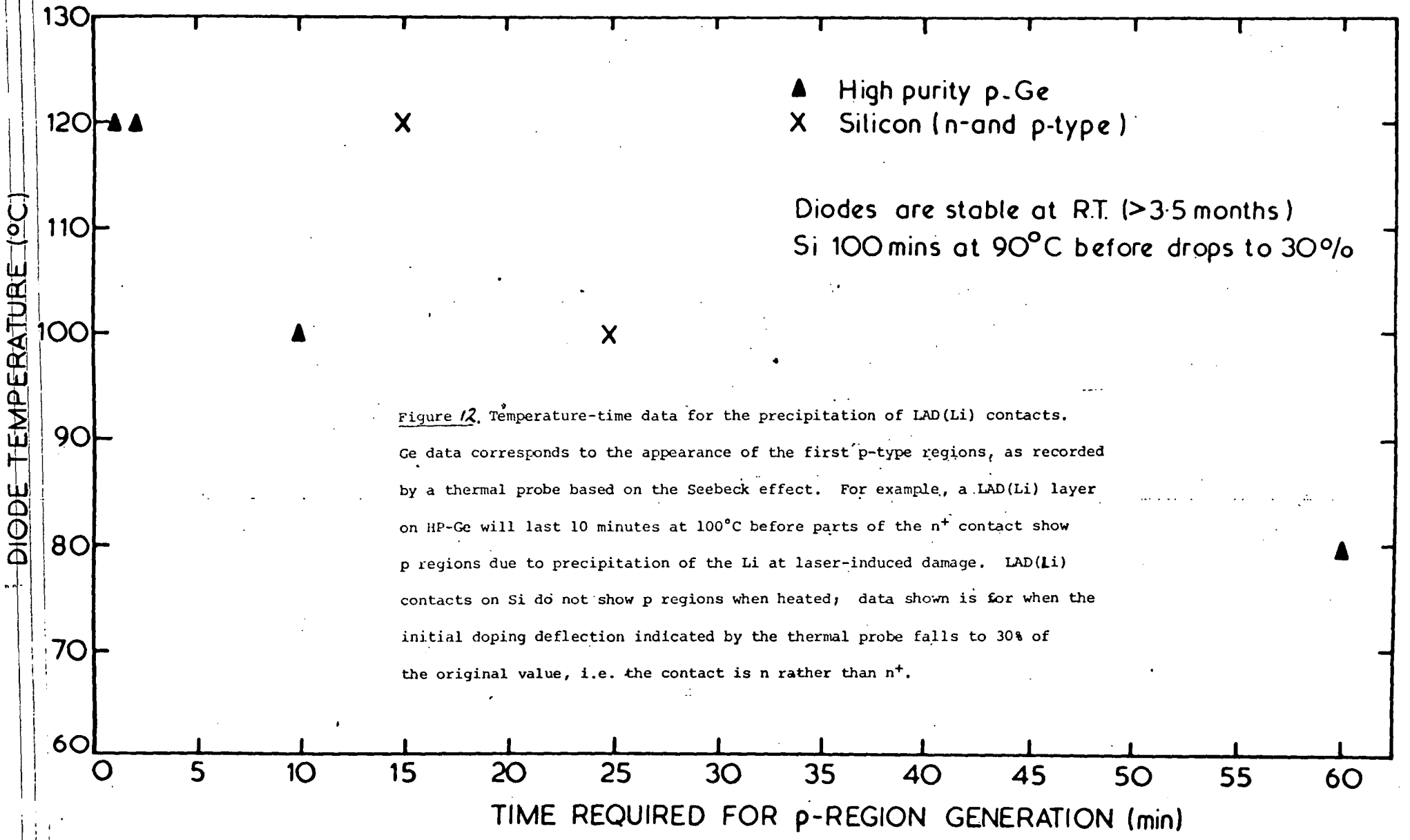

Figure 12. Temperature-time data for the precipitation of LAD(Li) contacts. Ge data corresponds to the appearance of the first p-type regions, as recorded by a thermal probe based on the Seebeck effect. For example, a LAD(Li) layer on HP-Ge will last 10 minutes at 100°C before parts of the n^+ contact show p regions due to precipitation of the Li at laser-induced damage. LAD(Li) contacts on Si do not show p regions when heated; data shown is for when the initial doping deflection indicated by the thermal probe falls to 30% of the original value, i.e. the contact is n rather than n^+.

most important disadvantage.

Figure 13(a) shows a deep level transient spectroscopy spectrum obtained on a HP Ge detector by pulsing the standing bias on the diode into the forward direction; this allowed the observation of deep level defects in the zero bias depletion region next to the contact. Acceptor level defects with a concentration of 1.1×10^9 cm^{-3} were present near the contact before precipitation, but after precipitation, their concentration was 5×10^{10} cm^{-3} (Figure 13(b)). The latter result was obtained by evaporating an In surface barrier contact onto the now p-type region.

It should be noted that the diodes had a wide range of defect densities before and after precipitation: 4.2×10^8 to 1.2×10^{10} cm^{-3} during laser-irradiation and 3×10^9 to 9×10^{11} cm^{-3} after heating. Such a density of generation-recombination centres in the contact region would have an effect on reverse leakage current. Generally, the DLTS spectra consisted of a smear of acceptor defects although, in some cases, data could be obtained on energy levels and cross sections of individual levels. Results for two acceptors were $E_v + 0.17$ eV ($\sigma_p \sim 6 \times 10^{15}$ cm^{-2}) and $E_v + 0.28$ eV ($\sigma_p \sim 5 \times 10^{-15}$ cm^{-2}).

Again, the Si diodes showed fewer trapping effects, both before and after heating, with little apparent change in DLTS spectrum between the two. Trap densities before and after heating were typically $\sim 8 \times 10^{-4}$ of the net background doping density.

DISCUSSION

It should be noted that the exact output of energy after homogenisation of the Q-switched ruby laser was never accurately known during this investigation. The crystal heating and DLTS data show that the laser energy was excessive in the case of the Ge detectors. Indeed, if one refers to Figure 2 of Meyer et al. (1980) showing the

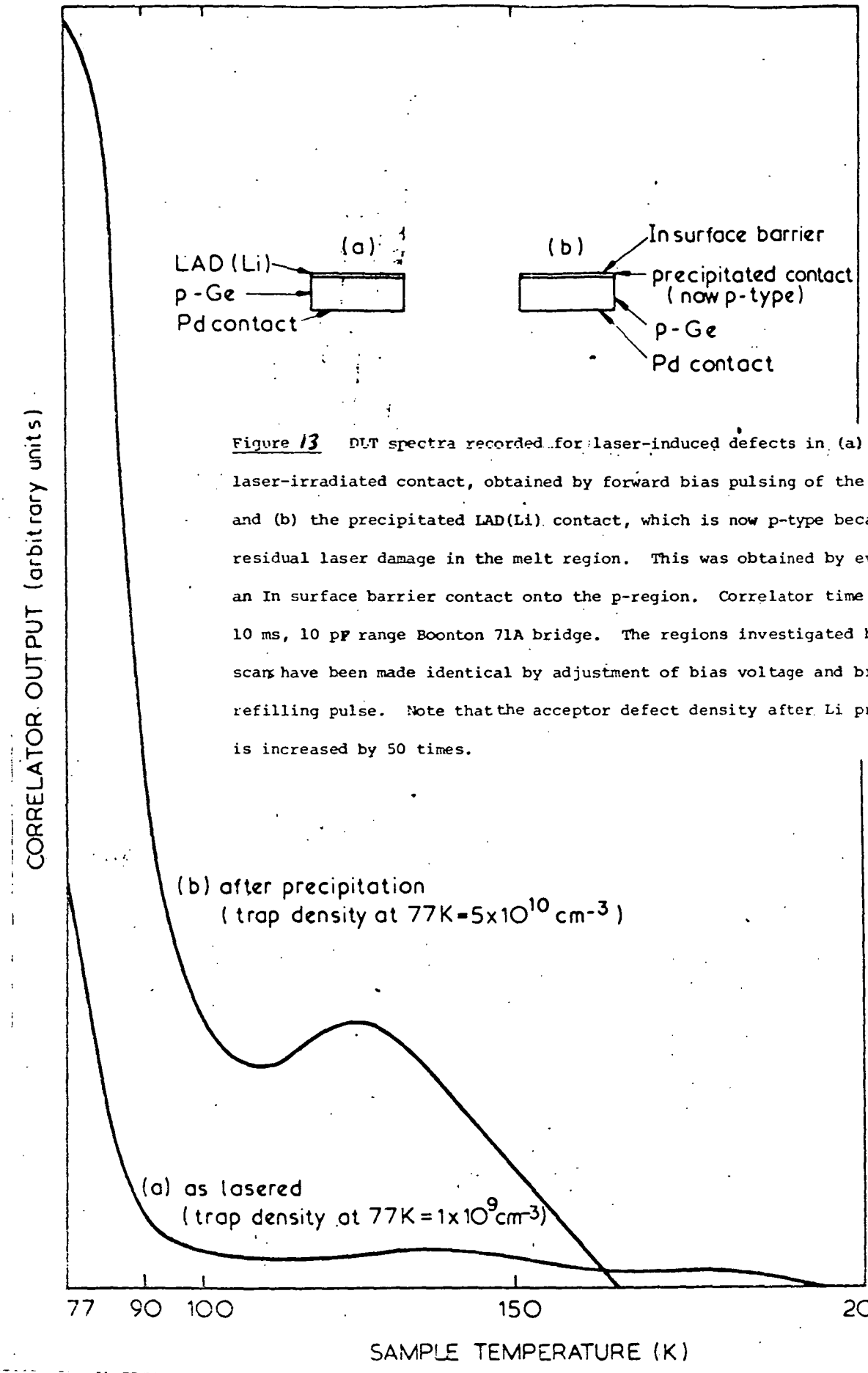

Figure 13 DLT spectra recorded for laser-induced defects in (a) the laser-irradiated contact, obtained by forward bias pulsing of the p-n^+ junction and (b) the precipitated LAD(Li) contact, which is now p-type because of residual laser damage in the melt region. This was obtained by evaporating an In surface barrier contact onto the p-region. Correlator time constant 10 ms, 10 pF range Boonton 71A bridge. The regions investigated by the DLTS scans have been made identical by adjustment of bias voltage and bias trap-refilling pulse. Note that the acceptor defect density after Li precipitation is increased by 50 times.

theoretical and experimental thresholds for melting damage versus pulse duration in Ge using a Q-switched ruby laser, one sees that 80 MW/cm^2 for 25 ns is just on the damage threshold, 240 MW/cm^2 is well above it. Similarly, Figure 4 of Meyer et al. (1980) shows the corresponding case for Si: our lower limit of 80 MW/cm^2 is well below the damage threshold and 240 MW/cm^2 just on the threshold. The results of this Chapter would support the Myer et al. data for both Si and Ge. A comprehensive theory of the melting process during pulsed laser irradiation has been published by Wood and Giles (1981). The actual amount of energy absorbed, of course, will depend upon the surface finish of the particular sample, and the reflectivity and absorption coefficients of the evaporated Li layer. As well, the Li vapour pressure during the melting process may have an effect on the absorbed energy.

Notwithstanding this, useful γ- and α-spectrometers have been fabricated from Ge by the laser melting technique. Doubtless, the useful window of laser energies (i.e. enough to melt the surface, but not enough to ruin the device through excess lattice damage) may be extended upward by the forgiving nature of the Li contact. The gettering action of Li on acceptor level defects is well known and has been demonstrated in these laboratories in ^{60}Co γ-irradiated Li-drifted and undrifted p-type Ge sections using DLTS. As no other shallow dopant exhibits this behaviour, it is expected that without annealing, LAD (Li) contacts will be consistently more successful than any other laser-aided doped contact.

The simple fabrication technique of these devices is worthy of brief comment. At no stage in the detector manufacture is the bulk crystal heated, and normally only two evaporations and a laser shot (apart from the normal polishing and etching) are required to produce

a workable diode. However, in Ge, the crystal can thereafter never be heated above, say, 60°C, which rules out the possibility of annealing radiation damaged detectors in situ. Typically these are heated to ∿150°C for tens of hours [Pehl et al. 1978] to remove proton and neutron damage. It may be possible, of course, to find the exact laser energy where little precipitation occurs on heating, but even so, any heating to significant temperatures will thicken the contact by thermal diffusion of the Li.

Oxidation of the evaporated Li layer before laser-irradiation has never been a problem. The incorporation of large concentrations of Li into the crystal are expected to dominate any other effect, although the incorporation of oxygen may prove to have a long-term stabilising effect on the movement of Li. Similarly, the storage of evaporated layers under N_2 before laser-irradiation has produced no significant difference in contact behaviour. Alpha particle resolutions of LAD (Li) HP p-type Ge detectors have not changed over several months, indicating that over this period there has been no significant movement of the Li.

As mentioned in section 1, no attempt was made to vary the Li layer thickness during evaporation. Qualitatively, it can be said that, in view of the results in section 4, the thick evaporated layers may have helped reduce the excess lattice damage by the laser.

Although the sensitive volumes of LAD (Li) detectors are at present small compared to conventional devices, this could be overcome either by homogenising the laser beam over larger areas, or by using laser irradiation in an overlapping pattern.

The fabrication yield of the technique is reasonably high; about 80% of the detectors manufactured could be classed as reaonable quality (<4 keV FWHM resolution at ^{137}Cs γ-rays for Ge, <25 keV FWHM resolution at ^{241}Am α-particles for Si). Twenty per cent of the detectors could

perhaps be classed as good quality (~3 keV resolution at ^{137}Cs for Ge; <20 keV at ^{241}Am for Si). However, it must be emphasised that approximately half of the detectors required parts of the laser-irradiated contact to be removed selectively by etching because of poor quality.

SUMMARY

A simple fabrication technique for the production of thin, mechanically robust n^+ contacts on nuclear radiation detectors has been described. The detectors fabricated by this method are at present small, but there is no heating of the bulk crystal and α-particle measurements indicate that the doped region is <0.1 μm thick. Good quality detectors of α-particles, γ- and X-rays have been produced from n- and p-type Ge and Si. The contacts cannot be heated, especially with Ge, owing to the precipitation of Li at laser-induced damage.

REFERENCES

Amann, J.F., Barnes, P.D., Dytman, F.A., Penkrot, J.A., Thompson, A.C. and Pehl [1975] - Nucl. Instr. and Meth. 126:193

Beech, A.McG. [1981] - private communication

Cullis, A.G., Webber, H.C. and Bailey, P. [1979] - J. Phys. E. Sci. Instrum. 12:689.

Gat, A., Gibbons, J.F., Magee, T.J., Peng, J., Deline, V., Williams, P. and Evans, C.A. [1978] - Appl. Phys. Lett. 32:276.

Meyer, J.R., Kruer, M.R. and Bartoli, F.J. [1980] - J. Appl. Phys. 51 (10) 5513.

Ortec Catalogue, Instruments for Research and Applied Sciences [1980].

Pehl, R.H., Varnell, L.S. and Metzger, A.E. [1978] IEEE Trans. NS 25:409.

Protić, D. and Riepe, G. [1977] - IEEE Trans NS 24:64.

White, C.W., Narayan, J. and Young, R.T. [1979] - Science 204:461.

White, C.W. and Peercy, P.S. (eds.) - Laser and Electron Beam Processing of Materials (Academic Press, 1980).

Wood, R.F. and Giles, G.E. [1981] - Phys. Rev. B 23 (6) 2923.

3.2 COMPOUND SEMICONDUCTORS GaAs AND CdTe

SUMMARY

A Q-switched ruby laser has been used to dope bulk and epitaxial n-GaAs ($n \simeq 2 \times 10^{16}$ cm^{-3}) from thin (<50 nm) evaporated Sn films. Rutherford backscattering and scanning electron microscope measurements (SEM) have been used to characterise the doped regions which are ohmic up to current densities of 300 mA/cm^2. SEM results also show evidence for incorporation into GaAs of Zn alloyed from a thin surface layer. No successful contacts were fabricated to CdTe, possibly because of excessive laser power.

INTRODUCTION

Considerable effort has been directed towards the doping of GaAs by laser melting of thin evaporated layers [Eckhardt 1980], usually to produce low resistance ohmic contacts. Difficulties have arisen in the control of various dopant layers owing to differing reflectivities and melting points. In addition, excess laser energy may result in the loss of As from the surface and produce problems associated with non-stoichiometry and Ga precipitation, although the evaporated layer may tend to reduce this effect. Previous work has described the formation of ohmic contacts by the laser irradiation of a double evaporated layer of Ag and Sn [Pounds et al. 1974]. In the present work, a technique for laser-assisted doping from thin single layers of Sn is demonstrated. The contacts have remained stable to current densities of 300 mA/cm^2, with maximum diameters of 16 mm. It may be possible to produce larger area contacts by using multiple laser shots in an overlapping pattern.

The formation of stable contacts to CdTe is still mostly a matter of black magic. A survey of the literature [2nd Int. Symp. Cadmium Telluride 1976] shows that evaporation of the same metal to opposite

faces of a semiconducting CdTe wafer will often produce a diode - one contact is rectifying, the other ohmic, depending on the surface layer to which it was evaporated. The production of thin, stable, consistent contacts to CdTe would be a useful procedure.

GaAs EXPERIMENTS

The material was nominally undoped n-type GaAs, both bulk ($n = 2 \times 10^{16}$ cm^{-3}) and epitaxial (LP, $n = 1.8 \times 10^{16}$ cm^{-3}). Polished surface were obtained by lapping the samples on a slurry of 600 # SiC grit on glass, and etching for three minutes in a mixture of $3HNO:2H_2O:1HF$. Thin films of Sn, generally <50 nm thick, were evaporated onto the samples at $<5 \times 10^{-6}$ torr.

A Q-switched ruby laser ($\lambda = 0.6943$ μm, FWHM 25 ns) was used to irradiate the samples. The beam was homogenised by passing it through a quartz or Perspex light pipe of the type described by Cullis et al. [1979]. Power densities after homogenisation were in the range 80 to 240 MW cm^{-2} and uniform over diameters 7 to 16 mm. The lower power is just on the threshold damage in GaAs for a 25 ns laser pulse, while the upper power is well over the threshold (see Figure 6 of Meyer et al. [1980]). Evidence that the sample surface had melted during irradiation was sought by observing the typical [Badertschev et al. 1980] melt pattern finish - an irregularly rippled 'orange peel' appearance (Figure 1).

Irradiations were performed both in air and in a gas cell with an inert (Ar) atmosphere. No effects due to the environment such as oxygen incorporation were discerned. After irradiation, excess Sn was removed by soaking for 15 minutes in HCl acid. The samples were then examined under the optical microscope for evidence of melting. A preliminary check for doping was performed with a thermal probe based on the Seebeck effect. The ten samples fabricated by the

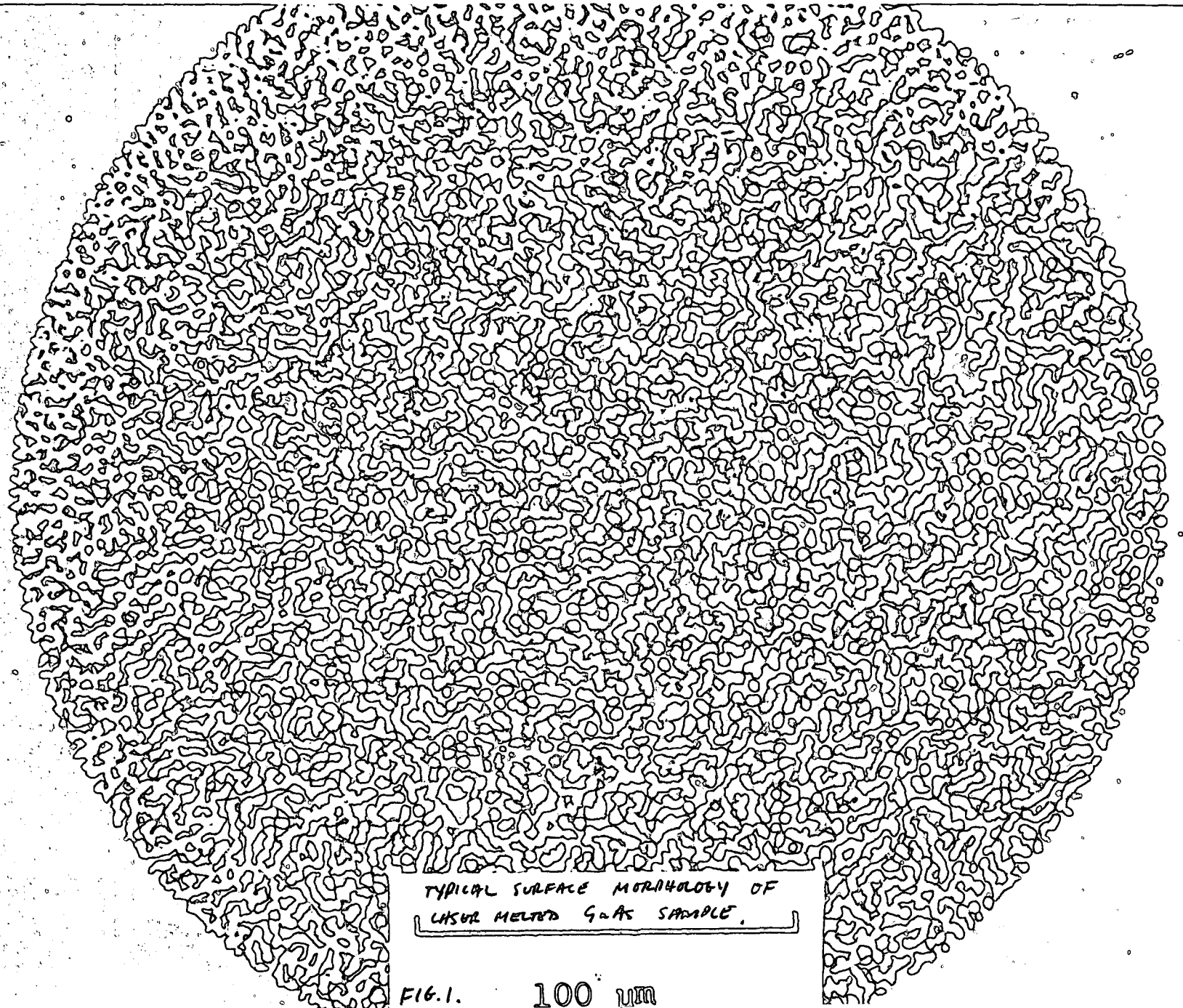

TYPICAL SURFACE MORPHOLOGY OF LASER MELTED GaAs SAMPLE.

FIG. 1.

100 μm

described procedure were all found to be heavily doped in the laser melted regions. I-V characteristics were recorded for some of these samples (measured between two laser-doped spots of area 0.05 cm^2) and found to be ohmic for current densities ≤ 300 mA/cm^2 (Figure 2). The degree of ohmicity can be determined by measuring the correlation coefficient from a least squares analysis; coefficients of better than 0.997 were obtained. The contact sheet resistance, 3.8 $\Omega/\square$, was obtained from I-V characteristics recorded between evaporated gold layers placed a fixed distance apart on the laser doped region. It is not possible to compare this to previous experiments [Pounds et al. 1974]. It should be noted that the contact areas in this work are several orders of magnitude larger.

RBS MEASUREMENTS

The Sn laser-doped contacts were further investigated by RBS of 2 MeV He^+ ions. Figure 3 shows a set of RBS spectra obtained at 170°†. A comparison can be made of aligned yields both off and on the Sn contact. Off the contact, the χ_{min} is poorer than the values obtained by Kular et al. [1979] who laser-annealed ion-implanted GaAs, perhaps suggesting that our power densities may have been excessive.

The Sn penetration depth was estimated to be 53 nm from the FWHM of the impurity peak. This gives a lower limit for the melt depth, assuming uniform incorporation of the Sn in the melt and no segregation. The melt depth is expected to be a function of both the laser output power density and the thickness of the evaporated Sn layer. Furthermore, the total Sn solubility (averaged over the penetration depth) is estimated to be 3.5×10^{20} cm^{-3} and the substitutional solubility to be 1.6×10^{20} cm^{-3}. It is not known what fraction of Sn is electrically active.

---

†Courtesy M. Scott and E. Lawson, AAEC.

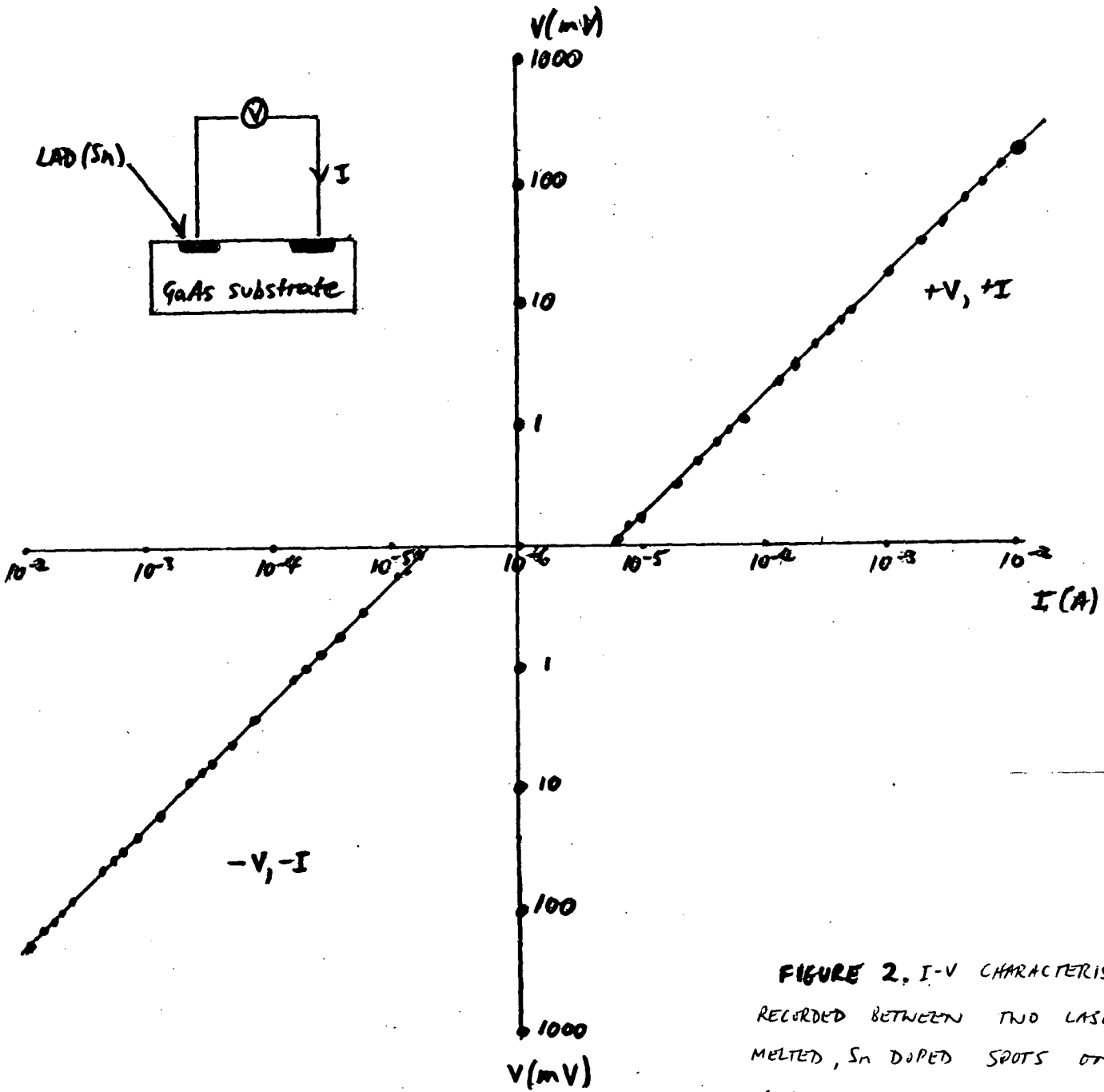

FIGURE 2. I-V CHARACTERISTIC RECORDED BETWEEN TWO LASER MELTED, Sn DOPED SPOTS ON A GaAs SUBSTRATE.

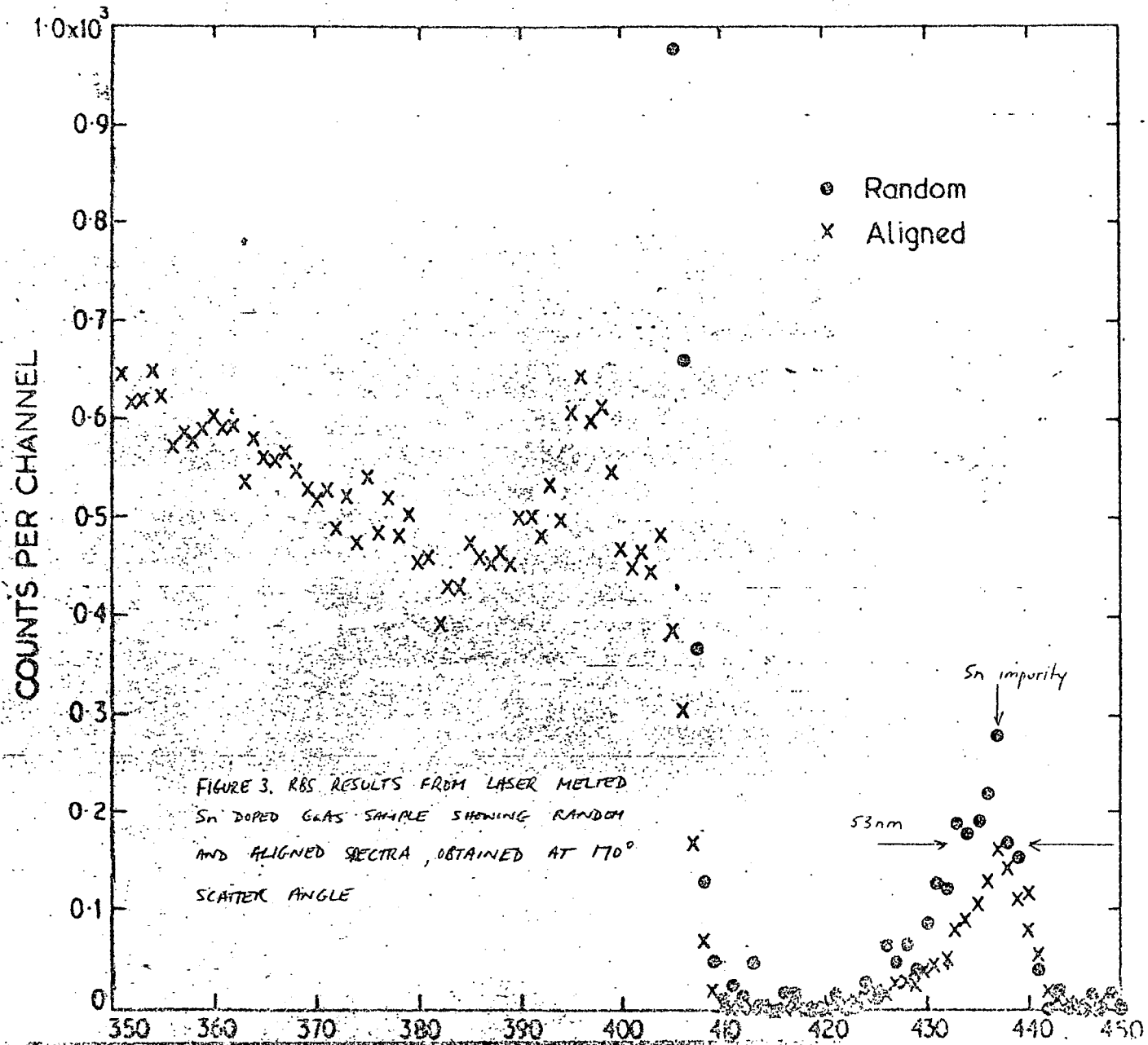

FIGURE 3. RBS RESULTS FROM LASER MELTED Sn DOPED GaAs SAMPLE SHOWING RANDOM AND ALIGNED SPECTRA, OBTAINED AT 170° SCATTER ANGLE

SEM MEASUREMENTS

The high spatial resolution of the SEM offers a possible useful tool in examining laser melted contacts. The diameter of the electron beam is 10 to 20 Å, which is much lower than the particle beam used in RBS. Figures 4 and 5 show X-ray fluorescence mode SEM measurements on a laser-doped Sn contact on GaAs[†]. Although Sn X-ray peaks are found in the lasered region, they are only just visible above the background. The signal was too low to allow a scan of the whole region. Measurements on another highly doped contact on a different sample confirmed the low sensitivity (Figures 6 and 7).

Zn DOPING ON GaAs

In an attempt to produce a p-type doped region on n-GaAs the procedure was repeated using Zn instead of Sn. The thermal probe indicated heavy doping and more obvious Zn X-ray peaks were detected using the SEM (Figures 8 and 9). The Zn distribution was non-uniform, possibly because of a non-uniform evaporation. It was difficult to evaporate a controlled thickness of Zn, and it was found that a thin layer was needed to achieve success with the laser melting. The junction I-V characteristics for these samples (p^+ on n-GaAs) were markedly non-linear, but often they were 'reverse' diodes, which may be evidence for the possible formation of an anomalous interface region at the melt front. Electron-beam induced current measurements on the SEM would be needed to confirm this.

Other dopants tried were Si, Te, Ge, Ga, Cd, Au and Ag. The only successful contact fabricated was with Ge, which has also been reported by Badertschev et al. [1980]. The others may also be suitable, as these investigations were performed at a time when the excessive laser energy problem was not fully appreciated (see next section).

[†]Courtesy K. Watson and E. Lawson, AAEC.

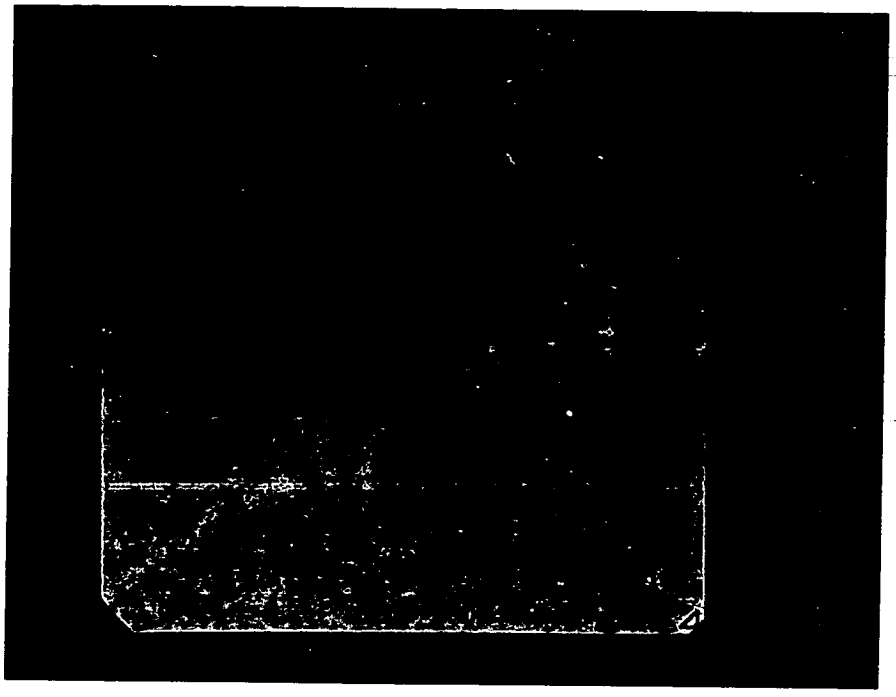

GaAs Sn CONTACT X80

MCP n-type material - boundary of laser treated region.

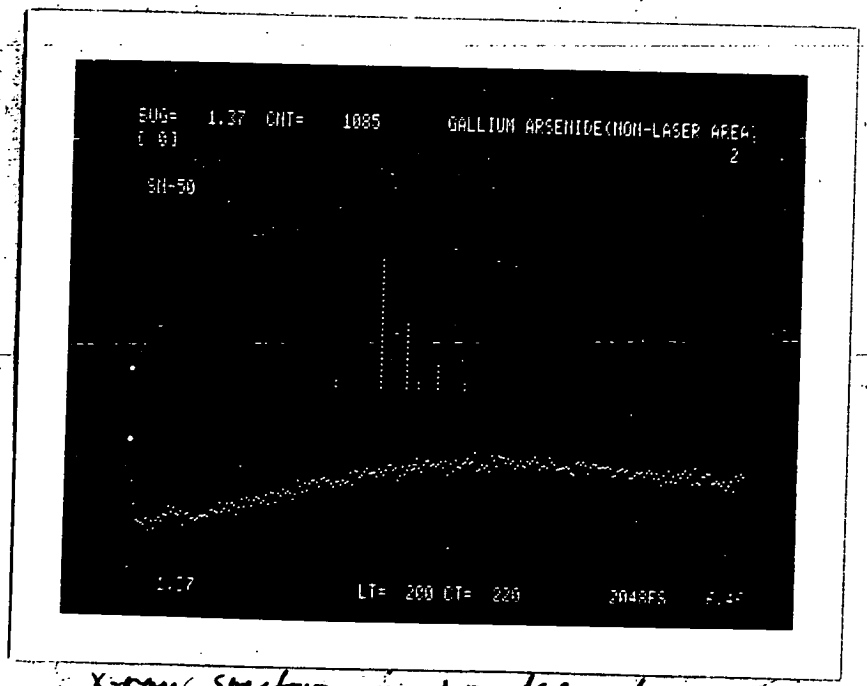

X-ray spectrum in non-lasered area

FIGURE 4. XRF DATA ON LASER DOPED Sn CONTACT ON MCP n-GaAs.

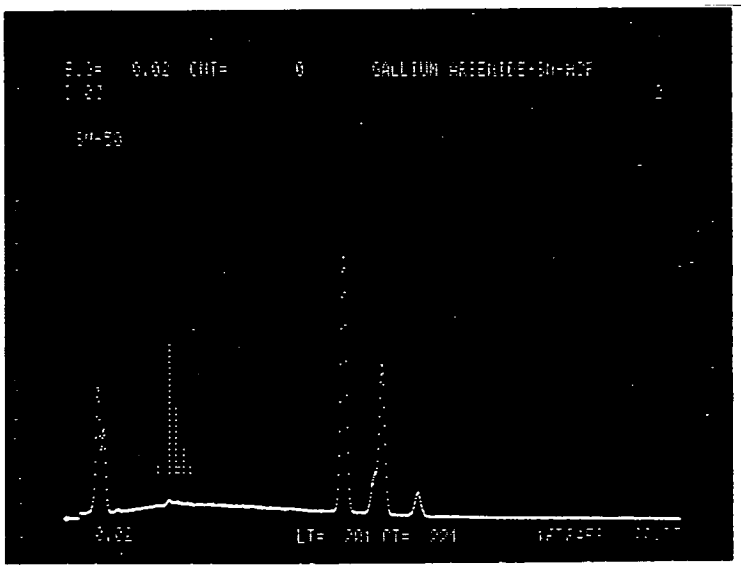

X-RAY SPECTRUM IN LASER TREATED REGION

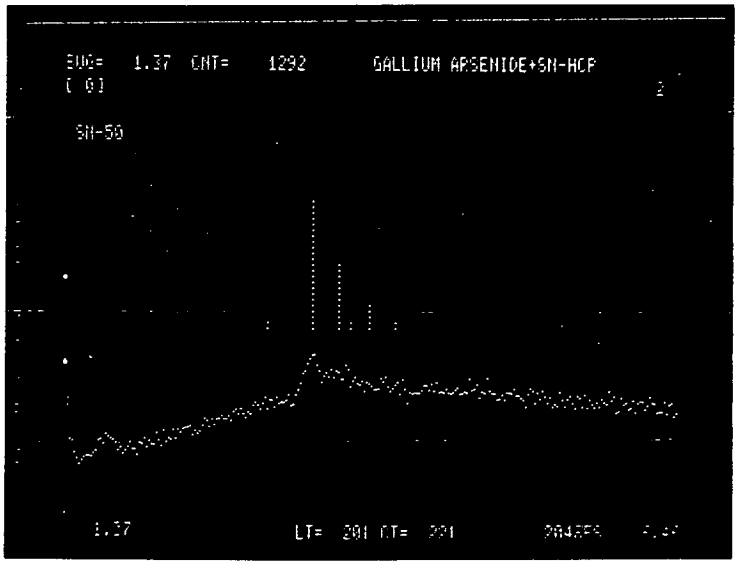

EXPANSION OF ABOVE.

FIGURE 5. XRF DATA ON LASER BONDED Sn CONTACT ON MCP n-GaAs.

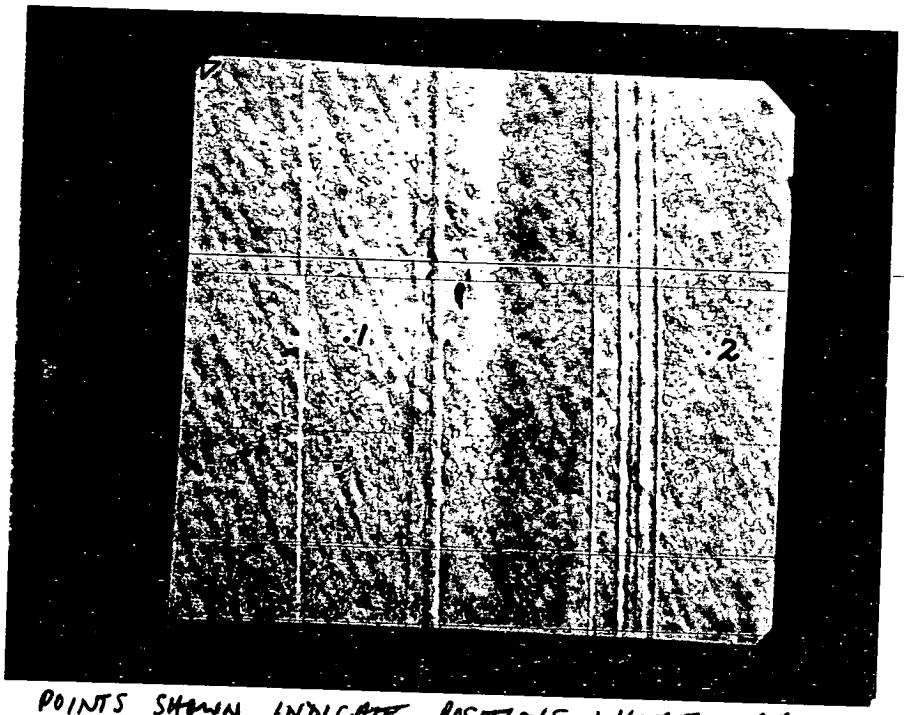

POINTS SHOWN INDICATE POSITIONS WHERE X-RAY SPECTRA ACCUMULATED. 1 IS ON BEAM
2 IS OFF BEAM

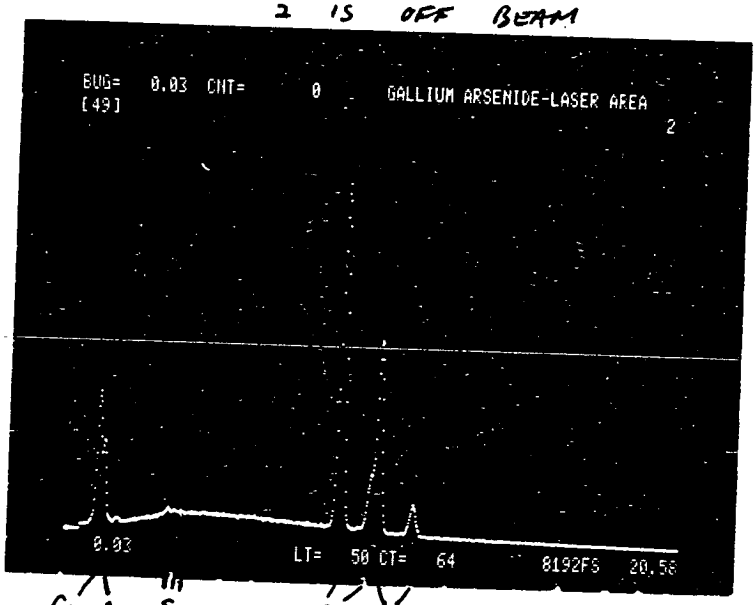

X-RAY SPECTRUM IN LASERED AREA - POINT 1 IN TOP PHOTO

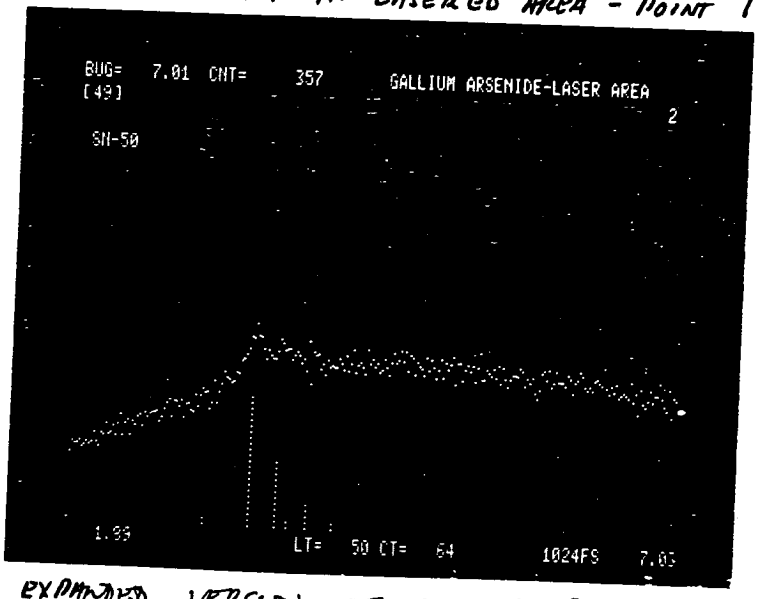

EXPANDED VERSION OF MIDDLE PHOTO.

FIGURE 6. XRF DATA FROM LASER DOPED Sn CONTACT, SWAS VP-8.

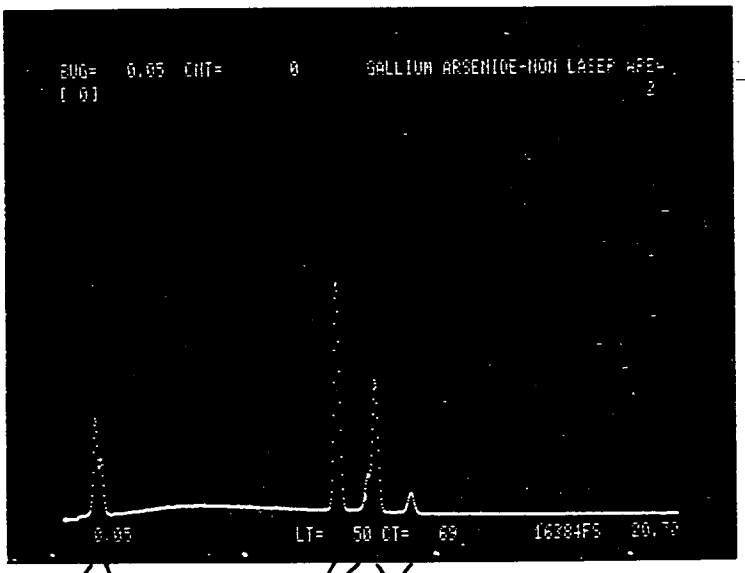

X-RAY SPECTRUM OUTSIDE LASERED AREA - POINT 2 IN PREVIOUS FIGURE.

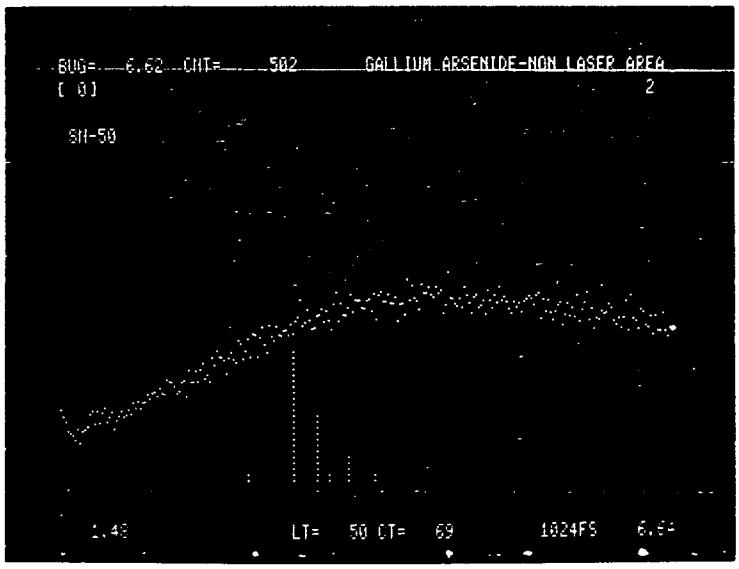

AS ABOVE, EXPANDED VERSION

FIGURE 7. XRF DATA FROM LASER DOPED Sn CONTACT (GaAs VP-8)

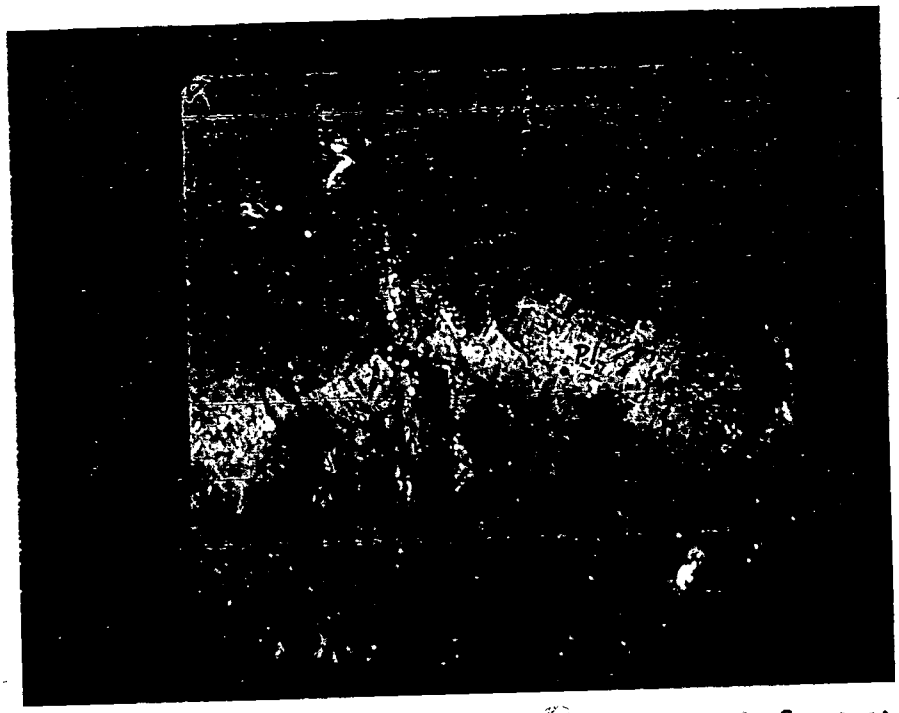

GaAs VP18 LASER MELTED Zn CONTACT - BOUNDARY OF LASER TREATED REGION - PI INDICATES WHERE PHOTOS IN FIGURE 9 TAKEN FROM.

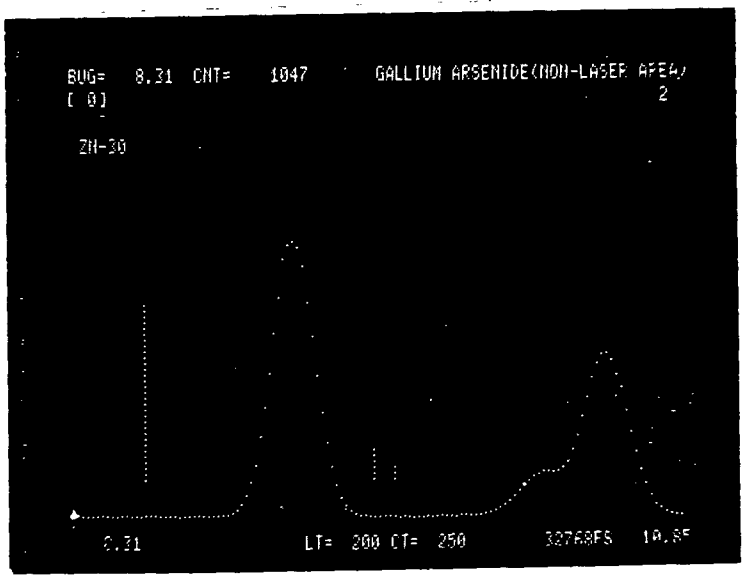

X-RAY SPECTRUM IN NON-LASERED REGION

FIGURE 8. XRF DATA ON LASER MELTED Zn CONTACT ON GaAs.

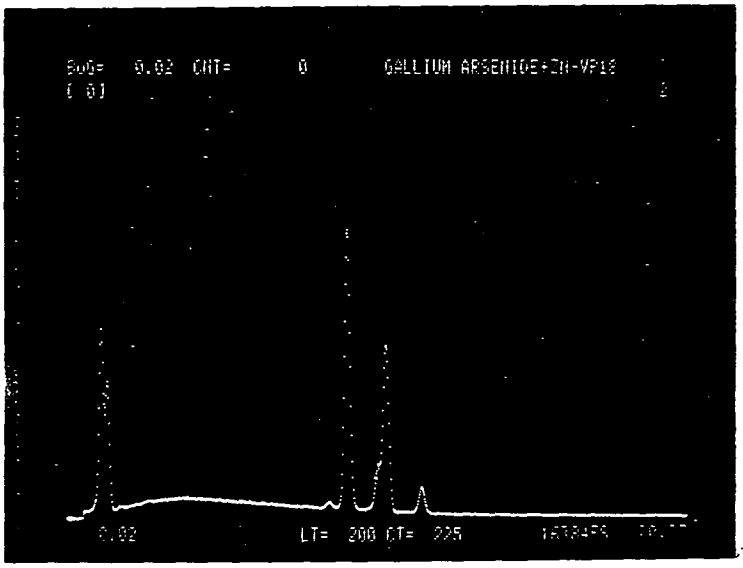

Zn SIGNAL FOUND AT P1 IN FIGURE 8 - THE SIGNAL WAS STRONGER ON THE PERIPHERY OF THE USERED REGION THAN IN THE CENTRE.

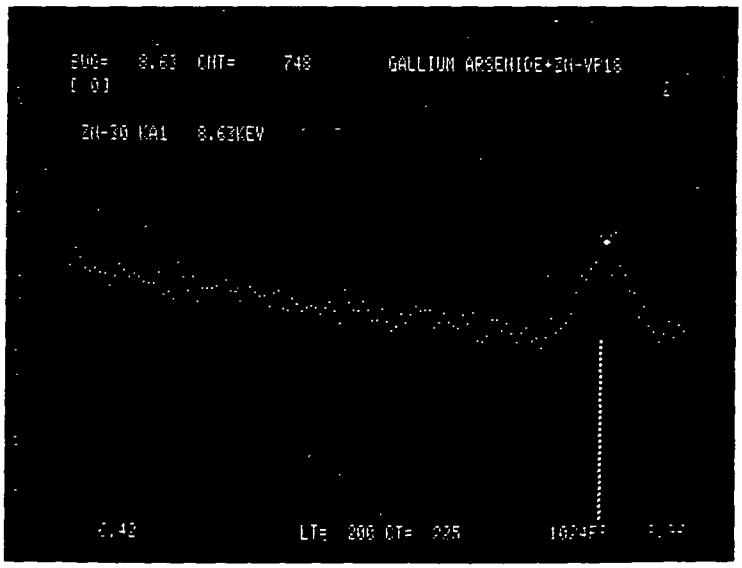

EXPANDED VERSION OF ABOVE.

FIGURE 9. XRF DATA FROM LASER MELTED Zn CONTACT (GaAs UP 18).

CdTe EXPERIMENTS

Wafers of low resistivity and semi-insulating CdTe grown in these laboratories were prepared by cutting, polishing on cloth with metallurgical media and etching in a mixture of 32 g $K_2Cr_2O_7$ in 80 mL HNO_3: 160 mL H_2O for 30 seconds [Inove et al. 1962]. The following dopants were evaporated onto the upper surface for laser melting: Si, Ge, Ga, Al/Cd, In/Cd, Cd/Sb, Sb and In. The double evaporations were performed in an attempt to reduce the loss of Cd from the surface during the melting. No combination was successful, probably due to lack of control of laser power and evaporated film thickness. Evidence for doping was sought by I-V and thermal probe measurements.

These investigations were performed almost certainly with excess laser power. Figure 10 shows microcracks induced in a CdTe sample coated with separate Cd and Sb evaporated layers. These effects have been seen on GaAs by Badertschev et al. [1980], and explained by shock waves being initiated by a plasma breakdown in the evaporated surface layer during the melting. The extreme situation of excess power is shown in Figure 11, with sections of a GaAs sample being blasted away by the laser energy[†]. With a better appreciation of this problem, some of these experiments might profitably be repeated.

CONCLUSIONS

In conclusion, it has been demonstrated that thin, highly doped layers can be produced on n-GaAs by laser-assisted doping from a thin film of Sn. There is some evidence that the upper limit of the laser power density may have been excessive. It is probable that the best contacts will only be formed within narrow ranges of laser power density and film thickness.

[†]Photographs courtesy of E. Lawson and J. Mellor, AAEC.

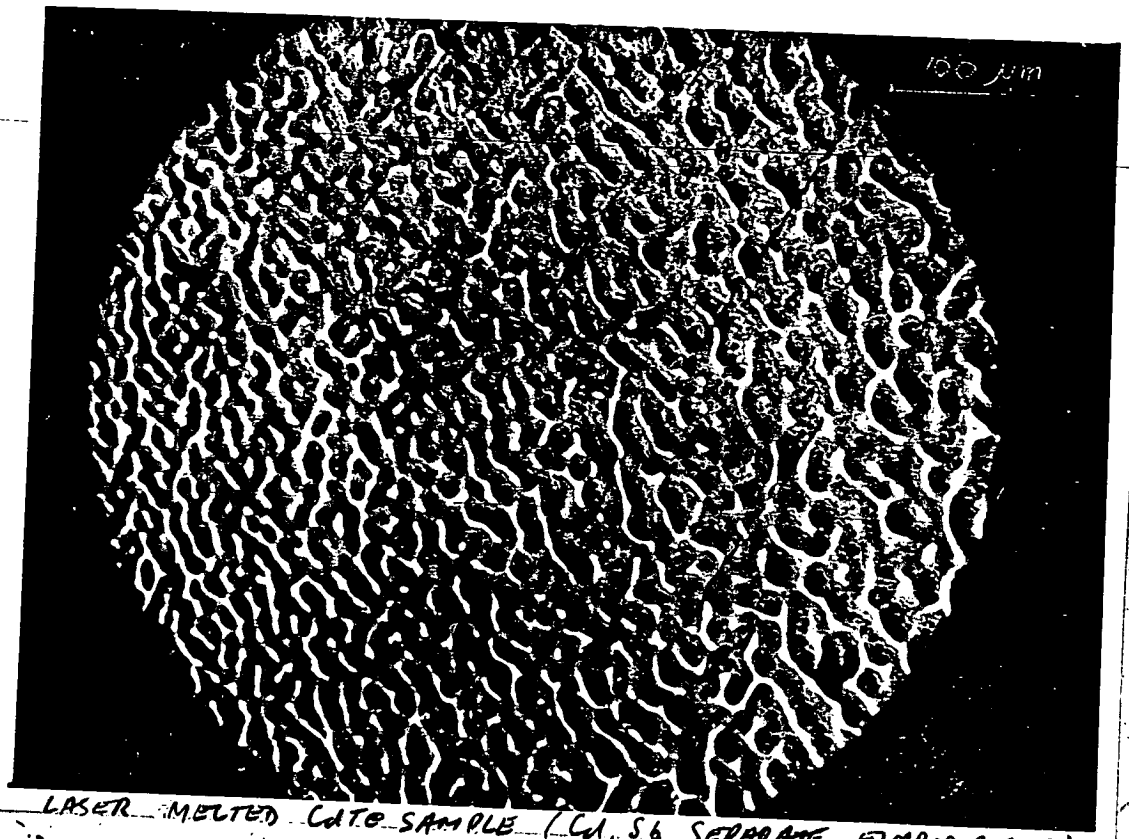

LASER MELTED CdTe SAMPLE (Cd, S6 SEPARATE EVAPORATIONS) ... CRACKS DUE TO EXCESS LASER ENERGY. ZEISS MICROSCOPE X 63.

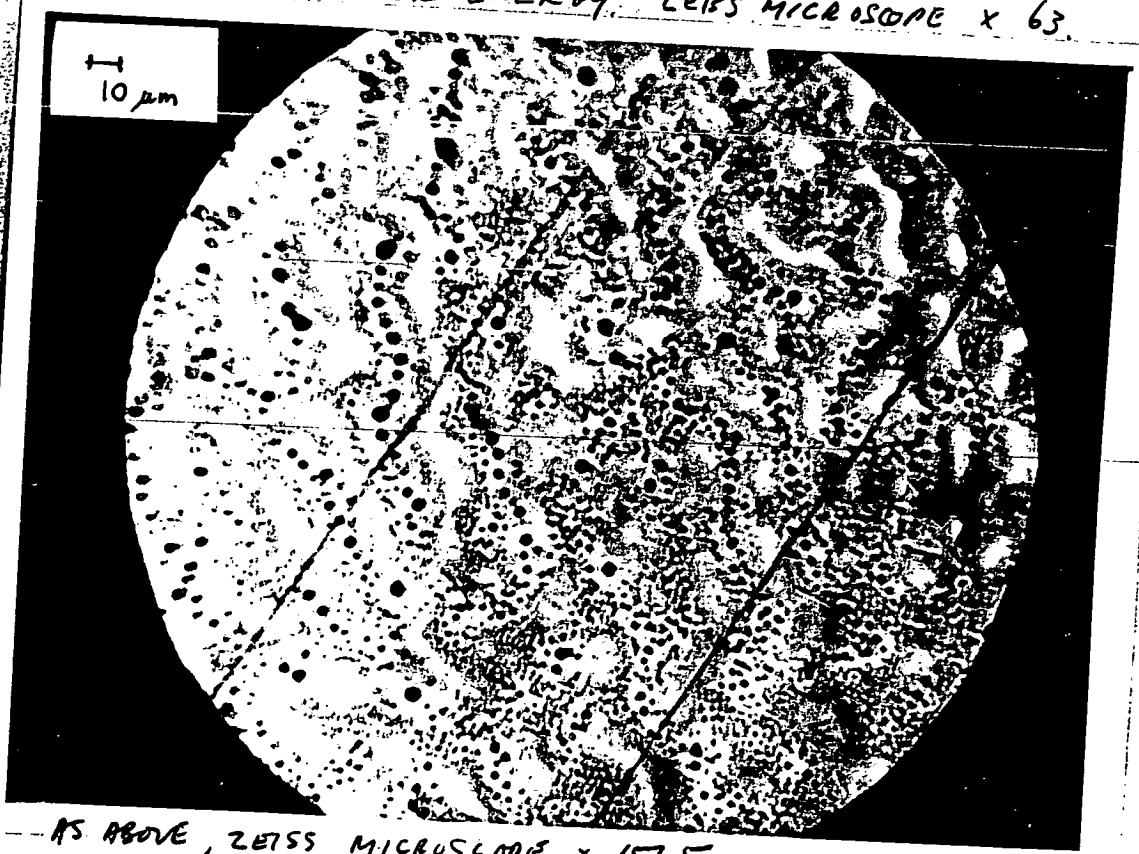

AS ABOVE, ZEISS MICROSCOPE X 157.5

FIGURE 10. EFFECT OF EXCESS LASER ENERGY ON CdTe SAMPLE OPTICAL MICROSCOPE DATA.

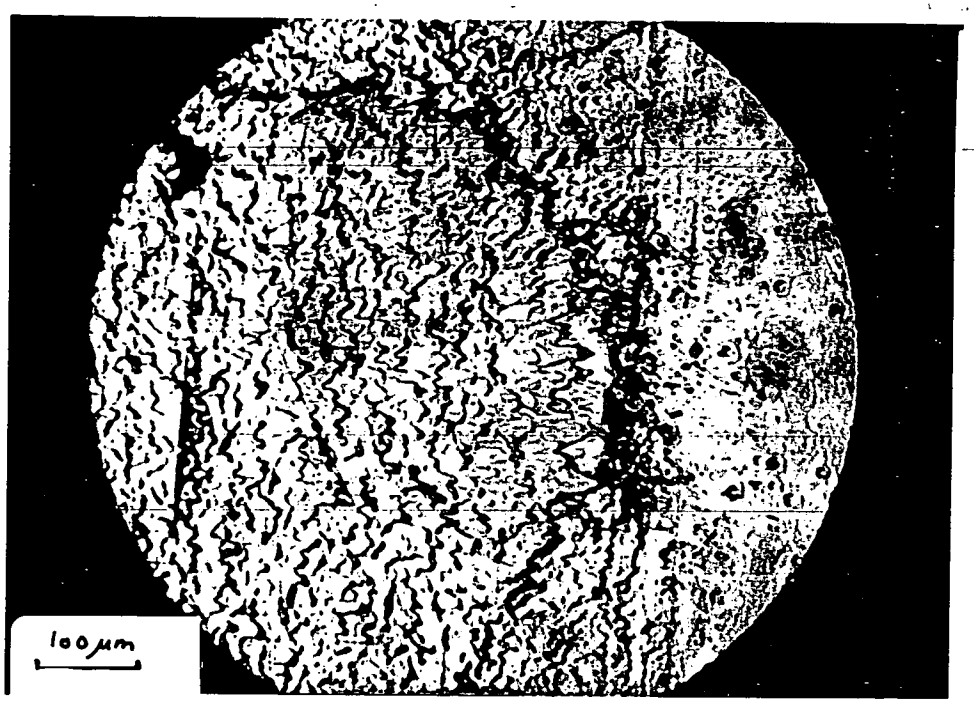

HOLE BLASTED IN GaAs. SAMPLE BY EXCESS LASER ENERGY - ZEISS MICROSCOPE × 63.

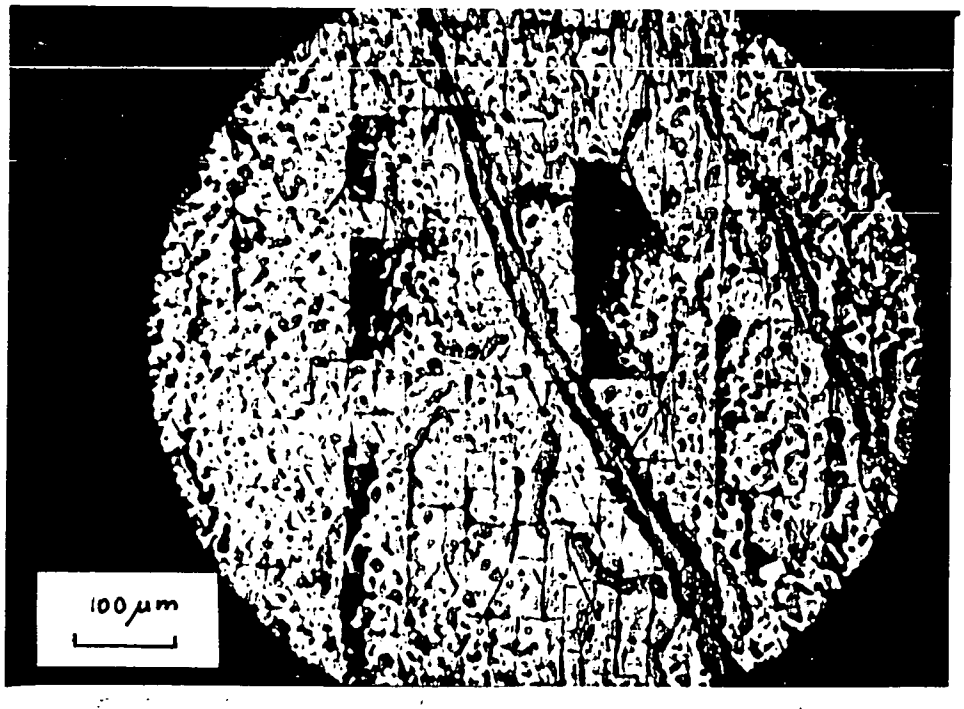

MICROCRACKS IN GaAs SAMPLE DUE TO EXCESS LASER ENERGY - ZEISS MICROSCOPE ×63.

FIGURE 11. OPTICAL MICROSCOPE PHOTOS OF GaAs SAMPLES ON WHICH EXCESS LASER ENERGY WAS USED TO MELT THE SURFACE

REFERENCES

Badertschev, G., Salathe, R.P. and Lathy, W. [1980] - Electron Lett. 16:113.

Cullis, A.C., Webber, H.C. and Bailey, P.J. [1979] - J. Phys. E. Sci. Instrum. 12:688

Eckhardt, G. [1980] - Overview of ohmic-contact formation on n-type GaAs by laser and electron-beam annealing. In: Laser and Electron Beam Processing of Materials, eds. C.W. White and P.S. Peercy (Academic Press, 1980) pp 467-480.

Inove, M. Teramoto, I and Takayanagi, S. [1962] - J. Appl. Phys. 33:2578.

Kular, S.S., Sealy, B.J., Badawi, M.H., Stephen, K.S., Sadana, D. and Booker, G.R. [1979] - Electron Lett. 15:413.

Meyer, J.R. Kruer, M.R. and Bartoli, F.J. [1980] - J. Appl. Phys. 51 (10) 5513.

Pounds, R.S., Saifi, M.A. and Hahn, W.C. [1974] - Solid State Electron 17:245.

Proc. 2nd Int. Symp. Cadmium Telluride, Strasbourg (1976); Revue de Physique Appliquée 12 (2) 1977.

CHAPTER 4

DEEP METAL-RELATED CENTRES IN Ge

OVERVIEW

It is perhaps surprising that more work on deep level defects in semiconductors has not been performed using Ge. As pointed out by Haller [1979], pure Ge provides a nearly perfect lattice in which to observe defect processes. It is also surprising, although perhaps inevitable, that the majority of the existing information on deep level defects in Ge has been 'solidified' in the literature from work published many years ago. An extreme example is information on the energy levels of deep metal related centres in Ge. The first source of reference, of course, is Deep Impurities in Semiconductors by Milnes, published in 1973. A closer look, however, shows the bulk of the deep levels coming from Tyler [1959]. Indeed, even in the eight years since Milnes' book appeared, there has been an explosion of information on deep levels in other semiconductors, particularly Si, due mainly to the advent of new detection techniques and the increased interest in the effect of deep impurities on devices. However, little work has been performed with Ge.

With these points in mind, we have determined to measure the energy levels related to many different elements in Ge. As with all work on deep level defects, the results obtained will not be the last word on the subject. On the contrary, they are simply a start in many instances to some recognition of the common levels associated with various impurities. In other cases they confirm results already in the literature. It is not the point of this Chapter to find a magical theory explaining all the results, but more realistically to provide a base from which to launch further effort. If the truth were known, very little is actually understood of the nature of deep level defects. When the nature of even the commonest levels in semiconductors can be disputed, such as oxygen in GaAs [Huber et al. 1979] and Au in Si

[Lang et al. 1980], the time is ripe for groundwork, not unsupported structures.

REFERENCES

Haller, E. E. [1979] - Defects and Radiation Effects in Semiconductors, 1978, Inst. Phys. Conf. Series No. 46, p. 205.

Huber, H. M., Linh, N. T., Valladon, M., Debrum, I. L., Martin, G. M., Mittonneau, A. and Mircea, A. [1979] - J. Appl. Phys. 50:4022.

Lang, D. V., Grimmeiss, H. G., Meyer, E. and Jaros, M. [1980] - Phys. Rev. B 22:3917.

Milnes, A. G. [1973] - Deep Impurities in Semiconductors (Wiley-Interscience, New York) pp. 35-44.

Tyler, W. W. [1959] - J. Phys. Chem. Solids 8:59.

INTRODUCTION

The study of deep impurity levels in semiconductors is an area of great current interest [Chen and Milnes 1980; Lang et al. 1980; Grimmeiss and Skarstam 1981]. The theoretical understanding of their nature is at present incomplete, and it is generally true that experimental studies have provided the new insights into deep level behaviour. The elemental semiconductors, Si and Ge, are particularly suited to the study of deep energy states as the problems associated with compound semiconductors, such as non-stoichiometry and high residual impurity concentrations, are avoided. While Si has been widely studied [Chen and Milnes 1980; Lange et al. 1980; Grimmeiss and Skarstam 1981; Grimmeiss et al. 1980a, Grimmeiss et al. 1980b], results on Ge have been lacking, with the exception of data on Cu and associated complexes [Haller et al. 1979; Evwaraye et al. 1979]. As part of an effort in these laboratories to tabulate the levels associated with various metals in Ge, we have applied the DLTS technique [Lang 1974] to n- and p-type Ge deliberately diffused with the following elements: Au, Ag, Ni, Pt, Pd, Se, Te, Cd, Mg, Ti, Cr, Mn, Fe, Zr, Co, Ba, Si, Sn, Zn, Pb, Nd, Gd, Tb, Tm, Ho, Er, S, Mo and Bi.

EXPERIMENTAL TECHNIQUE

(a) Semiconductor Material

The crystals were grown by the Czochralski technique from silica quartz crucibles in an H_2 atmosphere. Hall-effect and capacitance-voltage measurements (1 MHz) at 77 K revealed net shallow level impurity concentrations of 4×10^{12} to 1×10^{14} cm^{-3} for the n- and p-type material. The n-type material was nominally undoped, while the p-type material was either nominally undoped or lightly doped with Ga. The rectangular cubic shaped samples (area $\sim$0.5 cm^2, thickness $\sim$0.4 cm) were chemically etched, then a thin film of the appropriate metal

evaporated onto one face from an ohmically heated Mo or glassy carbon filament. All other faces were coated in GaIn eutectic alloy, which provided an effective gettering action for the fast diffusing Cu for all but the rare earth samples. Three separate sets of samples were fabricated, with different amounts of the metals evaporated onto the surface in an effort to more clearly identify the metal-related centres. Two sets of rare earth evaporated samples were used. The purity of the evaporants was six nines (Au, Ag, Ni, Pt, Pd, Cd, Te), five nines (Fe, Zr, Cr, Ti, Mn, Sn), four nines (Se, Mg, Co, Pb, Zn) or three nines (rare earth metals).

(b) Diffusion Conditions

Samples were mounted on a graphite block in an RF induction-heated furnace. Diffusions were performed at 650-750^{o}C for 8-10 hours under flowing H_2 or N_2 gas. Samples with an evaporated layer of one of the rare earths were diffused at 810^{o}C for 8 hours. The different temperatures of diffusion, together with the different quantities of evaporated metal dopant, helped to clearly identify the centres by measurement of the impurity concentration profile [Lang 1974]. Samples with a S, Se, Te, Cd, Bi, Pb, Ba (evaporated from a source of the hydroxide) or Zn surface layer were capped with a further evaporation of amorphous Ge to reduce mass transport due to high vapour pressures during the heat treatment. Extensive use was made of control samples, either uncapped or evaporated with an amorphous Ge layer.

After cleaning, contacts were formed to the samples as follows: all n-type samples were given Li diffused ohmic contacts (300^{o}C for 10 minutes) with evaporated Pd Schottky barrier front contacts, while p-type samples were given evaporated Pd ohmic back contacts with either evaporated In barrier front contacts or Li diffused n^{+} contacts (200^{o}C for 5 minutes). The latter contact was used for impurities with a

high diffusion coefficient in Ge: Au, Ag, Ni, Pt, Pd and Fe [Milnes 1973]. Delineation of the junction in these samples by copper staining showed Li diffusion depths of 18 to 25 μm.

(c) DLTS Measurements

DLTS scans were performed over the range 15 to 200 K using a system based on a 1 MHz capacitance bridge and an electronic correlator [Miller et al. 1975]. Energy levels for the observed defect states were obtained from Arrhenius plots with the usual 2 kT correction [Miller et al. 1977]. Cross sections and concentrations were directly measured from the dependence of correlator output signal on bias pulse width and pulse amplitude respectively. Forward bias pulsing the junction in p-type samples with a Li diffused n^+ contact enabled the measurement of minority (electron) traps. Pulsed infrared illumination of some of the Schottky diodes injected enough minority carriers to check on minority traps associated with the diffused metals; this provided an indication that the levels were present in both n- and p-type material. Concentrations of the observed centres were in the range 10^{10} to 5×10^{12} cm^{-3}. The solid solubilities of the elements are generally $\sim 10^{14}$ cm^{-3} at the temperatures used for the diffusions [Milnes 1973].

RESULTS

4.1 Group VII B, IB, IIB Impurities

Table 1 lists the impurity-related levels measured for group VII B, IB and IIB elements in Ge. The energy level, derived in the usual way from the emission rate-temperature data is given first, with D or A indicating donor or acceptor behaviour. The capture cross section for majority carriers (electrons for n-type material) is also listed, measured from the dependence of correlator signal output on trap-filling bias pulse width [Lang 1974]. The levels listed for each of the metals in the summary by Milnes [1973] are indicated by the arrows.

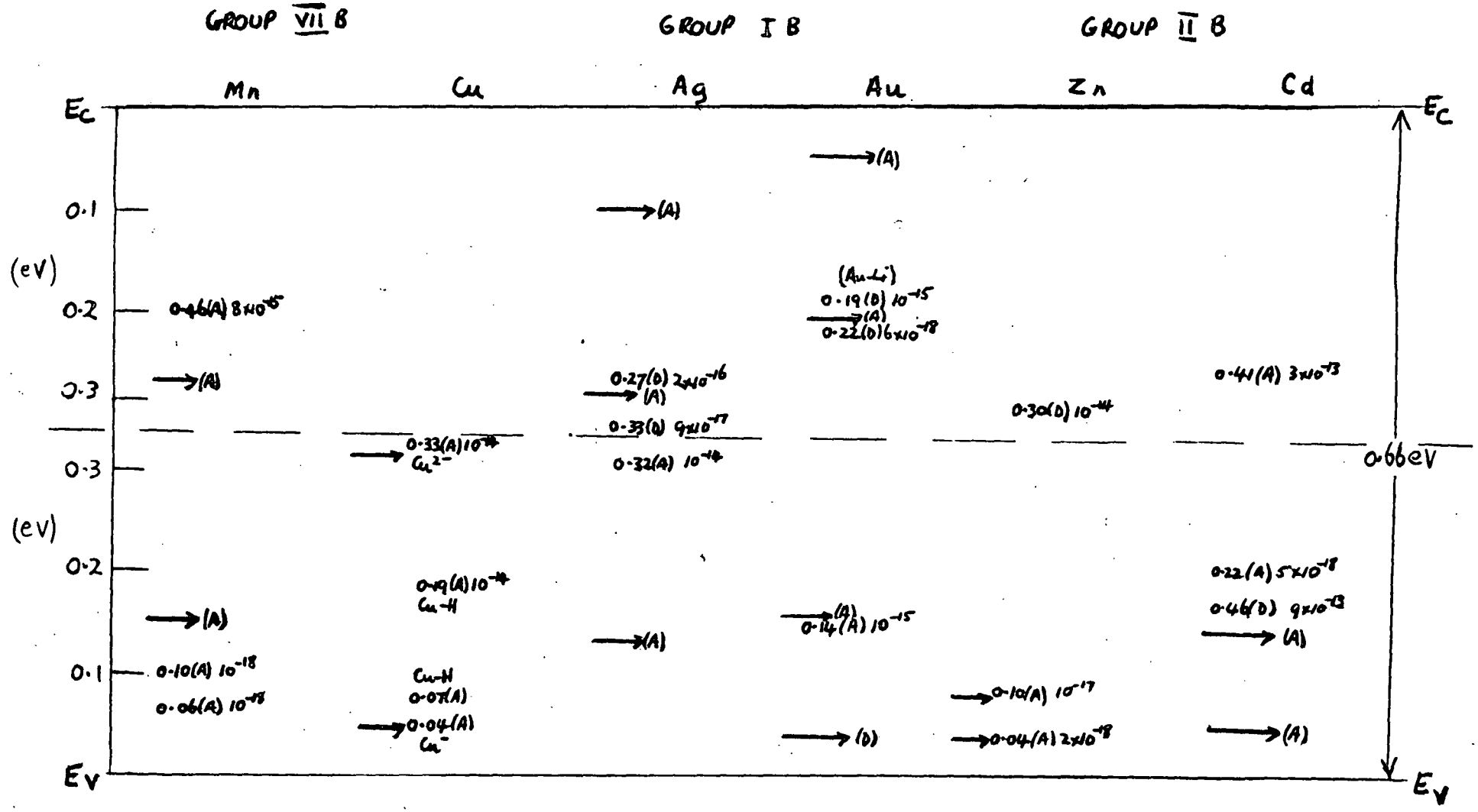

→ INDICATES LEVEL LISTED IN MILNES

D DONOR LEVEL

A ACCEPTOR LEVEL

TABLE I. ENERGY LEVELS AND CROSS-SECTIONS OF GROUP VII B, IB AND II B ELEMENTS IN Ge.

Manganese shows three acceptor levels: E_v + 55 meV, E_v + 0.10 eV and E_v + 0.46 eV in Ge. Silicon displays five acceptor centres related to Mn [Chen and Milnes 1980]. The concentrations of these three levels were similar, possibly suggesting they are related to the same centre. The DLTS spectrum for a typical p-type sample doped with Mn is shown in Figure 1(a), and the Arrhenius plots for these (and the other levels from this section) are shown in Figure 2.

Copper in Ge has been well tabulated using DLTS by Haller et al. [1979]. From measurements on samples subjected to heating under N_2 for extended periods (20 to 1000 hours) we confirm the identification of the E_v + 0.19 eV and E_v + 0.07 eV acceptor levels as being due to Cu-H complexes. In the samples used (grown from silica crucibles under an H_2 atmosphere) one saw a consistent reduction in the Cu-H levels concentration for longer heating period under N_2. We also confirm the identification of the E_v + 0.15 eV level as being due to a Cu-Li-H complex. Figure 3 shows a DLTS spectrum from a Cu-doped sample in which investigation of a region away from the Li contact shows trace (a), while forward bias pulsing the n^+ junction shows trace (b). The extra peak is correlated with the presence of Li, as well as Cu and H. Measurements on the passivation of Cu-related levels in Ge are described in Chapter 5.

Silver is a very rapid diffusant in Ge [Milnes 1973]. A DLT spectrum for an Ag-diffused, n-type diode is shown in Figure 4, displaying donor levels at E_c - 0.27 eV and E_c - 0.33 eV. Infrared illumination of the sample enabled sufficient minority carriers to be injected into the bulk material to allow observation of a deep acceptor centre at E_v + 0.32 eV with a large capture cross section for holes ($\sigma_p = 10^{-14}$ cm^2).

The behaviour of Au in Ge is of interest because of the extensive

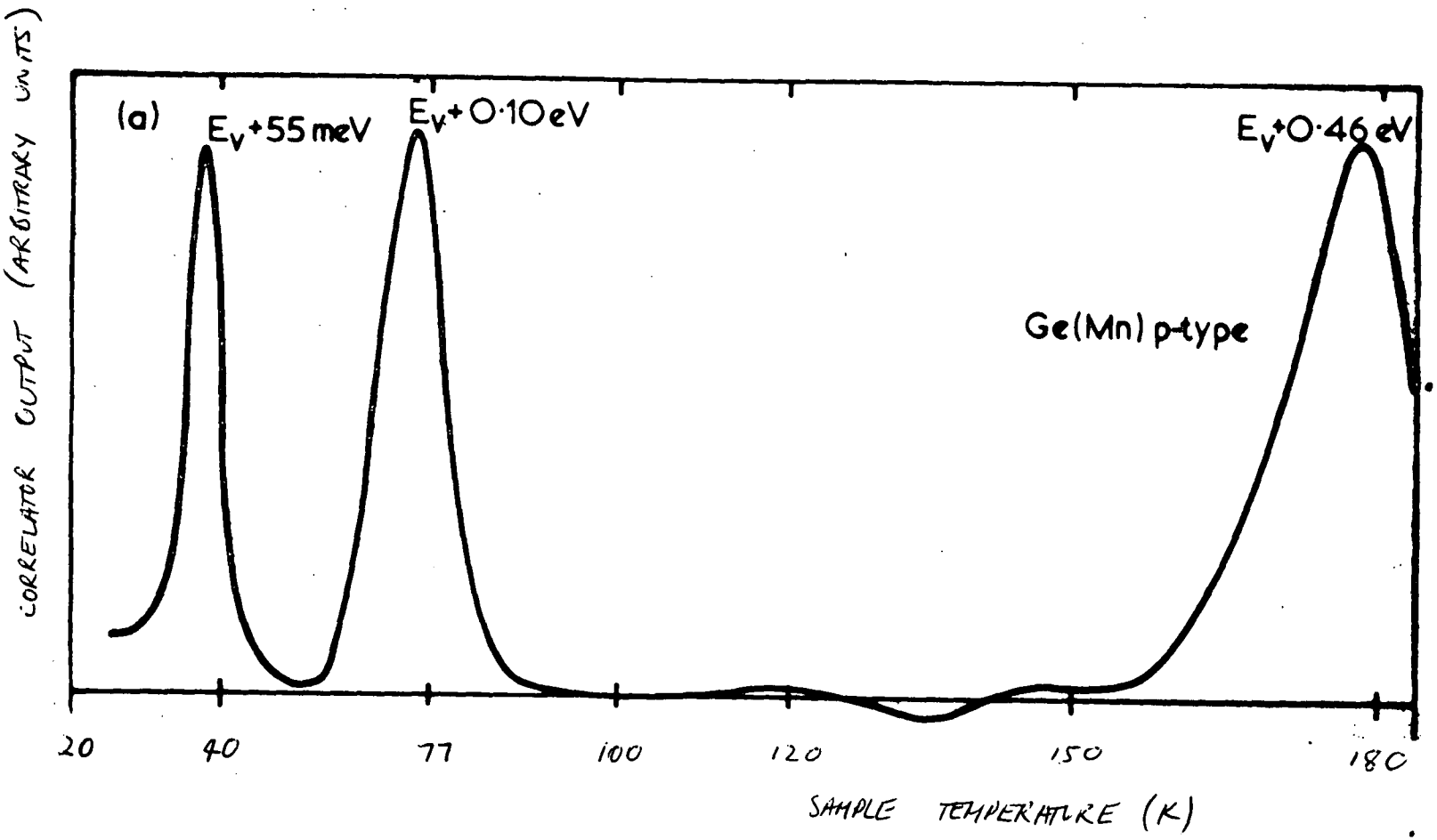

FIGURE 1

DLTS spectra for Mn diffused p-type Ge Typical reverse bias voltages used was 5 V with a 100 μs saturating bias pulse. The correlator time constant is 10 ms for all spectra.

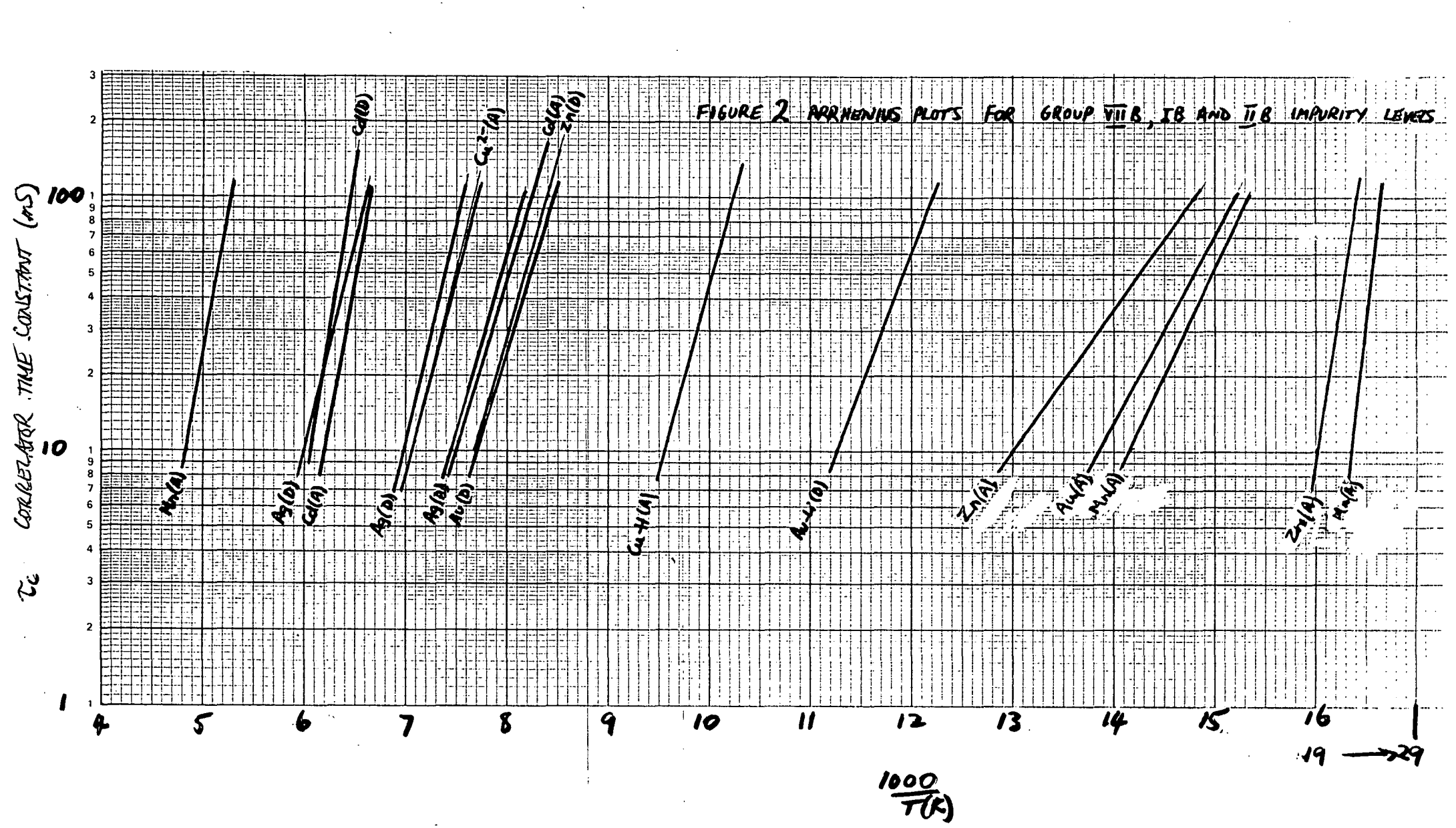
FIGURE 2 ARRHENIUS PLOTS FOR GROUP VIII B, IB AND IIB IMPURITY LEVELS
τ_c CORRELATOR TIME CONSTANT (nS)
100
10
1
4
5
6
7
8
9
10
11
12
13
14
15
16
19 → 29
$\frac{1000}{T(K)}$
Mn(A)
Ag(D)
Cd(A)
Cd(D)
Ag(D)
Ag(D)
Au(D)
Cu^{2+}(A)
Cu(A)
Zn(D)
Cu+(A)
Au-(D)
Zn(A)
Au(A)
Mn(A)
Zn(A)
Mn(A)

FIGURE 3.

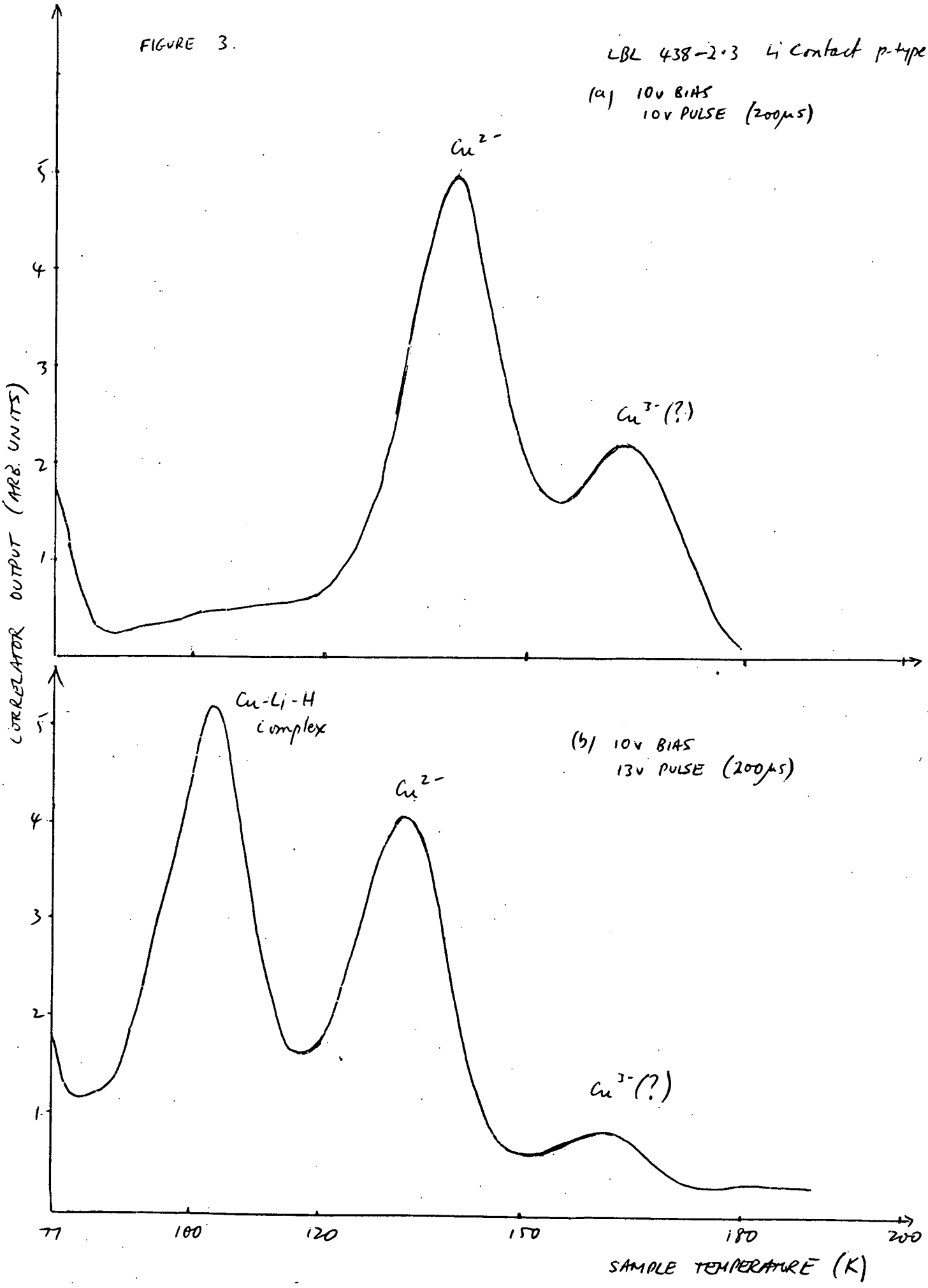
LBL 438-2-3 Li Contact p-type Ge
(a) 10V BIAS
10V PULSE (200μs)
Cu^{2-}
Cu^{3-} (?)
CORRELATOR OUTPUT (ARB. UNITS)
1
2
3
4
5
(b) 10V BIAS
13V PULSE (200μs)
Cu-Li-H complex
Cu^{2-}
Cu^{3-} (?)
77
100
120
150
180
200
SAMPLE TEMPERATURE (K)

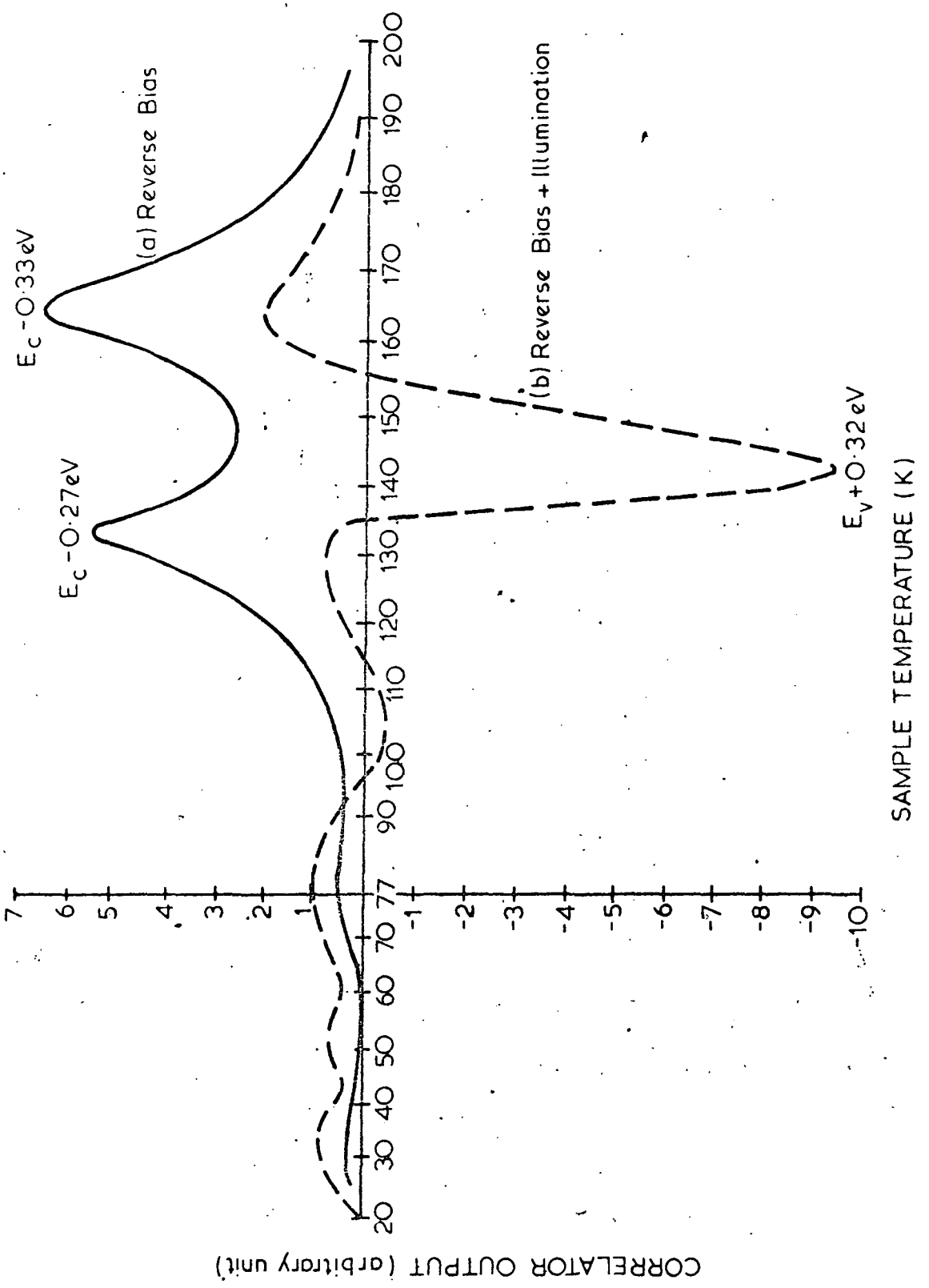

Figure 4

(a) DLTS spectrum for Ag diffused n-type Ge sample (b). The introduction of minority carriers by infrared illumination reveals a hole trap at E_v + 0.32 eV.

work performed on this element in Si [Lang et al. 1980] and past measurement in Ge [Milnes 1973]. Figure 5 shows the DLT spectra for Au-diffused, n- and p-type Ge samples. The E_c - 0.19 eV level is a Au-Li related complex. We may not have seen the higher acceptor states of Au in Ge because of incomplete filling of the lower state. A discussion of this is included in Milnes [1973].

We obtained good agreement with previous measurements [Milnes 1973] for the two acceptor states associated with Zn in Ge, and also observed a donor state at E_c - 0.30 eV present at concentrations approximately one-tenth those of the acceptor levels (Figure 6).

Cadmium in Ge was found to give rise to three levels, acceptor states at E_v + 0.22 eV and E_v + 0.41 eV, and a donor state at E_c - 0.46 eV. The E_v + 0.22 eV state may be the level measured as E_v + 0.16 eV during the Hall-effect measurements of Tyler [1959]. The other two levels have very large capture cross sections and may be Cd-related defect complexes. A typical DLTS spectrum is shown in Figure 7.

4.2 Group IVA, VA, IVB and VIB Impurities

Table 2 shows the electrically active levels measured for defect states related to group IVA, VA, IVB and VIB elements in Ge. Three acceptor states (E_v + 0.17 eV, E_v + 0.21 eV and E_v + 0.39 eV) associated with Pb were measured. The Arrhenius plots of these levels (and the other levels discussed in this section) are shown in Figure 8. Lead in Si has been observed to give rise to two deep acceptors (E_v + 0.37 eV, E_c - 0.17 eV) [Chen and Milnes 1980].

Bismuth is a shallow level donor impurity in Ge, as with the other group V elements. We also measured two deep Bi-related states at E_v + 0.07 eV and E_v + 0.17 eV present in concentrations of $\sim 7 \times 10^{10}$ cm^{-3} after diffusion at 700°C. The DLTS spectrum for a Bi-diffused p-type sample is shown in Figure 9. Control samples heated in the same fashion

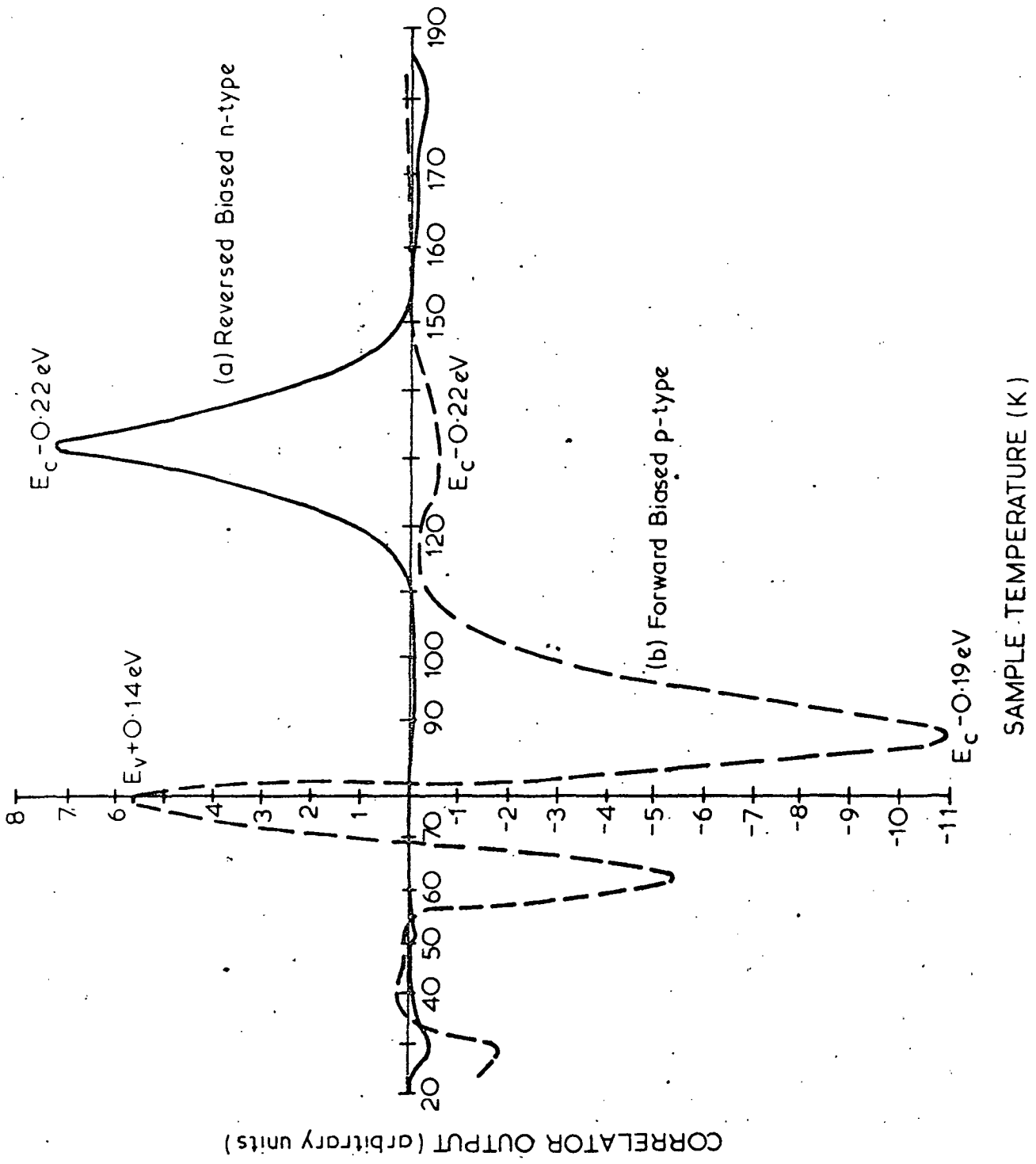

Figure 5

DLT spectrum for Au-diffused, n- and p-type Ge. Positive signals are due to the respective majority carrier traps for the two conductivity types.

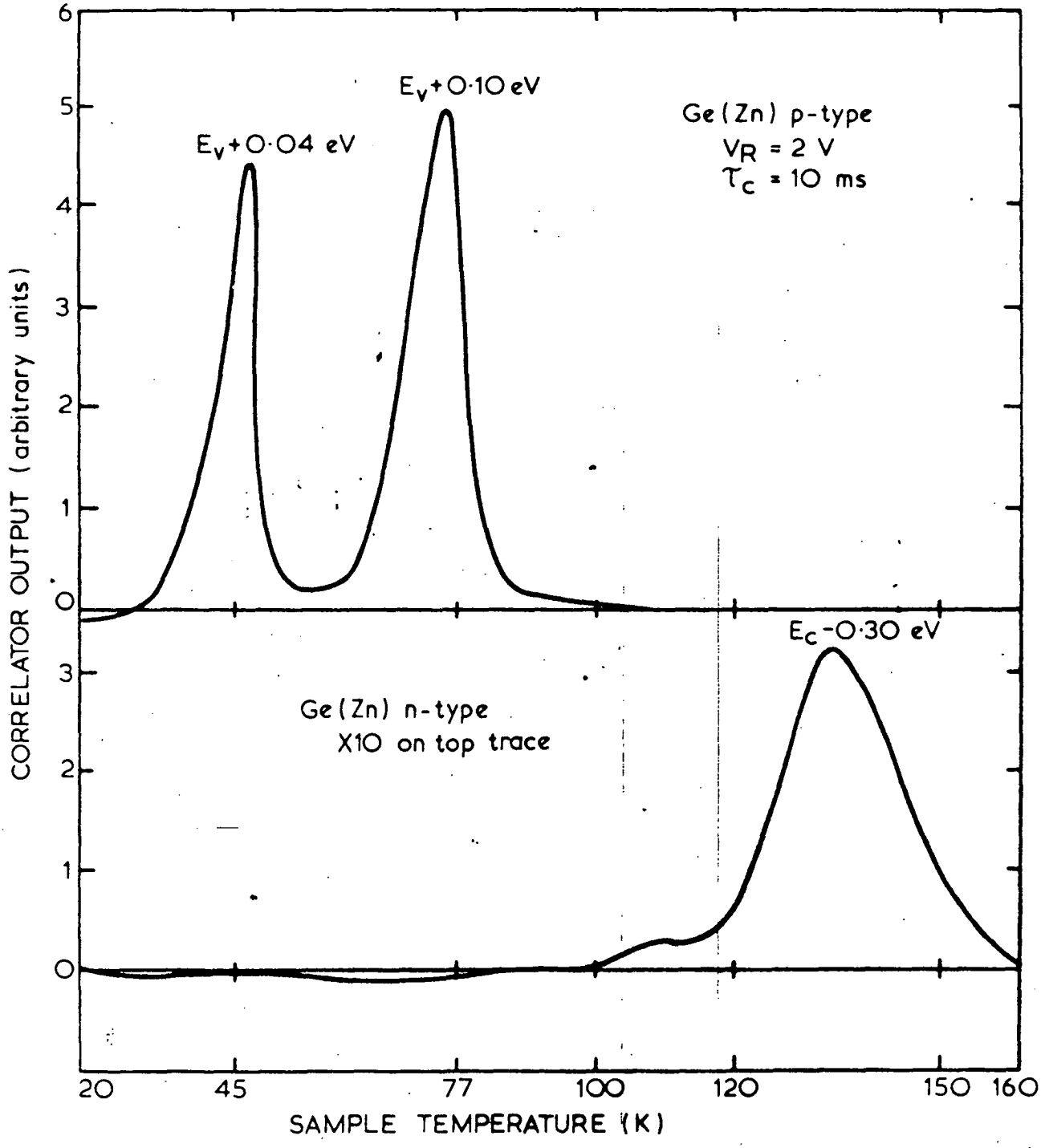

Figure 6. DLTS spectra for n- and p-type Ge samples diffused with Zn. The use of both conduction types enables observation of electron and hole traps introduced by the Zn.

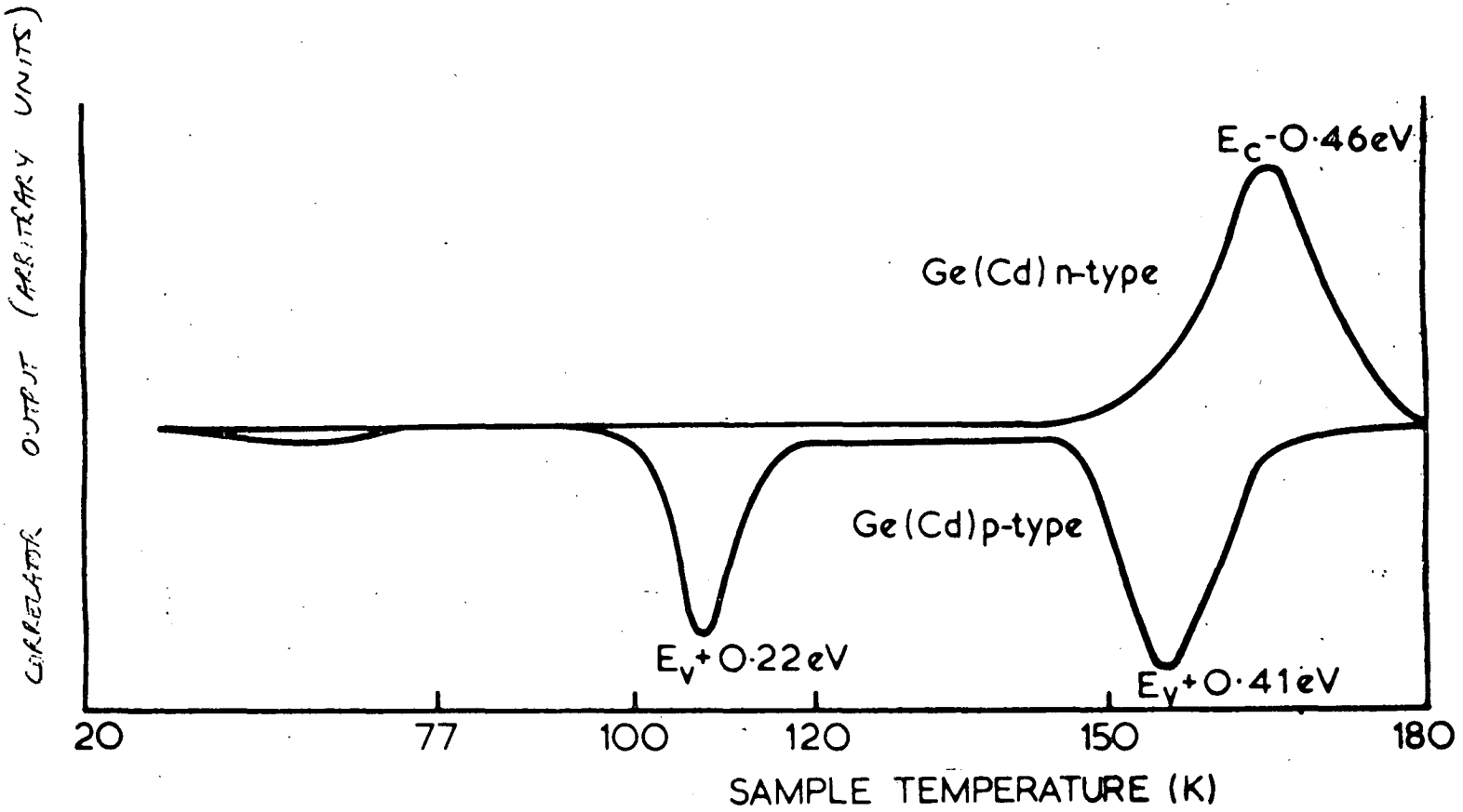

Figure 7. DLTS spectra of Cd diffused n-type Ge.

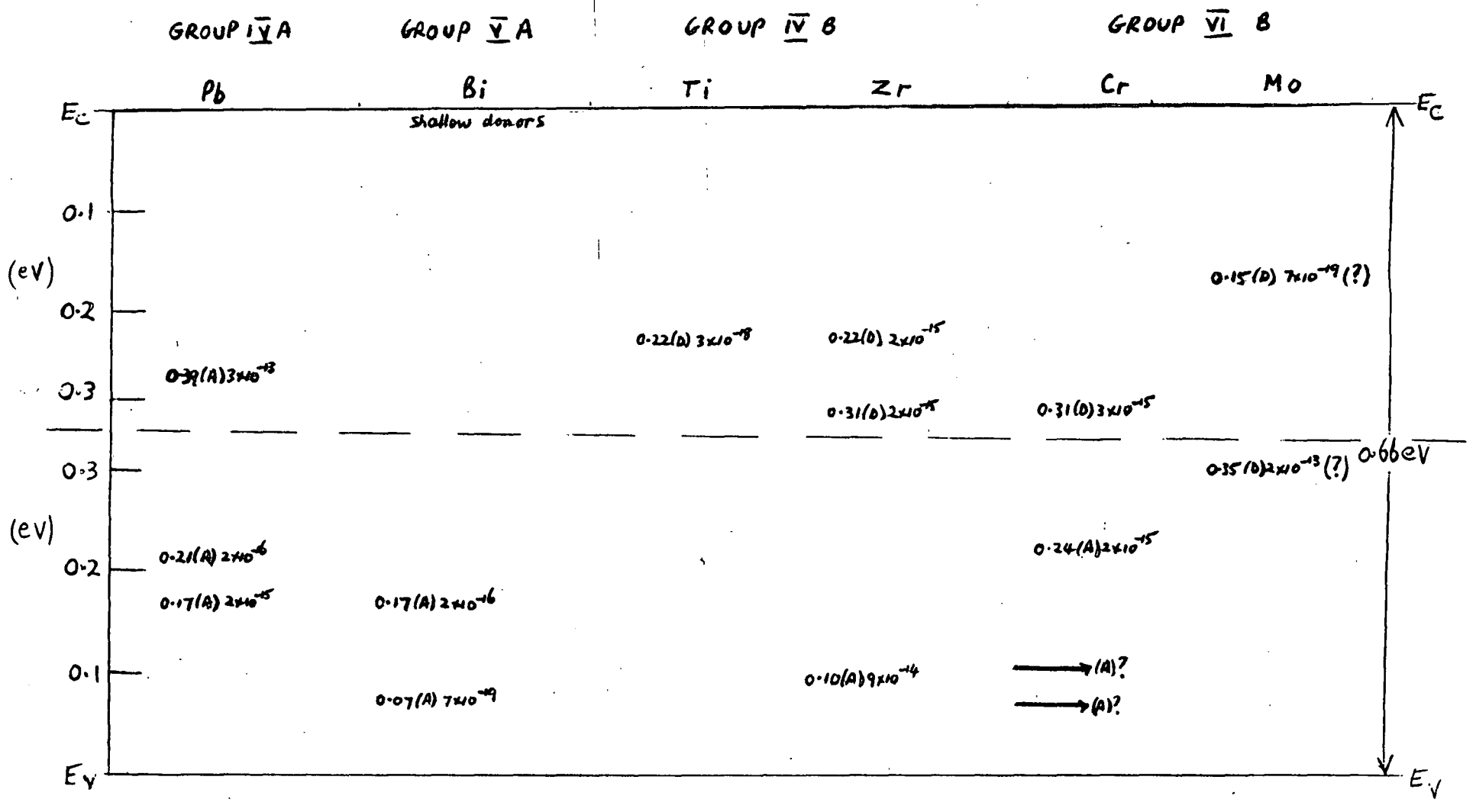

TABLE 2. ENERGY LEVELS AND CROSS-SECTIONS OF GROUP IV A, V A, IV B and VI B IMPURITIES IN Ge.

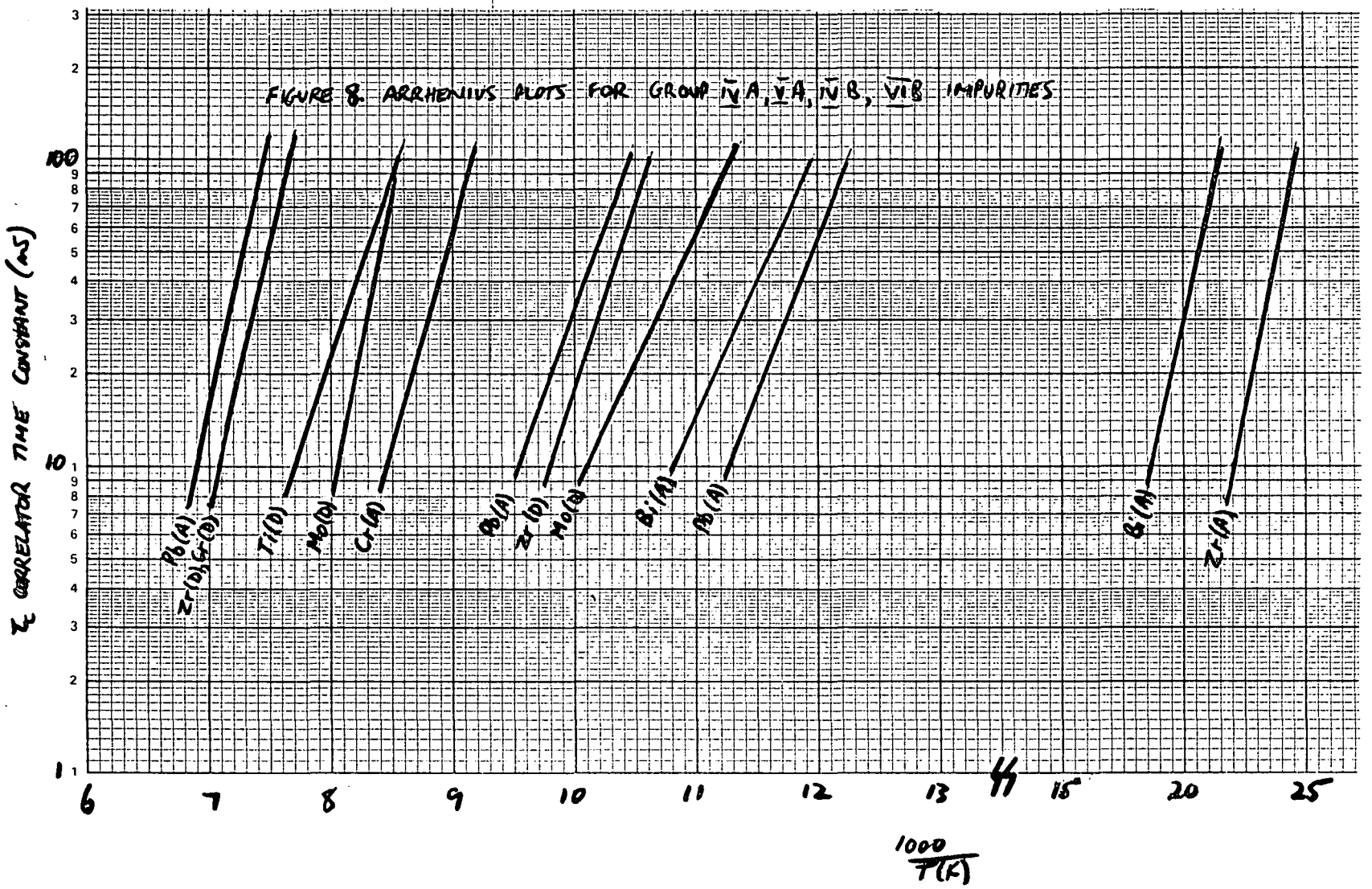
FIGURE 8. ARRHENIUS PLOTS FOR GROUP IVA, VA, IVB, VIB IMPURITIES
τc CORRELATOR TIME CONSTANT (nS)
100
10
1
6
7
8
9
10
11
12
13
15
20
25
1000/T(K)
Pb(A)
Zr(D),Sr(D)
Ti(D)
Mo(D)
Cr(A)
Pb(A)
Zr(D)
Mo(D)
Bi(A)
Pb(A)
Bi(A)
Zr(A)

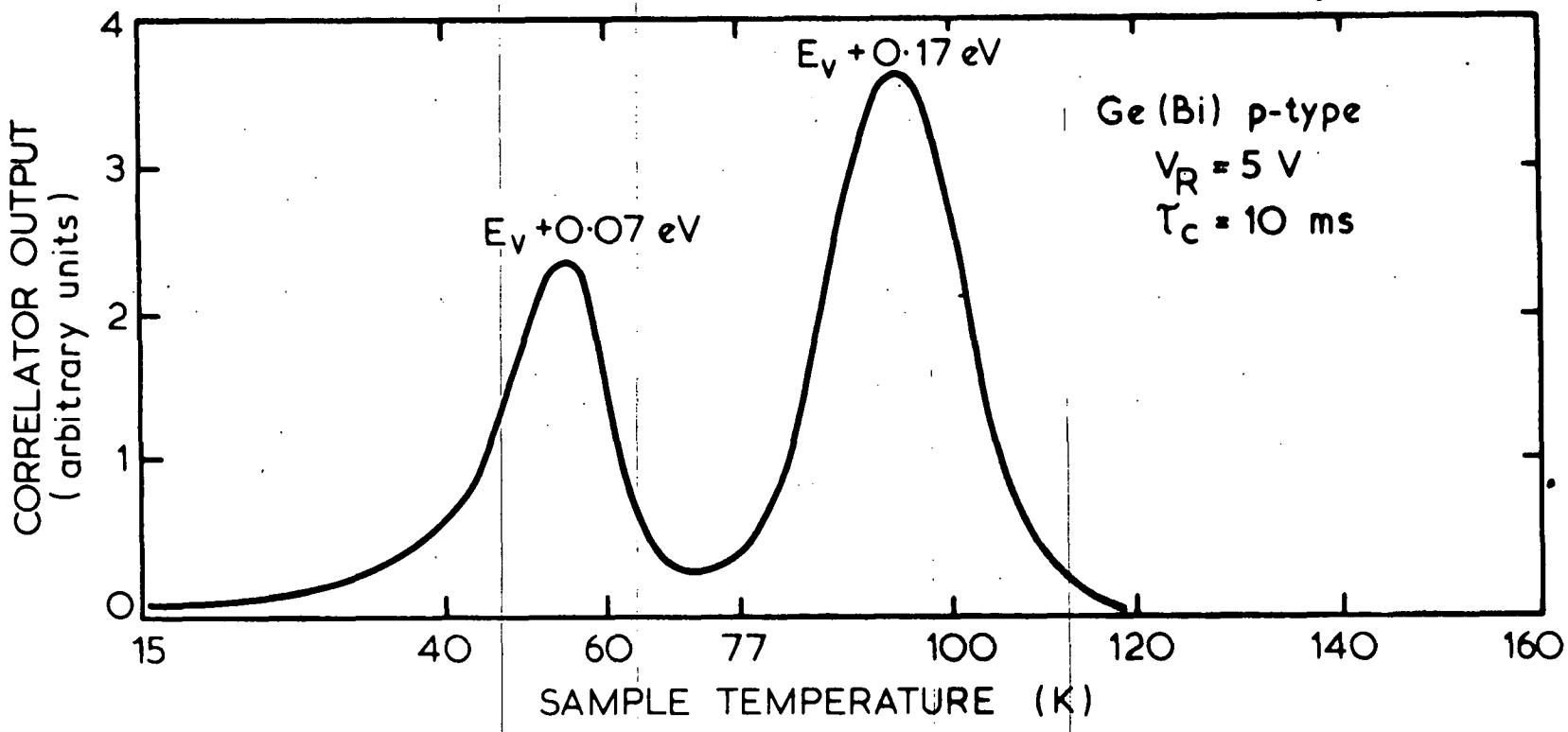

FIGURE 9. DLTS spectrum for a p-type Ge sample diffused with a low concentration of Bi. Spectrum conditions $V_R = 5V$, $\tau_c = 10ms$.

did not show these levels, or any of the other levels measured for the elements studied here.

Figures 10 and 11 display the DLTS spectra obtained for Ti and Zr diffused samples. As far as can be ascertained, these are the first reported measurements for Ti and Zr related centres in Ge. Results in Si [Chen et al. 1979] indicate that Ti may be capable of causing significant reduction in minority carrier lifetime. It displays a deep donor state in Si (E_c - 0.26 eV) as has been determined here for Ge (E_c - 0.22 eV). The diffusion coefficient for Ti at 750^{o}C was estimated to be 5±3 x 10^{-12} cm^2/s from the median range of the electrically active Ti ions. Zirconium acts as a shallow donor in Si when present in high concentrations (>10^{16} cm^{-3}), but is generally assumed to be present in neutral substitutional states. In Ge, however, it exhibits three levels: deep donors at E_c - 0.22 eV, E_c - 0.31 eV and an acceptor state at E_v + 0.10 eV.

Chromium in Ge has not been well tabulated (see summary by Milnes [1973]; it displayed a donor level at E_c - 0.31 eV and an acceptor level at E_v + 0.24 eV. The DLTS spectra for n- and p-type samples are shown in Figure 12.

Molybdenum appears to have a very low diffusion coefficient in Ge; an upper limit of ∿6 x 10^{-12} cm^2 s^{-1} at 650^{o}C was obtained. The tentative energy levels for deep states associated with Mo (E_c - 0.15 eV, E_c - 0.35 eV) were measured by pulsing the standing reverse bias on the diffused sample into forward direction. This enabled observation of impurity levels in the zero bias depletion region immediately under the Schottky barrier contact of the diodes. The DLTS spectrum of a Mo-diffused sample is shown in Figure 13. No previous measurements of impurity levels related to Mo in Ge appear to have been made, though the results reported here are not regarded as certain.

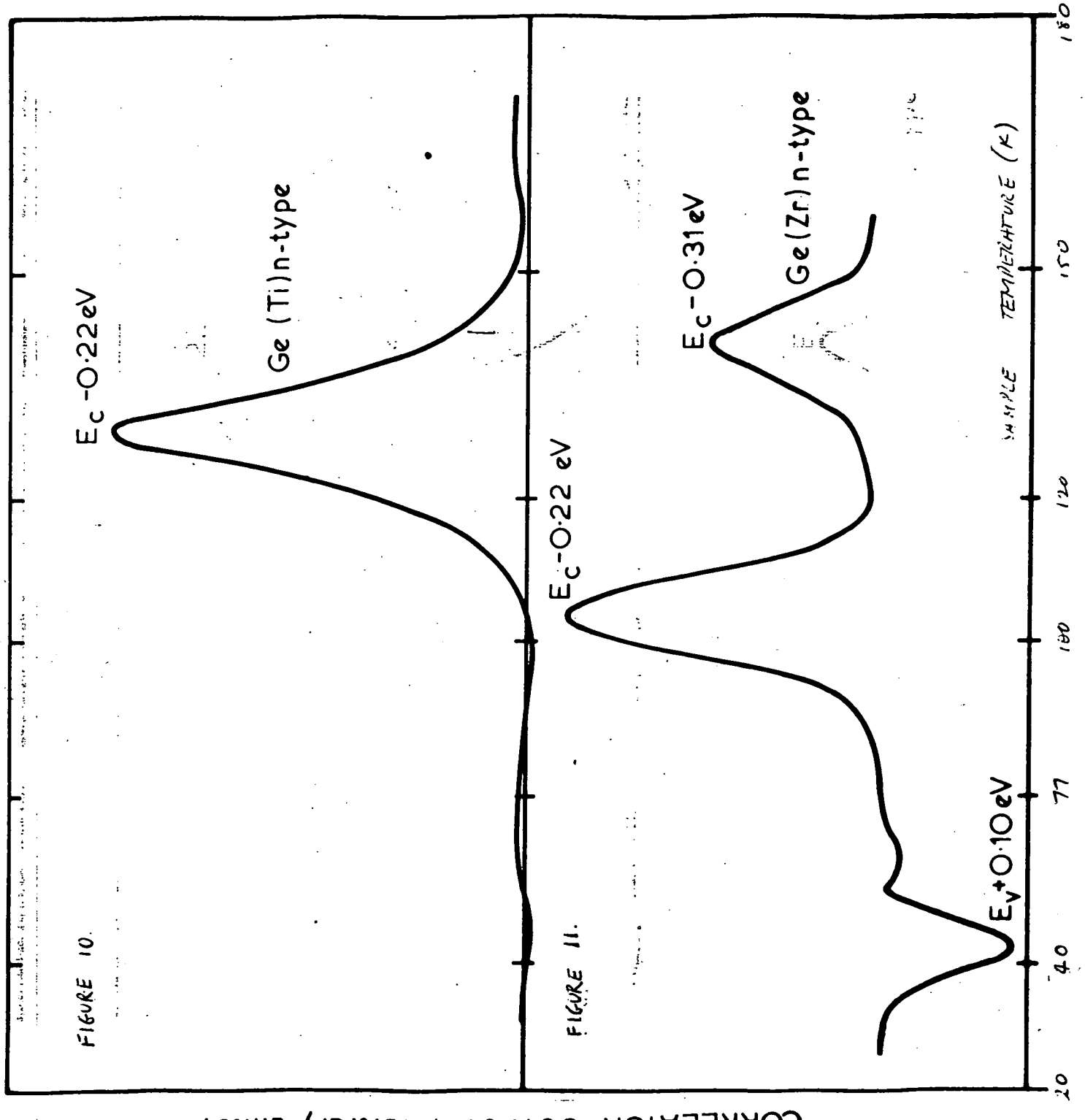

FIGURE 10.

FIGURE 11.

DLTS spectra for Ti diffused n-type Ge and Zr diffused n-type Ge, with infra-red illumination injecting enough minority carriers to reveal a hole trap at E_v+0.10 eV. This is observed as a minority trap in p-type material.

FIGURE 12.

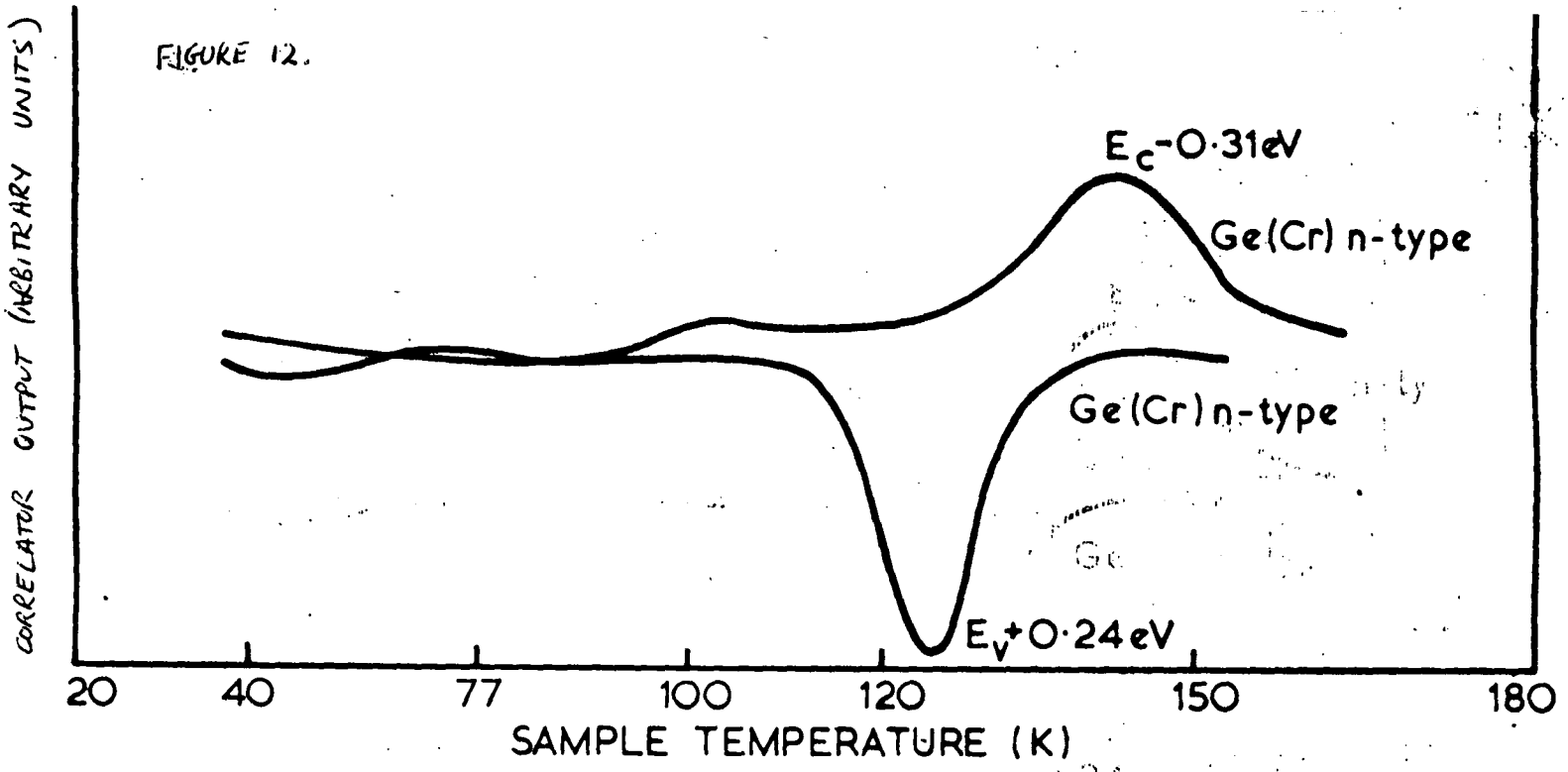

DLTS spectrum from Cr diffused n- and p-type Ge

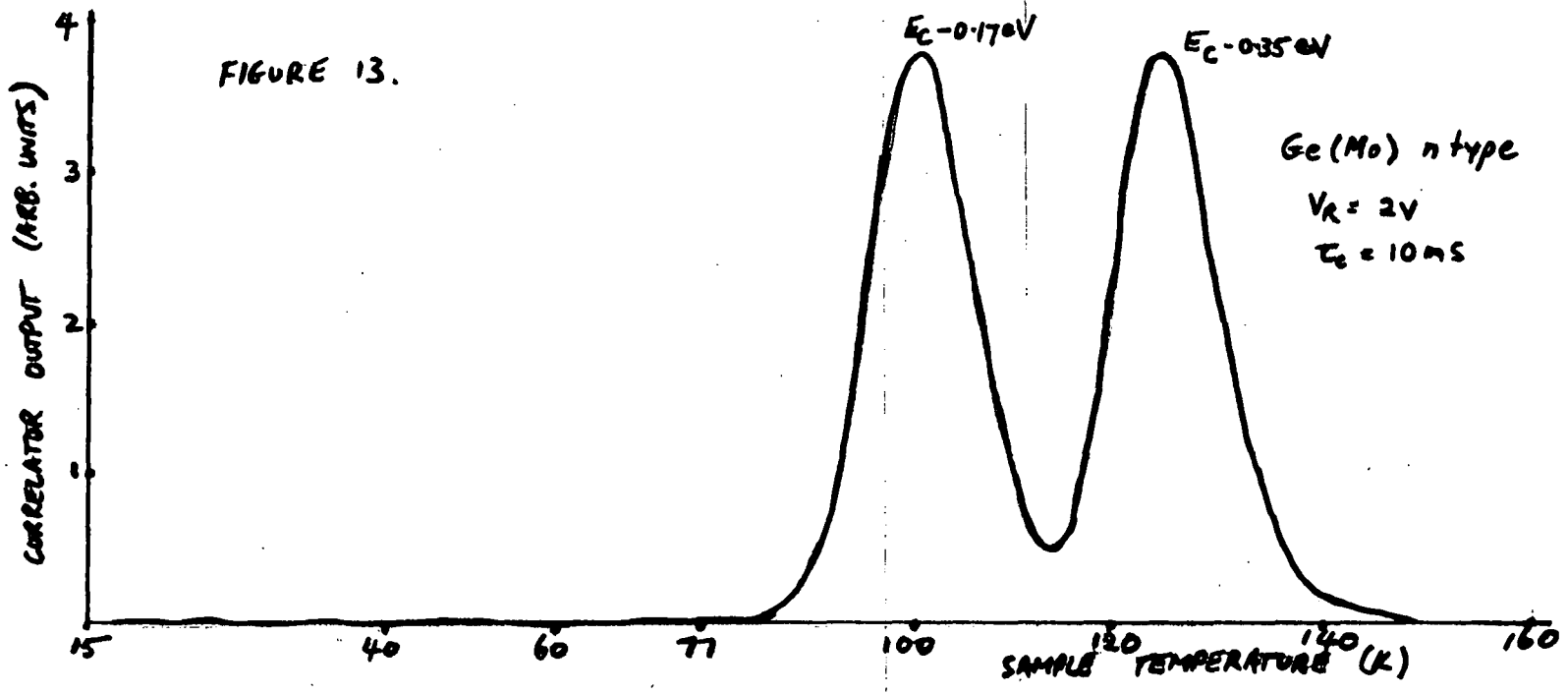

FIGURE 13. DLTS Spectrum for an n-type Ge sample diffused with Mo. Reverse bias 2V, τ_e = 10 mS.

4.3 Group VIA and VIII Impurities

Table 3 shows the levels measured for defect states related to group VIA and VIII impurities in Ge. The Arrhenius plots of the various levels are shown in Figure 14.

Sulphur-related states have previously been studied by Tyler [1959], who measured a donor state at E_c - 0.18 eV, using Hall-effect measurements. He also obtained evidence for deeper donor states, but did not give their energy levels. We obtained two deep donor levels for S, E_c - 0.21 eV and E_c - 0.25 eV. The DLTS spectrum for an S-diffused n-type sample is shown in Figure 15. From the median range of the electrically active concentration profile of these levels, we calculate an approximate diffusion coefficient of 5±3 x 10^{11} cm^2 s^{-1} at 700°C for S in Ge. The only other published value is $\sim 10^{-9}$ at 920°C [Tyler 1959].

Results on Se are in good agreement with past measurements [Milnes 1973], and the E_c - 0.31 eV centre in Te doped Ge has also been previously observed [Milnes 1973]. The deepest donor states measured (Pn, S, Se and Te) are progressively deeper for larger atoms. Tellerium in Ge also displays a deep acceptor with a very large hole capture cross section, 9 x 10^{-12} cm^2. The DLTS spectra for Se and Te doped samples are shown in Figure 16. From the concentration profile of the defects, and assuming a built-in bias of 0.35 V [Sze 1969], the diffusion coefficient of Se at 750°C was estimated to be 8±4 x 10^{-12} cm^2 s^{-1}. The only other reported value for the diffusion coefficient of Se at any temperature is $\sim 10^{-10}$ cm^2 s^{-1} at 920°C [Tyler 1959].

Iron in Ge was observed to give rise to two dominant donor levels at E_c - 0.18 eV and E_c - 0.34 eV (Figure 17), Because of the high diffusion coefficient of Fe in Ge [Milnes 1973], one p-type sample was prepared with a 20 μm thick Li diffused n^+ contact (5 minutes at

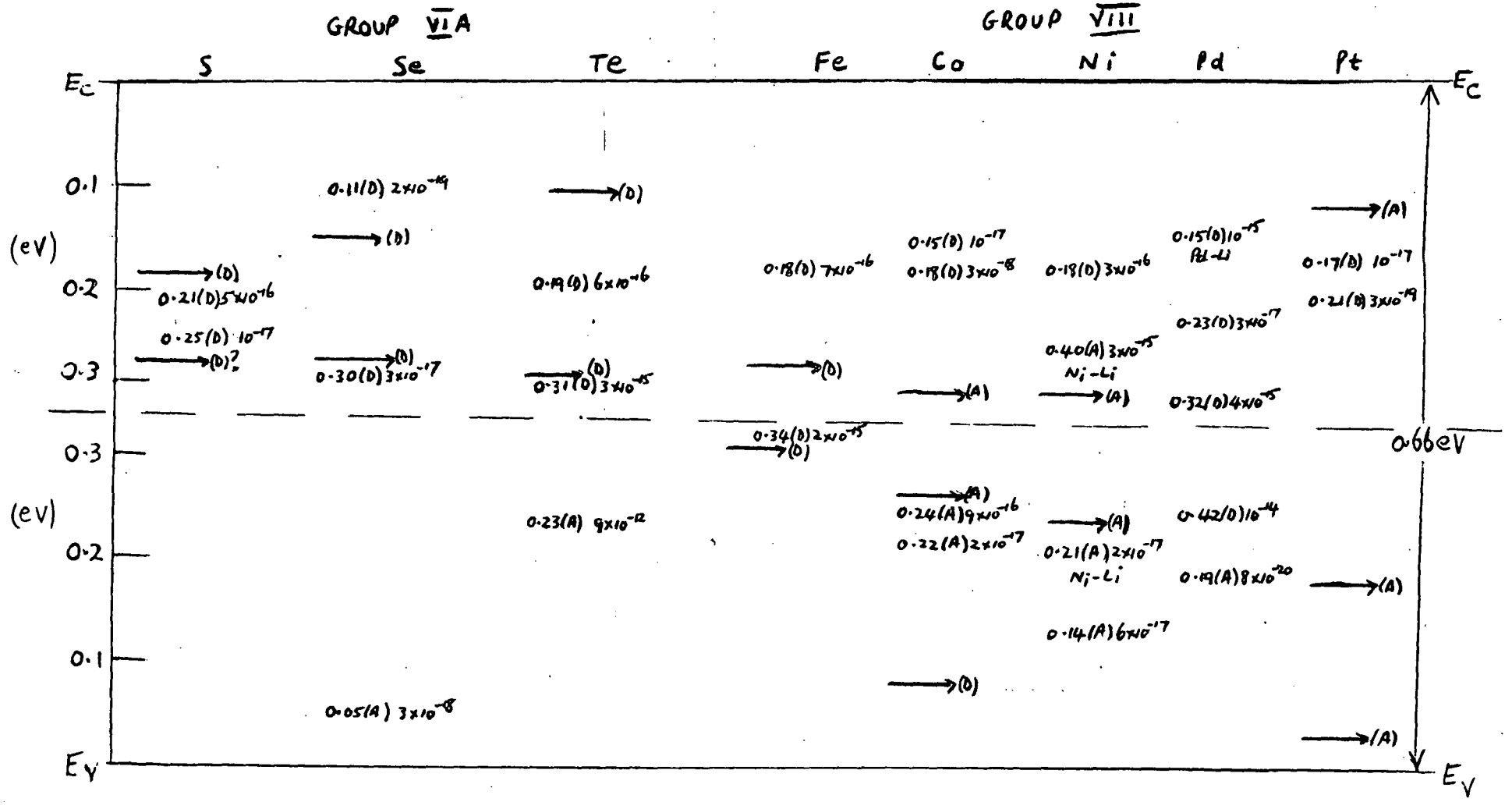

→ INDICATES LEVEL LISTED IN MILNES

D DONOR LEVEL

A ACCEPTOR LEVEL

TABLE 3. ENERGY LEVELS AND CROSS-SECTIONS OF GROUP VI A AND VIII IMPURITIES IN Ge.

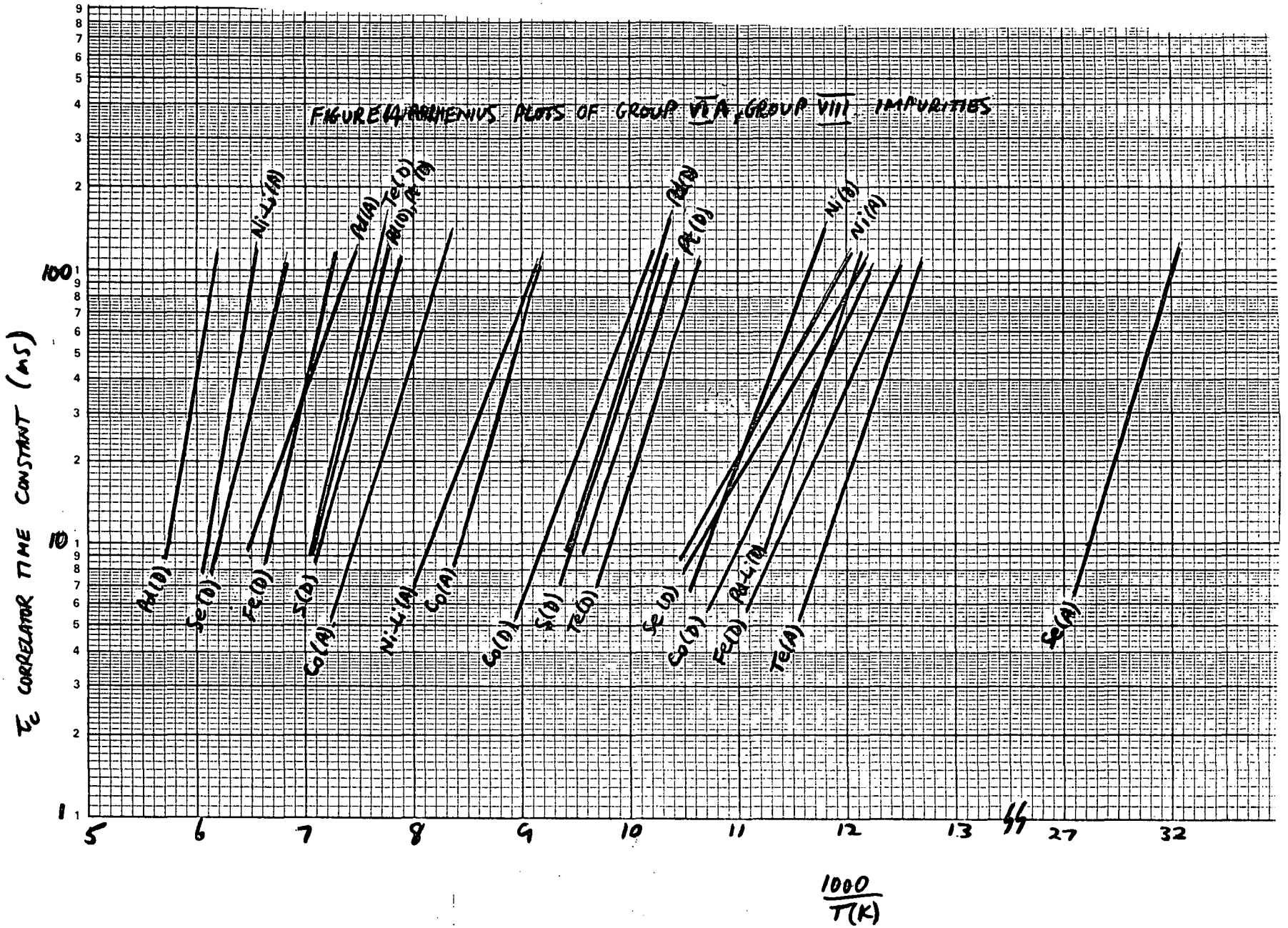
FIGURE 14 ARRHENIUS PLOTS OF GROUP VI A, GROUP VIII IMPURITIES
τ_c CORRELATOR TIME CONSTANT (nS)
$\frac{1000}{T(K)}$
Pd(D)
Se(D)
Fe(D)
S(D)
Co(A)
Ni-Li(A)
Co(A)
Co(D)
S(D)
Te(D)
Se(D)
Co(D)
Fe(D)
Pd-Li(A)
Te(A)
Se(A)
Pt(D)
Pd(A)
Te(D)
Pt(D),Pt(A)
Ni-Li(A)
Ni(D)
Ni(A)

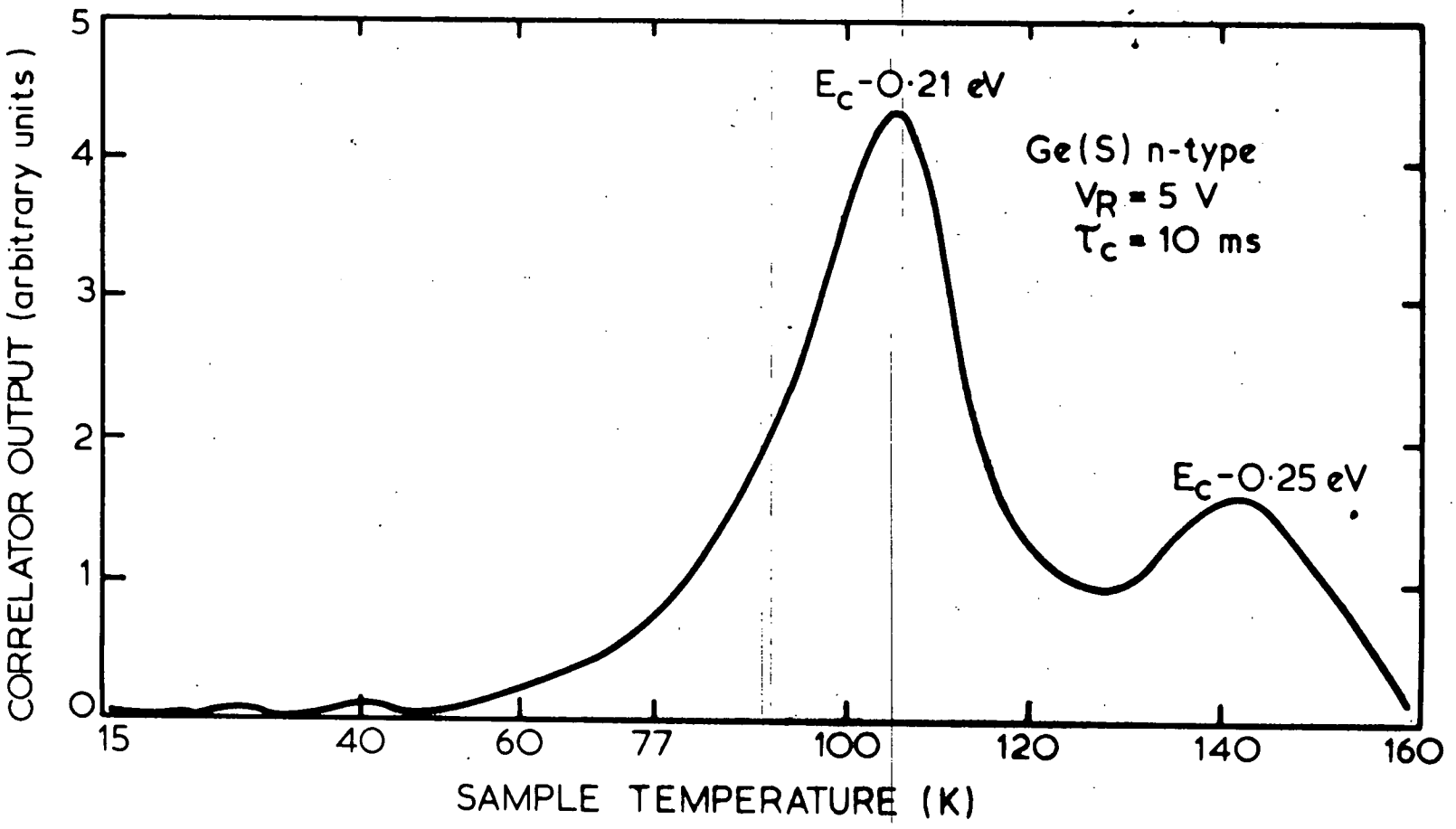

Figure 15. DLTS spectrum for an n-type Ge sample diffused with S. Reverse bias voltage is 5V, correlator time constant 10 ms.

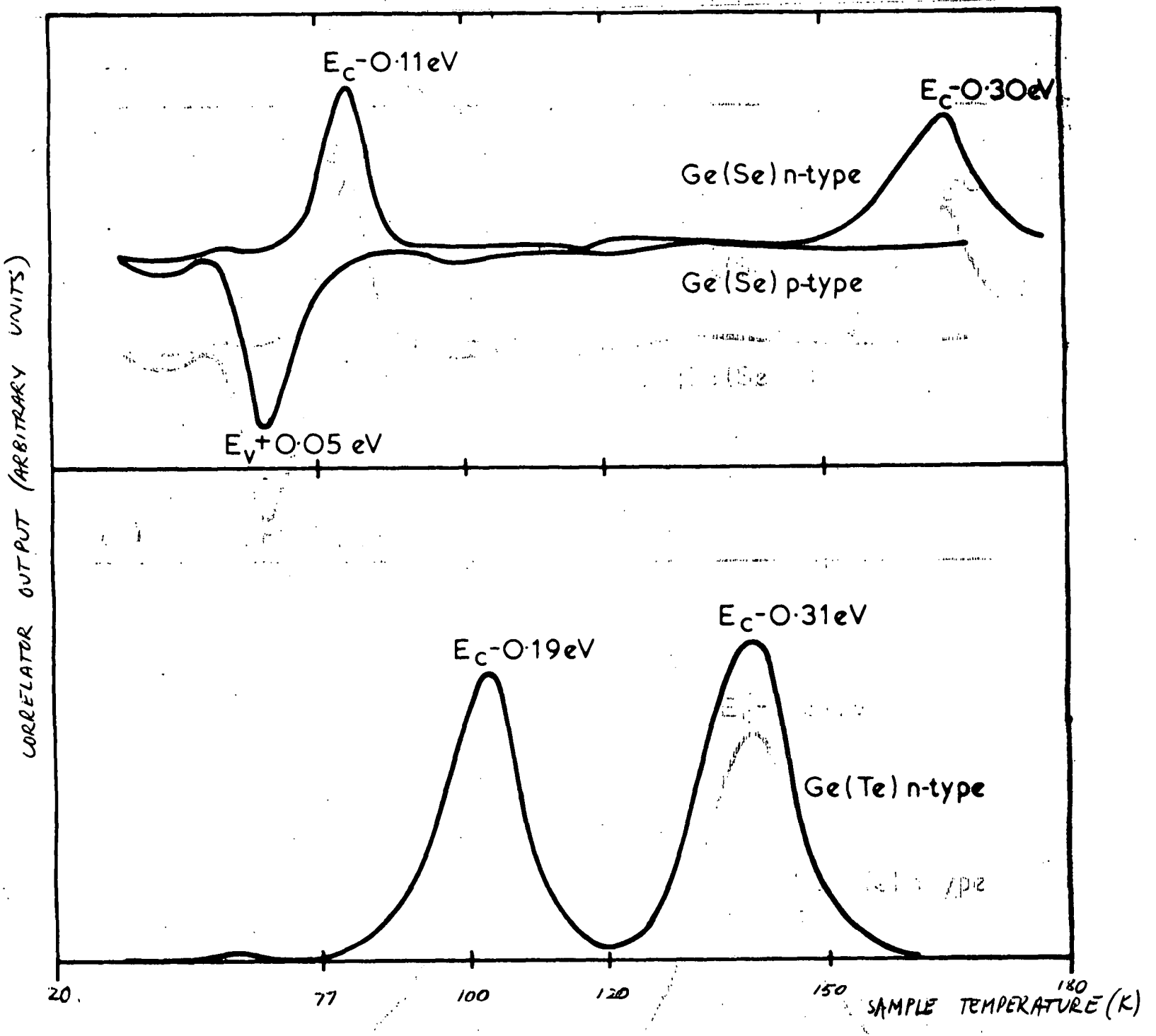

FIGURE 16 Se- diffused n- and p-type Ge diodes and Te diffused n-type Ge

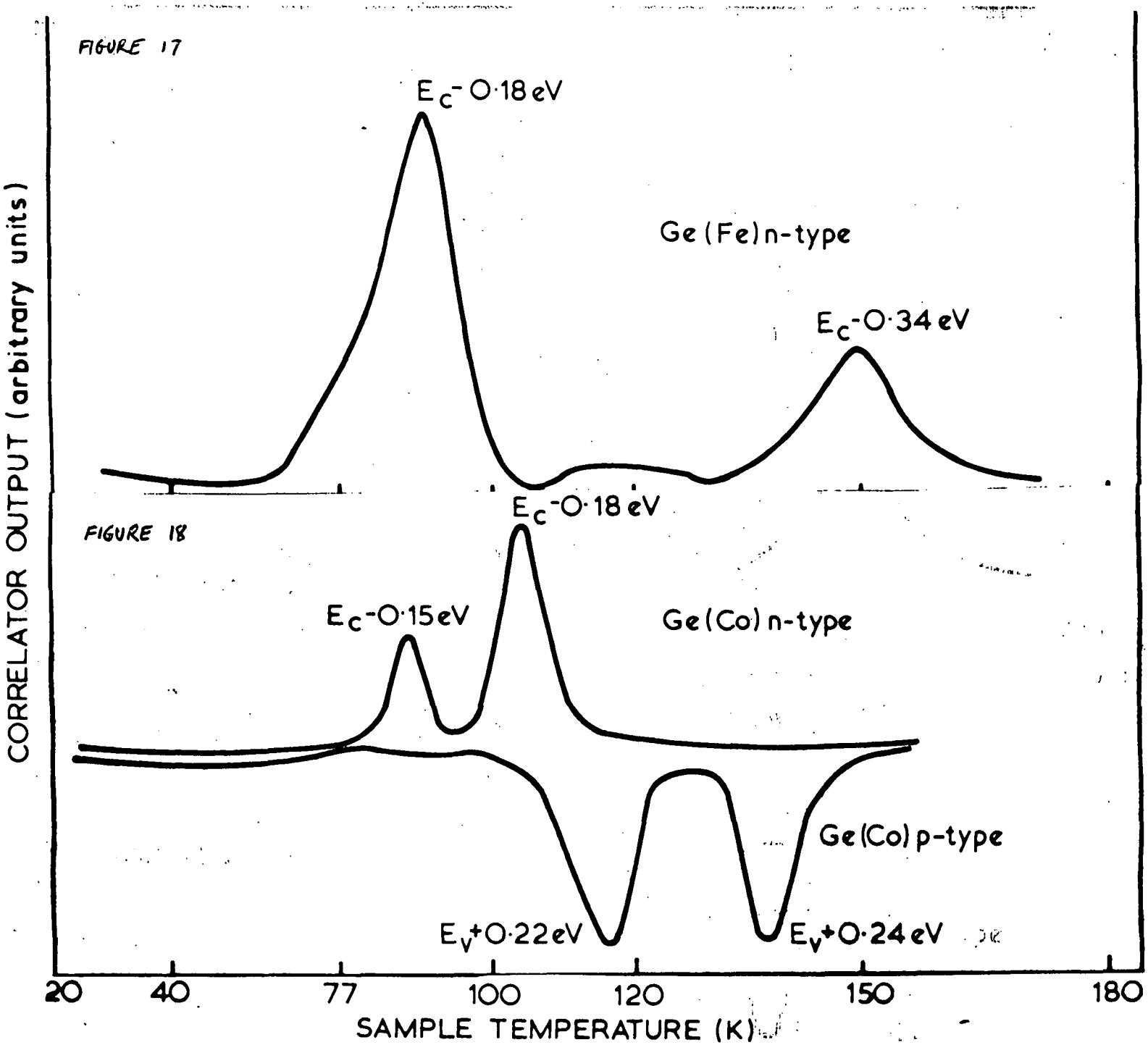

FIGURES 17 And 18.

Fe diffused n-type Ge and Co diffused n- and p- type Ge

200°C) to determine if Fe-Li pairing occurs, as with the elements Cu, Zn and Ni with Li. No such evidence was found.

Cobalt in Ge has been observed to exhibit an acceptor state at E_v + 0.25 eV [Milnes 1973]; with the spectroscopic DLTS technique we observed two acceptors present in equal concentrations with levels at E_v + 0.22 eV and E_v + 0.24 eV (Figure 18). The capture cross sections for holes of the centres are quite similar ($\sim 10^{-17}$ cm^2).

Figure 19 shows the DLT spectrum obtained for Ni-doped, p-type Ge. The E_c - 0.18 eV level is seen as a majority trap in n-type material. As the p-type samples are depleting from the Li-diffused side, Ni-Li related complexes may be identified by the concentration profile of the deep level; a sharply decreasing profile away from the contact means that Li is involved. The E_v + 0.21 eV and E_v + 0.40 eV acceptor levels are both Ni-Li-related complexes. Lithium shows a marked tendency to pair with Ni. It was noted that Li-diffused contacts on Ni-doped samples lost their n^+ nature within days if left at ambient temperature. Undoped samples of this material have retained their strong n^+ Li-doped contacts for more than 15 months at room temperature, due to stable Li-O donor formation. It is likely that Ni getters oxygen in the metal-diffused region, allowing Li to precipitate to its equilibrium solid solubility at ambient temperature. A similar effect involving Ni in Si has been observed [Bakhadyrkhov et al. 1976].

Figure 20 shows the DLT spectrum for a Pd-diffused, p-type sample. The E_v + 0.19 eV acceptor and E_c - 0.15 eV and E_c - 0.23 donor levels were observed in all Pd-diffused samples; the E_c - 0.15 eV centre is a complex involving Pd and Li. An additional donor level at E_c - 0.32 eV is observed in p-type material, but is masked by the other donors under injection conditions in a p-type diode.

Figure 21 shows the typical DLT spectrum for a Pt-diffused, n-type

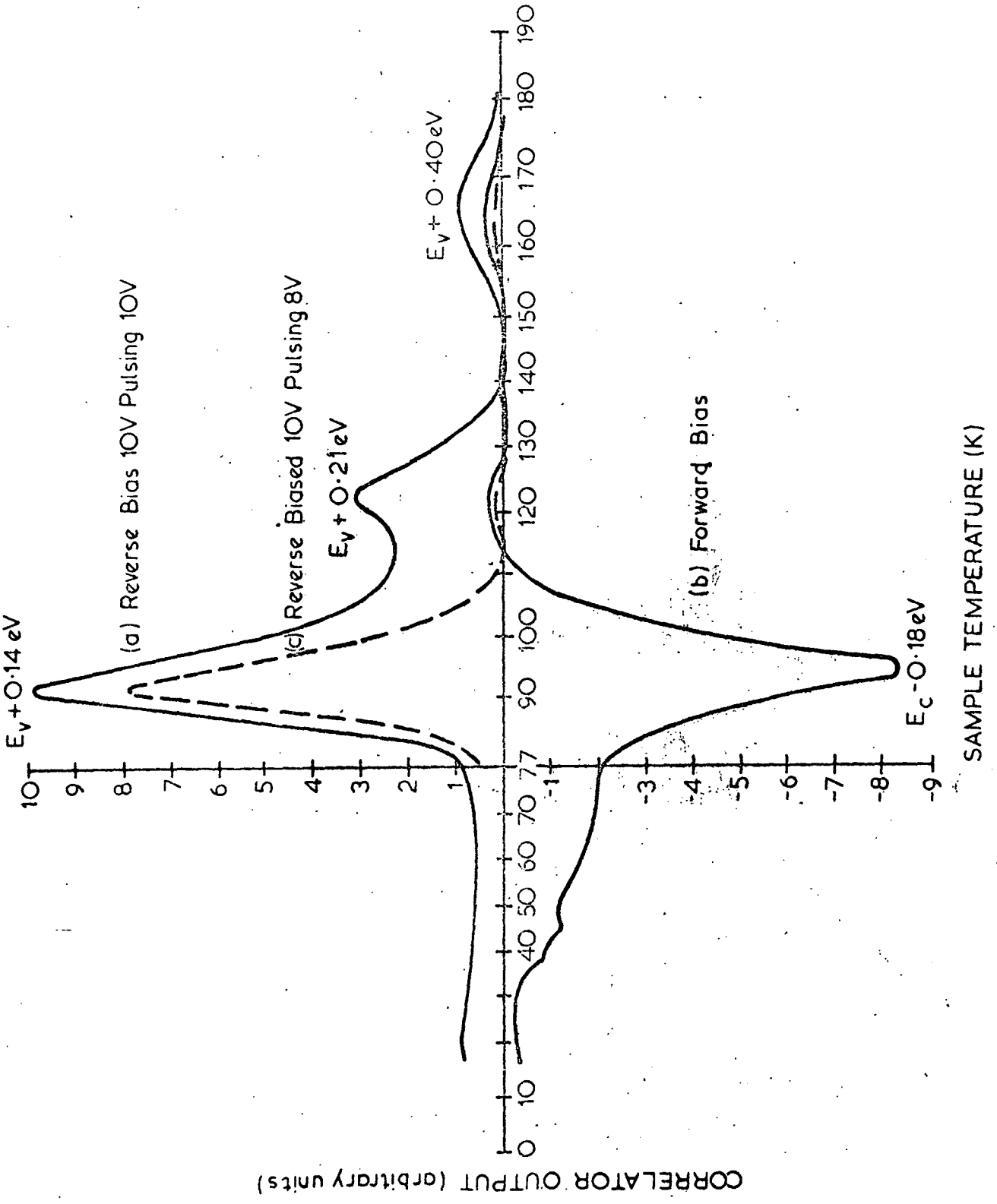

Figure 19

(a) DLTS spectrum for Ni-diffused, p-type Ge sample - forward biasing (b) the junction reveals a minority (electron) trap. (c) At 10 V bias, with a filling pulse of only 8 V, the region of the diode investigated is on the 'tail' of the Li-diffused contact-note the decrease in concentration of the Li-related centres.

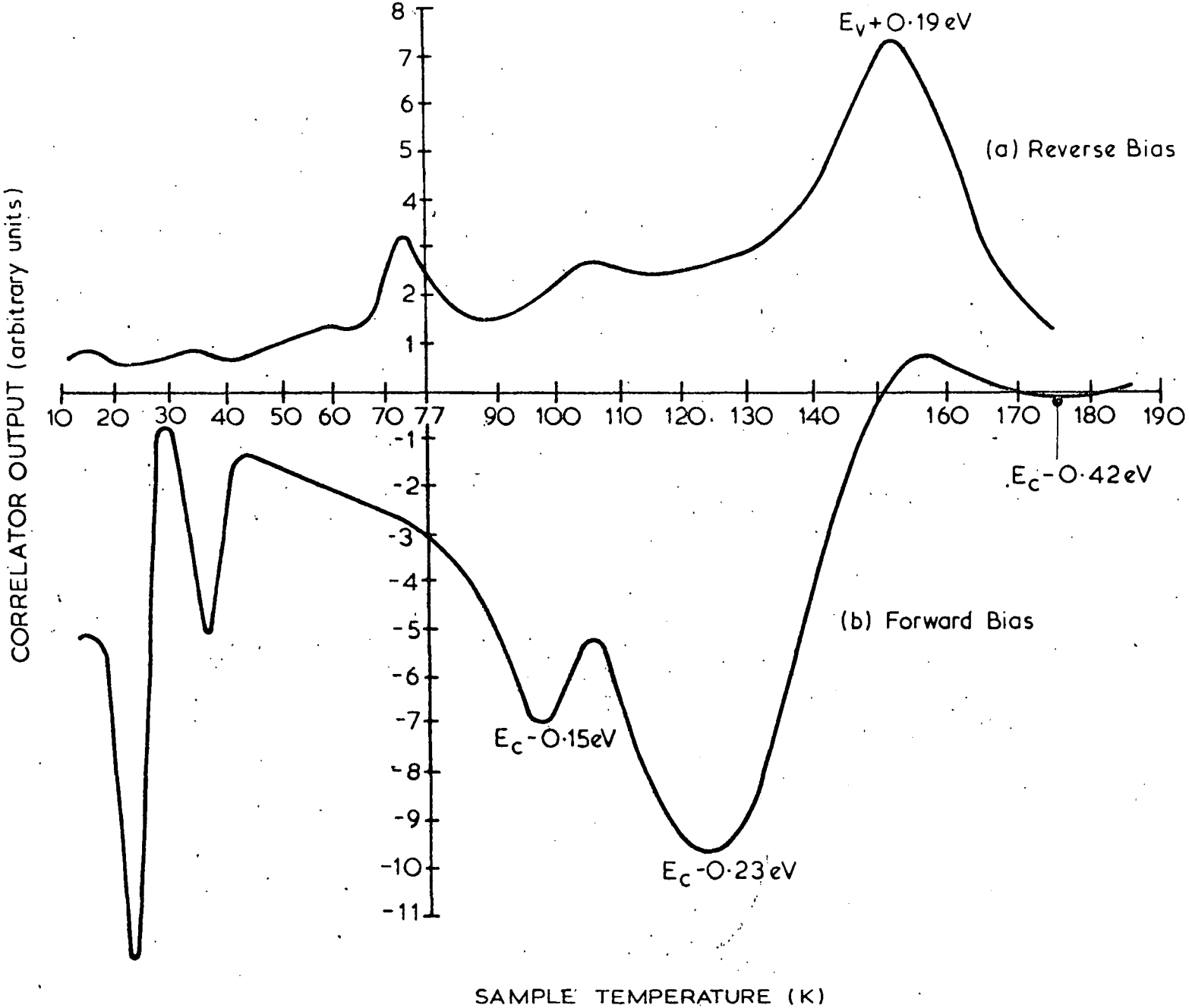

Figure 20

DLT spectrum for Pd-diffused p-type Ge sample. Only those levels which appeared in all Pd-diffused samples are labelled.

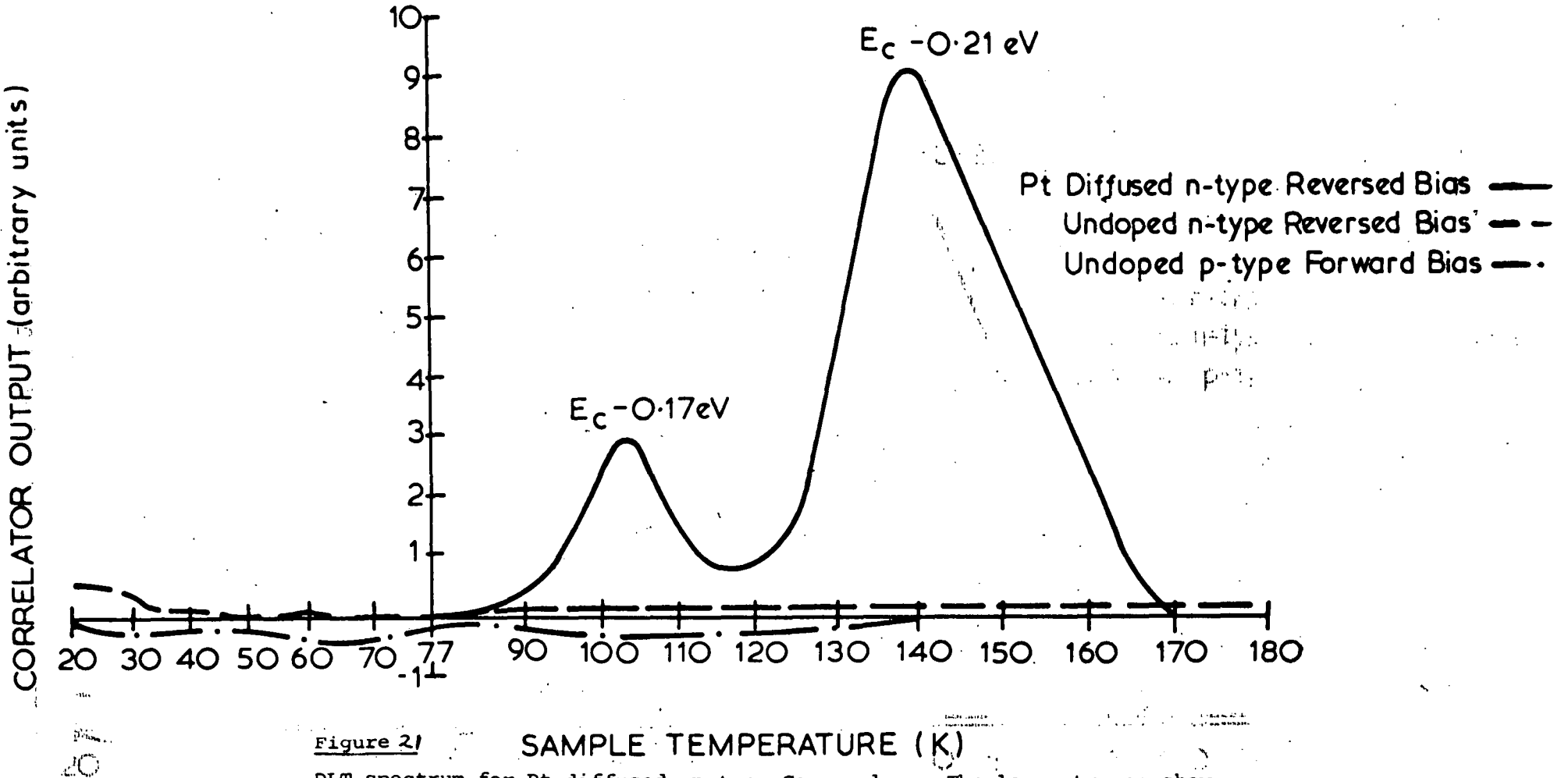

Figure 2

DLT spectrum for Pt-diffused, n-type Ge samples. The lower traces show defect spectra of the control samples used in the experiment. Typical reverse bias voltages were 10-20 V, with 200 μs saturating or injecting bias pulses to fill the defect states. Correlator time constant for all spectra is 10 ms.

Ge diode. As with the other elements, control samples fabricated and heated in exactly the same fashion as the test samples showed no electrically active impurities with concentrations comparable to the metal-related centres. Typical reverse bias voltages in these samples were 10 to 20 V (leakage current <50 μm for T ≤200 K) with 200 μs saturating or injecting bias pulses being used to fill the defect states. No acceptor states were measured for Pt in Ge, only donors at E_c - 0.17 eV and E_c - 0.21 eV. It should be noted that all the Group VIII elements measured displayed donor states between E_c - 0.15 eV and E_c - 0.23 eV.

Our correlation DLTS system did not have sufficient range of time constants to accurately measure the temperature dependence of the capture cross sections for the various levels.

4.4 Rare Earth Impurities

As far as can be ascertained, no measurements on the electrical behaviour of these elements in Ge have been previously reported [Milnes 1973], due partly to their low electrical activity and small diffusion coefficients. To overcome this, thick evaporated layers (>100 nm) of the elements were used and the diffusions performed at 810°C. At this temperature it was found impossible to keep copper out of the samples, although fortunately, one could readily identify the Cu^{2-} and Cu-H levels. Concentrations of these levels were in the range 10^{10} to 2×10^{11} cm^{-3}.

The DLTS scans were performed in the usual way, with the bias profiling technique allowing identification of the diffused impurities. A typical spectrum for a Ho diffused p-type Ge sample is displayed in Figure 22(a). Extra peaks due to Cu^{2-} and Cu-H related centres are present. The concentration profiles of these levels are constant throughout the sample, whereas the diffused rare earth impurity was

present only in the zero bias depletion region next to the rectifying contact, reached by forward pulsing the reverse bias on the sample. Investigating a region deeper into the material showed only the Cu-related centres (Figure 22(b)). One cannot rule out the possibility that copper-rare earth complexes are the cause of some of the levels. Table 4 shows the energy states measured for the elements investigated, together with their capture cross section for majority carriers. The Arrhenius plots of the energy states are displayed in Figure 23.

For the rare earth impurities Nd, Gd, Tb, Ho, Tm and Er we measured a common acceptor level of E_v + 0.13 eV with a capture cross section for holes of 4 x 10^{-17} cm^2, as well as other deep donor and acceptor states associated with these elements. The common acceptor level may be related to the stresses induced in the Ge lattice by the presence of large impurity atoms of similar structure; a previous attempt at modelling deep level behaviour in GaAs, GaP and Si used the relative lattice strain induced by transition elements (Sc to Cu) to obtain fair agreement of theoretical estimates of acceptor states related to these elements with experimental results [Partin et al. 1979]. Indeed, Tm and Ho gave rise to similar DLTS spectra with acceptors at E_v + 0.13 eV and E_v + 0.23 eV. The former level is not due to a copper-rare earth complex as it was often observed at concentrations far above the Cu contamination level.

4.5 Electrically Inactive Impurities in Ge

Magnesium was diffused into Ge in the same manner as for the other metals, but no electrical activity associated with the element was observed. This is in agreement with Hall-effect results [Borodovskii et al. 1977] suggesting that group II elements show no electrical activity in Ge at concentrations less than $\sim 10^{17}$ cm^{-3}, and then the electrically active fraction is $\sim 10^{-5}$. As the total Mg content after diffusion was

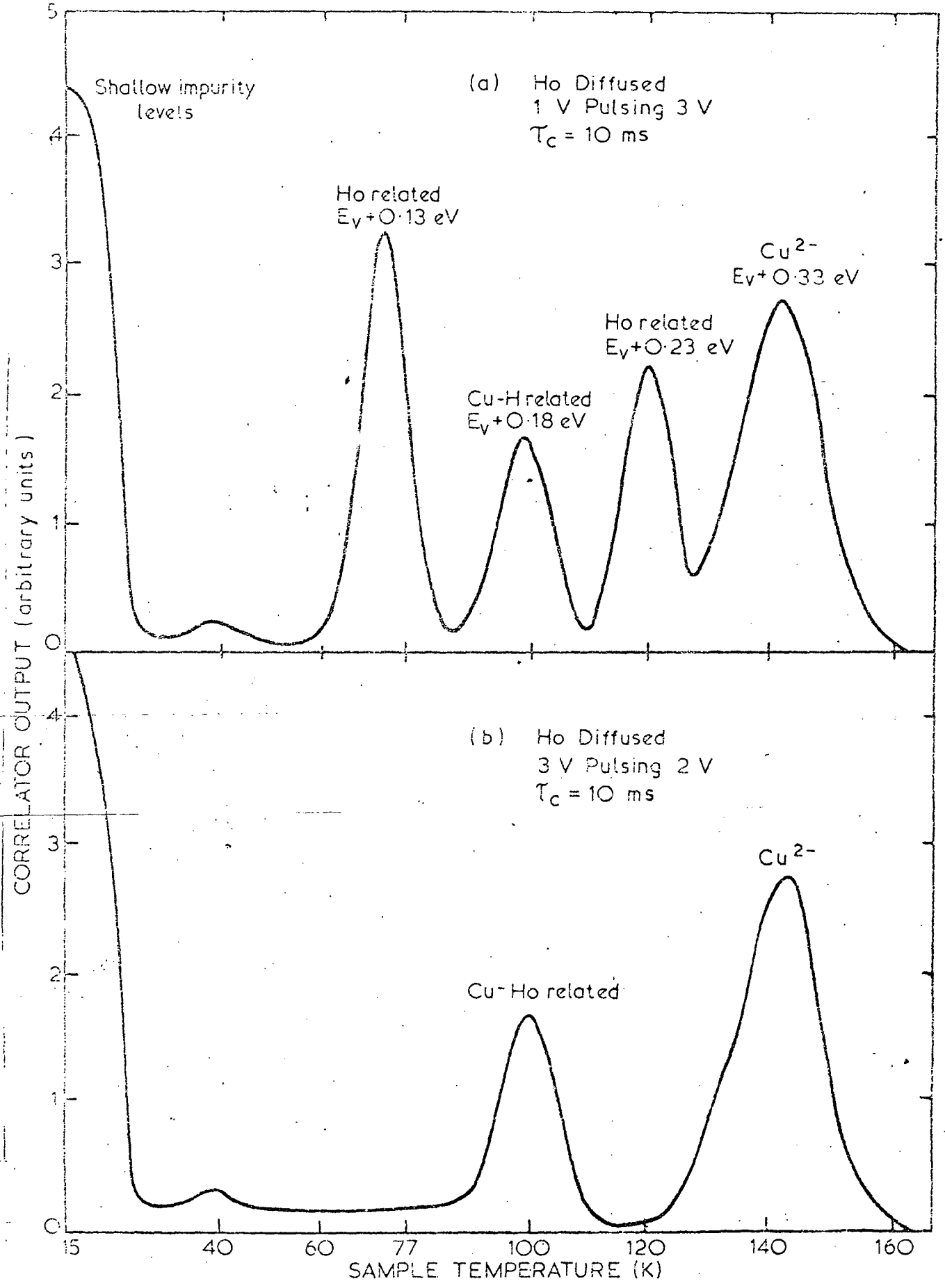
Shallow impurity levels
(a) Ho Diffused
1 V Pulsing 3 V
τ_c = 10 ms
Ho related
E_V + 0·13 eV
Cu-H related
E_V + 0·18 eV
Ho related
E_V + 0·23 eV
Cu^{2-}
E_V + 0·33 eV
(b) Ho Diffused
3 V Pulsing 2 V
τ_c = 10 ms
Cu-Ho related
Cu^{2-}
CORRELATOR OUTPUT (arbitrary units)
0
1
2
3
4
5
15
40
60
77
100
120
140
160
SAMPLE TEMPERATURE (K)

FIGURE 22.

RARE EARTHS

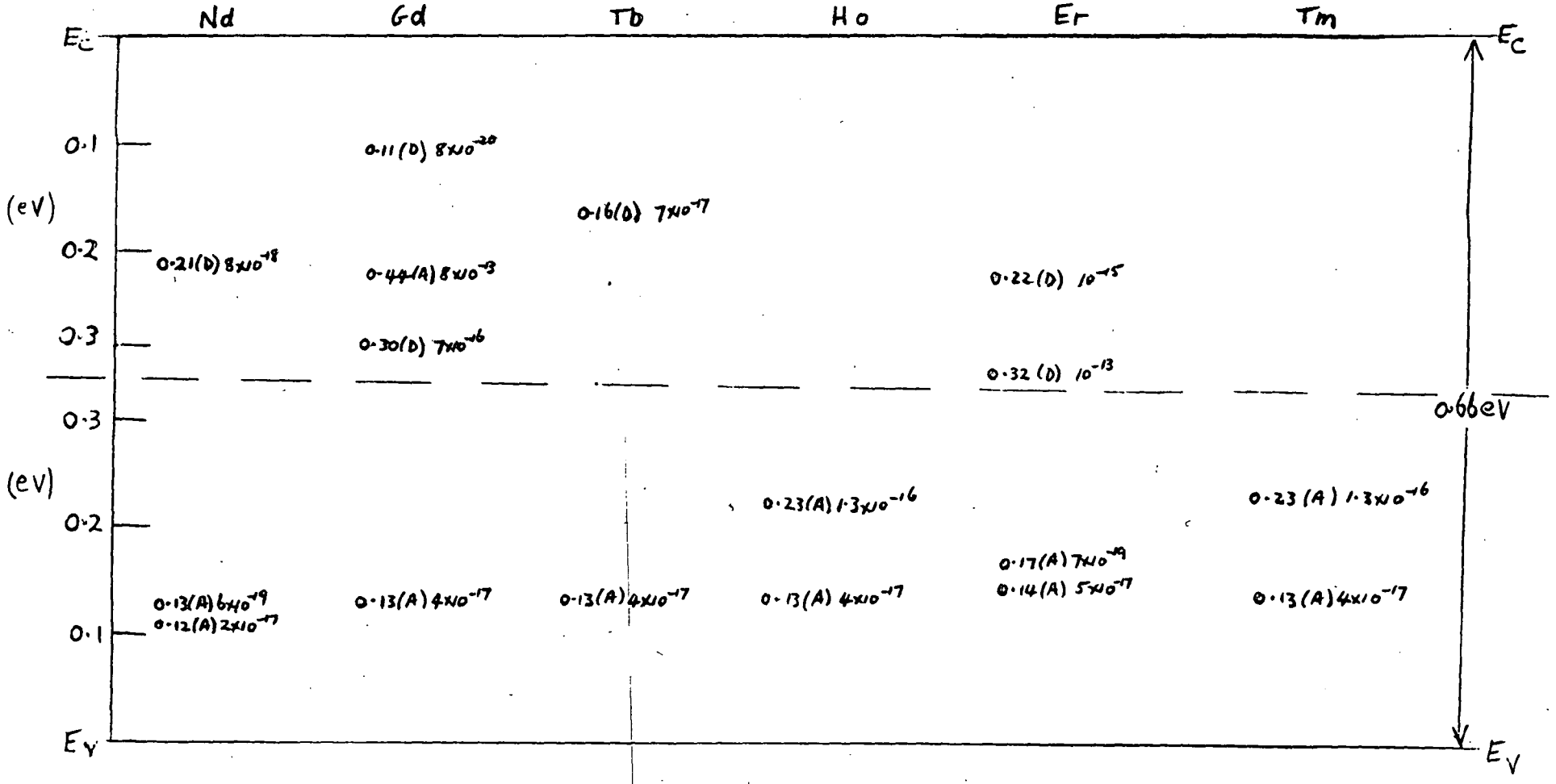

TABLE 4. ENERGY LEVELS AND CROSS-SECTIONS FOR RARE EARTH IMPURITIES IN Ge.

D DONOR LEVEL

A ACCEPTOR LEVEL

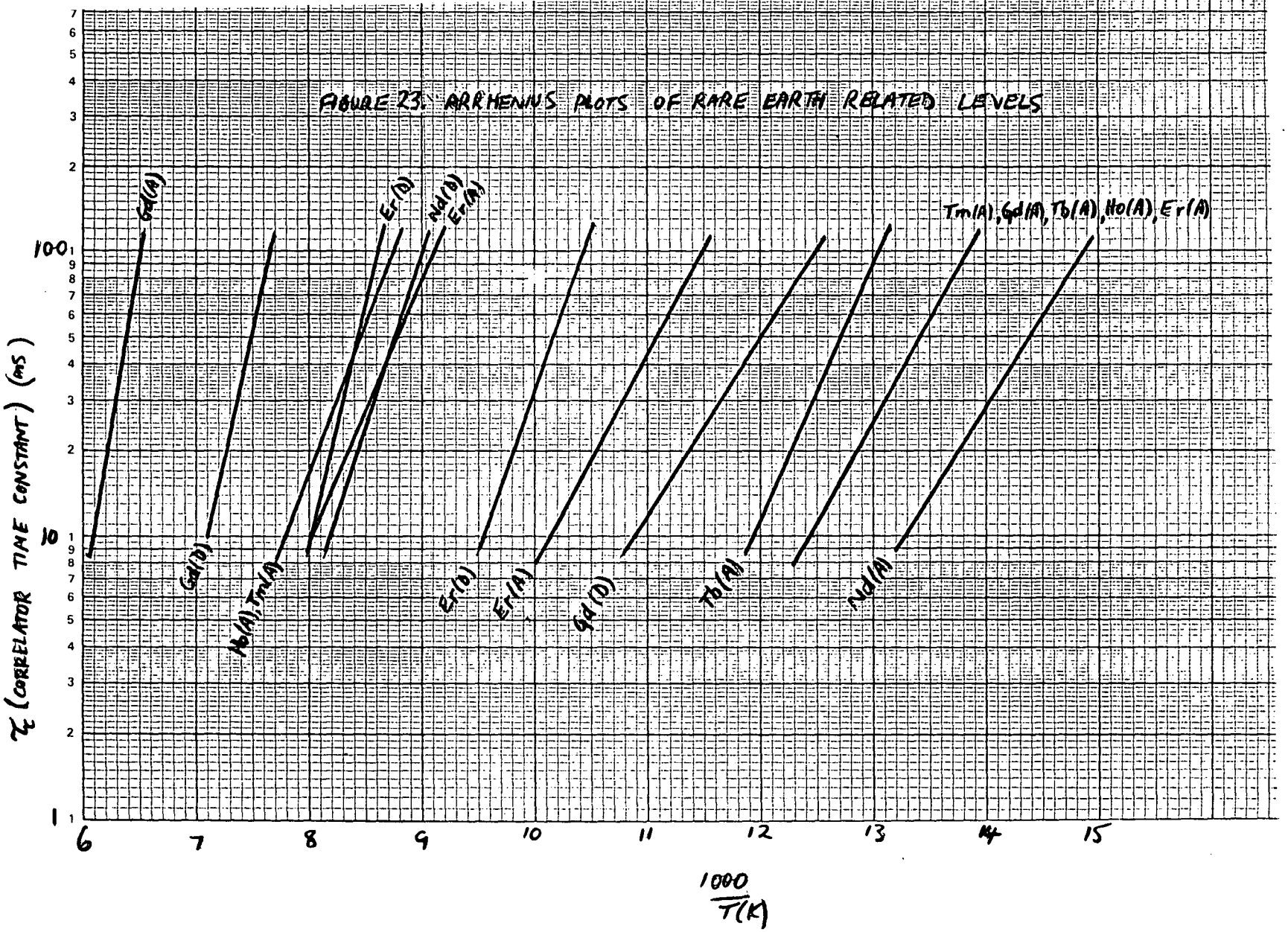
FIGURE 23: ARRHENIUS PLOTS OF RARE EARTH RELATED LEVELS
τc (CORRELATOR TIME CONSTANT) (ms)
1000/T(K)
Gd(A)
Gd(D)
Ho(A), Tm(A)
Er(D)
Nd(D)
Er(A)
Er(D)
Er(A)
Gd(D)
Tb(A)
Tm(A), Gd(A), Tb(A), Ho(A), Er(A)
Nd(A)

estimated to be less than 10^{14} cm^{-3} in the region investigated, the deep level concentration would have been less than 10^{9} cm^{-3} which is at the limits of sensitivity of the DLTS technique for the material used here. The diffusion of Ba also produced no measurable electrical activity.

For elements in the same column as Ge we measured no electrical activity for Si, Sn or Ge itself, although electrical activity has been measured for self-implanted Si samples [Chen and Milnes 1980]. It is possible that these may be related to radiation damage rather than the Si atoms themselves. The diffusion coefficient of Si in Ge is extremely small at 700°C, $\sim 3 \times 10^{-16}$ cm^2 s^{-1} [Rainsanen et al. 1981], making it difficult to observe its effect in high-purity material in which small biases cause relatively large depletion depths. Table 5 shows the elements diffused into Ge which did not show deep level activity.

DISCUSSION

Comparison of Tables 1-4 shows that there appears to be a band of energies from E_c - 0.15 eV to E_c - 0.25 eV into which many deep metal-related donor states in Ge fall, i.e. at approximately one-third the band gap of the material. The capture cross sections for these states are generally in the range 10^{-16} to 10^{-18} cm^2. Remembering that cross contamination between samples was impossible because of the separate diffusions and use of control samples, it is revealing that donor states related to Au, Pt, Pd, Ni, Nd, Tb, Er, Te, S, Co, Mo, Ti, Zr and Fe all fall into this band of energies. For example, a donor level at E_c - 0.31 eV ($\sigma_n = 3 \times 10^{-15}$ cm^2) was observed in Te, Cr and Zr diffused samples. It was apparent to different depths in samples diffused with these elements at the same temperature for the same period, correlating with the different diffusion coefficients.

TABLE 5.

ELECTRICALLY INACTIVE ELEMENTS IN Ge

GROUP II A	Mg, Ba
GROUP IV A	Si, Ge, Sn

THERE WERE ALSO NO DEEP LEVELS FOUND FOR Sb (SHALLOW LEVELS ONLY)

Likewise, Au-Li and Pd-Li donor complexes had similar emission rates over the temperatures investigated. Their cross sections are identical and bear a similarity to the cross section of a Ni-Li related complex. These are the first reported measurements on this group; others have observed pairing of copper [Haller et al. 1979], and zinc [Hannay 1960] with lithium in germanium.

Similarly, the deepest acceptor state measured for Bi-related levels, E_v + 0.17 eV, is similar in energy and capture cross section to acceptor centres related to Pb, Te, Cd, Co, Cr, Pd, Tm and Ho. There has been a level at E_v + 0.16 (±0.02) eV previously reported for γ-irradiated Bi-doped Ge, ascribed to a Bi-divacancy complex [Emtzev et al. 1973]. It is possible that the large Bi ion forms complexes with vacancies produced during the heat treatment and that this complex remains stable on cooling. The fact that Pb (which is next to Bi in the periodic table and in the same column as Ge) also displays an acceptor level of E_v + 0.17 eV may be further evidence that many of the energy levels measured may be due to impurity-defect associations or possibly latice strain, rather than specific to the impurity atom.

This behaviour is similar to that observed by Lang et al. [1980] for deep defect states in Si, where it has been noted recently that the Au donor and acceptor are not related to the same centre as was previously believed and, furthermore, that there are broad similarities for Au, Ag, Co, Rh, S and process-induced levels. In Ge it has also been the case that donor and acceptor states introduced by the same dopant do not have the same concentration as measured under saturation trap-filling conditions [Lang et al. 1980].

The data on Ge provide further evidence that deep metal-related levels in elemental semiconductors may be due to defects of complicated

structure, rather than simple substitutional or interstitial defects.

This complexing of metal ions with lattice defects or residual chemical impurities is one reason why many of the levels tabulated here have not previously been observed. The Ge used in this experiment is generally at least an order of magnitude more pure (in the electrical sence) than the material used in previous studies and this, combined with the sensitivity of the DLTS technique, enables a more effective study of the behaviour of metal-related defect centres. Indeed, the discrepancies between our data and that reported previously [Milnes 1973] may possibly be taken as evidence for the complicated nature of defect centres in Ge.

In general, crystals grown in different laboratories have different quantities of the various species of background chemical impurities, so there is a need for the cross correlation of results obtained in material grown under varying conditions. In this way, the most common metal-related centres will be identified.

CONCLUSION

Considerable evidence exists in Si that families of broadly-related defects exist, with similar emission and capture properties and that these centres are of a complicated nature, rather than simple, interstitial or substitutional defects [Lang et al. 1980]. Evidence for the same behaviour of impurities in Ge has been obtained; experiments along these lines will be of assistance in the formulation of more accurate models for deep level impurity behaviour. The Arrhenius plots of the various centres, together with the associated DLTS spectrum, provide a useful resource for identification of metal contamination in Ge devices.

REFERENCES

Bakhadyrkhov, H. K., Zainobidinov, S., Teshabaev, A. T. and Khodzkaeva, M. A. [1976] - Sov. Phys. Semicond. 10:593.

Borodovskii, Ya. A., Gavrilov, G. M., Goncharov, L. G., Kervalishivili, P. D., Litovchenko, P. G. and Khorvat, A. M. [1977] - Sov. Phys. Semicond. 11(10)1180.

Chen, J. W. and Milnes, A. G. [1980] - Ann. Rev. Mater. Sci. 10:157.

Chen, J. W., Milnes, A. G. and Rohatgh, A. [1979] - Solid State Electronics 22(9)801.

Emtzev, V. V., Mashovets, T. V. and Ryvkin, S. M. [1973] - Radiation Damage and Defects in Semiconductors, Inst. Phys. Conf. Series No. 16:17.

Evwaraye, A. O., Hall, R. N. and Soltys, T. J. [1979] - IEEE Trans. Nucl. Sci. 26(1)271.

Grimmeiss, H. G., Janzen, E. and Skarstam, B. [1980a] - J. Appl. Phys. 51(7)3740.

Grimmeiss, H. G., Janzen, E. and Skarstam, B. [1980b] - J. Appl. Phys. 51(8)4212.

Grimmeiss, H. G. and Skarstam, B. [1981] - Phys. Rev. B 23(4)1947.

Haller, E. E., Li, P. L., Hubbard, G. S. and Hansen, W. L. [1979] - IEEE Trans. Nucl. Sci. 26(1)265.

see for example Hannay, N. B. (ed.) [1960] - Semiconductors (Reinhold Publishing Corp., New York) pp. 203-213.

Lang, D. V. [1974] - J. Appl. Phys. 45:3023.

Lang, D. V., Grimmeiss, H. G., Meijer, E. and Jaros, M. [1980] - Phys. Rev. B 22(7)3917.

Miller, G. L., Lang, D. V. and Kimerling, L. C. [1977] - Ann. Rev. Mater. Sci. 7:377.

Miller, G. L., Ramirez, J. V. and Robinson, D. G. H. [1975] - J. Appl. Phys. 46:2638.

Milnes, A. G. [1973] - Deep Impurities in Semiconductors (Wiley and Sons, New York).

Partin, D. L., Chen, J. W., Milnes, A. G. and Vassamillet, [illegible] - [1979] Solid State Electronics 22:455.

Rainsanen, J., Hirvonen, J. and Antilla, A. [1981] - Solid State Electronics 24:333.

Sze, S. M. [1969] - Physics of Semiconductor Devices (Wiley and Sons, New York).

Tyler, W. W. [1959] - J. Phys. Chem. Solids 8:59.

CHAPTER 5

HYDROGEN PASSIVATION OF POINT DEFECTS IN Ge AND GaAs

SUMMARY

The passivation of copper-related centres in Ge, γ-irradiation centres in Ge and contaminating defects in GaAs by reaction with atomic hydrogen has been observed using DLTS. Data is presented on the efficiency of passivation as a function of the duration and temperature of the exposure to hydrogen.

INTRODUCTION

There is considerable interest in the effects of atomic hydrogen incorporation in amorphous [Pankove and Carlson 1980; Pankove et al. 1978] and crystalline [Seager and Ginley 1979; Benton et al. 1980] semiconductors. The passivation of dangling bands associated with electrically active defects by reaction with the H atom leads to lower leakage currents in p-n junctions [Pankove et al. 1978], improved efficiency of amorphous silicon solar cells [Pankove and Carlson 1980] and reduction of grain boundary recombination rates in polycrystalline silicon [Seager and Ginley 1979]. Recently, direct observation of hydrogenation passivation of recombination centres caused by laser irradiation has been reported for bulk silicon [Benton et al. 1980], using DLTS [Lang 1974]. This has raised the possibility of passivating defects caused during device processing and fabrication but, as yet, little work has been published on the efficiency and depth of hydrogen incorporation in various semiconductors as a function of the duration and temperature of the exposure to hydrogen. For example, the laser-induced defects in Benton et al. [1980] are present to a depth of ∿1 μm only. We have previously observed Li passivation of acceptor defects in Ge (Chapters 1 and 3), but Li is electrically active in Ge and Si; so the electrically neutral H has obvious advantages. We detail the results of experiments designed to measure the suitability of hydrogen neutralisation of bulk point defects related to γ-ray damage and

copper contamination during processing, of Ge, and defects incorporated during the crystal growth of GaAs.

5.1 Copper Related Centres in Ge

Extensive examination of copper in Ge has led to accurate measurements of its solubility and diffusion coefficient over a wide temperature range [Hall and Racette 1964; Frank and Thomas 1960; Williams 1969] and a good understanding of its electrical properties [Woodbury and Tyler 1957; Milnes 1968]. As well as introducing three acceptor levels at E_v + 0.04 eV (Cu^-), E_v + 0.33 eV (Cu^{2-}) and E_c - 0.26 eV (Cu^{3-}), it is known to form defect complexes with lithium [Haller et al. 1979] and hydrogen [Haller et al. 1977; Haller et al. 1979; Haller 1978]. Deliberate doping of Ge with copper is used to produce detectors of infrared radiation [Teich et al. 1966; Quist 1968], but in the large high-purity Ge nuclear radiation detectors, copper related defects act as trapping sites for free charge carriers, degrading the energy resolution of these detectors [see, for example, Evwaraye et al. 1979].

The Ge used in this work was high-purity p-type material (N_a-N_d = 5 x 10^{10} to 7 x 10^{11} cm^{-3}) obtained from Lawrence Berkeley Laboratory. Copper was introduced inadvertently as a background impurity during the diffusion of Sb (1 hour at 500°C) to form the blocking n^+ contact for diode structures. The diffused Sb contacts were thin (∿2 μm) and stable at the temperatures used in this experiment (150 to 350°C). Rear ohmic contacts were fabricated by a Pd evaporation. The net electrically active impurity concentrations of the samples, after introduction of the Cu, were in the range 2 x 10^{11} to 3 x 10^{12} cm^{-3}, obtained from C-V measurements (1 MHz) at 77 K.

DLTS measurements on the diode structures revealed two dominant copper related defects above 77 K: E_v + 0.19 eV (Cu-H complex) [Haller et al. 1977], and E_v + 0.33 eV (Cu^{2-} centre) [Woodbury and

Tyler 1957; Milnes 1968; Haller et al. 1977]. A typical DLTS spectrum is shown in Figure 1(a). In a few cases, measurements were extended down to ∿10 K; these scans revealed another copper-hydrogen complex defect level (E_v + 65 meV) [Milnes 1973; Haller et al. 1977] and in the singly ionized Cu level E_v + 44 meV [Woodbury and Tyler 1957; Milnes 1968; Haller et al. 1977]. The concentration of the Cu^{2-} level was in the range 2 x 10^{10} to 3 x 10^{11} cm^{-3}; its profile was constant to depletion depths ∿100 μm.

Samples were exposed to atomic hydrogen by insertion in a 0.5 W cm^{-3}, 27 MHz hydrogen plasma, at a pressure of approximately 0.5 torr. The plasma was created by inductively coupling RF power via a coil enveloping a quartz tube, with the samples mounted on a high purity Ge substrate placed on a heater block. The hydrogen gas was purified by passing it through a Pd diffuser at 200°C, and then entering the top of the quartz tube in which the samples were mounted. A vacuum system incorporating a turbomolecular pump maintained the required pressure [Alexiev, unpublished]. The experimental set up is shown in Figure 2. After exposure to the plasma for periods between 0.5 to 3 hours at temperatures of 150 to 350°C, the samples were allowed to cool in the plasma until their temperatures had reached 80°C (maximum time required approximately 45 minutes). Molecular hydrogen anneals were performed similarly, without the plasma.

Figure 1(b) shows the DLTS spectrum for a sample heated in molecular hydrogen for 3 hours at 350°C; heat treatment in H_2 for any of the times and temperatures used here had no effect on the concentration or constancy of the profile for the two acceptor defect states.

Heating in the H plasma, however, significantly reduced the density of electrically active Cu^{2-} and Cu-H defect centres. Figure 1(c) shows the DLTS spectrum recorded for the sample of Figure 1(b) heated

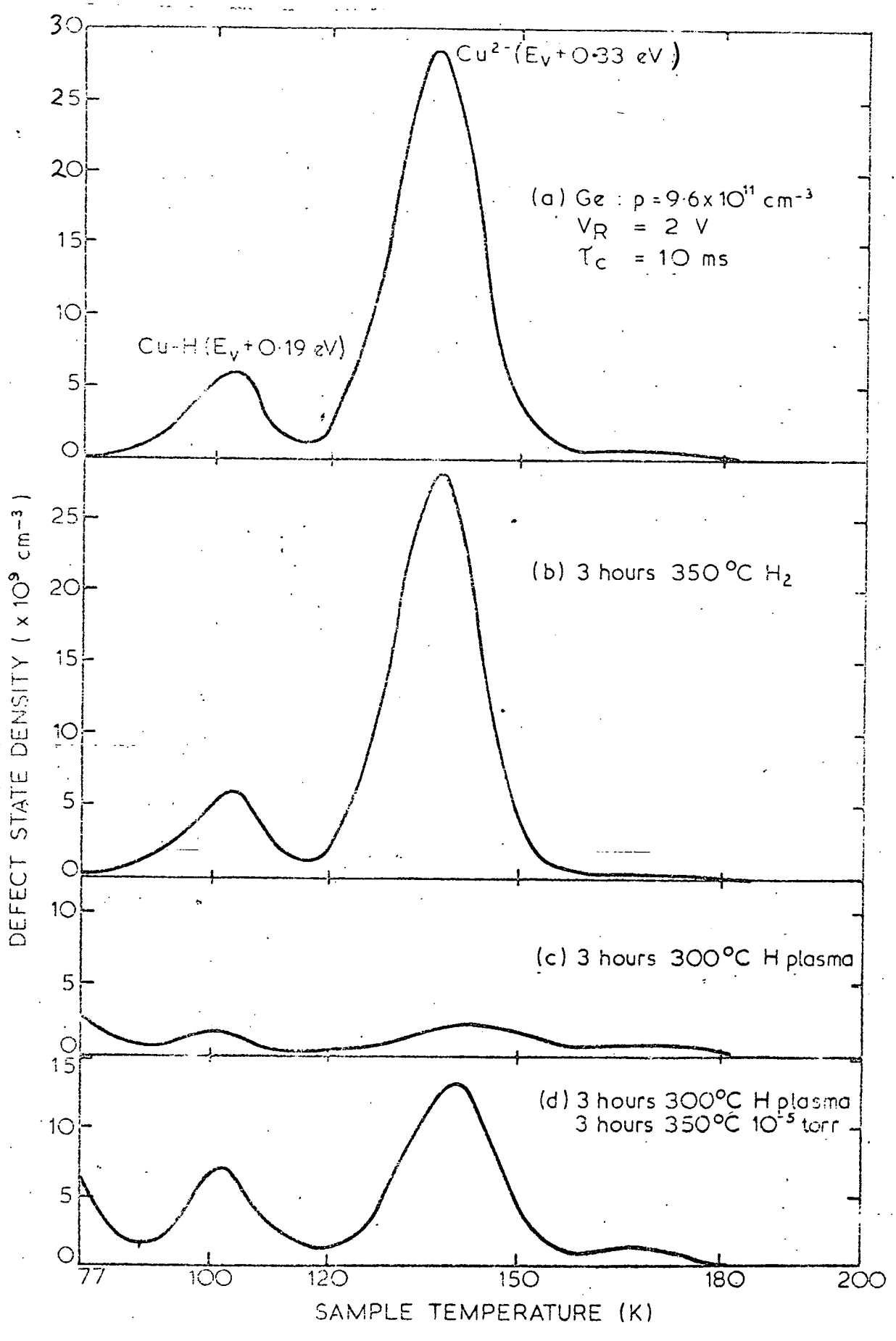
Cu²⁻ (Ev + 0·33 eV)
Cu-H (Ev + 0·19 eV)
(a) Ge : p = 9·6 x 10¹¹ cm⁻³
VR = 2 V
τc = 10 ms
(b) 3 hours 350 °C H2
(c) 3 hours 300°C H plasma
(d) 3 hours 300°C H plasma
3 hours 350°C 10⁻⁵ torr
DEFECT STATE DENSITY (x 10⁹ cm⁻³)
SAMPLE TEMPERATURE (K)
77
100
120
150
180
200

FIGURE 1.

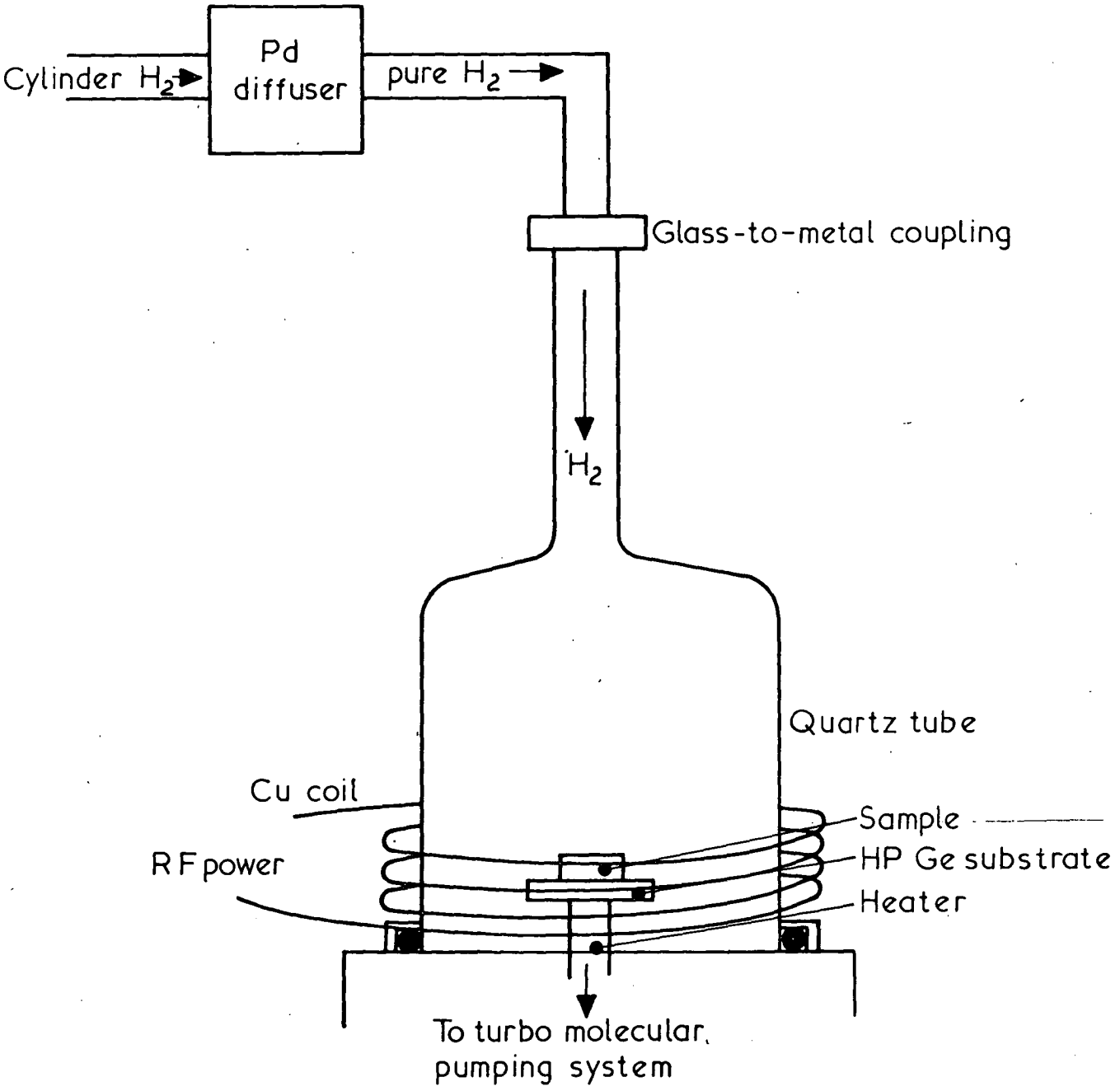

Figure 2. SCHEMATIC OF HYDROGEN PLASMA SYSTEM FOR INCORPORATION OF H IN SEMICONDUCTORS (D. ALEXIEV, UNPUBLISHED)

for 3 hours at 300°C in the H plasma. The sample capacitance was also reduced, confirming the evidence of the DLTS trace that deep defect states had been neutralised. Figure 3 shows a series of C-V curves for a sample exposed to the hydrogen plasma. Not only is the net doping density at 180 K reduced, but significantly, at 77 K also. At 180 K most of the Cu-H and Cu^{2-} levels will be ionized, and the reduction in capacitance at this temperature is due to their neutralisation by the hydrogen. At 77 K most of the Cu-H and Cu^{2-} levels will be frozen out and the reduction in capacitance will be due to neutralisation of copper related defects formerly active below 77 K, most notably the singly ionized copper level at E_v + 0.04 eV [Woodbury and Tyler 1957; Milnes 1958; Haller et al. 1977]. The fact that hydrogen is acting to neutralise the copper centres is evident after vacuum annealing hydrogenated samples; either evolution or recombination of the H to H_2 in the bulk brings an increase in the density of electrically active defects (Figure 1(d)) and hence the capacitance of the sample (Figure 3). Control samples initially without copper contamination did not show any copper related levels after similar vacuum anneals.

Plasma exposures for various periods and temperatures were carried out. Figure 4 shows the normalised concentration profile of the Cu^{2-} levels, obtained from DLTS measurements, as a function of the plasma exposure conditions. The normalisation to the pre-treatment concentrations allows for variations in the amount of copper present in different samples. In this pure Ge, only small bias pulses are needed to cover relatively large distances (tens of μm) and, due to the unusual profile encountered in this experiment (a low but not negligible concentration for a distance followed by a rapid increase over a short distance) and the method of obtaining the profile (comparison

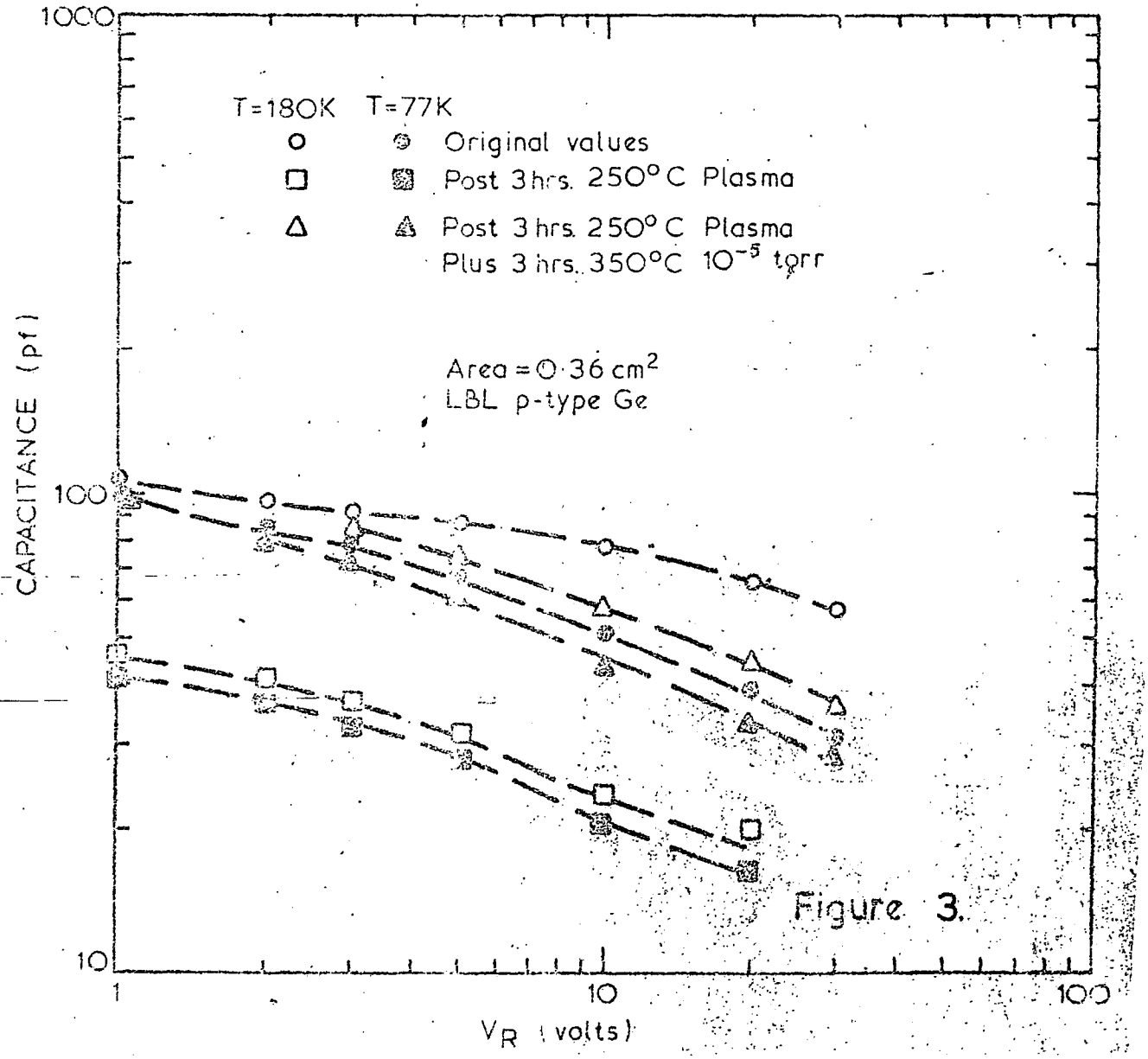
1000
100
10
1
10
100
CAPACITANCE (pf)
V_R (volts)
T=180K T=77K
Original values
Post 3 hrs. 250° C Plasma
Post 3 hrs. 250° C Plasma
Plus 3 hrs. 350° C 10^{-5} torr
Area = 0·36 cm²
LBL p-type Ge

Figure 3.

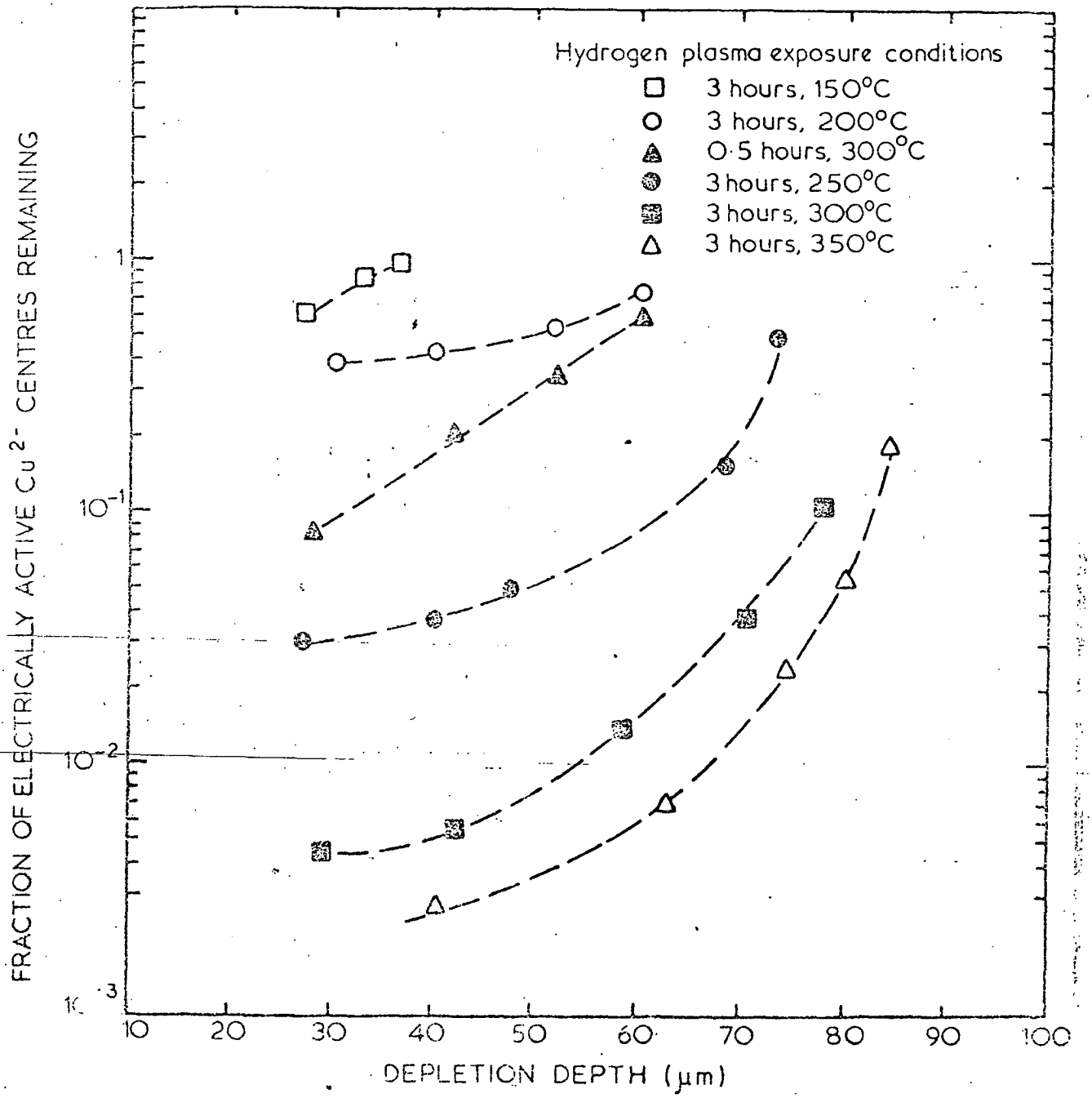
Hydrogen plasma exposure conditions
3 hours, 150°C
3 hours, 200°C
0·5 hours, 300°C
3 hours, 250°C
3 hours, 300°C
3 hours, 350°C
FRACTION OF ELECTRICALLY ACTIVE Cu 2- CENTRES REMAINING
1
10-1
10-2
10-3
10
20
30
40
50
60
70
80
90
100
DEPLETION DEPTH (μm)

FIGURE 4.

of output signals for small changes in bias pulse amplitude), large errors can be present in determining certain points. Only those points are shown on which reliance can be placed. The concentrations are accurate to ±30% and the distances to ±20%. The zero bias depletion depth, assuming a built-in bias of ∿0.2 V [Sze 1969] is between 18 and 40 μm for the range of samples used.

It is seen from Figure 4 that a 3 hour exposure at 300°C passivates 90% of the Cu^{2-} centres to a depth of ∿80 μm. Lower temperature exposures for the same time are less efficient, but still lead to a significant reduction in electrical activity of the acceptor level. The form of the concentration profiles will be related to the temperature dependence of the solubility and diffusion coefficient of hydrogen in Ge, and to the nature of the passivation mechanisms of the hydrogen with the ionized copper centre. Indeed, the hydrogen passivation of point defects may be a method of measuring the low temperature diffusion coefficients of hydrogen in semiconductor materials. For example, extrapolation to the original concentration of the 3 hours at 300°C exposure graph in Figure 4 would give an approximate H diffusion coefficient of 3.5×10^{-9} cm^2 s^{-1} at 300°C, i.e. diffusion depth = $(2D_H \times \text{diffusion time})^{\frac{1}{2}}$. At 430°C, Hall and Soltys [1978] have obtained a diffusion coefficient of $\sim 2 \times 10^{-8}$ cm^2 s^{-1}. Extrapolating the results of Frank and Thomas [1960], who measured the diffusion coefficient at 800 to 910°C and found a relationship of the form

$$D_H = 2.7 \times 10^{-3} \exp\left(- \frac{0.38}{kT} \right) \text{ cm}^2 \text{ s}^{-1} \quad ,$$

would give D_H (300°C) $= 1.2 \times 10^{-6}$ cm^2 s^{-1} .

It is likely that high temperature measurements cannot be extrapolated to lower temperatures because of much of the hydrogen being

in molecular form at lower temperatures [Hall and Soltys 1978]. In our measurement of the diffusion coefficient, errors are introduced because the sample is not quenched from the temperature of hydrogenation, so diffusion continues as the sample cools, and also because the hydrogen may actually have diffused further than the distance indicated by the copper passivation, without significantly neutralising copper centres over this 'tail' of hydrogen concentration.

Similar hydrogen passivation results were obtained with donor levels in n-type samples deliberately diffused with Pd or Ag. It is likely that passivation of many metal-related centres can be achieved Cu is obviously the most important. The passivation mechanism in the case of copper levels might be conversion to Cu-H_3, which is assumed to be neutral [Haller et al. 1977].

5.2 Gamma Radiation Defects in Ge

Gamma-induced defects were introduced into AAEC grown P- and As-doped n-type material (N_d-N_a = 4 x 10^{12} to 2 x 10^{14} cm^{-3}), Hoboken n-type material (N_d-N_a = 5 x 10^{13} cm^{-3}) and high-purity p-type Ge (N_a-N_d = 3 x 10^{10} to 7 x 10^{11} cm^{-3}) obtained from General Electric and Lawrence Berkeley Laboratory. p-type samples were prepared in the usual fashion with Li diffused (5 minutes, 250°C) contacts on one face and evaporated Pd contacts on the opposite face. n-type samples had GaIn eutectic alloy 'rub-on' ohmic contacts with Pd front contacts. Irradiations were performed in a 1.6 Mrad h^{-1} ^{60}Co facility; n-type material received a dose of 150 Mrad, the p-type material, 50 Mrad.

DLTS spectra are shown in Figure 5 from an n-type Hoboken sample containing the thermally stable deep donor level at E_c - 0.36 eV, after exposure to a H plasma for 3 hours at 150°C. Reduction in electrical activity of the donor centre was evident to depths of approximately 30 μm. The sample was then heated in the plasma for 4 hours at 350°C,

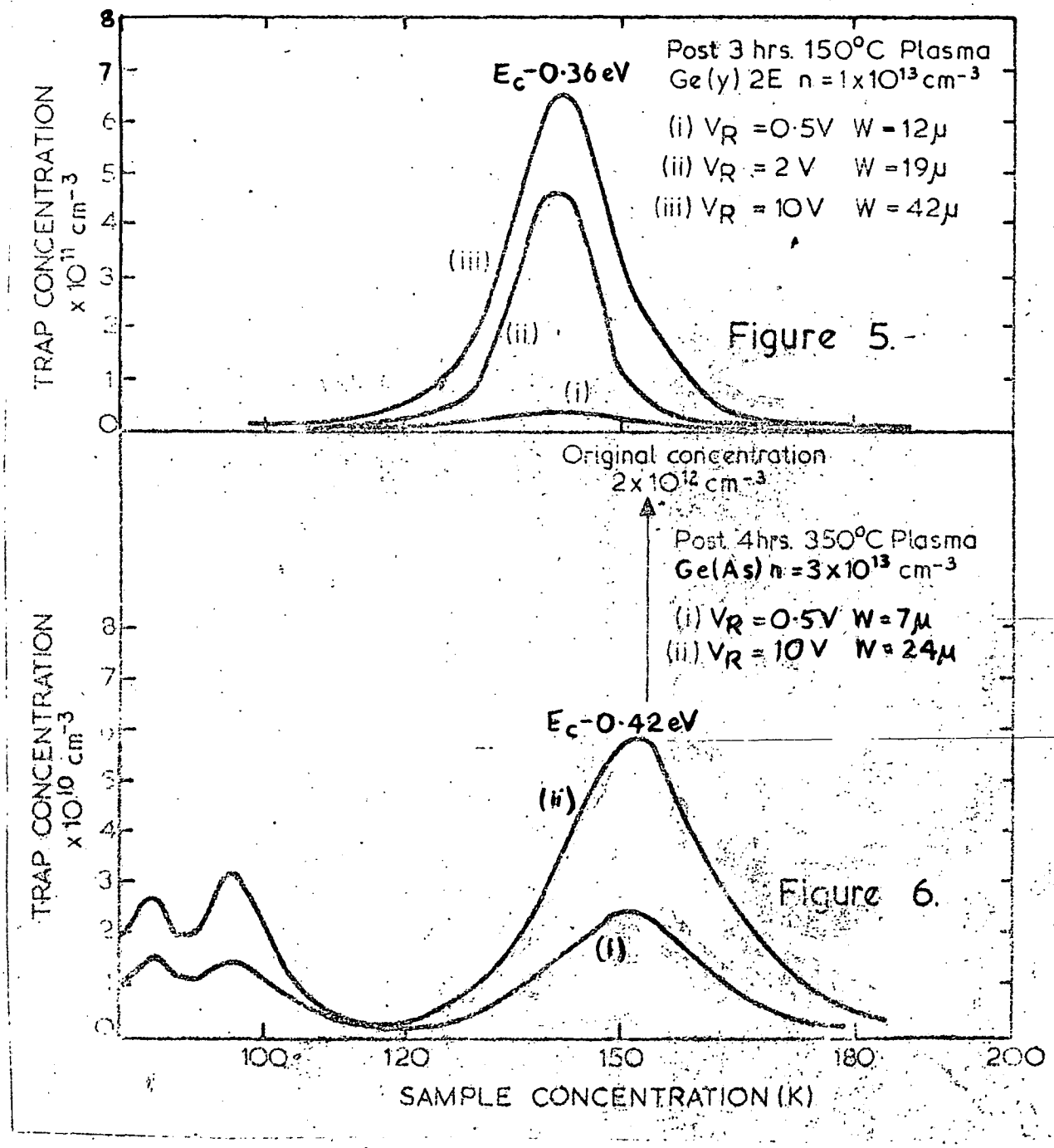

Figure 5.-

Figure 6.

neutralising the donor level to depths >80 μm. However, a vacuum anneal at the same temperature for 4 hours did not affect the sample. Possibly the hydrogen bonding to the donor defect is quite stable at these temperatures. A similar effect was seen with the E_c - 0.42 eV donor level in an As-doped sample (Figure 6). Hydrogenation for 4 hours at 350°C produced neutralisation of some of the donor levels, but vacuum annealing under the same conditions after hydrogenation did not affect the material.

Samples of General Electric and Lawrence Berkeley Laboratory material prepared with Li contacts and then irradiated also showed some neutralisation of the E_v + 0.23 eV and E_v + 0.38 eV acceptors after hydrogenation for 2 to 3 hours at 200°C, over and above the reduction due to thermal annealing (see Chapter 1). The fact that Li contacts were used on these samples and that the γ-induced centres start annealing at ∿200°C, precluded any further measurements on these levels.

5.3 Deep Donors in As-Grown GaAs

The GaAs used in this work was polycrystalline n-type bulk material obtained from Mining and Chemical Products (MCP) Electronics Ltd. (U.K.) The net electrically active donor concentration was measured to be 2.2×10^{16} cm^{-3} at 300 K by 1 MHz C-V measurements on Schottky diode structures. The diodes were fabricated by alloying GaIn eutectic to the rear surface of the sample and evaporating a 2 mm diameter Au barrier onto the previously polished and etched front surface. DLTS measurements revealed two donor defect states at E_c - 0.36 eV ($\sigma_n = 5 \times 10^{-15}$ cm^2) and E_c - 0.70 eV (σ_n ∿10^{-14} cm^2). A typical DLTS spectrum for this material is shown in Figure 7(a). The microscopic structure of the defects is unknown (Chapter 2), but measurements on sections of good crystallinity indicated no correlation with the presence of grain boundaries. The concentration profiles of these two

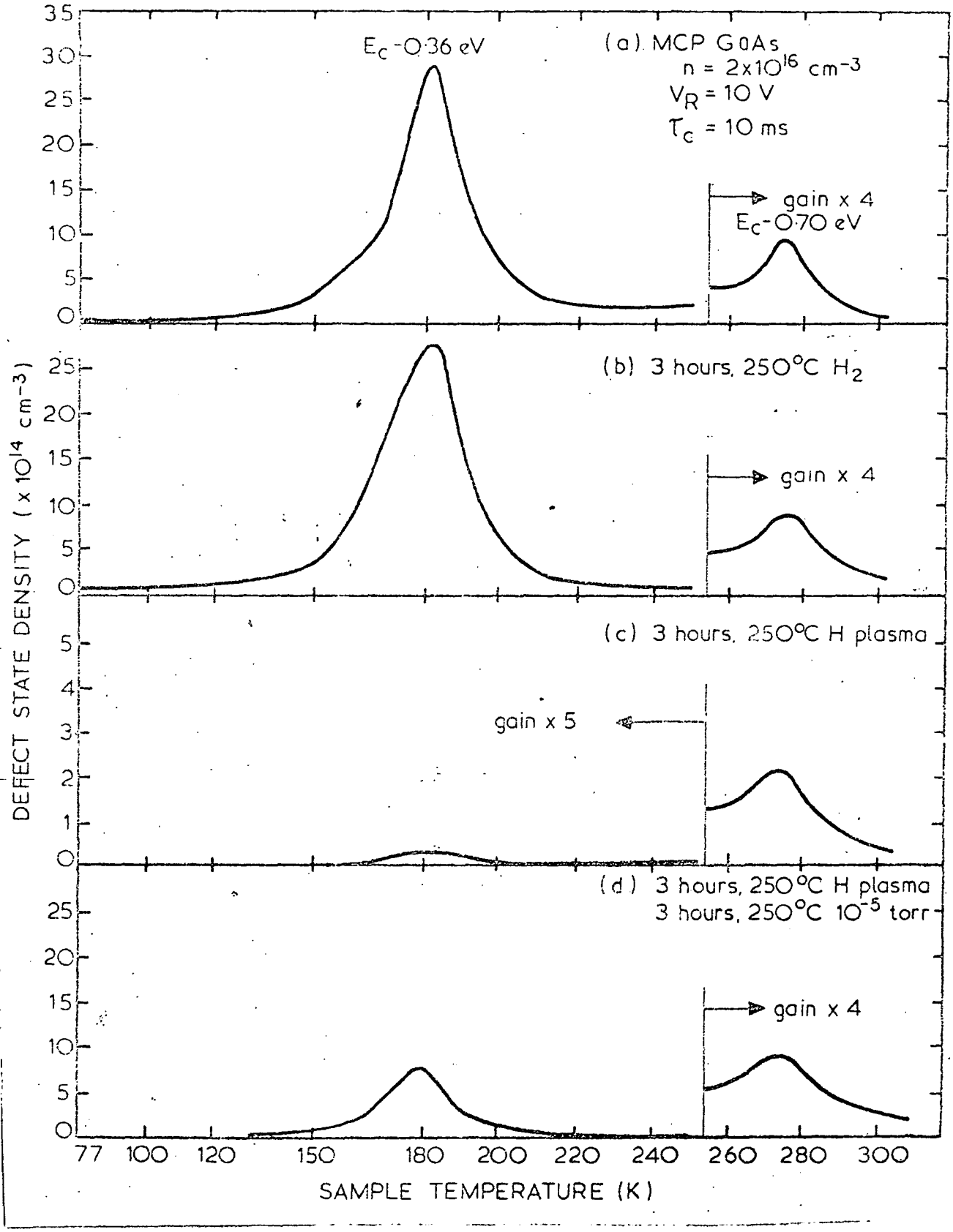
(a) MCP GaAs
n = 2x10^16 cm^-3
V_R = 10 V
τ_c = 10 ms
E_c - 0.36 eV
gain x 4
E_c - 0.70 eV
(b) 3 hours, 250°C H_2
gain x 4
(c) 3 hours, 250°C H plasma
gain x 5
(d) 3 hours, 250°C H plasma
3 hours, 250°C 10^-5 torr
gain x 4
DEFECT STATE DENSITY (x 10^14 cm^-3)
SAMPLE TEMPERATURE (K)
77 100 120 150 180 200 220 240 260 280 300

FIGURE 7.

defects were constant to a depth greater than 1.2 μm in the 12 samples used. The measurement depth was limited by diode breakdown at voltages in excess of ∿20 V.

Gold barriers were removed before heat treatments by soaking the samples in warm HCl acid; the rear contacts were marked during this procedure. Removal of the gold was necessary as Au is quite a fast diffusant in GaAs [Milnes 1973; Sze 1969]. The contacts were replaced after each heat cycle to allow testing on the DLTS system. Heating times of 0.5 to 3 hours at temperatures of 100 to 250°C were used.

Annealing in molecular hydrogen for any of the conditions used had no effect on the defect centres. Figure 7(b) shows the DLTS spectrum of a sample heated to 250°C for 3 hours. The spectrum conditions are the same as those used in Figure 1(a).

Heating in the H plasma, however, significantly reduced the density of electrically active E_c - 0.36 eV donor centres. Figure 7(c) shows the DLTS spectrum recorded for a sample heated to 250°C for 3 hours in the H plasma. Measurement of the net doping density at 300 K indicated that electrically active donor defects had been passivated, confirming the DLTS trace. Note that the E_c - 0.70 eV level showed no significant change in concentration. Annealing the sample at 250°C for 3 hours at a pressure of approximately 10^{-5} torr brought an increase in electrically active donor states again (Figure 7(d)). Bulk capacitance-voltage measurements again supported the evidence of the DLTS trace.

Plasma exposures for various times and temperatures were carried out. Figure 8 shows the concentration profile of the E_c - 0.36 eV centre, obtained from DLTS measurements for varying plasma conditions. Assuming a built-in bias of 1.35 V [Sze 1969], the zero bias depletion depth is 0.27 μm. A 3 hour exposure at the highest temperature used,

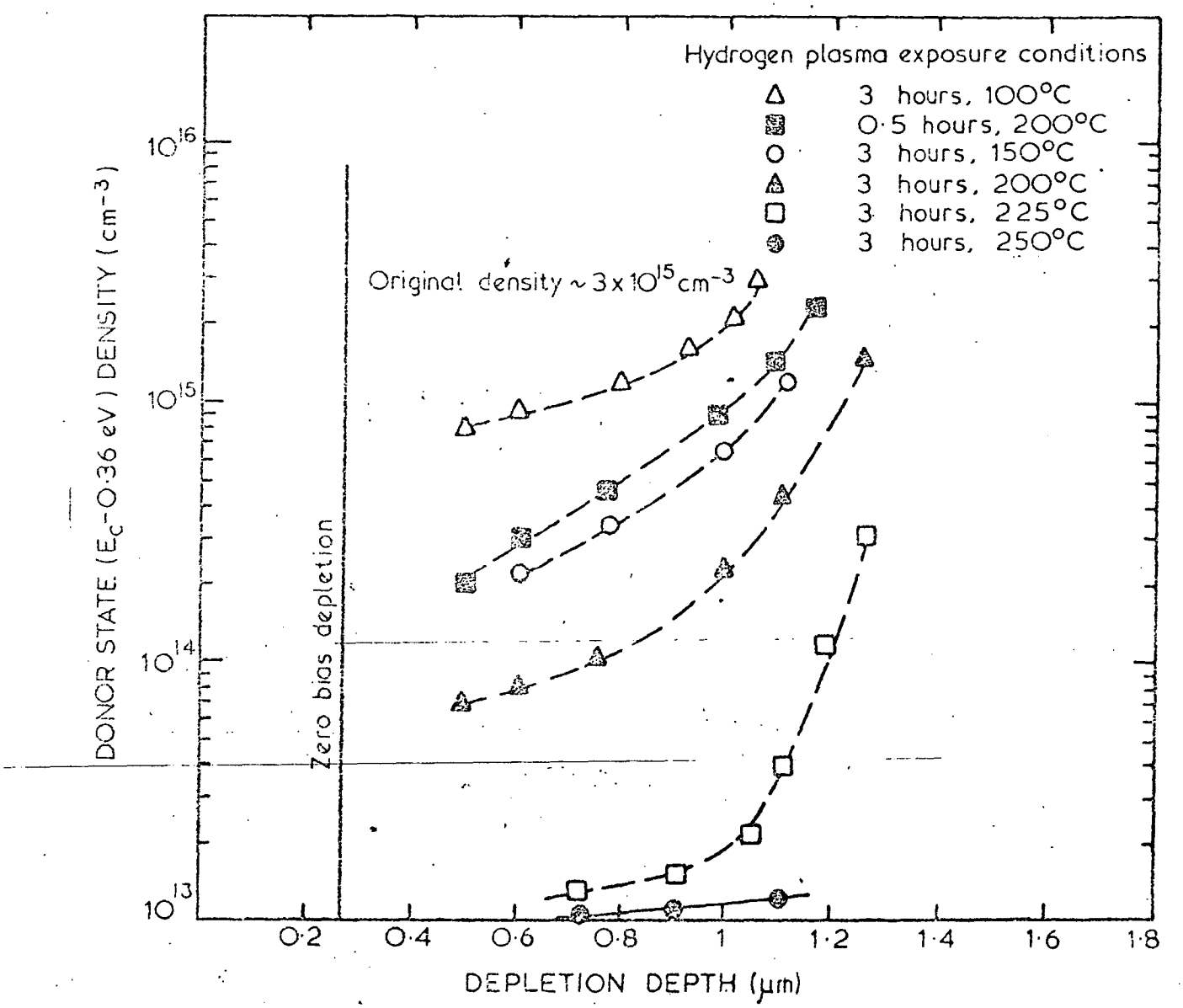
Hydrogen plasma exposure conditions
3 hours, 100°C
0·5 hours, 200°C
3 hours, 150°C
3 hours, 200°C
3 hours, 225°C
3 hours, 250°C
Original density ~ 3 x 10^15 cm^-3
Zero bias depletion
DONOR STATE (Ec-0·36 eV) DENSITY (cm^-3)
10^16
10^15
10^14
10^13
0·2
0·4
0·6
0·8
1
1·2
1·4
1·6
1·8
DEPLETION DEPTH (μm)

FIGURE 8.

250°C, passivated approximately 3 x 10^{15} donor defects cm^{-3} to distances greater than 1.1 μm. Lower temperature exposures for the same time were less efficient. Extrapolation of the 3 hours 225°C exposure graph to the original concentration would give an approximate H diffusion coefficient of 3 x 10^{-13} cm^2 s^{-1} at 225°C. At 100°C the corresponding number is ∿2.2 x 10^{-13} cm^2 s^{-1}, indicating the diffusion coefficient is not strongly temperature dependent at these low temperatures in GaAs.

DISCUSSION

The low temperature hydrogen passivation of defective bands related to point defects in semiconductor devices may be a useful technique for removing the effects related to these defects [Benton et al. 1980]. A note of caution might be added that not all electrically active defects appear to be amenable to passivation, as observed with the E_c - 0.70 eV donor centre here. It is likely that the microscopic structure of point defects will determine their susceptibility to neutralisation by hydrogen incorporation. Some defects may require higher temperature plasma treatments to overcome energy barriers to defect bonding, others may not be passivated at all at any temperature. In Ge the depth of passivation of Cu for example, is typically 100 μm for a 3 hour plasma exposure at 300°C. This depth may well be useful in device applications of hydrogen passivation. In GaAs, however, the hydrogen diffusion coefficient at the same temperature is much lower, and passivation of defects to depths of ∿1 μm for 3 hours at 250°C plasma exposures were observed. As with the initial flush of enthusiasm with laser annealing of semiconductors, it is more than likely that hydrogen passivation of defects will not be all things to all applications, but rather a useful tool in certain areas, both for devices and for basic physics, where incorporation of hydrogen might lead to families of defects being discovered (e.g. X-H, $X-H_2$, $X-H_3$ where X is a defect of some description)

or new understandings of defect complex formation and the bonding involved. DLTS measurements are not sufficient in these areas and more specific tools are needed, such as piezospectroscopy [Haller 1978] to observe, for example, isotopic shifts in the energy levels of these centres. No extra defects were observed in these experiments, but further work along these lines should prove useful in delineating the useful areas of hydrogenation of bulk semiconductors.

REFERENCES

Alexiev, D. [1981] - unpublished

Benton, J. L., Doherty, C. J., Ferris, S. D., Flamm, D. L., Kimerling, L. C. and Leamy, H. J. [1980] - Appl. Phys. Lett. 36:670.

see for example, Evwarage, A. O., Hall, R. N. and Soltys, T. J. [1979] - IEEE Trans. Nucl. Sci. 6(1)271

Frank, R. C. and Thomas, J. C. [1960] - J. Phys. Chem. Solids 16:144.

Hall, R. N. and Racette, J. C. [1964] - J. Appl. Phys. 35:379.

Hall, R. N. and Soltys, T. J. [1978] - IEEE Trans. Nucl. Sci. 25(1)385.

Haller, E. E. [1979] - Defects and Radiation Effects in Semiconductors, 1978, Inst. Phys. Conf. Series No. 46, p205 (1979).

Haller, E. E., Hubbard, G. S. and Hansen, W. L. [1977] - IEEE Trans. Nucl. Sci. 24(1)48.

Haller, E. E., Li, P. P., Hubbard, G. S. and Hansen, W. L. [1979] - IEEE Trans. Nucl. Sci. 26:265.

Lang, D. V. [1974] - J. Appl. Phys. 45:3023.

for a review of the properties of Cu in Ge see Milnes, A. G. [1973] - Deep Impurities in Semiconductors (Wiley-Interscience, New York) p. 40.

Pankove, J. I. and Carlson, D. E. [1980] - Ann. Rev. Mater. Sci. 10:43.

Pankove, J. I., Lampert, M. A. and Tarng, M. L. [1978] - Appl. Phys. Lett. 32:439.

Quist, T. M. [1968] - Proc. IEEE 56:1212.

Seagher, C.H. and Ginley, D. S. [1979] - Appl. Phys. Lett. 34:337.

Sze, S. M. [1969] - Physics of Semiconductor Devices (Wiley-Interscience, New York) pp.87-90.

Teich, M., Keys, R. J. and Kingston, R. H. [1966] - Appl. Phys. Lett. 9:357.

Williams, R. L. [1969] - J. Appl. Phys. 40:2932.

Woodbury, H. H. and Tyler, W. W. [1957] - Phys. Rev. 105:84.

CHAPTER 6

MISCELLANEOUS

6.1 SHALLOW LEVEL SPECTROSCOPY OF IMPURITIES IN SEMICONDUCTORS

SUMMARY

A method is described, based on transient conductance measurements, which allows the observation of shallow level impurities in a semiconductor. The technique involves a modified DLT capacitance spectroscopy system operating in the conduction mode, with an infrared LED used to disturb the equilibrium population of the ionized shallow impurities. The method has been confined to silicon at present, but in principle can be extended to other semiconductor detector materials, provided the carrier freeze-out temperature can be reached at the sample.

INTRODUCTION

Typically, the characterisation of shallow level impurities in semiconductors has been the domain of Hall measurements, the various forms of luminescence and, more recently, infrared spectroscopy, particularly far infrared photoconductivity. The shallow level population determines the conductivity type and general properties of the semiconductor, and in recent years it has become possible (at least in Ge) to produce material with very low net impurity concentrations ($<10^{10}$ cm^{-3}). Because of this, the characterisation and control of deep level impurities has increased in importance through their acting as generation-recombination centres or carrier traps.

A significant advance in deep level impurity detection has been the introduction of the sensitive DLTS technique [Lang 1974]. We detail the extension of this technique to the observation of shallow level impurities in semiconductors, confined at present to n-type Si, but in principle applicable to any other material.

EXPERIMENTAL PROCEDURE

The DLTS system is converted to the conductance mode, basically by adding phase to the RF test device signal so that the capacitance

bridge is observing transient conductance [Williams et al. 1980]. Samples are prepared with two ohmic contacts after the standard cutting, lapping and etching procedures.

In this experiment, only n-type Si was used (Table 1) with resistivities ranging from 200 Ω cm to 90 kΩ cm. The material was produced by three manufacturers, Wacker-Chemie, Dow Corning and Merck, and was phosphrus-doped in all cases. Contacts were formed by evaporating Li onto opposite faces of a slice and diffusing for 15 minutes at 350^{o}C. Slight lapping was necessary of the first diffused contact after the second diffusion had taken place in order to 'catch-up' with the rapidly diffusing lithium.

The Boonton meter was approximately balanced at room temperature by addition of a suitable resistance to the differential arm of the bridge and was used on the most sensitive range allowable for the test device. The range available is 160 Ω to 160 kΩ.

The pulsing waveform sequence is shown in Figure 1. The LED injects free carriers into the sample which are then available for trapping by defect centres. A bias pulse slightly longer than the LED pulse extracts the excess free carriers from the sample. The conductivity of the sample rises rapidly on injection of the free carriers, but after completion of the LED pulse some of the traps are now filled and the conductivity of the sample has decreased below its original value (i.e. its resistance has increased). As the trapped free carriers are thermally emitted to the appropriate band, the conductivity of the sample recovers exponentially back to its original value. The correlator delays its cross-correlation (via the holding time control) until after the initial transient caused by the trap loading process. The correlator output is at maximum when the trap emission rate is coincident with that set by

TABLE 1: SILICON USED IN THIS EXPERIMENT

Manufacturer	Resistivity (Ω cm)
Wacker-Chemie	200-300
Dow Corning	400
Wacker-Chemie	800
Wacker-Chemie	1000
Merck	3000
Dow Corning	3000
Wacker-Chemie	3500-6500
Wacker-Chemie	13000
Wacker-Chemie	20000
Wacker-Chemie	90000

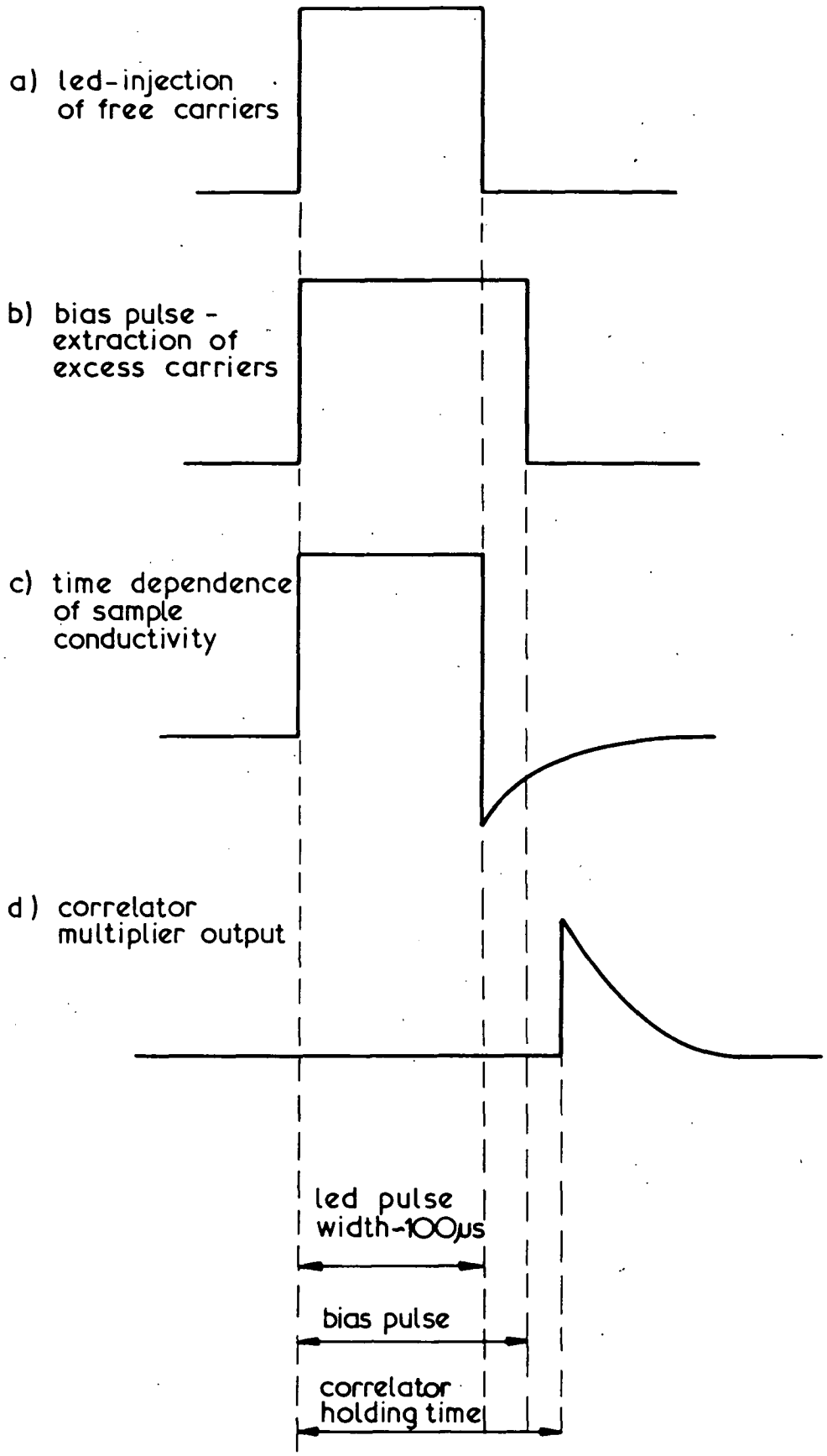

FIG.1 PULSING WAVE FOR TRANSIENT CONDUCTANCE SHALLOW IMPURITY DETECTION METHOD

the weighting function control. Note that there is no standing bias applied to the sample.

The sample temperature is scanned from ambient to below the carrier freeze-out point; in the case of Si, 30 to 50 K. The sample cryostat and the experimental apparatus have been described previously [Williams et al. 1980].

RESULTS

Figures 2 and 3 display the transient conductance spectra from a variety of samples and include a thermally stimulated conductance run (Figure 4) for comparison. The spectroscopic nature of the correlation technique is obvious. The spectra obtained were obviously quite similar in all cases, because all the samples were P-doped with Li contacts. The best values for the impurity activation energies obtained were E_c - 38 meV for the Li level and E_c - 48 meV for the P level. These compare to the theoretical value of 33 meV and 44 meV respectively [Geballe 1959], and to the experimentally measured values (using trapping-detrapping pulse rise time measurements and Hall effect results) of 31 mev and 44 meV respectively [Martini and McMath 1970; Sze and Irwin 1968].

It must be noted that the Arrhenius plots for the levels displayed in Figure 5(a) are the best obtained and that, in general, the experimental points showed quite a deal of deviation from linearity. One of the problems is that accurate control of the heating and cooling rate of the sample is very difficult at the low temperatures needed. This is true because the rate of cooling increases more rapidly as the temperature is lowered and manual control cannot maintain an even rate over one run, or a homogeneous rate over a set of runs. (The cooling and heating rate, of course, affect the hysteresis of the sample temperature compared to the thermocouple output and different

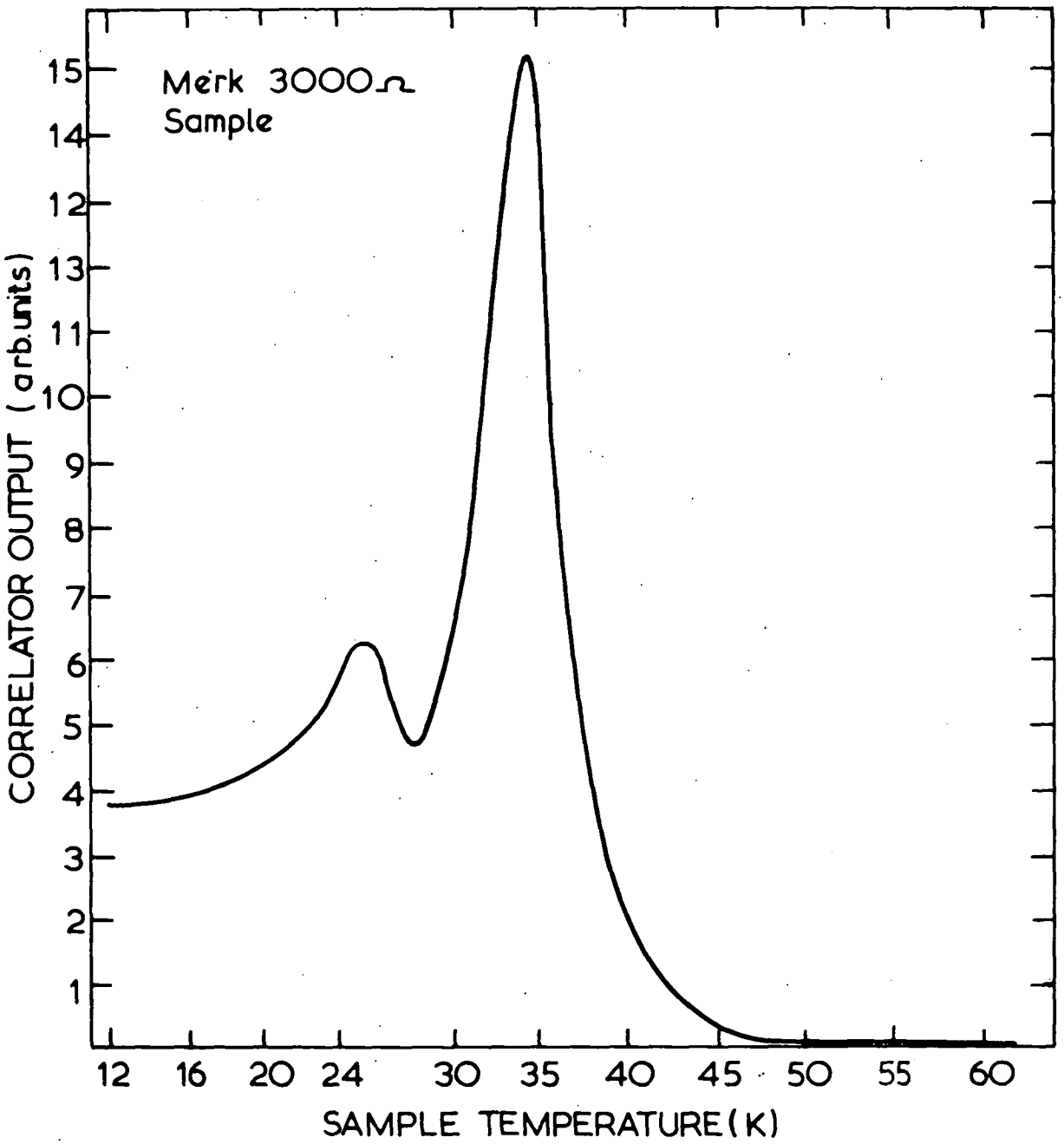
Merk 3000Ω
Sample
CORRELATOR OUTPUT (arb.units)
15
14
12
13
11
10
9
8
7
6
5
4
3
2
1
12
16
20
24
30
35
40
45
50
55
60
SAMPLE TEMPERATURE (K)

FIGURE 2

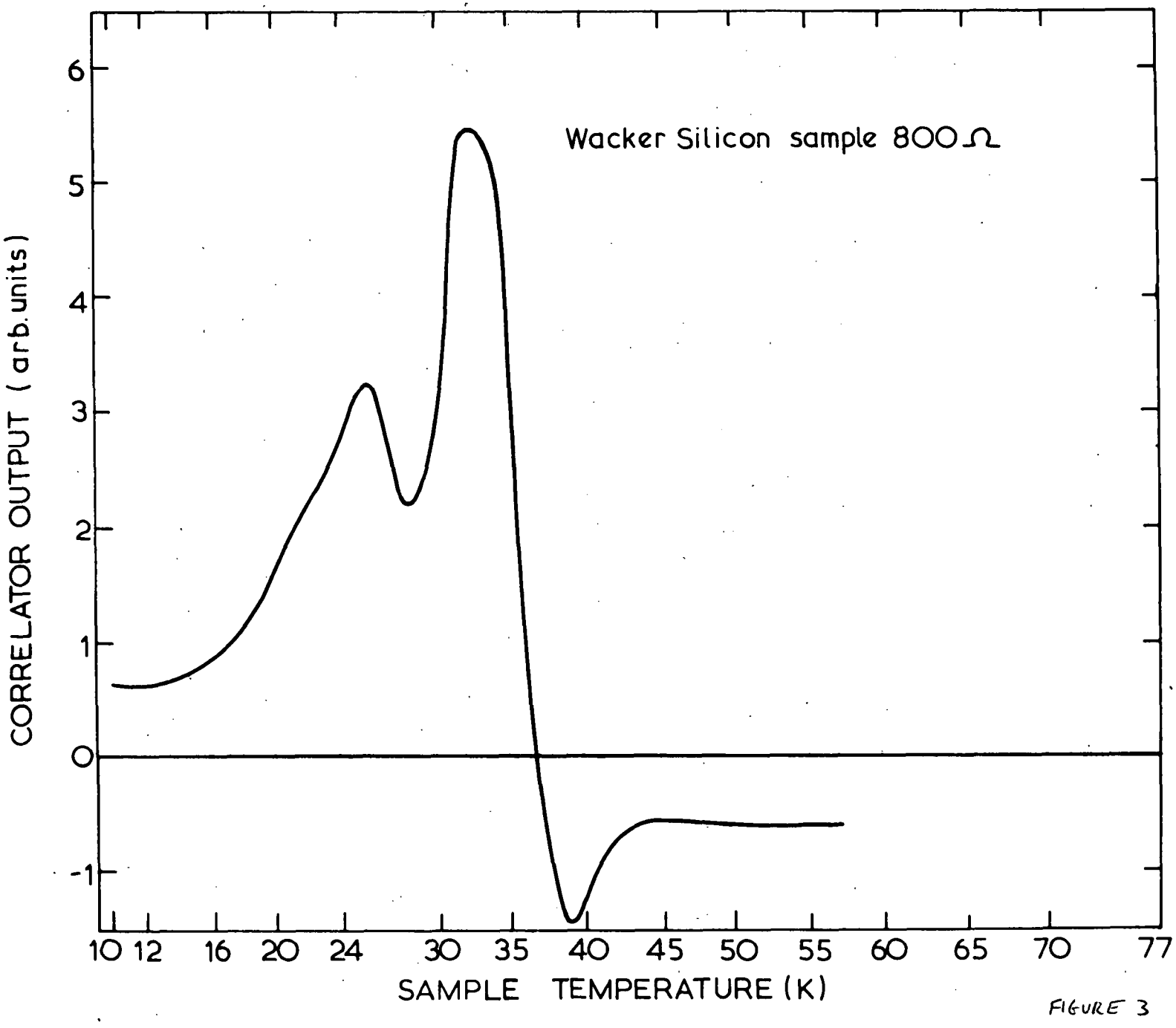
Wacker Silicon sample 800Ω
CORRELATOR OUTPUT (arb. units)
6
5
4
3
2
1
0
-1
10 12 16 20 24 30 35 40 45 50 55 60 65 70 77
SAMPLE TEMPERATURE (K)

FIGURE 3

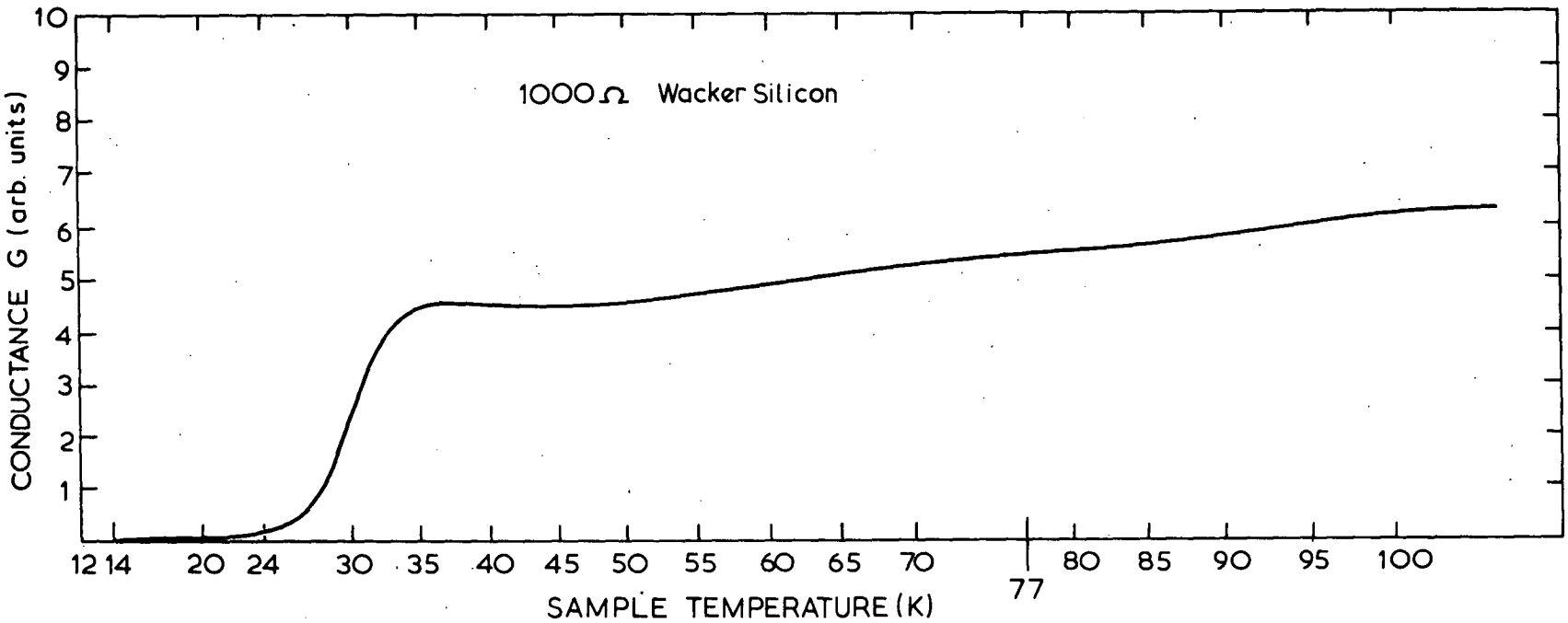

FIGURE 4 THERMALLY STIMULATED CONDUCTANCE SCAN OF 1KΩ SAMPLE

heating and cooling rates displace the peak from its mean position by a different amount.)

Capture cross sections were obtained from the intercept of the Arrhenius plot and were invariably $\sim 10^{-14}$ cm^2 for both donor impurities. This compares to the value of 1.5×10^{-13} cm^2 for the shallow impurities in Si obtained by Martini and McMath [1970] and Mayer et al. [1970]. A semi-quantiative direct measurement was made of the Li level (Figure 5(b)) by measuring the dependence of correlator output on LED pulse width for maximum LED intensity (400 mA pulse). However, the signal was not saturated at this value and an array of LEDs would be needed to achieve a more uniform illumination of the sample. The calculation also requires a knowledge of the number of carriers injected into the sample by the LED and it is difficult to determine this in a simple way. By comparison of the bulk conductivity with and without the LED on, a very approximate value of 10^{10} carriers cm^{-3} was obtained and, using this, the direct measure of cross section was $\sim 3 \times 10^{13}$ cm^{-3}. No allowance was made for recombination of the injected free carriers.

The concentration of the levels is also not possible to obtain in a simple way, but should come from the resistivity of the sample in any case. If one could obtain uniform illumination of the sample and saturation of the traps, then an approximate method might be as follows:

1. Measure the bulk conductance G of the sample at the peak temperature from the Boonton meter or by a simple d.c. voltage current reading, knowing the sample area and thickness.
2. Measure ΔG at the peak temperature from the CRO screen (monitoring the Boonton output), having calibrated the display in resistance or conductance units per division. Thus $\Delta G/G$ is known.

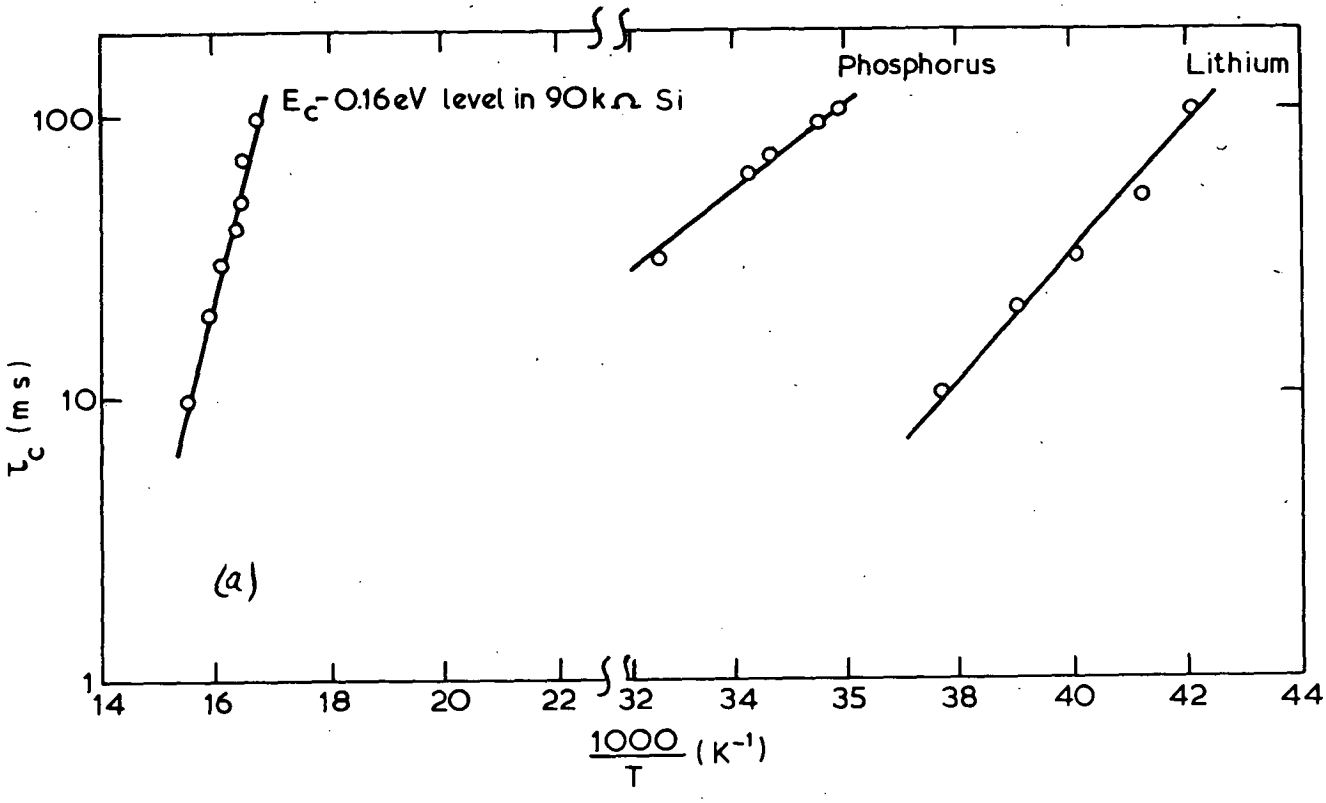

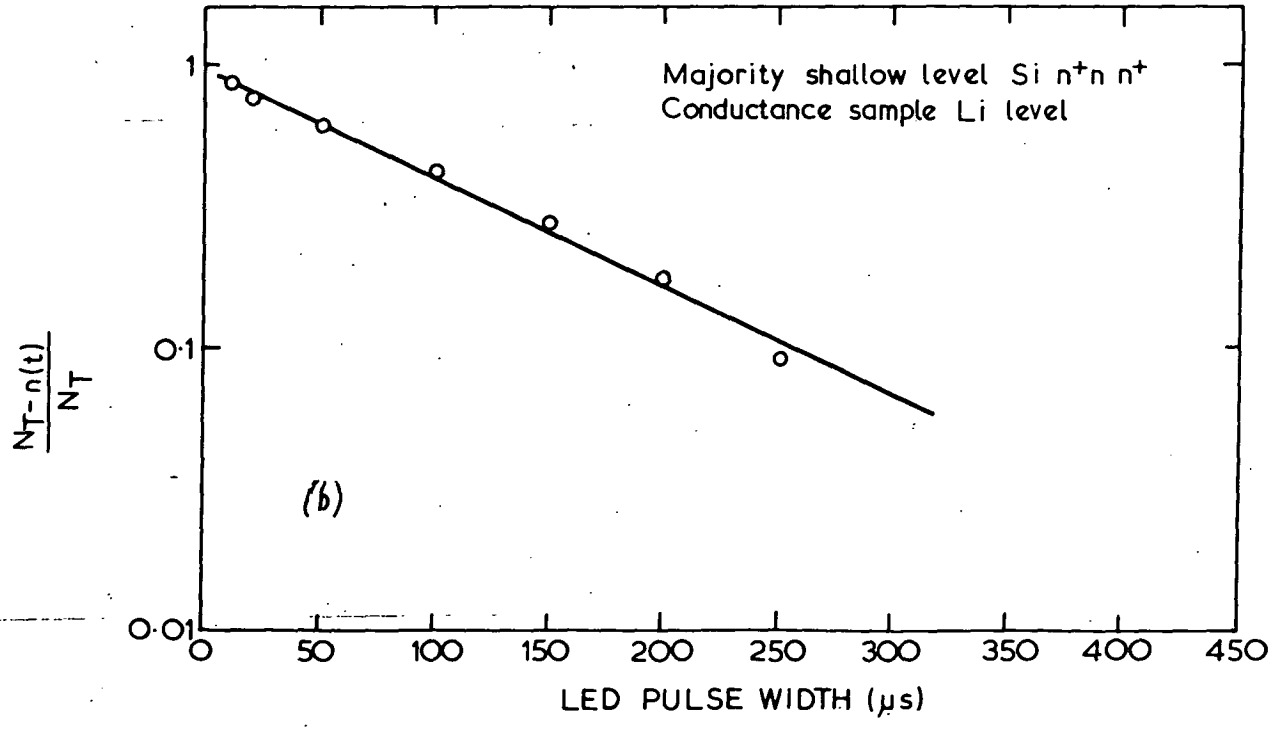

FIGURE 5. (a) Arrhenius plots for three of the levels observed.
(b) Relative correlator output versus LED pulse width for lithium level - data used to estimate cross-section.

3. From μ vs T curves, obtain the injected carrier density from the equation

$$\Delta G = e\Delta n\mu_n + e\Delta p\mu_p$$

$$= e\Delta n(\mu_n+\mu_p)$$

assuming electrons and holes are introduced in equal numbers. Then

$$N_T = \frac{\Delta G}{G}\Delta n$$

for the condition that there is complete saturation of the traps by the injected carriers.

Clearly, the assumptions and experimental uncertainties included above mean that the method is not accurate enough to displace current methods of shallow level impurity detection. The method would appear to be accurate to only ∿10 meV with very careful control of the heating and cooling rates, though this is not vastly different to the accuracy of the Hall system formerly used by the AAEC Semiconductor Radiation Detector Group [Lawson, private communication].

The common acceptor level centre observed had an activation energy estimated as E_v + 50 meV. It is not identified, but may be contaminating boron (theoretical activation energy E_v + 45 meV [Geballe 1959; Sze and Irvin 1968]). A donor level at E_c - 0.16 eV with a cross section of 7 x 10^{-14} cm^2 was also observed in the 90 kΩ sample. This is important, as its effect extends past 77 K, where X-ray detectors made from this material operate. The level is not identified and, in fact, because of its broadness, may actually be several levels that are not resolved. It appears too low in temperature to be the oxygen-vacancy level, E_c - 0.17 eV. The spectrum is shown in Figure 6.

The fractional resolution (FWHM) of the donor peaks in Figure 2 was $\Delta T/T$ ∿0.13, i.e. ΔT ∿4 K at T = 30.3 K. This translates to

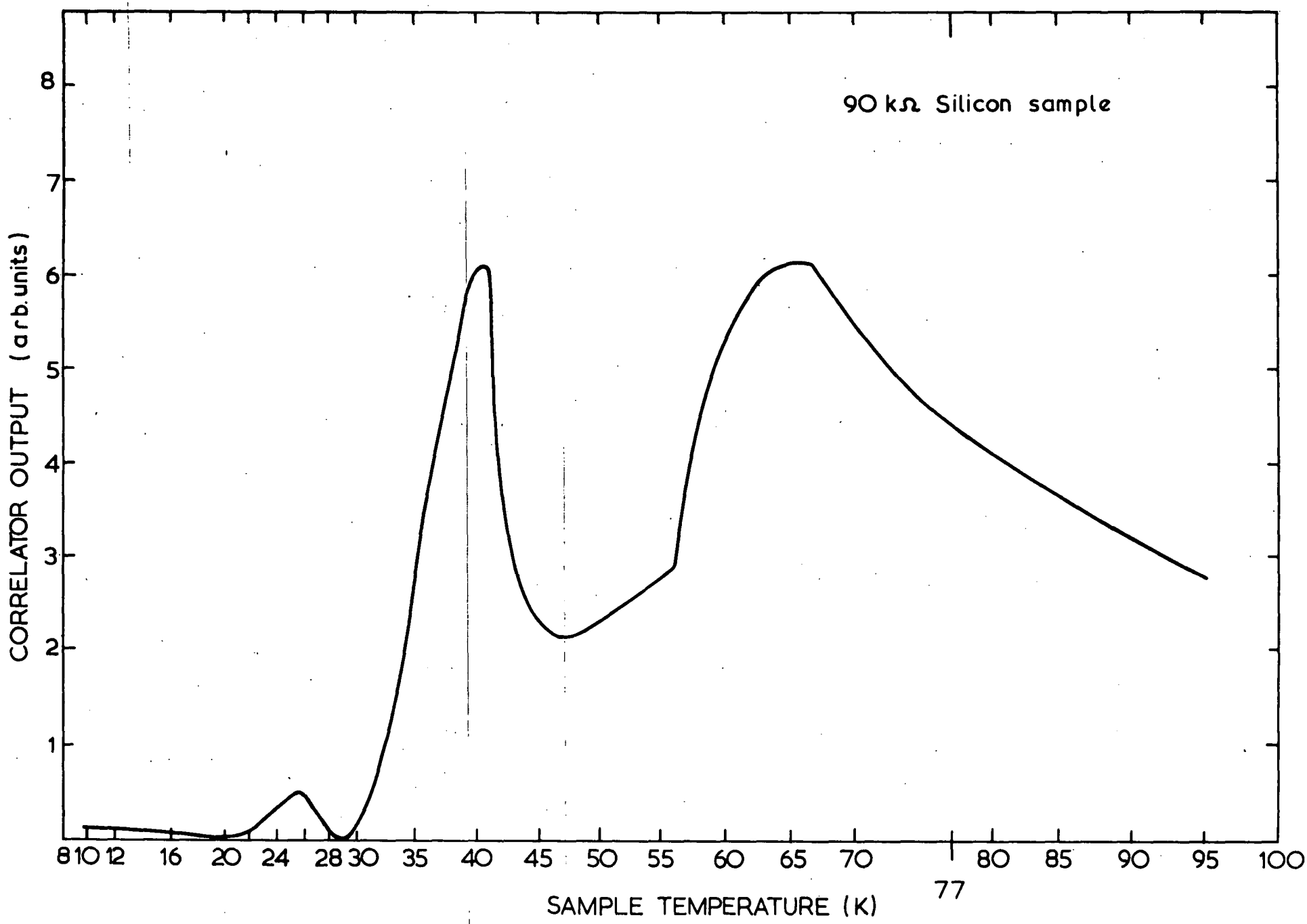
90 kΩ Silicon sample
CORRELATOR OUTPUT (arb.units)
1
2
3
4
5
6
7
8
8 10 12 16 20 24 28 30 35 40 45 50 55 60 65 70 77 80 85 90 95 100
SAMPLE TEMPERATURE (K)

FIGURE 6.

$\Delta E \sim 6.2$ meV at E = 48 meV.

CONCLUSIONS

What can we get from the shallow level detection method?

1. The trap activation energy, accurate to ±5 meV with careful control of the heating and cooling rates.
2. The trap capture cross section from the intercept of the Arrhenius plot.
3. An approximate concentration knowing the resistivity of the sample. Note that defects cannot be profiled in the conduction mode of operation.

The difficulty for materials other than Si will be to reach the carrier freeze-out temperatures and to control the heating and cooling rates at these temperature (<10 K). The shallow level activation energies for Ge are $\sim$12 meV and for GaAs are $\sim$6 to 9 meV. In principle, however, the information contained in (1), (2) and (3) is possible to obtain for these other materials.

REFERENCES

Geballe, T. H. [1959] - Semiconductors, ed. N.B. Hannay (Reinhold, New York), Ch. 8.

Lang, D. V. [1974] - J. Appl. Phys. 45:3014.

Martini, M. and McMath, T. A. [1970] - Nucl. Instr. and Meth. 79:259.

Mayer, J. W., Zanio, K. R., Martini, M. and Fowler, I. L. [1970] - IEEE Trans. Nucl. Sci. 17(3)221.

Pearton, S. J., Tavendale, A. J. and Williams, A. A. [1980] - AAEC report E504.

Sze, S. M. and Irvin, J. C. [1968] - Solid State Electron. 11:599.

Williams, A. A., Pearton, S. J. and Alexiev, D. [1980] - AAEC/TN147.

6.2 A SEARCH FOR MAGNETIC FIELD EFFECTS ON DEEP LEVEL DEFECTS

SUMMARY

The deep level transient spectroscopy technique was used to search for the effects of strong magnetic fields on deep level defects in three semiconducting materials, Ge, Si and GaAs. The defects were either present in the as-grown material (GaAs), formed by long-term annealing (Ge) or introduced by ^{60}Co γ-ray or 14.7 MeV neutron irradiation (Ge and Si). No effect on any 'normal' defect energy level or cross section was observed for axial magnetic fields up to 1.8 kG. However, in the VPE n-GaAs the E_c - 0.62 eV level, which displays electric field enhanced emission, has proved extremely sensitive to external magnetic fields.

INTRODUCTION

Semiconductor detectors must often be operated in the presence of strong magnetic fields, particularly in experiments involving charged particle beams [Byrne et al. 1970]. Marked deterioration of energy resolution may occur at fields of 3 x 10^4 G for Ge(Li) detectors and 6 x 10^4 G for Si surface barrier detectors operating at room temperature [Ganner and Rauch 1969]. Various temperature and magnetic field strength dependencies have been investigated for such detectors [Kiegle and Weber 1975; Byrne et al. 1974]. Strong magnetic fields cause the mean collection paths of free carriers to be increased in length and thus, being in the vicinity of trapping and recombination centres for a longer time, there is an increased chance of the carriers being lost to the output pulse. Carriers diverted to the surface may also be lost by recombination processes [Byrne et al. 1970].

All previous investigations of magnetic field effects have been performed using actual radiation detectors, hoping to observe changes in energy resolution due to enhanced trapping of free carriers. The

high frequency capacitance (or conductance) transient thermal scanning method (DLTS) allows the direct observation of individual trapping levels in semiconducting materials and thus is uniquely suited to the measurement of enhanced carrier capture. One might expect that by effectively increasing the cross section of deep level impurities, their detrapping time constants would increase, shifting the DLTS peak to lower temperatures. It is worth noting that because of the non-hydrogenic hehaviour of deep level impurities, theories relating to shallow level impurities cannot be extrapolated to the higher activation energies.

EXPERIMENTAL

This first investigation to directly observe the enhanced trapping at high magnetic fields was performed using the DLTS system described previously [Williams et al. 1980]. A solenoidal coil produced an axial field of 1.8 kG at the sample (Figure 1). The magnet calibration has been measured previously at 95.04 G/amp [Lawson, private communication].

Table 1 lists the Si, Ge and GaAs samples for investigation and the reasons for their choice. The defects were introduced by three separate methods: being present in the as-grown material, caused by irradiation (γ-ray or neutron), long-term room temperature annealing.

RESULTS

The DLTS measurements were performed in the usual way, either in capacitance or conductance mode (for the Si FET). The samples were scanned with no magnetic field operating and the resulting spectra compared to that for a field of 1.8 kG present. Representative spectra are displayed in Figure 2 for the Si FET, Figure 3 for the neutron damaged Ge and Figure 4 for the bulk GaAs. No peak shift or enhancement in these 'normal' defects is evident, nor have any additional

Fig. 1 SCHEMATIC OF EXPERIMENTAL SET-UP

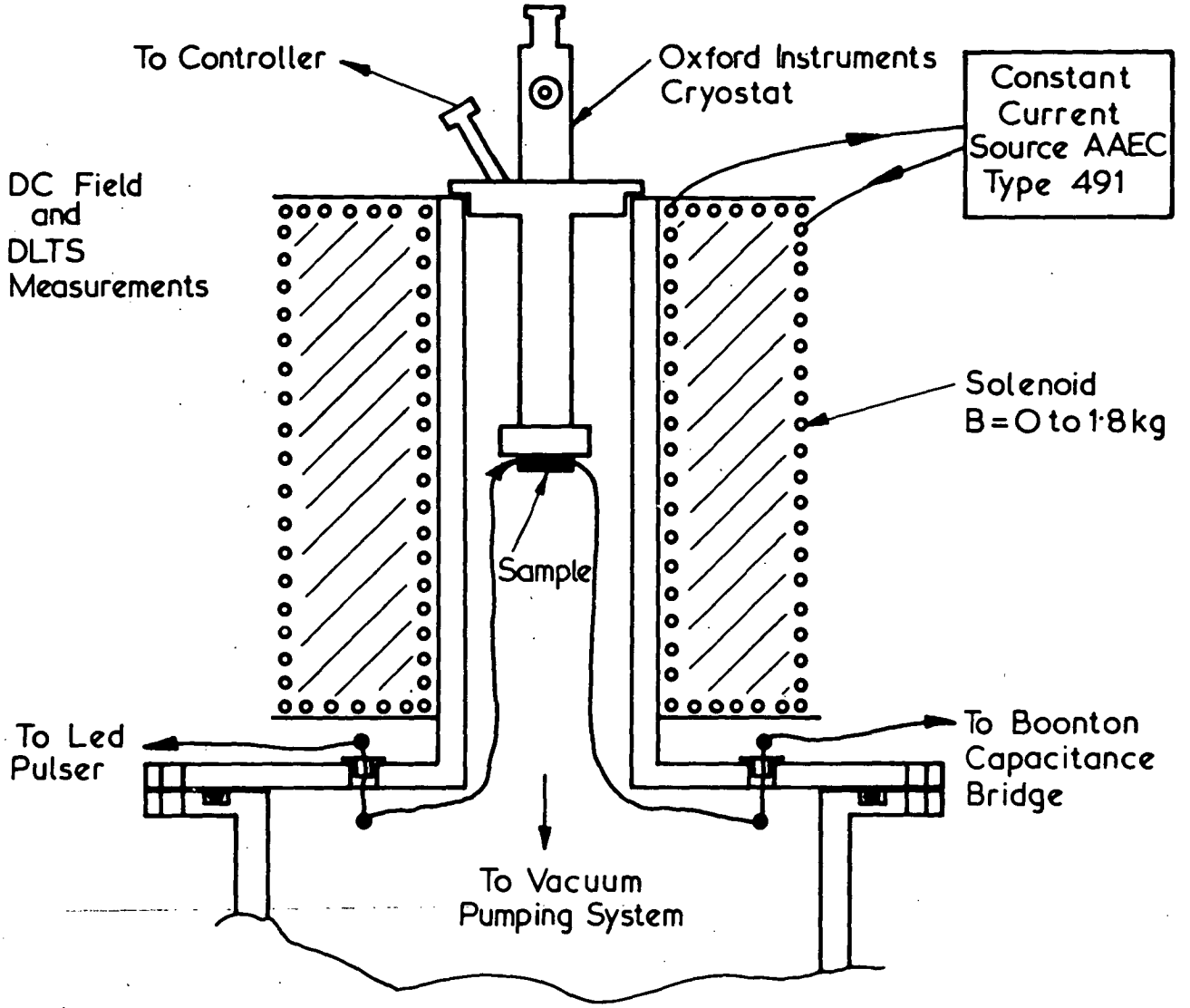

AC Field

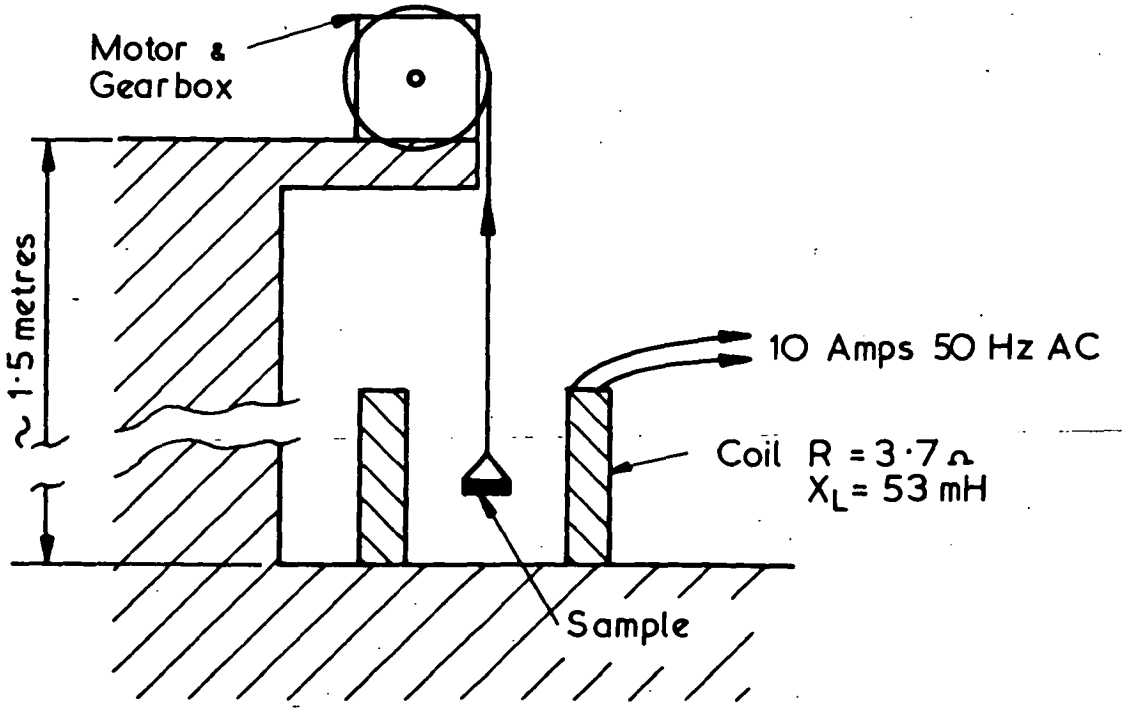

Fig. 2 DLTS SPECTRA FOR BULK GaAS

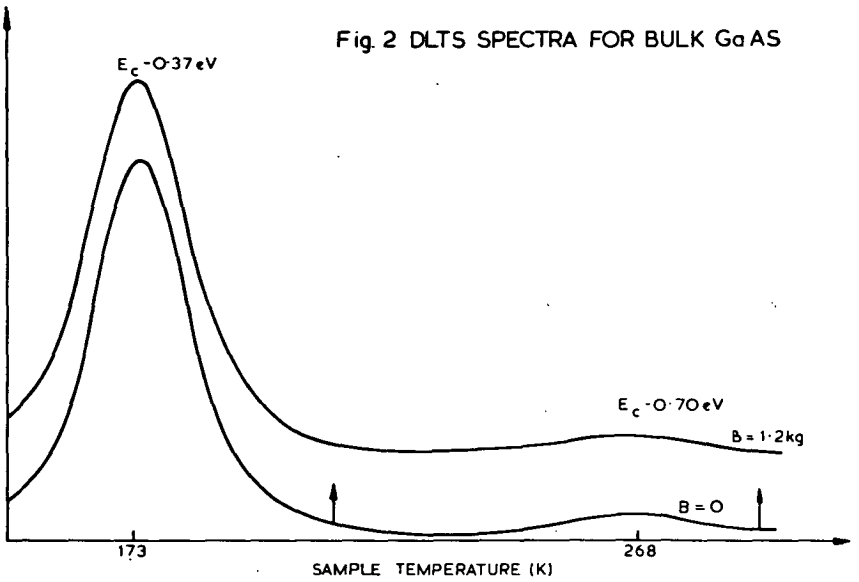

Fig. 3 DLTS SPECTRA FOR Si FET

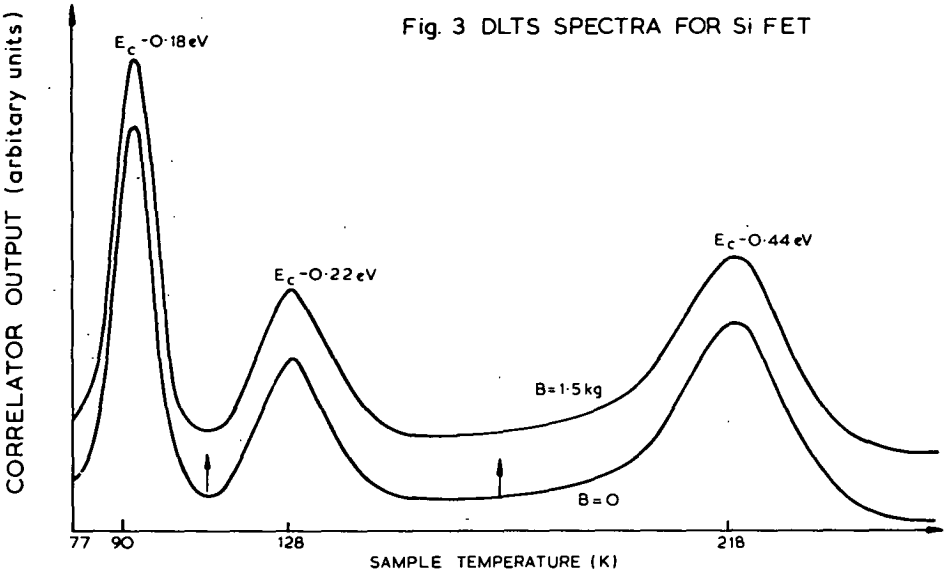

Fig. 4 NEUTRON DAMAGED Ge

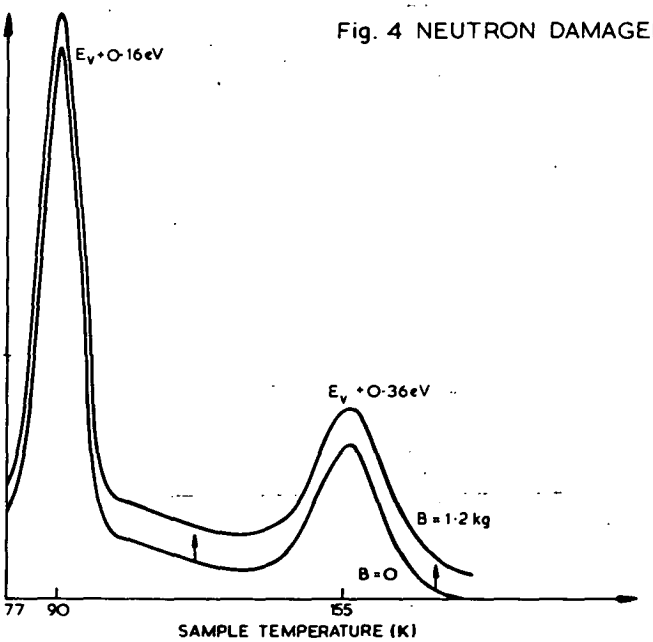

TABLE 1 LIST OF SAMPLES USED

SAMPLE	DEFECT SOURCE	N_T (cm^{-3})	DEFECT(eV)	COMMENTS AND AIMS
Ge 78-48-4 $n = 1.2 \times 10^{13}$ cm^{-3} (165K)	γ- Irrad 150 MRd	8×10^{8} 2×10^{10} 2×10^{12}	E_V + 0.12 E_V + 0.24 E_C - 0.42	To observe effect on deep acceptors and donors
Ge 78-48-3 $n = 1.3 \times 10^{13}$ cm^{-3} (160K)	γ- Irrad 160 MRd	3×10^{12} 3×10^{12} 2×10^{12} 4×10^{11}	E_V + 0.31 E_V + 0.36 E_C - 0.30 E_C - 0.44	Defect spectrum charge state dependent
Ge 78-8-6(RICH) $p = 2.4 \times 10^{13}$ cm^{-3} (77K)	γ- Irrad 150 MRd	2.9×10^{12} 1.3×10^{12}	E_V + 0.23 E_V + 0.38	To observe effect on deep acceptors
Ge 78-8-6 (POOR) $p = 10^{13}$ cm^{-3} (77K)	Neutron-Irrad 1.5×10^{8} n/cm^2	3×10^{10} 7×10^{10} 8×10^{10}	E_V + 71meV E_V + 0.16 E_V + 0.36	To observe effect on neutron damage levels
Ge(γ)2E $n = 9.9 \times 10^{12}$ cm^{-3} (77K)	Long-Term R.T. annealing	1×10^{12} 1×10^{12} 2×10^{12}	E_C - 0.36 E_C + 0.36 E_V + 0.33	To observe effect on stable donor
Ge 77-85-4 $n = 2.4 \times 10^{10}$ cm^{-3} (77K)	γ- Irrad 150 MRd	10^{9} 9×10^{9} 2×10^{11}	E_V + 0.20 E_V + 0.28 E_C - 0.46	To observe effect on deep donor
GaAs MCP Bulk $n = 1.2 \times 10^{16}$ cm^{-3} (77K)	As-Grown	3×10^{15} 2×10^{14}	E_C - 0.37 E_C - 0.70	To observe effect on donors in As-Grown matl.
GaAs MIT VPE $n = 1 \times 10^{14}$ cm^{-3} (300K)	As-Grown	4×10^{11} 2×10^{11} 5×10^{11}	E_V + 0.18 E_V - 0.36 E_C - 0.40	To observe effect on Poole-Frenkel defects

(CONTINUED)

TABLE 1 LIST OF SAMPLES USED (CONT'D.)

SAMPLE	DEFECT SOURCE	N_T (cm^{-3})	DEFECT (eV)	COMMENTS AND AIMS
		3×10^{12} 2×10^{12}	$E_C - 0.62$ $E_C - 0.73$	
Si 2N4416 FET $n = 7 \times 10^{15}$ cm^{-3}	γ- Irrad 500 MRd	$\sim 4 \times 10^{14}$ $\sim 2 \times 10^{13}$ $\sim 3 \times 10^{13}$ $\sim 3 \times 10^{13}$	$E_C - 0.18$ $E_C - 0.22$ $E_C - 0.44$ $E_V + 0.42$	To observe enhanced carrier path length (spiralling) in small channel width

low density defects been detected. The capture cross section of a range of defects was also measured as a function of magnetic field strength and no dependence observed.

For the MIT VPE n-GaAs, however, the E_c - 0.62 eV level proved susceptible to the magnetic field. This level also displayed the Poole-Frenkel effect [Pearton et al. 1980].

When the field was first applied (B = 1 kG) the DLTS peak, usually at 280 K for the conditions used (30 V reverse bias, 30 V bias pulse, correlator time constant 10 ms), shifted to 265 K when a pulsed infrared LED injecting minority carrier was turned on. Infrared is strongly absorbed near the shallow junction and carriers drift at their scattering-limited velocities through the depletion region, where they become available for trapping. Before the magnetic field was applied, this procedure had no effect on the peak position; consquently, without the injection of minority carriers, the peak temperature reamined at 280 K. The capture cross section, σ_n, at 265 K was greater than that at 280 K, i.e. 6.0 x 10^{-18} cm^2 compared with 3.7 x 10^{-18} cm^2. However, this increase is not enough to explain the shift in peak temperature, using the detailed balance relation:

$$e_n = \frac{\sigma_n \langle v_n \rangle N_c}{g} \exp\left(\frac{\Delta E}{RT} \right)$$

where e_n = emission rate of trap for electron,

$\langle v_n \rangle$ = average thermal velocity of carrier,

N_c = density of states in conduction band,

g = degeneracy of level (assumed g = 2),

ΔE = energy separation of defect from conduction band edge,

k = Boltzmann's constant, and

T = absolute temperature of sample.

Since the activation energy of the level had not changed within

the error of the measurement (±10%), we would need

$$\frac{\sigma_n\ (265)}{\sigma_n\ (280)} = 2.72 \quad ,$$

whereas the measured ratio is 1.62. It is possible that a significant lattice relaxation occurs when the orientation of the defect changes in the magnetic field, or perhaps that the degeneracy of the level (assumed g = 2) changes (e.g. to g = 1). Once in the new state (265 K, LED on; 280 K, LED off), the external d.c. magnetic field strength or orientation had no effect on the level.

The sample was then annealed in air for 10 minutes at 180°C without effect on the defect state. Subsequently, the diode was withdrawn slowly from an a.c. field (10 A, 50 Hz, coil inductance 53 mH, resistance 3.7 Ω); the Poole-Frenkel level remained at 280 K with the LED off, but was absent with the LED on over the temperature range 77 to 310 K. The d.c. magnetic field again had no influence on the defect. A second withdrawal from the a.c. field caused the return of the 280 K, LED off, 265 K, LED on state. The diode was then consecutively withdrawn from the a.c. field and scanned on the DLTS apparatus, which included the application of the d.c. magnetic field. Accordingly, the defect state in general, flipped between the 280 K, LED off, 265 K LED on and the 280 K, LED off, absent for LED on states. Again, in general, the d.c. field had no effect but, on one application, it did switch the defect state back to the 280 K LED off, 265 K, LED on state (Figure 5). The sample was cooled, with and without bias, and with and without the d.c. magnetic field; neither combination altered the defect state.

Two small Au barriers were then evaporated at the corners of the sample and the same defect spectrum (with the P-F level in the same state) obtained as for the original barrier. Table 2 lists the sequence of defect state 'flips'.

Fig. 5 DLTS SPECTRA FOR VPE n-GaAS
(POOLE - FRENKEL DEFECT E_c - 0·62eV)

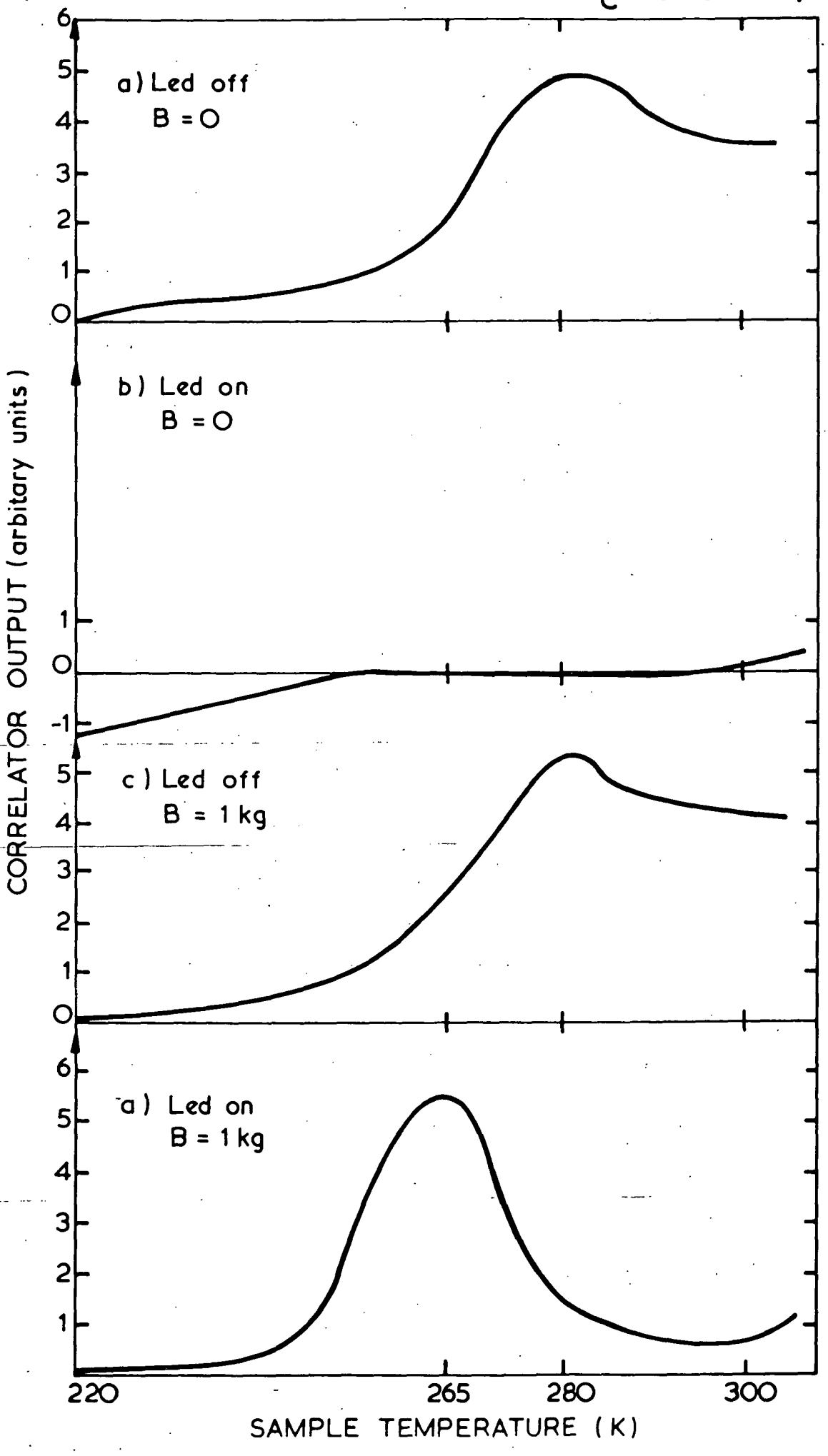

TABLE 2 SEQUENCE OF STATE CHANGES FOR P-F LEVEL

EXTERNAL STIMULI	DEFECT PEAK TEMP(K) LED ON	LED OFF	COMMENTS
Standard dlts	280	280	As for 1979 runs (over 11 days)
B = 1kG LED ON	265	280	After first flip, B has no effect
AC Field - Withdrawn	Absent	280	9A, 50Hz. DC Field no effect
AC Field - Withdrawn	265	280	10A, 50Hz. DC Field no effect
Left overnight	Absent	280	Stored in Vacuo at RT
AC Field - Withdrawn	Absent	280	No change from previous state
AC Field - Withdrawn (Same next morning after storing RT)	265	280	Sample at right angles to field in cryostat - DC field has no effect
AC Field - Withdrawn DC Field switched on	Absent 265	280 280	Withdrawn from field over ~15 mins by motor
Left Overnight	265	280	Stored in vacuo at RT
Two new barriers	265	280	No stimuli-new barriers give same spectrum in same state as original barrier
Left 9 days R.T. cooled without bias	265 265	280 280	No change since last check not withdrawn from cryostat B no effect.
Cooled with LED ON/No Bias	265	280	Left in cryostat; B no effect.
AC Field Withdrawn Left Overnight	265 265	280 280	No change; B not used stored in vacuo at R.T. B not used
AC Field (Withdrawn)	280	absent	Changed without DC Field

A companion piece of the original material was prepared in the standard way, except that a polishing etch of $4H_2SO_4:1H_2O_2:1H_2O$ for ∿5 seconds was used. The DLTS spectrum of this sample displayed only the P-F level - thus the other levels in the original sample must have been caused by the indiffusion of impurities in the final etch or rinse during the diode preparation. This is supported by the shallow depth (<8 μm) of these defects. Over the timescale involved, three possible contaminants which could have formed defect complexes with native defects are S, As and Sn. Because the newly evaporated contacts on the original sample displayed the same defect spectrum, the cause of the extra levels was clearly not impurity drift from the barrier under internal junction bias; however, while the remaining level indeed displayed the P-F effect, it did not respond to a d.c. magnetic field or two slow withdrawals from an a.c. field. A possible explanation is that a fast diffusant (e.g. Cu) has attached itself to the defect complex, sensitising it to the magnetic field, but not changing the defect activation energy.

In this way, the structure of the defect could determine its capture cross section for free carriers, while its chemical properties determine its activation energy. Annealing in air at 150°C for 100 hours did not change the behaviour of the second sample.

In conclusion, the facts could be explained by a linear, doubly charged defect complex which, in certain orientations determined by an external a.c. or d.c. magnetic field, changes its capture cross section for electrons (and possibly its degeneracy) sufficiently when its charge state is altered by capture of a hole, to appear with a different detrapping time constant τ_c.

CONCLUSIONS

There is no magnetic field dependence of capture cross section

for 'ordinary' deep level defects in Ge, Si and GaAs for magnetic fields $\leq$1.8 kG. Clearly a stronger magnet is required, perhaps with shaped pole pieces to concentrate the field at the sample. A small volume sample with high defect density, e.g. a γ-irradiated FET, with such a magnet configuration may then allow a clearer demonstration of enhanced trapping effects.

REFERENCES

Byrne, J., Shaikh, F. and Banner, B. E. [1979] - Nucl. Instr. and Meth. 86:323.

Byrne, J., Shaikh, F. and McCombe, T. J. L. [1974] - Nucl. Instr. and Meth. 122:347.

Ganner, P. and Rauch, H. [1969] - Nucl. Instr. and Meth. 76:295.

Kiegle, B. A. and Weber, H. W. [1975] - Nucl. Instr. and Meth. 123:285.

Pearton, S. J., Tavendale, A. J. and Williams, A. A. [1980] - Electronics Lett. 16(12)483.

Williams, A. A., Pearton, S. J. and Alexiev, D. [1980] - AAEC/TN147.

6.3 THE ELECTRICAL PROPERTIES OF POLYCRYSTALLINE Ge

SUMMARY

Polycrystalline germanium samples from the start end of zone-refined bars were characterised by I-V, C-V, DLTS and TSCAP measurements. No electrically active defects with energy levels $\gtrsim$150 meV and concentrations $\gtrsim 10^5$ cm^{-3} could be found when depleting through grain boundaries, although results consistent with the equivalent circuit of back-to-back diodes were obtained. Diodes fabricated from this material show poor rectification ratios ($\sim$100 at V_R < 5 V, $\sim$4 at V_R > 20 V), and DLTS peaks attributed to impurity defects. The material is generally p-type and high-purity (10^{11} cm^{-3}). One sample was unquestionably $N_a - N_d = 3.5 \times 10^9$ cm^{-3}.

INTRODUCTION

Imperfections such as twin and grain boundaries in semiconductor crystals act as localised trapping and recombination regions, degrading minority carrier lifetimes in their vicinity. As polycrystalline material becomes increasingly important for device applications, a more complete knowledge of the properties of these line defects is desirable. In an earlier chapter (Deep Levels in GaAs), we investigated 'badly' polycrystalline GaAs and concluded that native and impurity point defects were dominant in that material. Here the investigation is extended to high purity (10^{10} to 10^{13} cm^{-3} net ionized impurity density) polycrystalline Ge from zone-refined bars, in which large (>5 mm^3) crystallites were evident. This is the starting material for the large high purity single crystals for nuclear radiation detectors. Standard semiconductor characterisation techniques were used to gain an insight into the material properties.

EXPERIMENTAL PROCEDURE

The base material (from zone-refined bar Ge-NF-80-7) was first

cut, lapped, polished and etched in the usual way to delineate the grain boundaries more clearly. Seven samples were then further shaped so that a single grain boundary was running parallel to the lapped faces and approximately 1.0 to 1.5 mm from the nearest face. This face was then Li diffused (10 minutes, 350°C) to form a blocking contact. On a further nine samples, the grain boundaries were allowed to run in a random fashion throughout the material. On the initial seven samples, a Pd evaporation on the opposite face provided an ohmic contact (sample volumes were typically 10 mm^3), while evaporated Au dots (ϕ = 2 mm) were evaporated onto the larger, random orientation samples (volume typically 100 mm^3).

The C-V characteristics of all samples generally had a $-1/3$ slope, indicating a graded junction, and all could be easily pulsed into the forward biased direction, indicating that the material was indeed p-type and hence depleting from the Li diffused contact. The net ionized impurity densities at 77 K determined from the C-V data (taken at 1 MHz) indicated that generally $N_a - N_d \simeq 10^{11}$ cm^{-3}. The experimental procedure and apparatus for the measurements have been described previously [Pearton and Lee 1980].

RESULTS

The DLTS measurements for the parallel grain boundary measurements were performed by using a constant 25 V bias pulse (pulse width = 300 μs) and increasing the standing reverse bias in 25 V increments, from 25 V to 20 V. In this way, the entire diode is investigated. A typical set of spectra obtained is shown in Figure 1. For this sample, $N_a - N_d \sim 3.5 \times 10^9$ cm^{-3}, thickness 2.4 mm, so the diode was fully depleted at ~20 V. Even though two acceptor level defects are evident, these defects were observed only in this particular sample, and were not observed in the other six diodes in

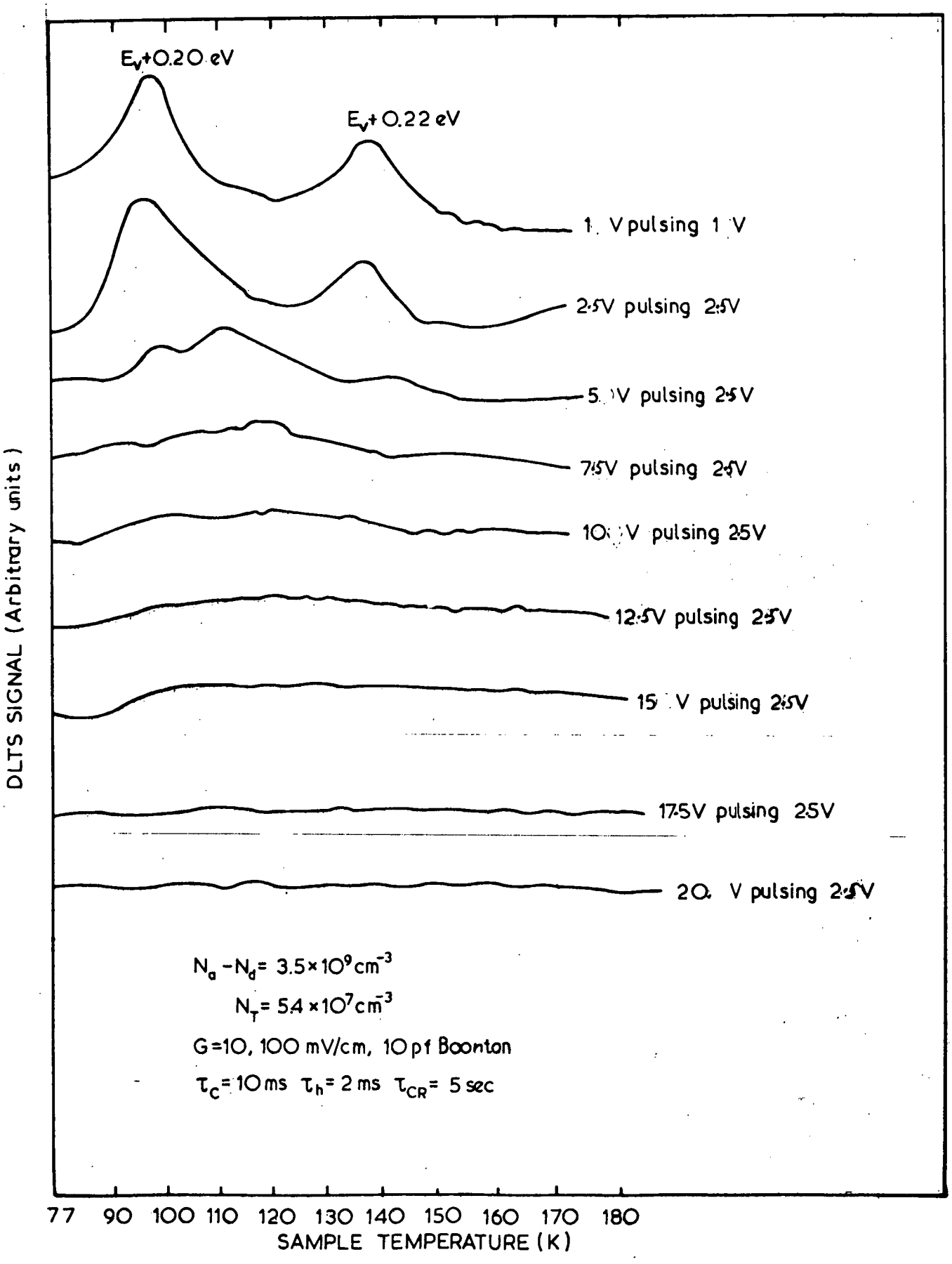

Figure 1: DLTS Spectra for a high-purity ($N_a - N_d = 3.5 \times 10^9$ cm^{-3}). Sample with a grain boundary parallel to the Li contact. No electrical activity positively attributable to the boundary was found on depleting through this region. Sample thickness 2.4 mm, area 0.75mm^2.

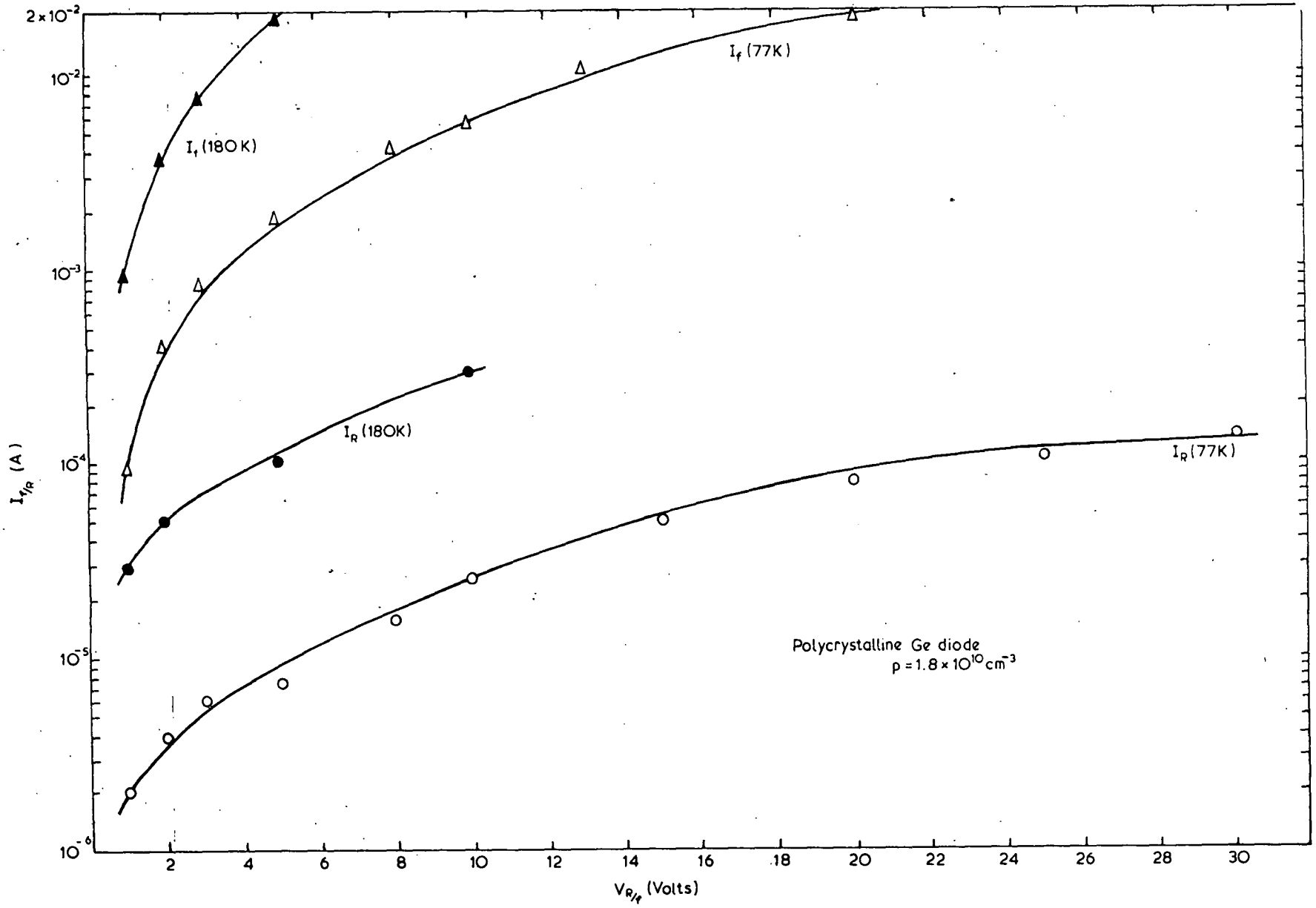

Figure 2: I-V characteristics for a polycrystalline - Ge sample $N_a - N_d$ = 1.8×10^{10} cm^{-3}. Note the high reverse leakage currents due to poor crystallinity.

which equally obviously, we had depleted through a grain boundary. However, both of these levels appear to decrease into the sample, so possibly the impurities are pinned at the grain boundary. In none of the seven samples were common levels observed which could be correlated with the electrical activity of grain boundaries.

I-V characteristics for a typical polycrystalline sample of the random orientation type are recorded in Figure 2. The net ionized impurity concentration at 77 K was $p = 1.8 \times 10^{10}$ cm^{-3}, thus the saturation reverse leakage current should be noted, $I_R \sim 10^{-4}$ A; this is approximately six orders of magnitude higher than the expected reverse leakage current for a single crystal Ge diode of the same purity. In many of the diodes the rectification ratio showed marked deterioration at higher volts, ~100 at $V_R < 5$ V to ~4 at $V_R > 20$ V). The high leakage currents are a stark reminder to those who would produce nuclear radiation detectors with laser melt contacts. Unless the melt regrowth is perfect, the current injection from the poor crystallinity will thwart attempts to achieve low leakage currents and thus excess laser energy is to be avoided, particularly in Ge where melting is achieved at lower energies than in Si. It can be reasonably expected that many of the earlier disappointing results were due to poor crystallinity on regrowth of the melt region.

A DLTS spectrum for one of the randomly oriented grain boundary samples, together with the thermally stimulated capacitance plot, is shown in Figure 3. The two acceptor level defects ($N_T \sim 9 \times 10^7$ cm^{-3}, $N_T/p \sim 4 \times 10^{-3}$), $E_v + 0.22$ eV ($\sigma_p \sim 2.4 \times 10^{-15}$ cm^2) and $E_v + 0.20$ eV ($\sigma_p \sim 2.9 \times 10^{-14}$ cm^2) were observed in three of the nine random orientation grain boundary samples, as well as the very high-purity parallel grain boundary sample (Figure 1). Note that the capacitance peaks and then decreases on heating the sample from 77 to 180 K.

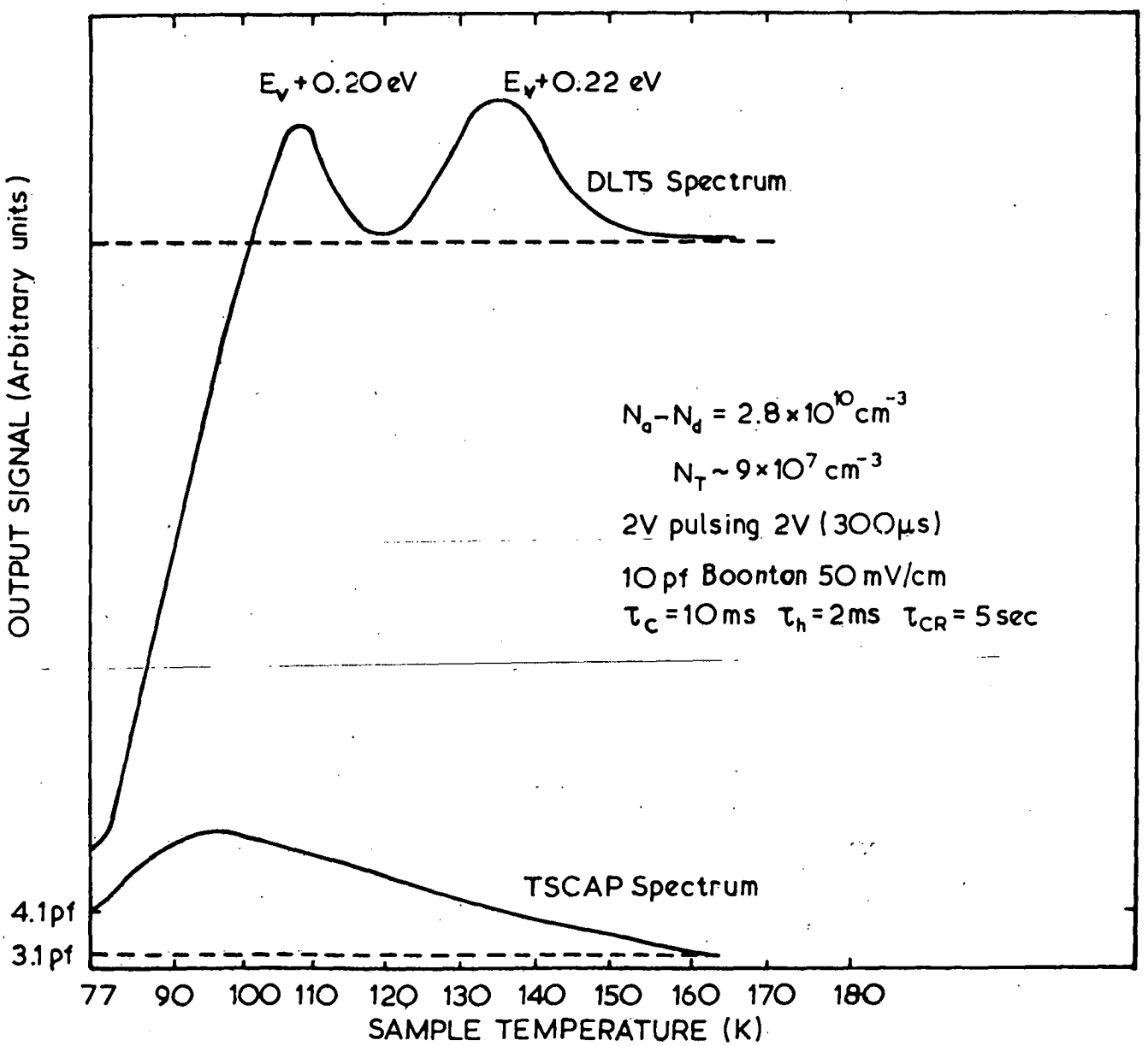

Figure 3: DLTS and TSCAP spectra for a polycrystalline Ge sample $N_a - N_d \simeq 2.5 \times 10^{10}$ cm^{-3}. Grain boundaries have random orientation to Li contact.

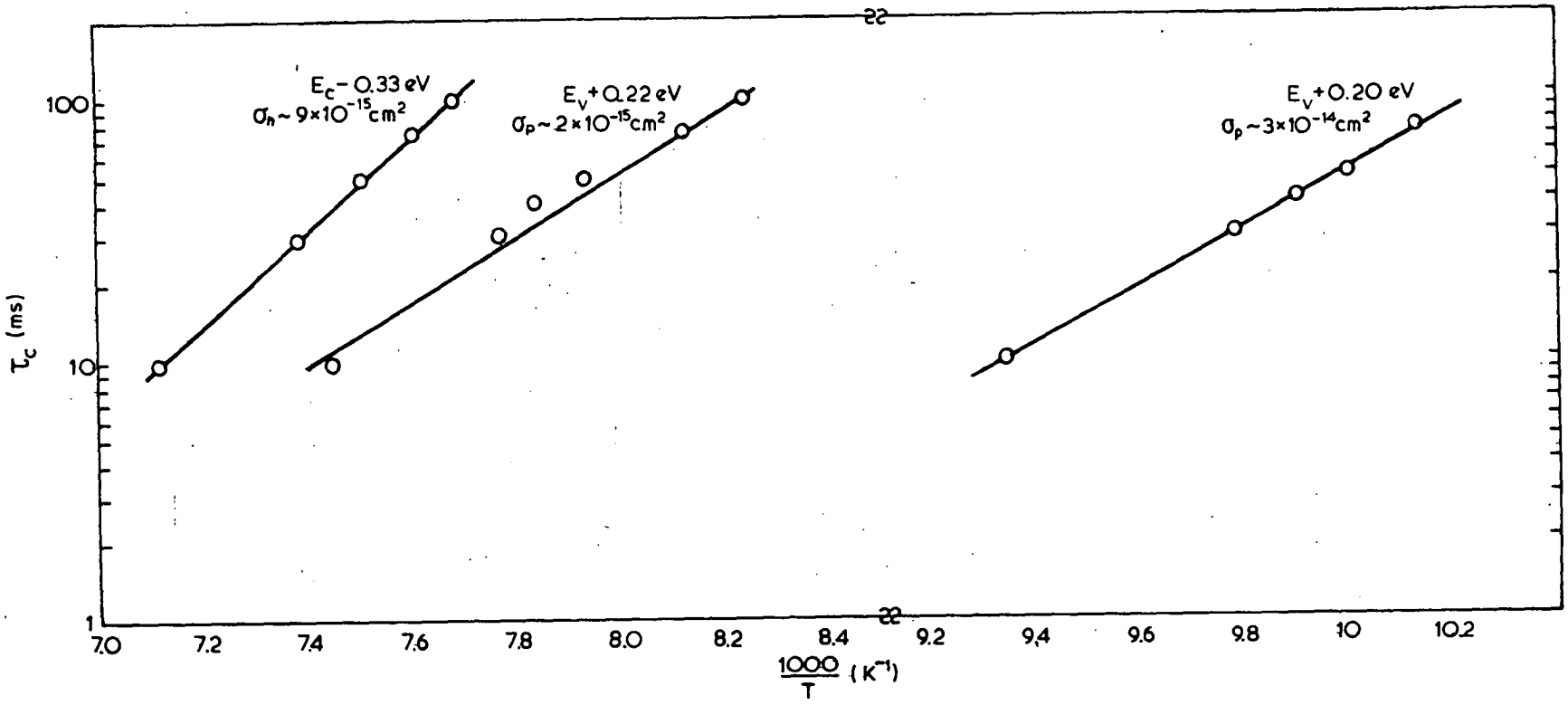

Figure 4: Arrhenius plots for three impurity levels measured in zone-refined bar material.

Because the capacitance bridge measures $N_a - N_d$ it is possible that deep donors which are unobservable by the DLTS technique because of very small (or very large) capture cross sections, are ionizing. Arrhenius plots for three levels observed are shown in Figure 4.

DISCUSSION

The crystallinity and purity of this material was far superior to that investigated previously, and one could reasonably expect to observe the electrical effects of grain boundaries without the masking effect of a high-impurity and native point defect concentration. Even though conventional DLTS measurements may, in some circumstances, give an erroneously low concentration for very thin regions of high electrical activity, the conclusion of the experiment must be that no impurity levels $\gtrsim$150 meV with cross sections $<10^{-14}$ cm^2 and concentrations $>10^5$ cm^{-3} can be associated with grain boundaries in the Ge investigated. Of course, if the trapping cross sections of the boundaries are very high, $>10^{-13}$ cm^2, then the levels may still be deep ($\sim$100 meV), but observable only below 77 K because of the high detrapping rates. Similarly, the boundaries may have the usual cross sections (10^{-14} to 10^{-17} cm^2) and semi-deep activation energies (20 to 80 meV); these also will be observable only below 77 K. An interesting prospect is that the electrical activity of the boundaries has been passivated by the material preparation - zone-refining under hydrogen - although this was molecular hydrogen rather than the atomic hydrogen known to passivate point and line defects.

REFERENCE

Pearton, S. J. and Lee, P. J. [1980] - AAEC/TN152.

6.4 DEFECT STATES IN γ-IRRADIATED n-CHANNEL SILICON FIELD EFFECT TRANSISTORS

SUMMARY

The common and well-characterised A- and E-centres have been observed in the gate junction of γ-irradiated n-channel silicon FETs using a modified DLTS system to enable transient conductance measurements. The possibility exists of using commercial FETs as dosemeters for the flux range 50 kGy to 10 x 10^3 kGy (5 to 1000 Mrad). A dedicated FET structure, suitably doped for more sensitive defect detection, could prove useful in the technologically important flux ranges 500 Gy to 25 kGy (50 krad to 2.5 Mrad).

INTRODUCTION

The technique of DLTS [Lang 1974] is standard for analysis of defect levels in semiconductors. By periodically reducing the reverse bias on a diode, trapping centres are filled, and their emission is monitored as a function of temperature by measuring transient changes in the device capacitance. In this way, individual defect levels may be observed.

The fundamental limit to the sensitivity of the technique is reached for semi-insulating devices, or for those in which capacitance change with bias is very small. In this case, transient current or conductance measurements may be performed. For FET structures, the drain conductance may be monitored as detrapping from defect states modulates the channel depletion depth. This section describes observation of the common deep level A- and E-centres in γ-irradiated silicon FETS, using a modified transient capacitance spectroscopy system.

APPARATUS

The capacitance bridge used in the system is a Boonton model 71A L-C meter and signal processing is by an electronic correlator

[Miller et al. 1975]. To convert to the conductance mode, the sample RF signal voltage into the phase detector of the bridge is interrupted and the phase of the signal shifted 270^{o} to enable observation of the real component of device impedance. This is effected by using a Canberra 1457 delay amplifier and a calibrated coaxial cable acting as a phase trimmer. The phase is optimised by noting the maximum response when a resistor is placed across the test terminals (or alternatively a null response if a capacitance is added). The modifications to the bridge and setting up of the system are minor [Williams et al. 1980], so any standard DLTS apparatus without a transient conductance capability may be converted.

EXPERIMENTAL

The experiment involved six groups of three FETs selected from different batches. One set was used as a control group and the others received doses of 50, 250, 500, 5×10^3 and 10×10^3 kGy (5, 25, 50, 500 and 1000 Mrad) respectively, at 21 kGy h^{-1} (2.1 Mrad h^{-1}). Irradiations were performed in a cobalt-60 irradiation facility at ambient temperature, fluxes being calibrated by the AAEC's Isotope Division. The I-V characteristics of each FET were recorded before irradiation so that each group contained FETs of similar transconductance (g_m). Transient conductance scans were performed over the temperature range 77 to 300 K by locating the FETs in a brass holding block which was mounted in a continuous flow cryostat (Oxford Instruments CF-100). The FET gate was pulsed towards or into forward bias to obtain the majority or minority defect level spectrum. A 400 μs bias reduction pulse was used, supplied by a Systron-Donner 100A pulse generator. The drain voltage was 1.35 V; this voltage is not critical as long as the FET is below pinch-off and above zero volts, since the I-V characteristic is linear in this region.

RESULTS

Figure 1(a) shows a typical majority carrier spectrum. The E_c - 0.17 eV level is the A-centre, oxygen-vacancy, and has been studied after irradiation of silicon by protons [Kimerling et al. 1978], neutrons [Whan 1966] and electrons [Kimerling 1977]. The E_c - 0.22 eV level is commonly assigned to a divacancy defect, and the E_c - 0.44 level to phosphorus-vacancy [Kimerling 1977]. Apart from the three dominant defects, there is evidence for levels estimated as E_c - 0.19 eV and E_c - 0.36 eV respectively. These are probably levels E4' and E6 of Kimerling et al. [1978]. When our results are compared with those of Kimerling [1977] it can be inferred that the starting material for the FETs is low oxygen content, float-zoned, phosphorus-doped silicon.

Figure 1(b) shows the appearance of the hole trap E_v + 0.42 eV when the gate is forward biased. This is commonly thought to be either a higher charge state of the A-centre, or an interstitial related defect [Kimerling 1977]. From Figure 1(c) it can be seen that at a dose of 50 kGy (5 Mrad), the A-centre is visible, but it is not until 500 kGy (50 Mrad) that the other levels are clearly defined.

Cross sections were measured from the dependence of correlator output signal on trap filling time. The results correlate closely with those of Kimerling [1977]. Figure 2(a) shows the reduction in relative correlator output signal as a function of bias reduction pulse width (during which time the traps are filled).

The conductivity, g, of a semiconductor in which electrons are the majority carriers, is given by

$$g = e\mu_n n \qquad (1)$$

where e = electronic charge, μ_n = electron mobility and n = net free carrier density (= $N_d - N_a$ where these are the total donor and acceptor

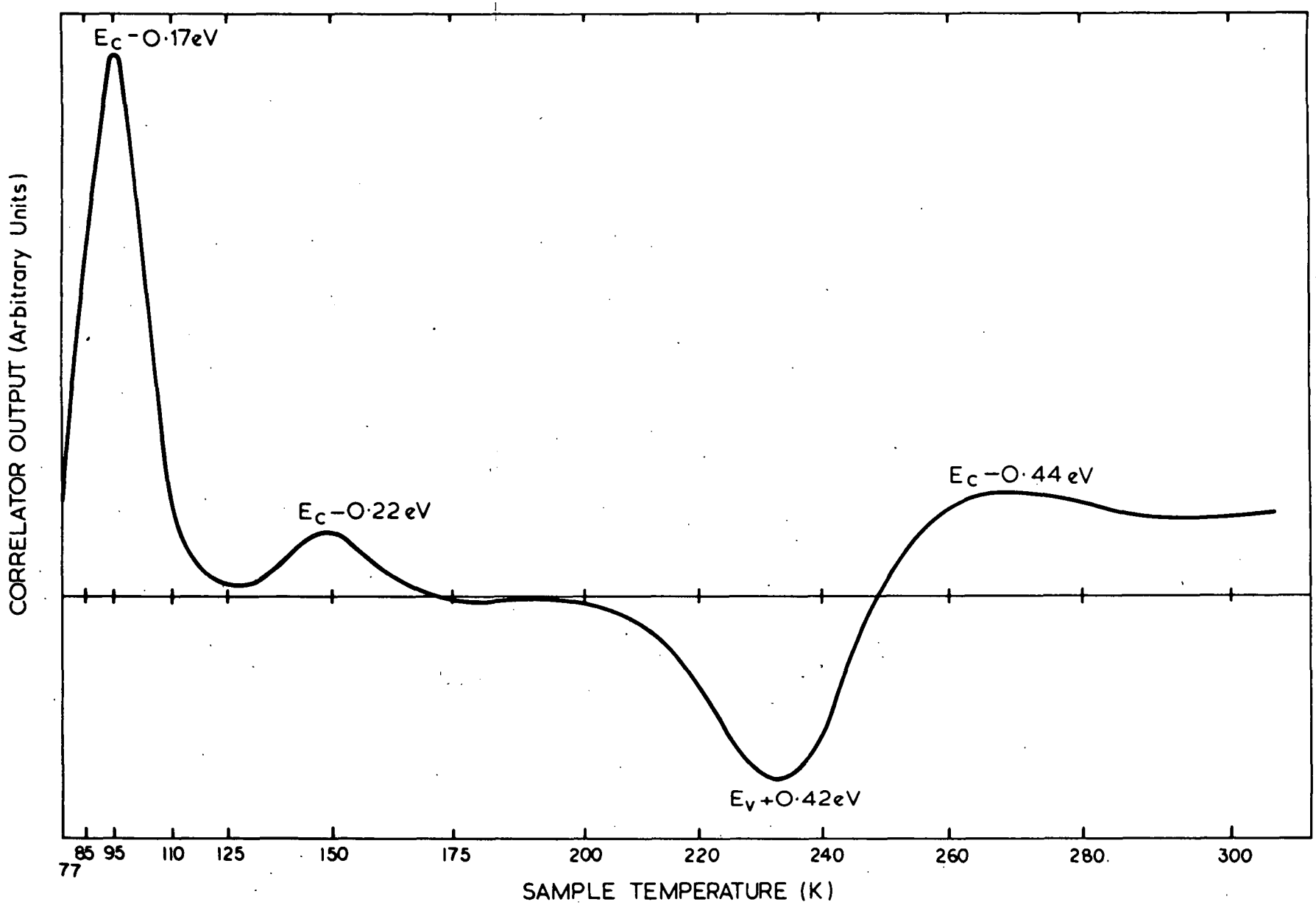

FIGURE 1(a) DLT CONDUCTANCE SPECTRUM FOR DOSE OF 5 MGy (500 Mrad), GATE FORWARD BIASED TO DISPLAY MINORITY DEFECTS

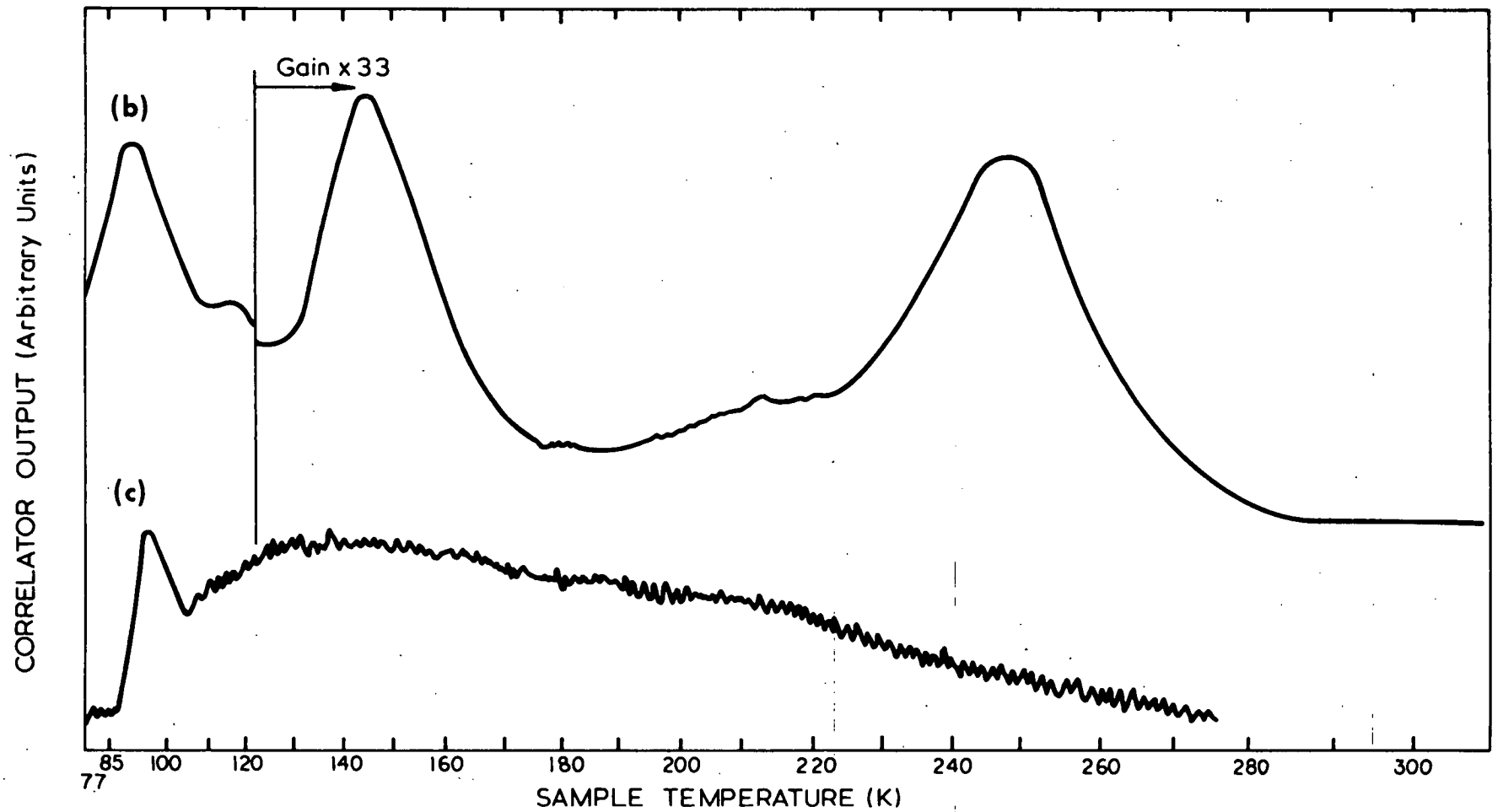

FIGURE 1 (b) TRANSIENT CONDUCTANCE MAJORITY DEFECT SPECTRUM FROM A γ-IRRADIATED 2N4416 FIELD EFFECT TRANSISTOR FOR DOSE OF 5 MGy (500 Mrad)

(c) DLT CONDUCTANCE SPECTRUM FOR DOSE OF 50 kGy (5 Mrad)

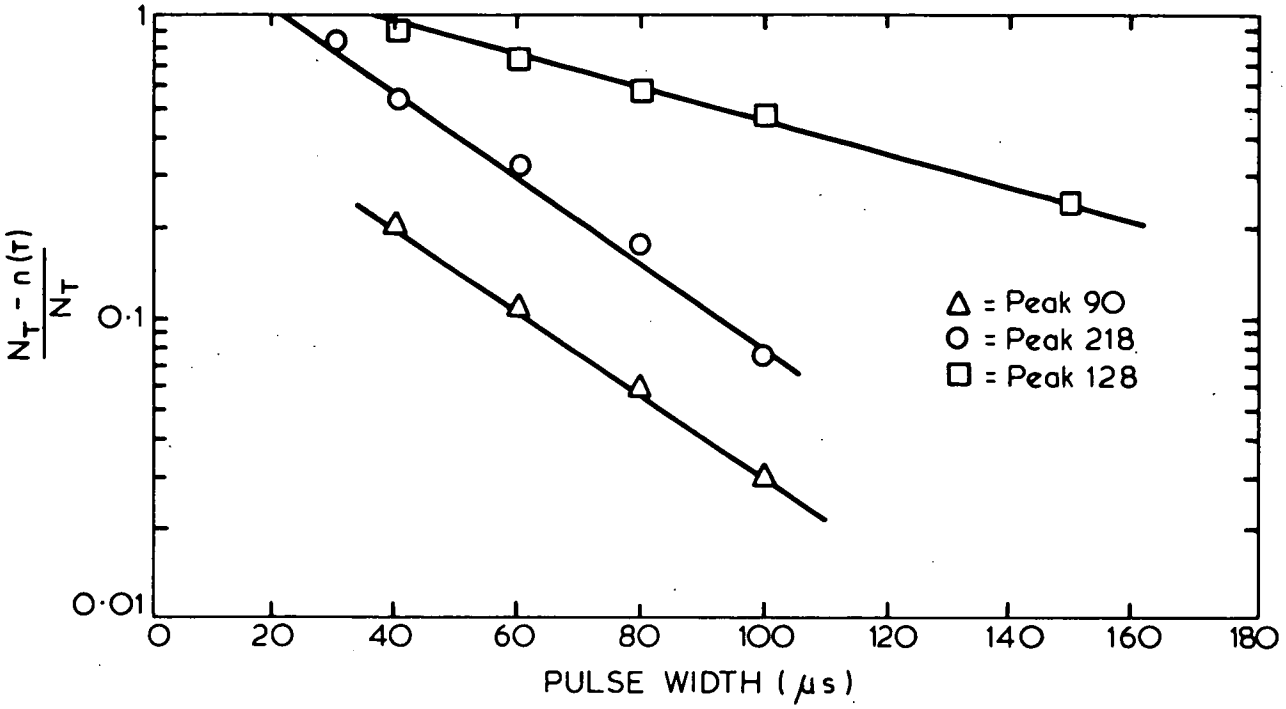

FIGURE 2 (a) RELATIVE CORRELATOR SIGNAL OUTPUT v. PULSE WIDTH FOR THREE DOMINANT MAJORITY LEVELS

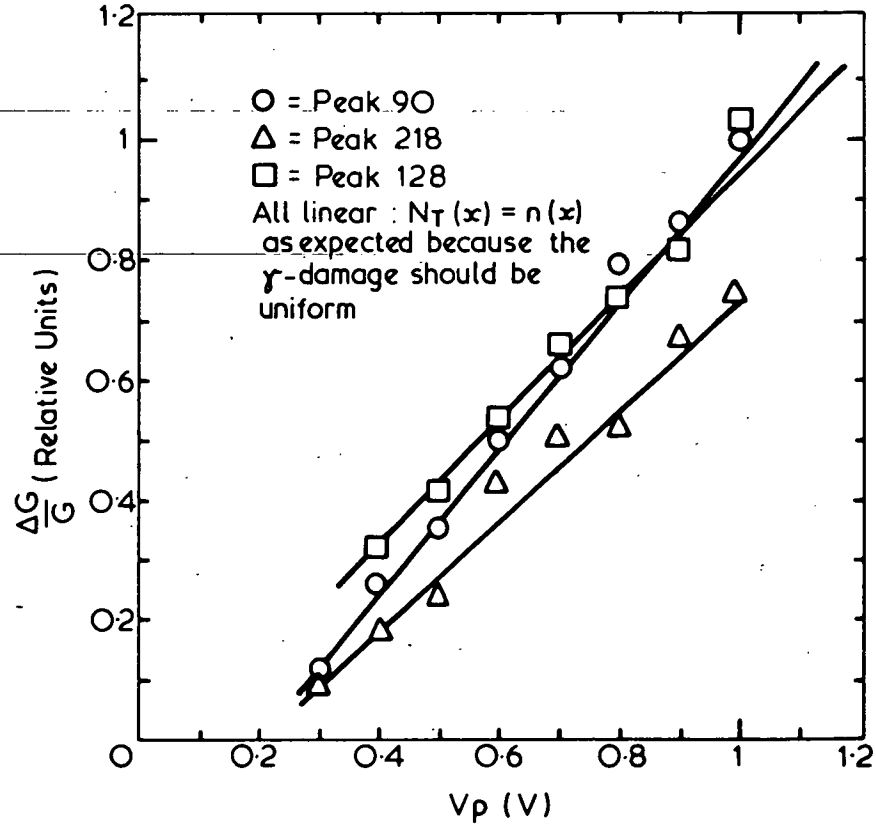

FIGURE 2 (b) TRANSIENT CONDUCTANCE CHANGE v. PULSE AMPLITUDE FOR THREE DOMINANT MAJORITY LEVELS

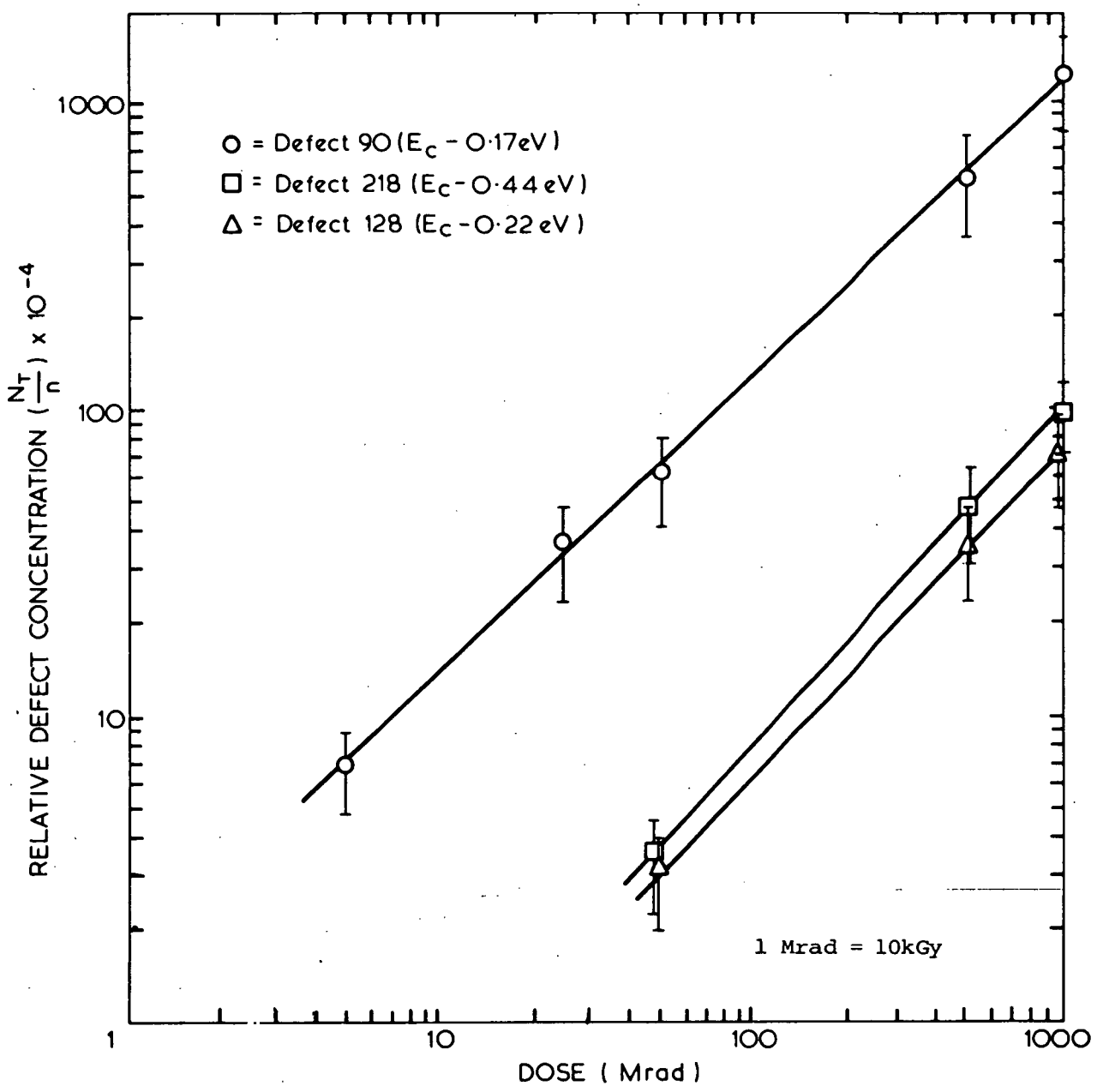

FIGURE 3. DOSE DEPENDENCE OF RELATIVE DEFECT CONCENTRATION FOR THE THREE DOMINANT MAJORITY LEVELS

concentrations, respectively). A slight increase Δn ($<<n$) in the free carrier density leads to a slight increase, Δg, in the conductivity of the sample. In this technique the thermal detrapping of electrons from defects provides such an increase, i.e.

$$\Delta n = N_T$$

where N_T is the concentration of the particular defect level. For the condition $\Delta g/g << 1$,

$$N_T = \frac{\Delta g}{g} n \qquad (2)$$

This equation was used to estimate trap concentrations by measuring Δg_d, the magnitude of the transient conductance change by pulsing to zero bias and g_d, the drain conductance of the FET at the peak temperature. Figure 2(b) shows the dependence of $\Delta g/g$ on the bias pulse amplitude; the linearity of the plot indicates that the defects are uniformly distributed through the region.

Figure 3 shows a plot of relative defect concentration versus dose received. The slopes are

E_c - 0.17 eV	1.2×10^{-5} kGy^{-1}
	(1.2×10^{-4} Mrad^{-1})
E_c - 0.22 eV	7.23×10^{-7} kGy^{-1}
	(7.23×10^{-6} Mrad^{-1})
E_c - 0.44 eV	9.48×10^{-7} kGy^{-1}
	(9.48×10^{-6} Mrad^{-1})

Absolute defect concentrations require a knowledge of n, which may be obtained from a measurement of the FET pinch-off voltage and a knowledge of the channel depth. It appears that the ultimate sensitivity of this system is approximately 10^{-4} of the net background doping density, which is similar to the capacitance mode operation. Figure 4

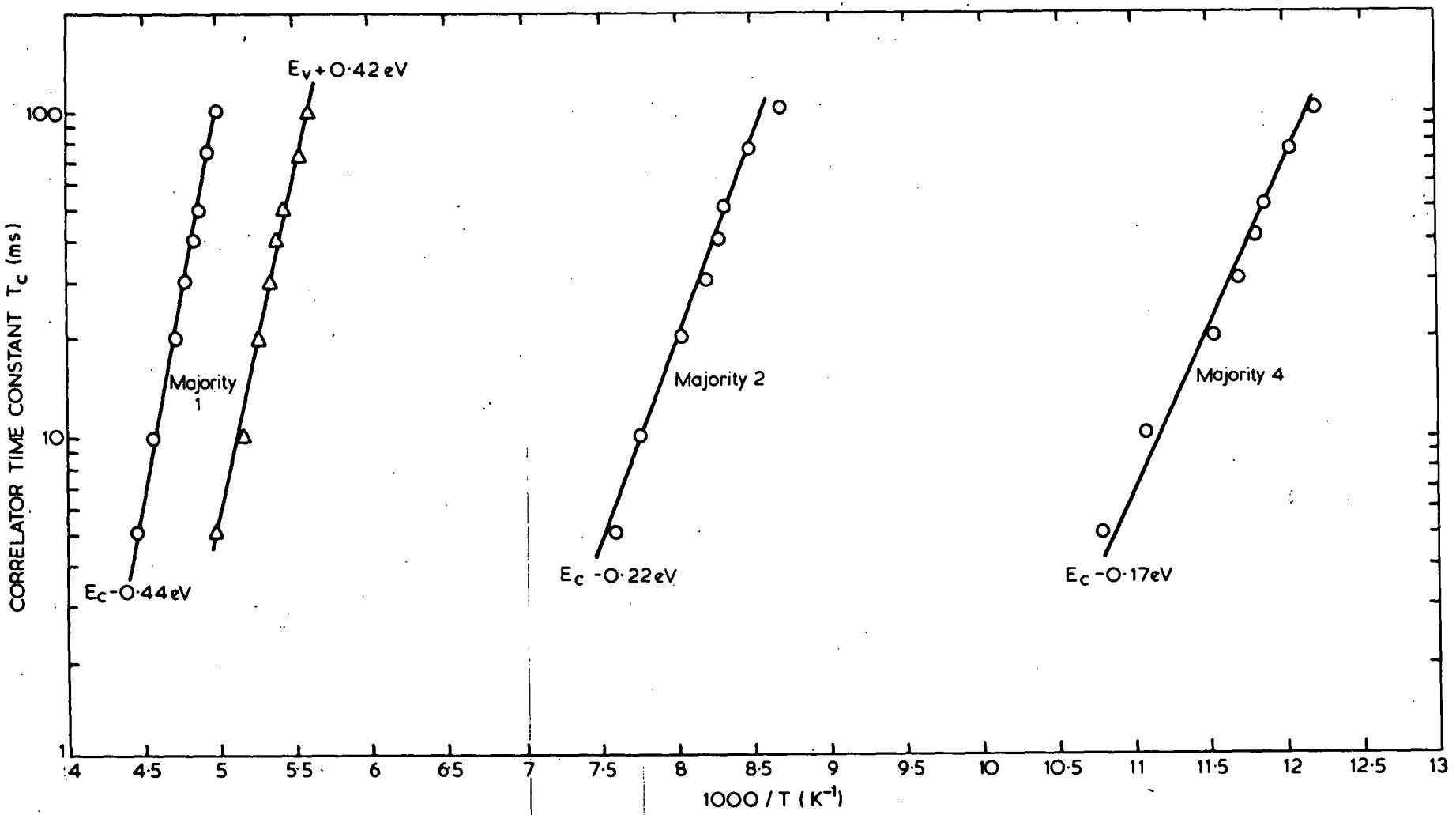

FIGURE 4. ARRHENIUS PLOTS OF THE FOUR MAIN DEFECT LEVELS

shows the Arrhenius plot of the four main levels, these data leading to the activation energies of the traps.

DISCUSSION

The homogeneity of the FETs (results within any dose group were within 15% of each other, aided by preselection on the basis of similar g_m* (~±10%), combined with the linearity of defect concentration with dose suggests that, at least in the range ~500 kGy to ~10 x 10^3 kGy (~50 to ~1000 Mrad), they may be useful as dosemeters. They may be particularly useful in situations where conventional monitoring is difficult, for example, where there is a demand for physically small, readily available, mass produced monitors (e.g. flux-mapping). It is intended to use them at the AAEC Research Establishment as a secondary check for flux measurements when irradiating other semiconductor materials for DLTS studies.

For general application, of course, a DLTS system must be available, but as the technique is now standard, 2N4416 FETs are cheap (and widely available) and the levels monitored are well characterised, this may be a simple and novel means of γ-flux measurement.

It may be possible to construct a 'sensitised' FET structure dedicated to flux measurement using DLT conductance spectroscopy. For example, a highly oxygen-doped silicon FET would give improved sensitivity of the oxygen-vacancy level. If it were possible to increase the oxygen content by two orders of magnitude, this would allow measurement of fluxes in the 25 kGy (2.5 Mrad) region, the approximate legal minimum for the γ-ray induced sterilisation of medical items, and the 500 Gy to 50 kGy (50 krad to 0.5 Mrad) dose range used in food processing. Defect introduction rates vary with temperature, particle type

*Note that preselection on the basis of g_m (related to $\sqrt{n}$) is essential as the doping density of Texas Instruments 2N4416 JFETs extends over the range 5.3 x 10^{15} to 1.0 x 10^{16} cm^{-3}.

and energy [Kimerling et al. 1978], so a prior calibration would be needed before the FET is used as a dosemeter. The FETs would also need a fairly strict (say ±10%) constancy of the oxygen and possibly phosphorus (or As or Sb) content. Operation as a dosemeter at elevated temperatures would be no problem as the levels of interest do not begin to anneal out until at least 120°C [Evwaraye 1977; Kimerling 1977].

REFERENCES

Evwaraye, A. O. [1977] - J. Appl. Phys. 48(5)1840.

Kimerling, L. C. [1977] - Radiation effects in semiconductors. Inst. Physics Conf. Series No. 31:222.

Kimerling, L. C., Gibson, W. M. and Blood, P. [1978] - Int. Conf. on Defects in Semiconductors, Nice, France. Inst. Physics Conf. Series No. 46:273.

Lang, D. V. [1974] - J. Appl. Phys. 45:3023.

Miller, G. L., Ramirez, J. V. and Robinson, D. A. H. [1975] - J. Appl. Phys. 46(16)2638.

Whan, R. E. [1966] - J. Appl. Phys. 37(9)3378.

Williams, A. A., Pearton, S. J. and Alexiev, D. [1980] - AAEC report, unpublished (AAEC/TN147).

APPENDIX

Following a suggestion by Dr A. J. Tavendale, it was decided to scan a variety of standard FETs in the hope that a correlation existed between deep level defects and noise performance. Low noise FETs are the first amplifying element (and the most important) in nuclear spectroscopy systems. Using the transient conductance method the following FETs were investigated: 2N4393 (n-chanel), 2N4416 (n-channel), 2N5465 (p-channel), 2N6435 (n-channel), 2N3823 (n-channel). A typical gate bias of 1.3 V was used with a 300 to 500 μs, 1 to 2 V bias pulse. Only one FET from approximately 15 tested showed a significant defect density above 77 K, the 2N4393 (Figure 1). The peaks are possibly due to the Au contamination of the base Si. Included in the study were an approximately even number of low noise and mediocre FETs; no correlation of noise performance with deep level defect density was found. The method is not a useful one for selecting low noise FETs.

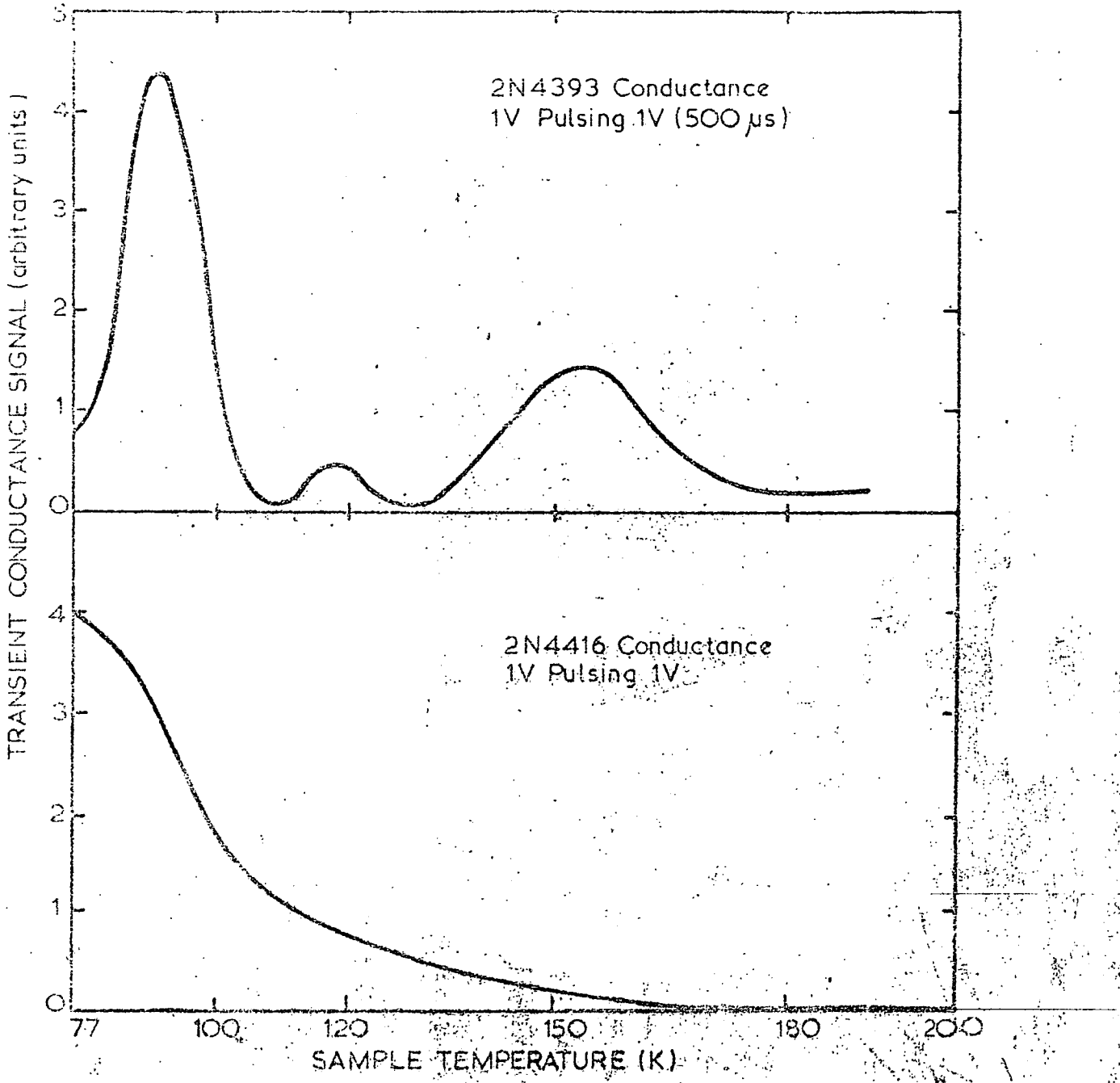

Figure 1. SHOWING TRANSIENT CONDUCTANCE SPECTRA FROM 2N4393 FET SHOWING DEEP LEVELS, & 'NORMAL' LOW NOISE 2N4416 FET SPECTRUM. NO CORRELATION OF DEFECT DENSITY WITH NOISE PERFORMANCE WAS FOUND

6.5 ELECTRONIC STIMULATION OF DEFECTS IN RADIATION DAMAGED Ge

SUMMARY

Defects produced by the γ-, electron- or laser-irradiation of Ge show DLTS spectra sensitive to infrared illumination and the thermal cycling history of the sample.

INTRODUCTION

Electronically stimulated defect processes in semiconductors such as GaAs, GaP and Si are the subject of much current interest. The role of electronic stimulation mechanisms in deep level defect behaviour has been discussed at length recently [Kimerling 1976,1978,1979; Lang and Henry 1975; Lang and Kimerling 1974; Lang et al. 1976]. Three specific areas are generally defined:

1. Electric field effects which have the weakest enhancement factor because the field exists over distances large compared to defect dimensions. Examples are the motion of Li in Si and Ge, and also radiation damage defects [Baruch 1961] in an applied field. Also, internal fields at defect clusters in neutron irradiated Li drifted Si cause the capture of mobile Li ions, removing the Li and reducing the net charge on the defect clusters [Kimerling 1978].
2. Recombination enhancement arising from local deposition of vibrational energy at a defect site. An example of this is the extremely efficient annealing of some radiation damage centres in compound semiconductors under forward bias (injection conditions).
3. Configureational processes due to a change in potential energy contours surrounding a defect site upon a change in the electronic state of the defect. These lead to charge dependent annealing of defect centres (P-V defect

in Si [Kimerling 1979]), changes in emission rate of a defect in an electric field due to polarisation effects (electron damage centres in GaAs [Kimerling 1979]) and capture cross section changes due to excited state processes (F_A centre in NaCl [Kimerling 1979]).

The changes in defect behaviour are therefore due to modifications in local binding energy, defect configuration or electron-photon coupling. In practical terms, the above mechanisms account for some of the tendency of semiconductor devices such as LEDs and lasers to fail under injection conditions.

We have already mentioned the motion of γ-damage centres in an electric field (Chapter 1), the sensitivity of the E_v + 0.23 eV and E_v + 0.38 eV centres in γ-irradiated p-type Ge to infrared illumination (Chapter 1), the removal of proton-damage induced acceptors by infrared illumination (Chapter 1) and the electric and magnetic field sensitivity of a donor state in epitaxial GaAs (Chapters 2 and 6.2). This section details DLTS [Lang 1974] measurements on defect centres in γ-, electron and laser irradiated Ge, which show sensitivity of the defect states to infrared illumination or prior heat cycles.

RESULTS

Sections of a n-type Hoboken crystal (N_d-N_a $\sim 10^{14}$ cm^{-3}) were irradiated by 1 MeV electrons to a dose of 1.6×10^{15} electrons/cm^2. Pd contacts were evaporated onto the irradiated face. The DLTS spectrum displayed two donor levels, the concentrations of which were non-uniform in the irradiated region (Figure 1). One defect had a concentration profile decreasing away from the contact, the other increasing slightly away from the contact. It is possible that the extremely bright light from the tungsten filament during evaporation of the Pd contact favoured annealing of one level and

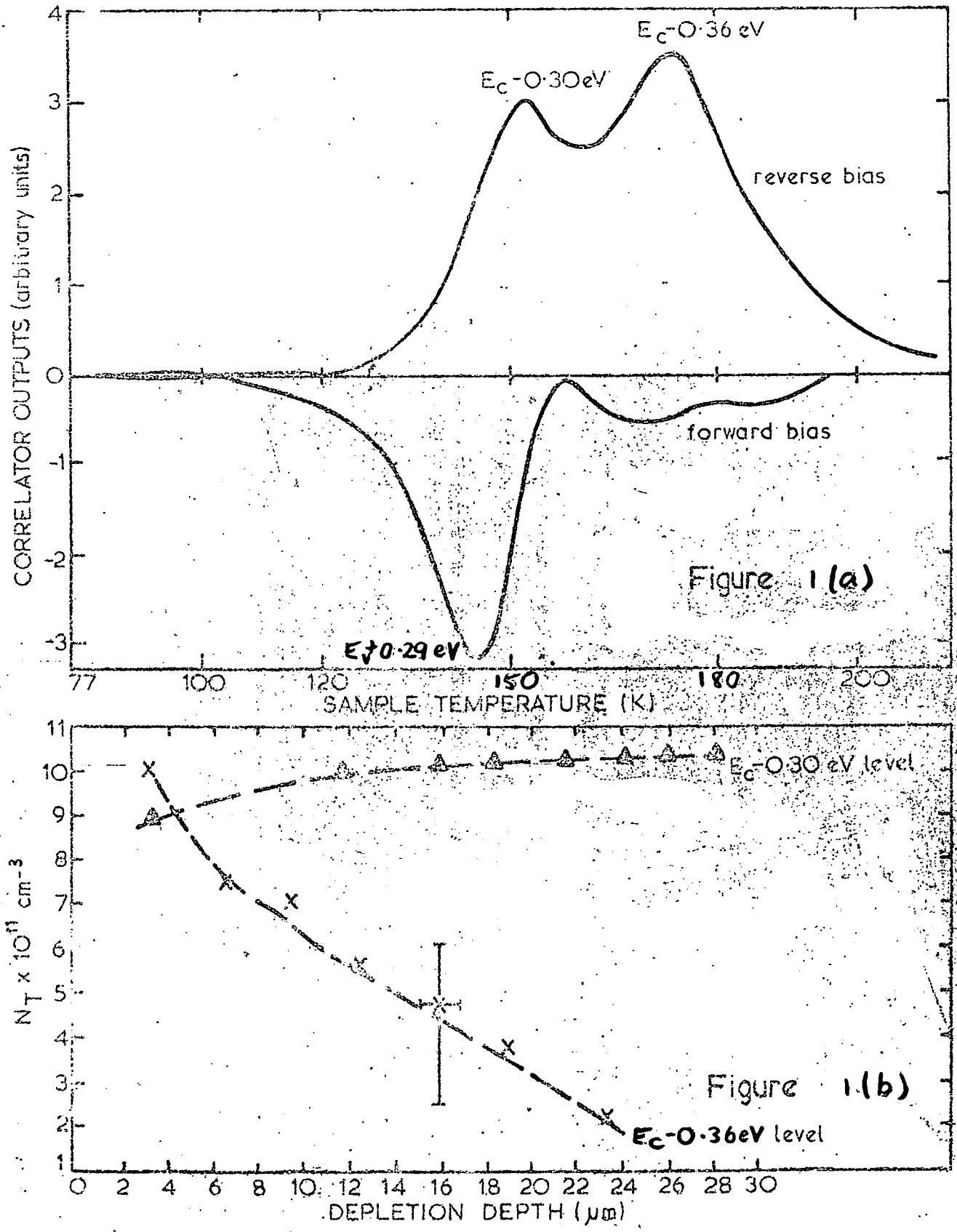

Figure 1 (a) DLTS spectrum of e-irradiated Hoboken n-type Ge

(b) Concentration profile data in e-irradiated region- note non-linear profiles

production of another, as the DLTS measurement depth was far less than the range of the electrons and to the damage profiles should have been constant. Samples etched to remove the top layer and processes with a further Pd contact showed constant defect profiles.

A nitrogen-implanted, pulsed laser annealed n-type Ge sample displayed a DLTS spectrum in the melt region composed of donors and acceptors sensitive to infrared illumination by a LED in the DLTS cryostat. The concentrations of the levels were excessive for correct determination by the DLTS technique.*

The sample on which most information was accumulated was a section of n-type AAEC grown Ge (78-48-3, see Chapter 1). The DLTS spectrum for reverse bias conditions is shown in Figure 2(a). The spectrum was unchanged for the 5½ hours required to obtain the data for the energies, cross sections and concentrations of the donor levels induced. Upon foward bias pulsing and infrared illumination, five acceptor levels were evident; cycling the diode in temperature changed the number and concentration of these levels (Figure 2(b)). Reverting to reverse bias conditions (with no minority carrier injection) revealed one acceptor level but no donors (Figure 3(a)). Possibly the reverse leakage current of the diode was enough to fill the minority (acceptor) traps. Under infrared illumination again the original acceptor spectrum was obtained (Figure 3(b)). This set of results was repeated on three separate, successive days.

It is revealing, that once in the single acceptor state (Figure 3(a)), one could 'revive' the donors by heating at 220 K (above the detrapping temperature of the defect) for four minute intervals (Figure 4). The bulk capacitance of the sample was also changing during the DLTS spectrum changes, confirming the latter (Figure 5). Six monthly checks of the

*Sample courtesy of Dr A. J. Tavendale, AAEC

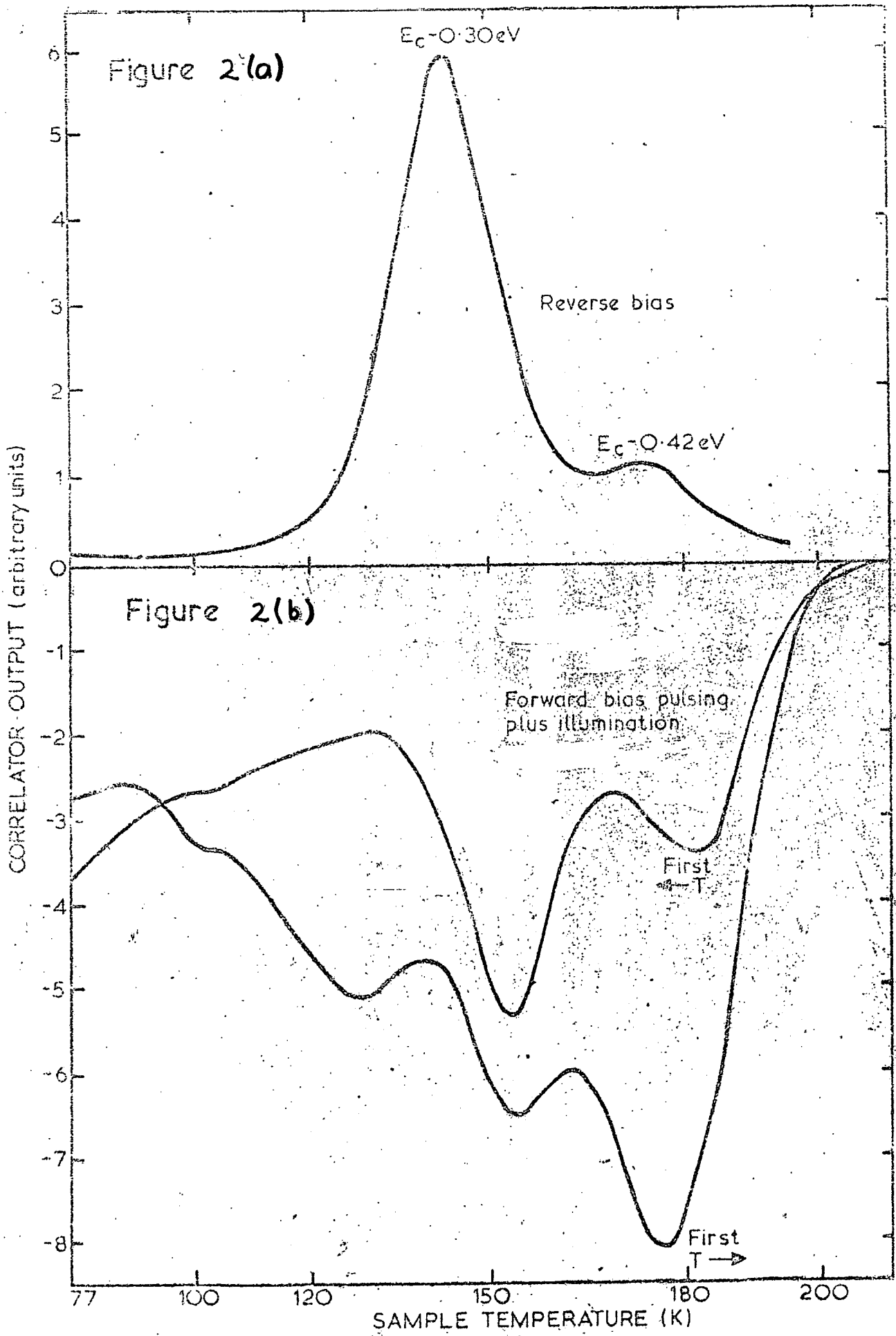

Figure 2 (a) DLTS spectrum for reverse biased γ-irradiated n-Ge diode

(b) Changing minority spectrum on cycling in temperature after infra-red illumination

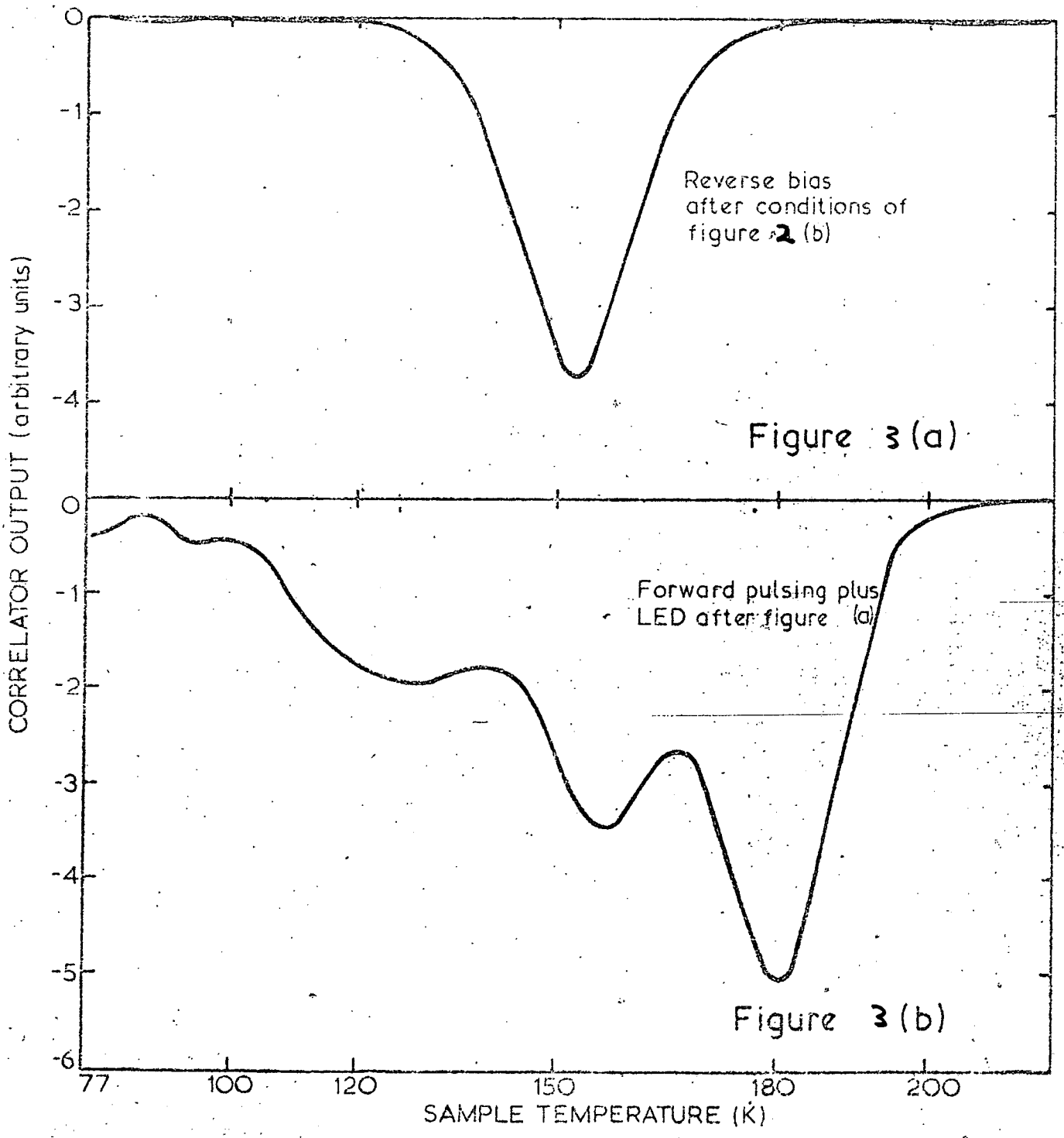

Figure 3 (a) Reverse biased spectrum for sample of figure 2 after cycling under injection conditions

(b) Forward biased spectrum after running in conditions of figure 3 (a)

Figure 4

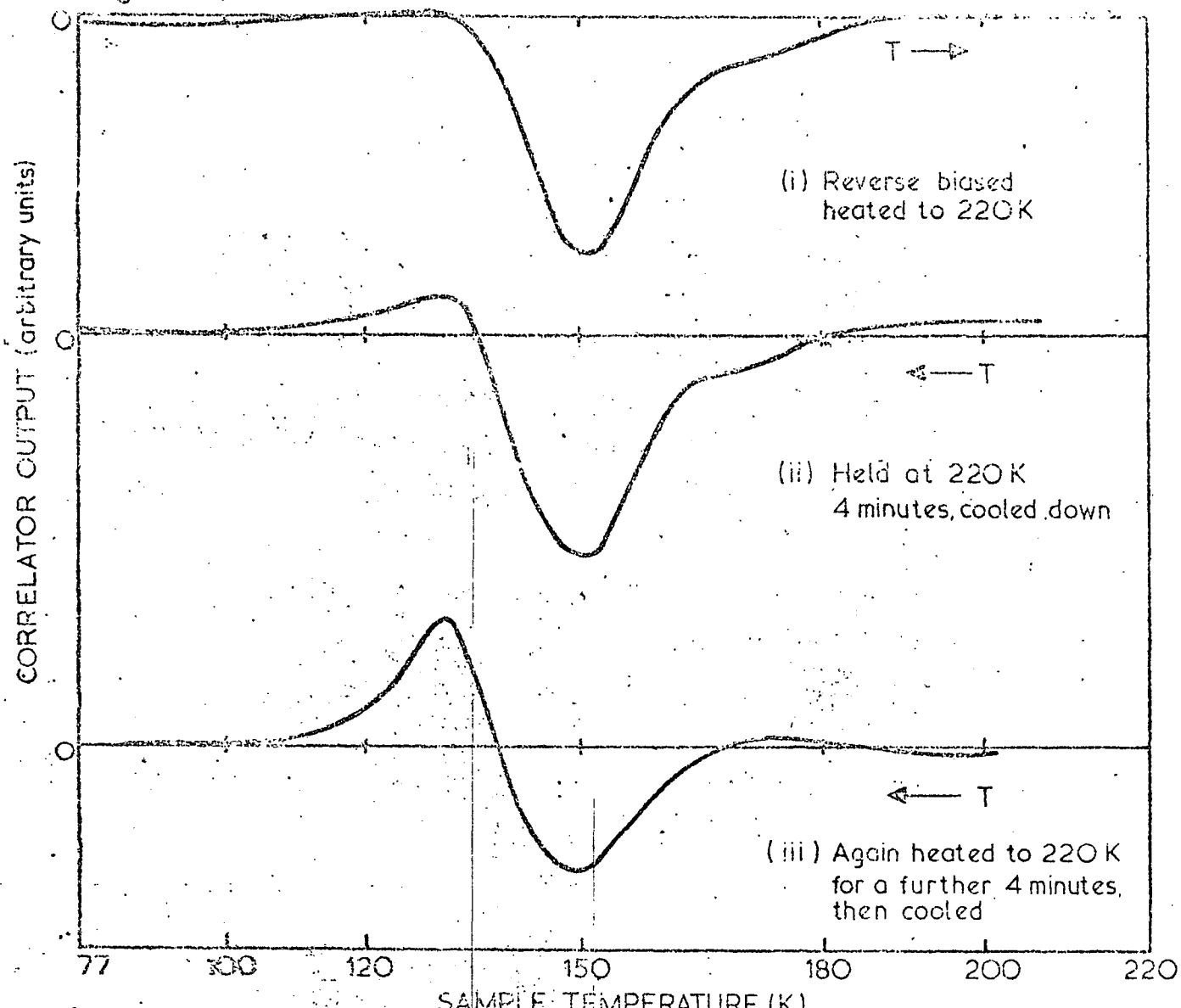

Figure 4 DLTS spectrum for conditions in Figure 3(a) after heating at 220K for 4 minute periods - note the donors returning to the spectrum

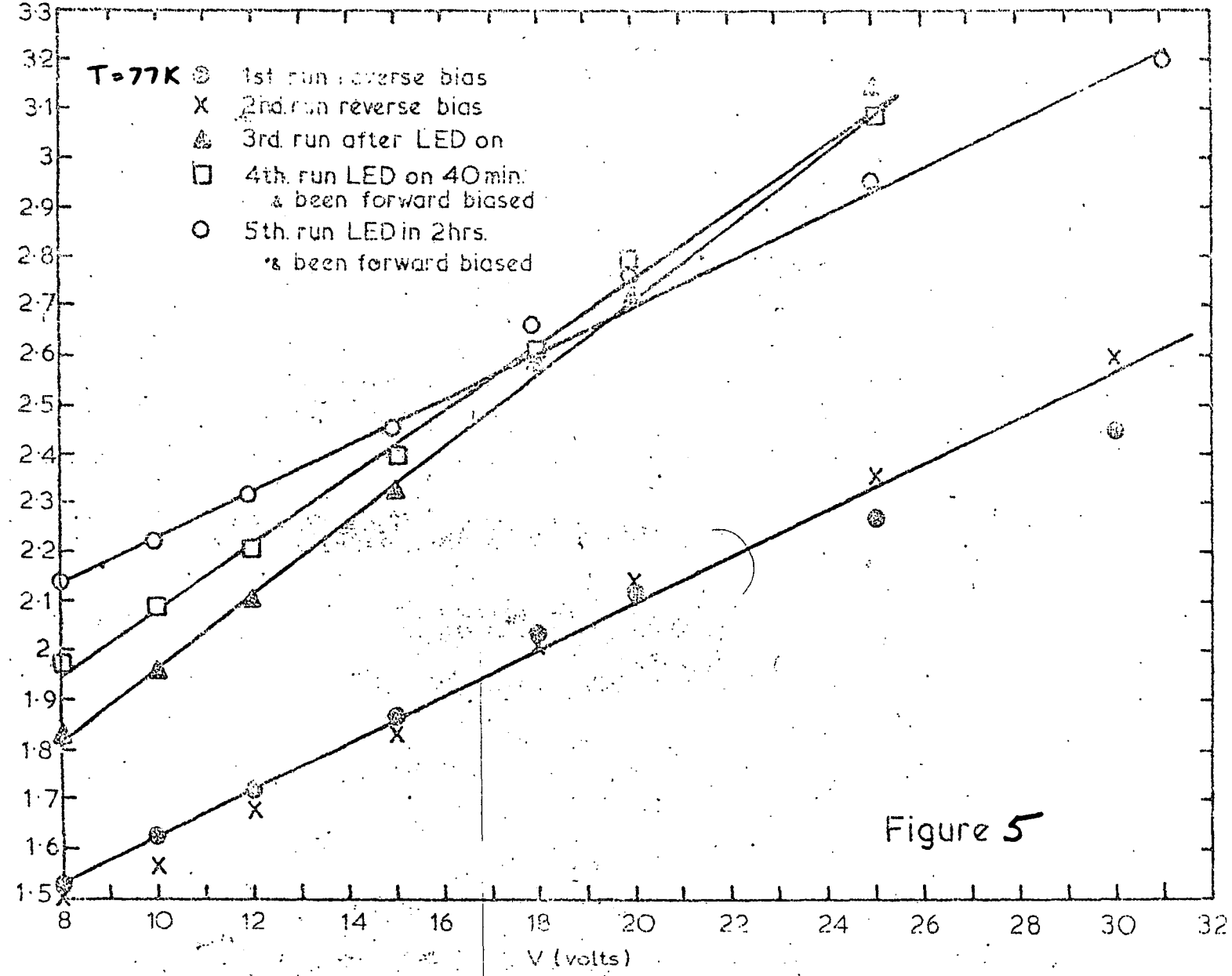

Figure 5

Figure 5 During the cycling and charge state dependent spectra of figures 2-4, the bulk capacitance at 77K showed significant changes

sample showed room temperature annealing of the acceptor defects, with the infrared sensitivity still present.

DISCUSSION

One of the interesting points of this work has been the question of why the deep level defects are light sensitive in some samples and not others which have been taken from the same crystal slice and treated in an analogous fashion. At least four samples exist of 74-48-3 discussed above, and 78-93-4 discussed in Chapter 1, which had been irradiated to the same γ-dose at various times and even under similar conditions on the DLTS apparatus. As evidenced from section 2, the charge states of the defects are extremely sensitive to the history of thermal cycling and infrared illumination of the same and probably to the exact conditions of the defect production (ambient temperature, dose rate) as well as post-irradiation processing.

Ge samples irradiated at 77 K which show sensitivity to white light illumination have been studied since 1959 [Basman et al. 1974], mainly by Hall effect measurements. A model has been proposed for such behaviour involving intermediate quasi-stable defects, through which radiation damage centres pass between stable states [Basman et al. 1974]. As sensitivity to illumination has also been seen in quenched, unirradiated Ge samples [Hall 1975], the phenomenon is clearly an important one in understanding the defect chemistry of Ge. It may also be interesting to try annealing radiation damaged Ge devices by minority carrier injection, in certain circumstances. Indeed, the study of this effect by DLTS may give some clue to defect centre identity by revealing the number of charge states and hence possibly the number of vacancies attached to the centre. The results in this section would be explained by the semi-quantitative model of Basman et al. [1974], though it does not provide the identity of the damage complexes.

REFERENCES

Baruch, P. [1961] - J. Appl. Phys. 32:653.

Basman, A. R., Gerasimov, A. B., Kakhidze, N. G., Konovalenko, B. M. and Tsertsvadze, A. B. [1974] - Sov. Phys. Semicond. 7(7)903 and references contained therein. For a recent publication, see Ito, K., Ito, T. and Oka, M. [1979] - Inst. Phys. Conf. Series 46:212.

Hall, R. N. [1975] - Inst. Phys. Conf. Series 23:190.

Kimerling, L. C. [1976] - IEEE Trans. Nucl. Sci. 23(6)1497.

Kimerling, L. C. [1978] - Solid State Electron. 21:1391.

Kimerling, L. C. [1979] - Inst. Phys. Conf. Series 46:56.

Lang, D. V. [1974] - J. Appl. Phys. 45:3023.

Lang, D. V. and Henry, C. H. [1975] - Phys. Rev. Lett. 35(22)1525.

Lang, D. V. and Kimerling, L. C. [1974] - Phys. Rev. Lett. 33(8)489.

Lang, D. V., Kimerling, L. C. and Yeung, S. Y. [1976] - J. Appl. Phys. 47(8)3587.

CONCLUSIONS

Excellent reviews on the theoretical treatment of deep levels in semiconductors [Pantelides 1978; Jaros 1980] have noted the many problems of explaining their nature. Also, the sensitivity of experimental results on the preparation process of the semiconductor sample has led to a lack of unambiguous data in most areas. As noted by Pantelides [1978], a re-examination of what is known and accepted about deep levels is necessary and new experimental and theoretical work is required to aid this process. It would be presumptuous to think that this thesis has done any more than provide a few useful results and, indeed, it has probably raised more problems than it has solved. Probably its major asset is that deep levels in the long neglected Ge have been studied. Haller [1979] has promoted several reasons why defects in Ge should be investigated, including taking advantage of its extremely high purity to study fundamental radiation damage processes and the interaction of hydrogen with point defects.

In Chapter 1 we have attempted to study radiation damage (mostly by γ-rays) centres in Ge. The dominant defects created by γ-rays in Czochralski crystals grown from silica crucibles under H_2 atmospheres seem to be oxygen-vacancy complexes. Indeed, the result may be a method of measuring low oxygen content in some Ge crystals. Many other levels have been observed and tabulated, but little is known of their microscopic structure. The major claim of the chapter would be that at least here is a starting point for a more systematic study of damage centres in Ge.

In Chapter 2 we measured deep levels in n-type GaAs, observing the Poole-Frenkel effect, and a sensitivity to magnetic fields, in the E_c - 0.62 eV level in VPE material. No crystal growing program was being undertaken at the time and, although a wide range of material

was used, only small quantities of each type was available. Consequently, no systematic doping experiments were carried out. The major point of the chapter is simply that the compound semiconductors are a mess in terms of the deep levels they contain. Even the purest epitaxial GaAs wafers had high trap densities and many different defect species.

Chapter 3 dealt with laser doped contacts to Si, Ge and GaAs, and demonstrated that under the right conditions, useful solid state detectors could be fabricated. Larger area contacts and control of the laser output power are required to give a more realistic comparison with conventional contacting methods.

Chapter 4 attempted to provide a starting place for the measurement of impurity levels in deliberately doped Ge. Much more experimental work is needed to identify the commonest levels related to the various elements, but some evidence in Ge was gained to support the results of Lang et al. [1980] on the complex nature of many impurity centres in Si.

In Chapter 5 the hydrogen passivation of defect centres in Ge and GaAs was studied. An important result was that the troublesome copper-related centres in Ge could be neutralised over considerable depletion depths. The microscopic study of this passivation mechanism and the possible production of new hydrogen-related defects during the incorporation of hydrogen could be of fundamental importance. The copper-related centres in Ge are well studied [Haller et al. 1981] and their interactions with atomic hydrogen could further this knowledge.

Chapter 6 was a collection of interesting but not especially important results. They were included for completeness sake.

If the uncertain wisdom of two and a half years were to be

distilled into a sentence, it would be that the unusual is the usual with deep level defects, and that defect complexes are much more important than first thought, probably crucial to the whole subject.

REFERENCES

Haller, E. E. [1979] - Int. Conf. Radiation Physics in Semiconductors and Related Materials, Tbilisi, USSR, Sept.

Haller, E. E., Hansen, W. L. and Goulding, F. S. [1981] - Advances in Phys. 30(1)93.

Jaros, M. [1980] - Advances in Phys. 29(3)409.

Lang, D. V., Grimmeiss, H. G., Meijer, E. and Jaros, M. [1980] - Phys. Rev. B 22(7)3917.

Pantelides, S. T. [1978] - Rev. Mod. Phys. 50(4)797.

REPORTS ARISING FROM THIS PROJECT

CHAPTER 1

New γ-radiation damage centres observed in Ge by deep level transient spectroscopy - Pearton, Tavendale and Williams, Rad. Effects, 60 129 (1982).

Thermal and electrical stability of γ-ray induced defects in Ge - Pearton, Rad. Effects, 61 135 (1982).

Radiation hardening to γ-rays of Ge for nuclear radiation detection by thermal annealing - Pearton, Rad. Effects Letters 67 (3) 63 (1981).

Transient capacitance measurements of deep level defects introduced by long-term, room temperature annealing in γ-ray compensated Ge - Pearton, Tavendale and Williams, AAEC/E501 [1980].

Deep level transient spectroscopy of γ-ray induced defects in Ge - Pearton, Tavendale and Williams, AAEC/E502 [1980].

The nature of the E_v + 0.23 eV and E_v + 0.38 eV γ-induced centres in Ge - Pearton and Tavendale, AAEC/E535.

Fast neutron and knock-on proton damage in Ge - Pearton, AAEC/TN151 [1980].

Electrical properties of γ-irradiated polycrystalline GaAs and Ge - Pearton, AAEC/TN156 [1981].

CHAPTER 2

Deep trapping centres in n-GaAs surface barrier diodes for nuclear radiation detection - Pearton, Tavendale and Williams, Electron. Lett. 16(12)483 [1980].

Electrical properties of polycrystalline GaAs - Pearton and Lee, AAEC/TN152 [1980].

Deep level transient spectroscopy of n-GaAs surface barrier diodes for nuclear radiation detection - Pearton, Alexiev, Tavendale and Williams, AAEC/E503 [1980].

CHAPTER 3

Ultra-thin laser aided doped Li contacts on HP Ge nuclear radiation detectors - Pearton and Williams, Nucl. Instr. Meth. 188 261 (1981).

The use of laser aided doped Li contacts on semiconductor nuclear radiation detectors - Pearton, Nucl. Instr. Meth. 189 589 (1981).

Pulsed laser alloying of Sn evaporated films on GaAs - Pearton and Lawson, Phys. Stat. Sol. (a) 68 K63 (1981).

CHAPTER 4

Deep metal-related centres in Ge - Pearton, Solid State Electron. 25 (4) 305 (1982).

A study of deep metal-related levels in Ge by capacitance spectroscopy - Pearton, Solid State Electron. 25 (6) 499 (1982).

Energy levels of some rare earth impurities in Ge - Pearton, Phys. Stat. Sol. (b) 109 K135 (1982).

The electronic states of some metal impurities in Ge - Pearton Aust. J. Phys. 35 53 (1982).

CHAPTER 5

Hydrogen passivation of copper-related defects in Ge - Pearton, Appl. Phys. Lett. 40 253 (1982).

Hydrogen passivation of the E_c - 0.36 eV centre in GaAs - Pearton, J. Appl. Phys. 52 4509 (1982).

Neutralization of point defects in Ge and GaAs by hydrogen incorporation - Pearton, AAEC/E 523 (1981).

CHAPTER 6

A method for observing shallow level impurities in semiconductors - Pearton and Tavendale, AAEC/TN148 [1980].

Magnetic field dependence of defect states in GaAs - Pearton, Phys. Stat. Solidi B 105(1)K19 [1981].

A search for magnetic field effects in deep level defects in semiconductors - Pearton, Williams and Tavendale, AAEC/TN150 [1980].

Electrical properties of polycrystalline Ge - Pearton, AAEC/TN153 [1980].

Transient conductance spectroscopy measurements of defect states in γ-irradiated n-channel Si FETs with possible γ-dosemeter application - Pearton, Tavendale and Williams, AAEC/E504 [1980].

Electronic stimulation of defects in radiation damaged Ge - Pearton, AAEC/TN161 [1981].

GENERAL

Deep level transient capacitance spectroscopy of point defects in semiconductors for nuclear radiation detection - Pearton, Tavendale and Williams (12th Aust. Spectroscopy Conference, UNSW, August 1980), reprinted as AAEC/TN149 [1980].

Capacitance spectroscopy measurements of deep defect states in semiconductors - Pearton, J. Electron. Electr. Engin. (Aust) Sept. (1982).

Instrumentation for DLTS of semiconductors - Williams, Pearton and Alexiev, AAEC/TN147 [1980].

DLTS system manual - Pearton, AAEC/TN165 [1981].